International PhD Program in Biomolecular Sciences
Department CIBIO
XXXI Cycle

"Impact of ETV7 on chemoresistance and cancer stem-like cell plasticity in breast cancer"

Advisor

Dr. Yari Ciribilli

Laboratory of Molecular Cancer Genetics

Department CIBIO, University of Trento

Tutor

Prof. Alessandro Provenzani

Laboratory of Genomic Screening

Department CIBIO, University of Trento

Ph.D. Thesis of

Laura Pezzè

Laboratory of Molecular Cancer Genetics

Department CIBIO, University of Trento

Academic Year 2017-2018

INDEX

ABSTRACT

ETV7 is a poorly characterized transcriptional repressor that belongs to the large family of ETS transcription factors, whose members have been associated with several cancer-related processes. ETV7 is a well-recognized Interferon-stimulated gene (ISG), and it was shown that its expression can be synergistically induced by the combined treatment with the chemotherapeutic drug Doxorubicin and the inflammatory cytokine TNFα in different cancer cell lines, including the breast cancer-derived MCF7 cells. Recently, it has been shown that ETV7 expression is significantly increased in breast cancer tissues, compared to the normal breast; however, the roles and the impact of ETV7 expression in breast cancer have still to be elucidated.

This project aimed at understanding the effects caused by increased ETV7 expression on breast cancer (BC) progression and resistance to conventional anti-cancer drugs.

We first observed that ETV7 expression can be induced by different stimuli, particularly by the treatment with several chemotherapeutic drugs able to induce DNA damage. We also demonstrated that the expression of ETV7 could affect the sensitivity of BC cell lines to standard anti-cancer therapies, such as Doxorubicin, 5-Fluorouracil and radiotherapy, and this evidence was correlated with an increase in ABC transporters and anti-apoptotic proteins expression. By investigating the possible mechanism responsible for ETV7-dependent Doxorubicin resistance we identified a novel target gene of ETV7, *DNAJC15*, which is a co-chaperone protein whose repression was previously associated with drug resistance.

Given the ability of cancer stem cells (CSCs) to be more chemoresistant, we analyzed the effects of ETV7 expression on the sub-population of breast CSCs. We found that ETV7 expression could exert a strong effect on breast cancer cells stemness, confirmed by both an increase in $CD44^{+}/CD24^{low}$ population and mammosphere formation efficiency.

In order to investigate the mechanisms responsible for these effects, we performed an RNA-seq analysis, which revealed significant repression of a signature of Interferon-

stimulated genes, suggesting a possible negative feedback mechanism in the regulation of the response to Interferon. Finally, prolonged treatment of breast cancer cells with IFN-β was able to rescue the effects on CSCs content.

Taken collectively, our data revealed that ETV7 can affect the sensitivity of breast cancer cells to some chemotherapeutic drugs and we propose ETV7 as an important contributor to the tumor-initiating capabilities of BC cells.

INTRODUCTION

1. Breast cancer

The breast is made up of adipose tissue, together with blood and lymph vessels and connective tissue. Each breast is divided into 12 to 20 sections called lobes, which are subdivided into lobules, glands responsible for milk production; and the lobes are linked by ducts, thin canals that drain milk from the lobules to the nipple [1].

Breast cancer (BC) refers to a malignant tumor occurring when cells in the breast start to divide and grow uncontrollably. Most frequently, breast cancer starts in the milk ducts (ductal carcinomas) or can originate from the cells of the lobules (lobular carcinomas). Less commonly, it can originate from the stromal tissues, which include the fibrous and fatty connective tissues in the breast.

Breast cancer is the second most common cancer overall and the most common cancer in women worldwide, and it is estimated that about 1 woman in 8 will develop breast cancer in her lifetime. The mortality rate is decreasing in the last years thank to earlier diagnosis and treatment strategies improvements, however, breast cancer still represents the fifth cause of cancer-related deaths in women [2,3]. Risk factors include increasing age, family history with the main inheritance susceptibility represented by germline mutations in *BRCA1* and *BRCA2* genes, alcohol consumption, hormone therapy, obesity, and radiation exposure [4].

In the past, breast cancer was recognized as a single disease, with differential features and systemic treatment responses. However, thanks to the development of high throughput technologies for gene expression analysis, breast cancer is now considered a highly heterogeneous disease, both at the clinical and at the genetic level [5].

1.1 Breast cancer classification

In an attempt to standardize breast cancer heterogeneity, thus helping in treatment and prognostic evaluation, several types of classifications have been developed, including histopathological and molecular classification of breast cancers.

1.1.1 Histopathological classification

The histopathological classification of breast cancer consists of classifying breast carcinomas based on the morphological features of the tumor. This type of classification is spread worldwide and allows the distinction of 20 major types and 18 minor subtypes of the tumor. Breast tumors can be classified as in situ or invasive (infiltrating) carcinomas. In situ carcinomas can be further subdivided into the more common ductal (DCIS) or lobular (LCIS) carcinoma in situ and include a heterogeneous sub-group of breast cancer types. Similarly, also invasive carcinomas represent a heterogeneous group of malignant tumors and include tubular, ductal/lobular, invasive lobular, infiltrating ductal, mucinous, medullary and papillary carcinomas [6]. However, about 70-80% of all invasive breast cancer belong to invasive ductal carcinomas (IDC), revealing the need to use molecular biomarkers to further classify the status of this breast cancer subtype [7]. Indeed, it is of fundamental importance to improve patients' stratification according to the relative risk of relapse or progression.

1.1.2 Molecular classification

Thanks to the advancement in gene expression analyses, it is now possible to better stratify breast cancer patients according to the "intrinsic" (or biological) molecular classification [5]. Perou and collaborators proposed the classification of breast cancer into subtypes based on the hierarchical clustering of gene expression profiles [8], identifying the following subtypes: luminal A, luminal B, HER2+, basal-like and normal breast-like subtype (Figure I), which has been proved to have good prognostic values and to be predictive of the response to commonly used chemotherapy [9–11]. However, this type of classification was obtained from fresh-frozen samples and is not possible to easily apply it to the more commonly used formalin-fixed and paraffin-embedded (FFPE) samples, reducing the applicability of this classification to the clinical practice. In order to overcome this

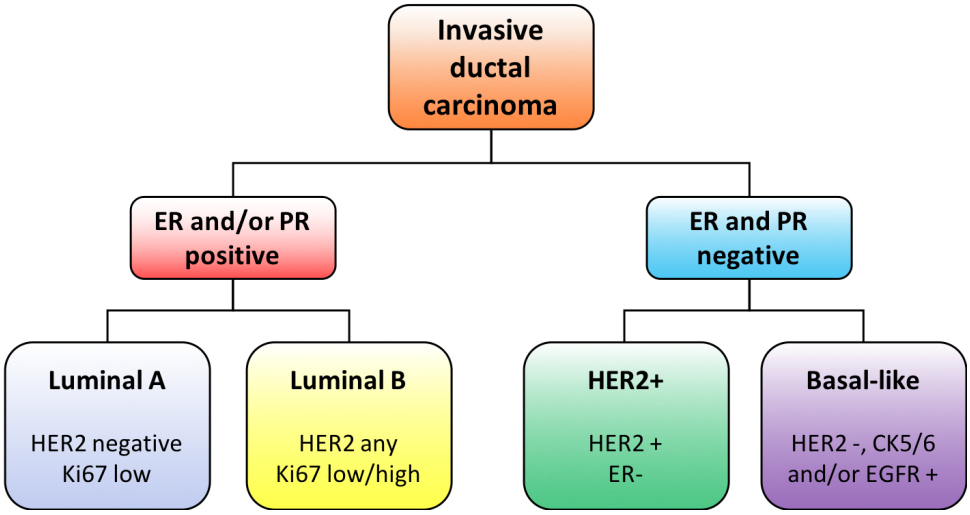

Figure I. Schematic illustration of the breast cancer subtypes (invasive ductal carcinoma) according to the expression of immunohistochemical markers ER, PR and HER2. Luminal subtypes are characterized by ER and/or PR positivity, variable expression of HER2 and Ki67. Her2+ subtypes are usually ER negative and HER2 positive. Basal-like subtypes are mainly represented by triple negative breast cancers (ER, PR and HER2 negative), or can also be characterized by high levels of expression of mesenchymal markers, CK5/6 and /or EGFR positivity.

problem, a gene expression assay of 50 genes based on qRT-PCR, called PAM50, has recently been developed and has shown to be able to generate risk-of-relapse scores with good prognostic values [12].

A further improvement of the applicability of the molecular classification to the clinical practice has been obtained with the identification of surrogate immunohistochemical markers ER, PR, HER2 and Ki67 [13].

The luminal subtypes account for approximately 70% of all breast cancer cases, they are usually characterized by estrogen receptor (ER) and progesterone receptor (PR) positivity and present a favorable prognosis. Luminal B subtype can be negative for PR, show HER2 positivity or high levels of Ki67, it is often poorly differentiated and usually Luminal B breast cancer patients have a worse prognosis compared to luminal A.

Normal-like tumors represent 5-10% of cases in a lymph node negative cohort and are characterized by an IHC status similar to luminal A, but they present a normal breast tissue profiling [14].

The HER2 subtype accounts for the 10-15% of breast cancers and it is characterized by the amplification and over-expression of the *ERBB2* gene and thus high membrane expression of the HER2 protein. Despite the high aggressiveness, this tumor subtype is predictive of good responsiveness to the targeted therapy with anti-HER2 treatment strategies [15].

The basal-like subtype is the most aggressive subtype of breast cancer and it represents a highly heterogeneous type of tumor. Most of the cases of basal-like subtype (80%) are represented by the triple negative profile, which is ER, PR, and HER2 negative, and are often associated with mutations in *BRCA1* gene [16]. This subtype of breast cancer is showing a very poor prognosis with frequent metastases and reduced sensitivity to standard therapeutic approaches [17]. Interestingly, given their heterogeneity, the basal-like BCs have been also sub-divided into 6 groups using gene expression analyses from 21 available breast cancer datasets: basal-like 1, basal-like 2, immunomodulatory, mesenchymal, mesenchymal stem-like, and luminal androgen receptor [18].

1.2 Therapeutic strategies

Current therapeutic approaches for breast cancer depend on the subtype of breast cancer, its mass, the localization, the stage and the physical condition of the person affected. Therapeutic strategies most commonly used include both local, and systemic treatments. Local treatments are represented by surgery and radiation therapy, whereas systemic treatments include chemotherapy, endocrine (hormonal) therapy and targeted therapy.

The leading approach for the treatment of localized breast cancer is conservative surgery, which can be preceded by neoadjuvant therapy to shrink the tumor and is usually followed by other systemic adjuvant therapies to reduce the risk for local recurrence [19].

Neoadjuvant therapy is chosen for the treatment of large and locally advanced operable tumors in order to reduce the tumor and facilitate surgery and can exploit chemotherapy, endocrine therapy and targeted therapy [20].

Adjuvant therapy strategies for breast cancer are determined by the characteristics of the tumor and particularly are distinguished between endocrine-responsive and non-responsive histology [21].

Endocrine therapy aims at balance or block hormones and is indicated for the treatment of patients with detectable ER and PR expression and it is therefore commonly used for the treatment of luminal subtypes of breast cancer, either alone or in combination with chemotherapy or targeted therapies [22].

Chemotherapy is recommended for the treatment of most of the triple negative, HER2+, and high-risk luminal breast cancers, and can reduce breast cancer mortality by about one-third [23]. However, chemotherapy is not specifically selective for cancer cells and can eliminate also normal healthy cells, especially fast dividing cells, like immune cells, resulting in immune suppression and organ toxicity [24]. Chemotherapy treatment for breast cancer has various side effects, which most frequently include myelosuppression, nausea and vomiting, alopecia, weight gain and ovarian failure [25].

Most commonly used chemotherapeutic regimens include anthracyclines (i.e. Doxorubicin and Epirubicin), taxanes (i.e. Paclitaxel and Docetaxel), 5-Fluorouracil (5-FU), Cyclophosphamide, Methotrexate, and Carboplatin [26].

1.2.1 Doxorubicin

Doxorubicin (also known as Adriamycin) is a cytotoxic anthracycline, an antibiotic with anti-neoplastic activity isolated from the bacterium *Streptomyces peucetius* [27]. Doxorubicin is one of the most effective anti-cancer agents and has been used for the treatment of osteosarcoma, breast cancer, lung cancer, prostate cancer, and many other cancers for over 30 years. Unfortunately, Doxorubicin causes also life-threatening toxicity to most major organs, such as brain, liver, kidney and heart [28].

Doxorubicin can exert its anti-tumor activity by intercalating the base pairs of the DNA's double helix, thereby preventing DNA replication and inhibiting RNA transcription [29]. Furthermore, it can inhibit topoisomerase enzymes I and II, thus preventing the ligation of the nucleotide strands after double-strand breaks. These mechanisms induce a range of cytotoxic and anti-proliferation effects resulting in DNA damage [30]. Other Doxorubicin actions include the generation of free radicals resulting in further DNA damage and unwinding, increased alkylation and inhibition of macromolecule production [31]. Moreover, Doxorubicin can directly affect the cell membrane by binding to plasma proteins, causing the formation of highly reactive species of hydroxyl free radicals, which are responsible for the dangerous side effects of toxicity, with cardiotoxicity being the most prominent one [32].

1.2.2 5-Fluorouracil

5-Fluorouracil (5-FU) is a widely used chemotherapeutic drug for the treatment of a range of cancers, including breast, colorectal and skin cancer. 5-FU is one of few clinically useful anti-tumor agent rationally designed based on tumor biochemistry studies. Its discovery dates back to 1957 [33], after the observation of an increased use of exogenous uracil in malignant tissues compared with normal tissues in rats' hepatic tumors [34], suggesting that uracil analogs might interfere with tumorigenesis. A rational study of physicochemical properties allowed the design of 5-FU, a heterocyclic aromatic organic compound which is an analogue of uracil with a fluorine atom at the C-5 position in place of hydrogen.

The cytotoxic effects of 5-FU are caused by alterations of RNA and DNA normal synthesis and functioning [35]. In mammalian cells, 5-FU enters the cells via the same transport mechanism as uracil and it is then converted into fluorodeoxyuridine monophosphate (FdUMP), which can interact with the enzyme thymidylate synthase (TS) by binding to its nucleotide binding site. This interaction causes the inhibition of the synthesis of new deoxythymidine monophosphate (dTMPs), which are highly required by rapidly dividing cells, like cancer cells. Moreover, TS inhibition results in depletion of dTMP with the accumulation of deoxyuridine monophosphate (dUMP), which causes an imbalance in intracellular nucleotides level, and accumulation of deoxyuridine triphosphate (dUTP), which, together with FdUTP, can be misincorporated into the DNA. Both these effects result in excessive endonuclease-induced double-strand breaks in the DNA, ultimately resulting in cell death [36].

Furthermore, 5-FU can exert its cytotoxic effects via interference with the RNA. Indeed, 5-FU has been shown to interfere with normal processing and function of various RNA species, such as pre-rRNAs [37], tRNAs [38] and small nuclear RNAs [39]. Moreover, FdUTP can also be incorporated into mRNA, which can alter its metabolism and expression [40].

1.2.3 Radiotherapy

Radiotherapy, or radiation therapy, is a type of local cancer treatment exploiting high doses of radiation (predominantly X-rays) to kill cancer cells, resulting in tumor shrinkage. The use of radiation for cancer treatment was first introduced by Emil Grubbé in Chicago, who used the just discovered X-rays for the treatment of an incurable breast cancer [41].

Subsequent technological advancements allowed the improvement of doses and precision of the treatment. Now, breast-conservative surgery followed by radiation therapy is a widely accepted standard approach, able to halve the overall recurrence rate and reduce BC mortality of more than 15% [42].

Radiotherapy can be administered both from the outside or the inside of the body. Internal administration can be performed by implanting radioactive sources in tissues or cavities of the body (i.e. brachytherapy), or by systemic administration of radiopharmaceutical agents [43]. Administration of radiation from the outside of the body is called external beam radiation therapy and it is conducted with a linear accelerator (LINAC) machine, which produces a photon beam and directs it to the tumor site. The radiation dose is measured with the standard unit called Gray (Gy), which express the radiation dose in terms of absorbed energy per unit mass of tissue; in particular, 1 Gray corresponds to 1 Joule of energy per kilogram of matter.

Radiation therapy can use low and high linear energy transfer (LET) radiation, which measures the number of ionization caused per unit distance while it traverses the living tissue. Low LET radiations include X-rays, γ-rays and β-particles and can deposit a relatively small amount of energy, whereas charged radiation particles (electrons, protons, α-rays, *etc*.) deposit more energy on the targeted areas causing more biological effects and allowing for dose minimization [44].

The radiotherapy approach is based on the observation that rapidly proliferating cancer cells are more sensitive to ionizing radiations compared to normal cells since cancer cells have a slower DNA repair system and also produce more DNA breaks than normal cells [45,46]. Indeed, the mechanism of action of radiotherapy includes both direct and indirect effects which both result in DNA damage and subsequent cell death [47].

Radiation can induce direct DNA damage by inducing ionization on the DNA, resulting in double-strand breaks (DSBs) or single strand breaks (SSBs). Furthermore, it can produce free radicals derived from ionization or excitation of water molecules inside the cell, which finally result in DNA damage [44]. Radiation-induced DSBs are the most dangerous types of DNA damage, which can lead to cell death if not repaired by the DNA damage response (DDR) system.

2. Chemoresistance and radioresistance

One of the main challenges in cancer treatment is the development of resistance to standard therapies, such as chemoresistance and radioresistance, which causes failure of the therapy, with subsequent disease relapse and metastases formation. This event can appear when patients initially responsive to the treatment show a reduced response later on, which can result in the regrowth of the tumor [48].

This phenomenon can be explained by two causes: either the tumor cells are intrinsically resistant to the therapy possibly due to genetic features (intrinsic resistance), or they can become resistant after the exposure to the therapy (acquired resistance) [49]. Since intrinsic resistance is usually present in about 1 in 10^6-10^7 cancer cells, the probability of successful elimination of the cancer cells is related to the tumor size at the beginning of the treatment [48].

Given the high individual variability and complexity of the biological processes altered in resistant cells, as well as the absence of proper diagnostic tools to evaluate the resistance before the start of the therapy, it is an urgent need to better understand the mechanisms involved in the processes of resistance.

2.1 Molecular mechanisms of chemoresistance

Chemoresistance can be influenced by genetic and epigenetic alterations affecting drug uptake, metabolism, and export. There are several mechanisms contributing to chemoresistance, such as tumor heterogeneity, increased drug efflux, drug inactivation, evasion of apoptosis, deregulation of oncogenes and tumor suppressor genes, enhanced DNA repair, mitochondrial alteration, autophagy, epithelial-to-mesenchymal transition (EMT), cancer stemness, and exosomes production, but also the tumor microenvironment (TME) has been shown to be a key player in this process [50,51] (Figure II).

A typical molecular mechanism of resistance to chemotherapy is the increased expression of transporter pumps, which are responsible for enhanced efflux of cytotoxic molecules across the cellular membranes, keeping the intracellular concentration of the drugs below the lethal threshold. These types of transporters belong to the ATP-binding cassette (ABC) superfamily and are responsible for the absorption, distribution, and excretion of many

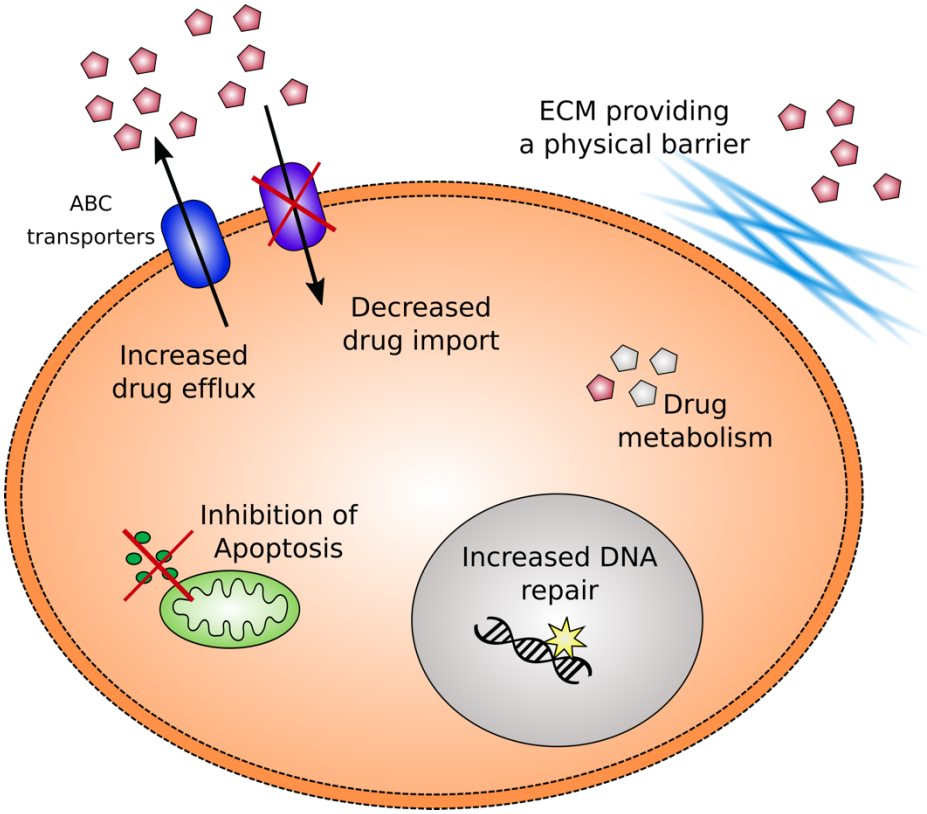

Figure II. A schematic representation of some of the processes that can be involved in the development of chemoresistance. The shown processes include the enhanced drug inactivation via drug metabolism, decreased drug import or increased drug efflux via ABC transporters, inhibition of apoptosis, increased DNA repair and increased production of extracellular matrix (ECM) proteins which provide a physical barrier against the drug intake.

drugs. In addition to their role in cytotoxic chemotherapeutics transport, it has been proposed that ABC transporter can also transport cell-signaling molecules that may contribute to tumorigenesis, such as peptides, inorganic ions, proteins, amino acids, polysaccharides, and vitamins [52,53]. There are at least 48 genes encoding ABC transporters, and ABC proteins have been divided into 7 subclasses named from A to G (ABCA, ABCB, ABCC, ABCD, ABCE, ABCF, and ABCG) based on sequence homology and genomic organization [54,55]. The most commonly deregulated ABC transporters in breast cancer are ABCB1 (also known as MDR1 or P-glycoprotein), ABCC1 (MRP1) and ABCG2 (BCRP), that can drive the so-called multidrug resistance (MDR) [56].

Alternatively, some metabolic effects can alter the effective concentration of the drug within the plasma, reducing its efficacy. The over-expression of drug-metabolizing enzymes or carrier molecules can reduce the sensitivity to anti-cancer drugs by reducing its concentration [57,58], or, on the other side, the reduced expression of drug-metabolizing

enzymes can instead reduce the efficacy of the drug when the administered pro-drug needs to be metabolized in order to get activated [59].

Another factor contributing to chemoresistance is the hyper-activation of oncogenes or the inactivation of tumor suppressor genes. Examples of oncogenes responsible for enhanced chemoresistance include epidermal growth factor receptor (EGFR), which can activate STAT3 and NF-κB pathways, thus leading to inflammation-associated chemoresistance, the PI3K/Akt pathway and ERK. Alternatively, the inactivation of tumor suppressor genes like p53 can enhance chemoresistance. In particular, p53 inactivation, either due to mutations or its inhibition, was shown to be involved in the resistance to several chemotherapeutic drugs, mainly via the impairment of apoptosis and cell cycle arrest [51]. Indeed, another mechanism of resistance to therapy is based on defects in the apoptotic pathway, which usually affect the efficacy of most of the anti-cancer agents. In this case, cancer cells can acquire the resistance by inducing the expression of anti-apoptotic proteins such as BCL-2/BCL-xL and IAP proteins, or, alternatively, by mutating or down-regulating the expression of pro-apoptotic proteins (i.e., BAX or Caspase-8) [60].

Among the many ways cancer cells can become or be intrinsically resistant to chemotherapy, mitochondrial alterations need to be mentioned. Indeed, mitochondria are the centers of cellular energy production and play key roles in cancer progression, metabolic reprogramming and response to chemotherapeutic drugs. As previously mentioned, mitochondrial apoptosis is one of the mechanisms which can mediate the resistance to therapy, and it is mainly regulated by the B-cell lymphoma 2 (BCL-2) proteins. Pro-apoptotic (BAX, BAK, and BCL-xS) and anti-apoptotic (BCL-2, BCL-xL, and MCL-1) proteins can regulate the mitochondrial apoptosis by stabilizing mitochondrial permeability and thus regulating the release of Cytochrome c from the mitochondria into the cytosol, where it can activate Caspase-3 and Caspase-9, finally leading to apoptosis [51]. Moreover, mitochondria functioning can alter the sensitivity to chemotherapy by altering cellular metabolism. In fact, most of the cancer cells harbor somatic mutations or alterations in the mitochondrial genome (mtDNA), resulting in mitochondrial dysfunction. However, cancer cells do not turn off completely the mitochondrial metabolism, but rather they alter the bioenergetic profile of the cells by changing the transcription and activation of cancer-related genes and signaling pathways. Cancer cells can then undergo

different bioenergetic choices, increasing the tumor heterogeneity, which will include both more glycolytic or more oxidative cellular metabolisms [61].

A further way by which cells can become resistant to chemotherapy, in particular to those therapies which exploit the DNA damage as the main mechanism of action, is the increased ability to repair the DNA efficiently. DNA repair is a biological system able to identify and correct the damage to DNA molecules which can be induced by several causes, such as ultraviolet (UV) radiation, X- and γ-rays, endogenous ROS, toxins, mutagenic chemicals and some chemotherapeutics [51]. Thus, the over-expression or the hyper-activation of DNA repair proteins can mediate the resistance to chemotherapy. For example, the over-expression of ERCC1, which participates in the Nucleotide Excision Repair pathway, has been linked to resistance to platinum-based chemotherapies in various cancer types [62], and the up-regulation of the DNA repair enzyme O(6)-methylguanine DNA methyltransferase (MGMT) has been involved in the chemosensitivity to alkylating agents [63].

A common resistance mechanism, which is particularly effective for targeted therapies, is the development of alterations in the target molecules. In fact, during the course of the treatment, the target of the drug can be modified or reduced in the expression, ceasing to have any biological influence useful to target. For example, in endocrine-resistant breast cancers, the tumor initially responsive to anti-estrogen therapy (e.g., tamoxifen), undergoes a loss of estrogen receptors, resulting in treatment resistance [64]. Similarly, mutations in the Topoisomerase protein can alter its nuclear localization, making cancer cells resistant to the chemotherapeutic drugs targeting the activity of Topoisomerase II, such as Etoposide [65].

2.2 Molecular mechanisms of radioresistance

The determination of failure or success of radiotherapy is based on what is called the 5 R's of radiobiology: Repair of the DNA, Redistribution of cells in the cell cycle, Repopulation, Reoxygenation of hypoxic tumor areas and Radiosensitivity [66].

Repair of the DNA is the primary source of resistance to radiotherapy. In fact, ionizing radiation induces direct DNA damage, which leads to the activation of the ATM-p53 pathway, responsible for replication blockage and induction of DNA repair systems [67].

Therefore, similarly to the mechanisms of resistance to chemotherapy, radioresistant cancer cells usually have a higher expression of DNA repair enzymes and anti-apoptotic proteins.

The second R of radiobiology is Redistribution of cells in the cell cycle and refers to the fact that the sensitivity of cells to radiation is different during the different phases of the cell cycle. Cells in mitosis are in fact the most sensitive to DNA damaging agents, whereas the cells in late S-phase are the most resistant [68]. Thus, the redistribution of radiotherapy treated surviving cells into less sensitive phases of the cell cycle may account for increased resistance to the following doses.

Repopulation of tumors is another common reason for the failure of radiation therapy. Repopulation refers to the tissue's response to a decrease in cell number, however, also the tumor can undergo an accelerated repopulation, which results in a faster cellular growth rate of treated tumors compared to untreated ones [69].

Reoxygenation of hypoxic tumor areas is also believed to improve the efficacy of radiotherapy. Indeed, several experiments have shown that oxygen is one of the most potent modifiers of radiosensitivity and that hypoxic cells are more resistant to radiation therapy [69,70]. Hypoxia can be either transient or chronic, based on the presence of blood vessels or their intermittent closure, thus affecting the reoxygenation process [71,72]. It is now clear the importance of targeting the hypoxic areas of the tumor in order to improve the therapeutic outcome. However, it is still to be elucidated whether acute or chronic hypoxia is the most relevant for radioresistance.

The last and newest R is Radiosensitivity, which refers to the fact that some cells are more sensitive to radiotherapy than others. Radiosensitivity is the response of a tumor to irradiation and can be measured by the rapidity of response, its durability and the extent of regression [73].

3. Cancer stem cells

Despite the molecular mechanisms of chemoresistance and radioresistance can partially explain the appearance of the resistance to therapy, the recently proposed theory of

cancer stem cells (CSCs) can improve the understanding of resistance and implement it within a better model.

The cancer stem cells theory opposes to the stochastic model of cancer in the explanation of cancer formation.

According to the stochastic (clonal evolution) model, every cell within the tumor is potentially capable of propagating and forming a tumor. This model proposes that a normal somatic cell, which undergoes at least five genetic mutations in order to acquire the ten hallmarks of cancer, can originate a tumor. However, this theory cannot explain the higher incidence of some types of cancer during the childhood compared to adulthood or the fact that usually a large number (more than 10,000) of cells is required to initiate a tumor in immunocompromised mice [74].

On the opposite, the CSC theory is based on the observation that cancer cells within a tumor are different, but are hierarchically organized, with some rare undifferentiated CSCs able to give rise and to maintain the whole population of cells within the tumor [75].

The cancer stem cells theory is based on two related concepts stating that: 1) tumors can originate from either tissue stem cells or their immediate progeny because of self-renewal dysregulation and 2) tumors contain and are driven by cells displaying some stem cells properties [76].

The origin of this theory dates back about 150 years ago when Rudolf Virchow proposed the idea that cancer is a disease which originates from an immature cell, paving the basis for the concept of cellular hierarchy [77].

However, the modern concept of CSCs was first described in 1971, when Pierce and Wallace showed that some malignant undifferentiated cells were able to originate benign, well-differentiated cells in squamous cell carcinoma, giving the first experimental evidence of the existence of cellular hierarchy in a tumor [78]. Another critical evidence came in 1990, when Fialkow and colleagues, by labeling and tracing the lineage of cancer cells in chronic myeloid leukemia (CML), demonstrated that a pluripotent stem cell is initially transformed and can then give rise to malignant clonal progeny [79].

A few years later, cancer stem cells were first isolated from acute myeloid leukemia (AML) using a phenotypic cell isolation strategy based on fluorescently labeled cell surface protein, and the authors showed that a population of the isolated cells was able to transplant AML into severe combined immunodeficiency (SCID) mice [80].

Subsequent studies recognized CSCs in various solid tumors, including breast, prostate, ovarian, melanoma, brain, bone sarcoma, colon, and renal cancer [81]. Nevertheless, the identification and characterization of CSCs in most tumor types is still evasive and, it is still under debate whether CSCs could exist in all human tumors.

With cancer stem cells or tumor-initiating cells, we now refer to the subset of cancer cells thought to be the main drivers of tumorigenesis, which are responsible for tumor growth, resistance to therapy and metastatic spread [82]. The definition of CSC describes it as a cell within the tumor which has self-renew capacity and differentiation potential, meaning that it can give rise to the heterogeneous lineages of cancer cells within the tumor. Basically, CSCs are defined by their intrinsic ability to propagate tumor cells [83]. Similarly to stem cells (SCs), which are essential for maintaining tissue homeostasis, CSCs have long term self-renew potential, meaning that upon division they give origin to cells that retain the ability of self-renewal. This can be accomplished by either symmetric or asymmetric divisions [83]. During symmetric division, one CSC will originate two identical daughter cells, whereas with asymmetric division it will produce one daughter cell which will retain its CSC identity, and another which could undergo several rounds of division and post-mitotic differentiation, accomplishing the second task defining a cancer stem cell [84].

3.1 Drug resistance of cancer stem cells

Another important property of CSCs is their intrinsic capacity to resist to both chemotherapy and radiotherapy (Figure III).

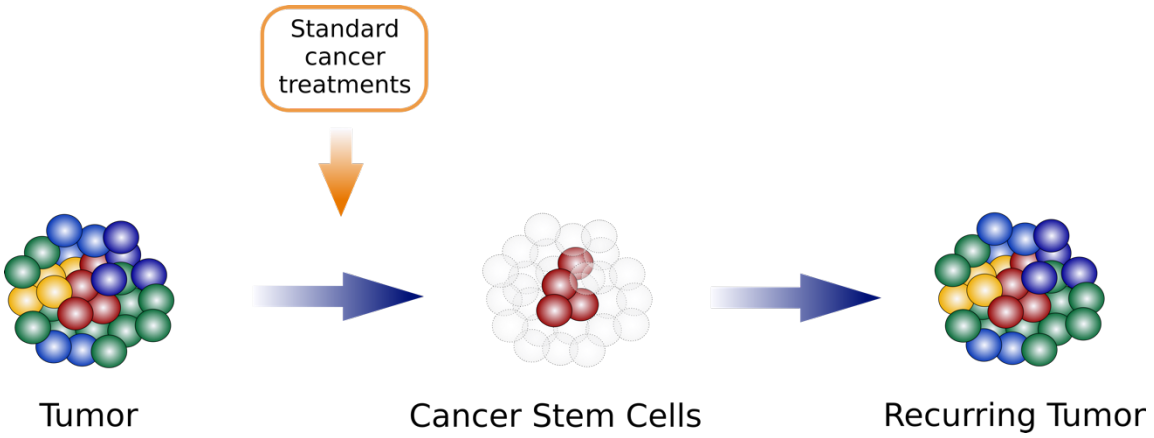

Figure III Model of cancer stem cells resistance to standard cancer treatments. Heterogeneity within the bulk initial tumor is represented by different colors of the cells. In response to the treatment with standard anti-cancer agents, the cancer stem cells population (in red) can survive and subsequently give origin to a recurring tumor which will present heterogeneity similar to the initial tumor.

There are several molecular mechanisms responsible for the increased resistance of CSCs to anti-cancer therapy, including cell cycle kinetics, DNA replication and repair mechanisms, asymmetric cell division, anti-apoptotic proteins, and transporter proteins expression, *etc.* [76].

Cell cycle kinetics of cancer stem cells differs from that of cancer cells because most of the cancer stem cells are not- or slowly-cycling and are usually in G0 phase of the cell cycle, in a state called quiescence, thus becoming resistant to radiotherapy or chemotherapy agents who depend on cell cycle progression for their function [85].

As previously mentioned, the resistance to DNA damaging agents can also be mediated by alterations in the DNA replication and repair mechanisms, which are often found deregulated in cancer stem cells, given the fact they can undergo asynchronous DNA synthesis and usually present an increased DNA repair potential compared to cancer cells [86,87].

The property of cancer stem cells to undergo asymmetric cell division is also contributing to the resistance to therapy, as, during the asynchronous DNA synthesis, the parental DNA strand selectively segregates with the cancer stem cell and not with the differentiated daughter, a process regulated by the oncosuppressor p53 [88,89]. In this way, the undifferentiated compartment is protected by the accumulating mutations and by the DNA-damaging agents.

Another characteristic of cancer stem cells mediating drug resistance is the elevated expression of anti-apoptotic proteins, including BCL-2 and IAP family members, which protect the cells from therapy-induced apoptosis [90].

Finally, cancer stem cells were shown to express high levels of transporter proteins often involved in chemoresistance such as ABC transporters [91]. However, there are several other mechanisms driving resistance in cancer stem cells including ROS detoxification, EMT induction, increased telomerase activity, and the activation of stemness signaling pathways.

3.2 Cancer stem cell plasticity

According to the CSC theory, cancer stem cells are placed at the top of the cellular hierarchy and are usually originated from normal stem cells or progenitor cells which have

gained the ability to generate tumors when they encounter particular genetic mutations or some environmental cues. An alternative origin of CSCs could be the de-differentiation of normal somatic cells acquiring stem-like characteristics and malignant behavior through genetic or heterotypic alterations, such as EMT [84].

However, accumulating evidence shows that cancer stem cells can also arise from the transition of non-stem cells, revealing the possibility of a bidirectional conversion between self-renewing and non-self-renewing cells, which adds a level of complexity to the origin of heterogeneity. When CSCs are generated by non-stem cells acquiring CSC properties, we usually refer to them as "cancer stem-like cells" (CSC-like) [92].

This dynamic process in which cancer cells can bidirectionally shift from non-CSC state to CSC-like state is referred to as "cancer stem cell plasticity" (Figure IV) and can be modulated by specific stimuli which are often regulated by endogenous transcription factors [92]. An important contributor to CSCs plasticity is the tumor microenvironment, which is composed of non-tumorigenic cells including mesenchymal stem cells, stromal cells and immune cells such as macrophages and myeloid-derived suppressor cells [93]. The particular TME surrounding CSCs creates a specialized environment providing secreted factors and cell to cell contact critical for CSCs function and plasticity, which is defined as "cancer stem cell niche" [94].

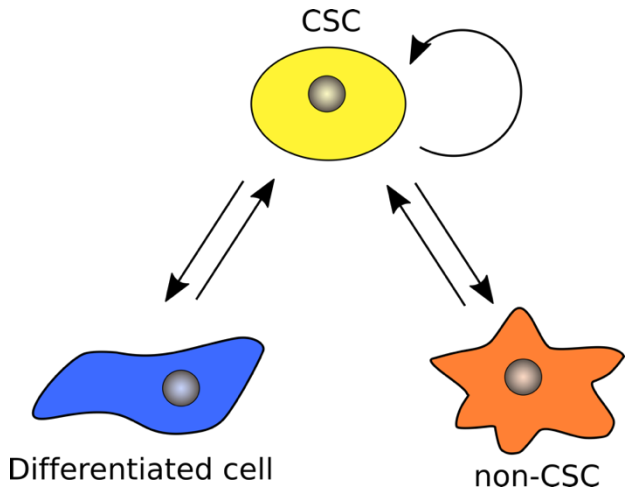

Figure IV. The dynamic model of CSCs plasticity. Cancer stem cells (yellow) have self-renewal and differentiation potential and can give origin to differentiated cells (blue) or non-cancer stem cells, which can dynamically interconvert into CSCs.

The dynamics in CSC plasticity supports the fact that the CSC and non-CSC states are not permanent, but are instead transitory and can regulate the equilibrium in the proportions of cellular states [95]. Based on this concept, the conversion of non-CSCs into CSCs may account for another way of resistance to therapy. Indeed, according to the original interpretation of the relapse process, non-CSCs were killed by the therapy, whereas pre-existing CSCs could survive the treatment and re-populate the tumor. However, recent evidence suggests that chemotherapy and radiotherapy can induce the *de novo*

generation of cells with CSC properties, by causing the transition of non-CSCs into drug-tolerant CSC-like cells [96].

These observations sustain a model of acquired and transitory resistance to therapy, a concept that has to be taken into consideration for the therapeutic targeting of CSCs. It is therefore of fundamental importance to consider targeting the CSC plasticity processes, rather than merely the CSC properties.

3.3 Breast cancer stem cells

Breast cancer stem cells (BCSCs) were first identified and isolated about 15 years ago when Al-Hajj and colleagues isolated a subpopulation of cells from human breast cancer specimens able to form tumors in mice. They showed that a small amount of these cells, identified by flow cytometry fractionation based on cell surface markers expression, was able to originate a tumor when injected into the mammary fat pads of non-obese diabetic/severe combined immunodeficiency (NOD/SCID) mice. Moreover, the tumors initiated by this population of tumor-initiating cells were able to reproduce the heterogeneity found in the original tumor [97]. The isolation of this sub-population was based on the detectable expression of CD44 and the low expression of CD24 surface markers ($CD44^{+}/CD24^{low/-}$), which are still nowadays reliable markers for the identification of breast cancer stem cells.

The identification, isolation, and characterization of CSCs have always been a challenging factor, given the fact that CSCs usually constitute a very small fraction of the total population of cells within the tumor and can express the same surface markers of non-stem cancer cells. It is thus of fundamental importance to define specific CSCs markers, which can be very diverse in different tumor types and should also consider the heterogeneity of tumors, in particular for very heterogeneous tumors such as breast cancer [98].

Breast cancer stem cells research has now identified several putative markers to accurately identify BCSCs; most of those are surface markers, which do not only contribute to cell interactions, but also provide them with peculiar features. The most well-accepted surface markers for BCSCs are still CD44 and CD24, but other surface markers used for BCSCs isolation include CD133, EpCAM, CD49f, CD29, CD133/2 and CD61 [99].

CD44 is a cell surface glycoprotein acting as a specific receptor for hyaluronan. Moreover, CD44 can mediate cell-cell and cell-matrix interactions by also interacting with osteopontin, collagens and matrix metalloproteinases, thereby affecting cell adhesion, migration, and invasion, but also proliferation and tumor angiogenesis, resulting in tumor progression [100,101]. CD24 is also a surface glycoprotein involved in modulation of growth which can play a role in cell differentiation [102].

Another recently recognized marker for BCSCs is the aldehyde dehydrogenase (ALDH), which is a family of cytosolic enzymes responsible for the detoxification by oxidation of intracellular aldehydes and are involved in the retinol to retinoic acid oxidation during stem cells differentiation [103]. ALDH family is composed of nineteen members, of which four (ALDH1A1, ALDH1A2, ALDH1A3, ALDH8A1) can interfere with retinoic acid signaling, which has been shown to negatively interfere with BCSCs [104]. A standard method to measure ALDH activity, and thus to analyze the BCSCs sub-population, uses ALDEFLUOR assay, a non-immunological fluorescence system (see Methods section for details).

However, $CD44^{+}/CD24^{low/-}$ BCSCs can overlap only partially with $ALDH^{+}$ BCSCs, and present different properties. Liu *et al.* recently demonstrated that BCSCs exist in two distinct states: a mesenchymal-like and an epithelial-like state [105]. $CD44^{+}/CD24^{low/-}$ cells belong to the mesenchymal-like BCSCs, are primarily quiescent, highly invasive and are localized at the tumor invasive front. Conversely, the $ALDH^{+}$ cells are the epithelial-like BCSCs, are highly proliferative, characterized by the expression of epithelial markers and are localized more centrally within the tumor mass [105] (Figure V). This model can somehow explain the

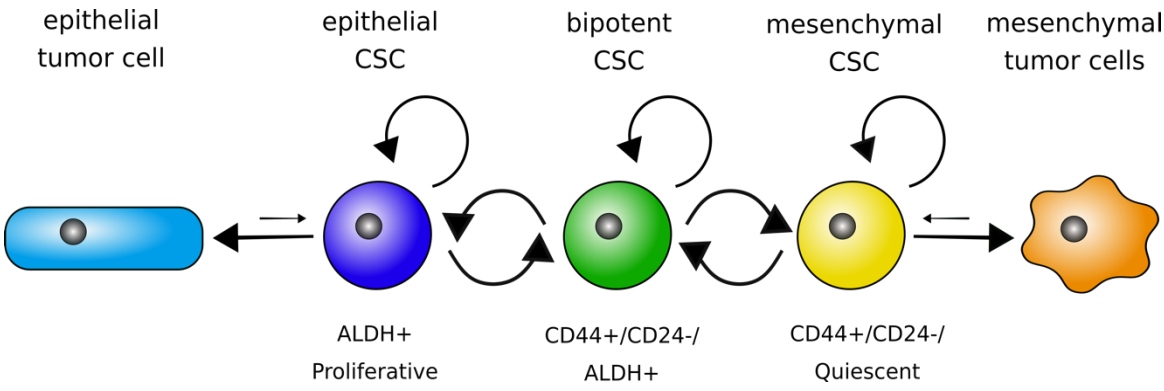

Figure V. Model of the epithelial and mesenchymal breast cancer stem cells switch suggested by Liu and colleagues. According to this model we can distinguish between different types of BCSCs based on the expression of the CD44/CD24/ALDH markers. These states are dynamic and cells can interconvert between the different states, giving origin to either epithelial-like or mesenchymal-like breast cancer cells.

contradictory data about CSCs and the EMT state, as some studies suggest a commonality between the two states [106], whereas others suggest that these processes are mutually exclusive [107], and this is a further proof of cancer stem cell plasticity in BC, as BCSCs can switch between the two states.

Given the contradictory data regarding BCSCs makers, another option to identify and isolate cancer stem cells is based on their self-renew capability. Commonly used methods measure their clonogenic potential in vitro or their ability to form mammospheres, which are single cell-derived clumps of mammary cells generated by clonal expansion when cells are grown in non-adherent and non-differentiating conditions [108].

Testing the BCSCs activity *in vivo* is usually achieved by xenotransplantation of the cells into immune-compromised mice and, in particular, by their ability to generate serially transplantable tumors [98].

Regarding the molecular mechanisms involved in breast cancer stem cells maintenance, several pathways and proteins have been shown being often deregulated in these cells. The Wnt, Notch, and Hedgehog pathways are among the most well characterized, however also the transcription factors associated with embryonal stemness have been related to BCSCs activity [109]. However, the Wnt, Notch, and Hedgehog pathways can be regulated by several signaling cascades, which have also been involved in breast cancer stem cells maintenance, such as NF-κB, TGF-β, JAK/STAT, PI3K/AKT, and MAPK pathways. Understanding the molecular determinants in both breast cancer stem cells maintenance and plasticity is of fundamental importance, as it can allow the development of CSCs direct targeting, thereby paving the way to overcome chemotherapy and radiotherapy resistance and avoid subsequent tumor relapse.

In this work, we identified ETV7 as a novel factor involved in breast cancer stem cells plasticity and its associated chemoresistance.

4. ETV7

4.1 The ETS family of transcription factors

ETV7, also called TEL2 or TELB, is a member of the large family of ETS (E26 Transforming Specific) transcription factors, whose members can regulate the expression of genes

involved in various processes, such as development, differentiation, cell proliferation, migration, and apoptosis.

Given their role in essential cellular functions, their dysregulation can result in severe impairments within the cell, as demonstrated by the involvement of ETS factors in various diseases. In particular, many ETS factors have been associated with cancer initiation, transformation and metastatic spread [110]. ETS transcription factors are mainly involved in oncogenesis, however, some of them can also act as tumor suppressor genes [111].

There are several mechanisms by which ETS can mediate oncogenesis. Tumorigenesis can be caused by ETS hyper-activation by mRNA/protein over-expression or gene amplification, which are frequently observed in breast, prostate and hematological cancers. Several ETS factors, including ELF3, PEA3, ETS-1, ETS-2, and ELF5 have been shown to be up-regulated in tumor tissues and were associated with poor prognosis by affecting the expression of HER2/NEU, UPA, MMPs, MET, BCL2, VEGF and Survivin, oncogenes that regulate transformation, proliferation, migration, invasion, angiogenesis and apoptosis [112].

The most common mechanisms of ETS activation in hematological cancers is the process of gene fusion caused by chromosomal translocation, which usually involves the fusion of TEL (ETV6) with different partners, such as AML1, EVI1, TRKc, ABL and JAK2 [110]. Gene fusions involving ETS factors are instead rarer in solid cancer, except for prostate cancer, with ERG and ETV1 commonly rearranged, and Ewing sarcoma, which usually involves EWS gene fusion [113].

ETS-mediated oncogenesis can also be initiated by cytoplasmic localization of ETS factors [114] or by their expression in the stromal tissue, which can contribute to cancer progression by stimulating tumor growth and promoting angiogenesis, invasion and metastasis [115].

ETS factors can also exert oncogenic functions by gaining transcriptional activity through the binding to genome regulatory regions undergone *cis*-acting mutations, as seen for example for telomerase reverse transcriptase (TERT), which can frequently harbor mutations generating an ETS-binding site in its promoter [116].

Furthermore, ETS proteins can also gain increased transcription activity due to post-translational modification, protein-protein interaction or protein stabilization, or can switch their functions from activator to repressor and vice versa [110].

The ETS family is one of the largest family of TFs and include 27 genes in humans, which can be structurally characterized into 11 subfamilies: ETS, ERG, ELG, ELF, ESE, ERF, PEA3, SPI, TCF, PDEF, and TEL, to which belong ETV6 and ETV7 [117].

4.2 ETV7 structure and function

All the ETS proteins share a conserved helix-turn-helix DNA binding domain of about 85 amino acids called ETS domain, which binds to a consensus purine-rich 5'-GGA(A/T)-3' motif in the regulatory regions of target genes [118].

ETV7 was recently isolated and shown to be highly related to TEL/ETV6, the only other characterized member of the TEL subfamily. ETV7 and ETV6 both act as transcriptional repressors, they bind similar DNA sequences, and can directly interact; however, they play separate biological functions [119].

Also their structure is very similar, as they both contain an N-terminal pointed (PNT) domain, a central domain, and the following ETS domain. Given the presence of the PNT domain, which is a protein-protein interaction domain required for the formation of homo-/heterodimers or oligomers and involved in transcriptional repression, ETV7 can either self-associate or form hetero-dimers/oligomers with ETV6, which indeed also acts as transcriptional repressor [120]. The central domain is less conserved and has been shown to be the main contributor to the repressor activity of TEL factors [121], whereas the ETS domain is highly conserved (>85% identity) and can strongly bind to a core "ccGGAAgt" sequence [118] (Figure VI).

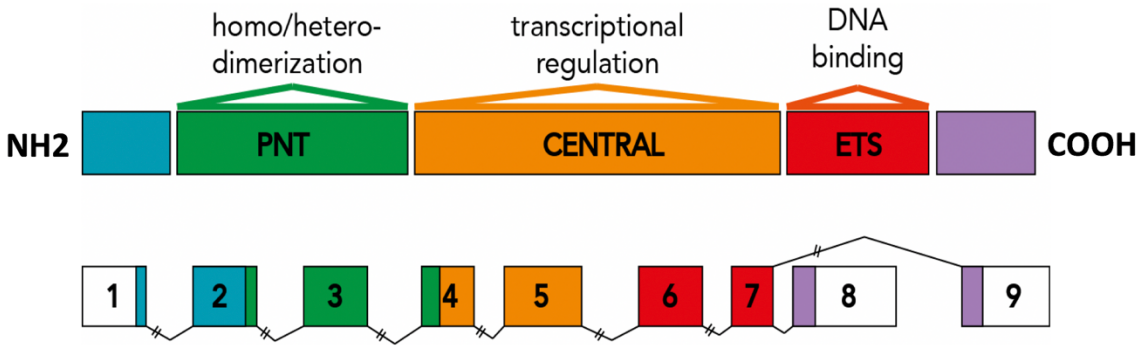

Figure VI. The structure of ETV7 gene and the encoded proteins. A schematic representation of the ETV7 gene with numbered boxes corresponding to exons, which are shaded according to the corresponding domains on the encoded ETV7 protein, whose function is shown above.

Despite their high similarity, these two proteins exert different biological effects. For example, ETV6 has been shown to inhibit colony formation, whereas ETV7 stimulates it [122]. In contrast to ETV6, which is ubiquitously expressed, ETV7 expression is low in most of the tissues but significantly higher in the hematopoietic ones [123].

The regulatory mechanisms mediating ETV7 expression are still to be uncovered; however, the presence of alternative isoforms may remove putative MAPK phosphorylation sites within the PNT domain, suggesting possible regulation from the MAPK pathway. Indeed, *ETV7* gene can encode six differentially expressed alternative splicing isoforms, which can vary in the N-terminal PNT domain or in the C-terminal, possibly altering the regulation of their expression [124].

In a previous study, it was observed the synergistic induction of ETV7 in cancer cells treated with a combination of Doxorubicin and the inflammatory cytokine TNFα and reported p53 and NF-κB as direct regulators of ETV7 [125]. *ETV7* is also recognized as an Interferon-stimulated gene (ISG), as its expression was shown to be induced by type I, type II and type III IFN treatment in different cell types [126–129]. Moreover, ETV7 was up-regulated in hESCs-derived hepatocytes infected with Hepatitis C Virus (HCV) [130], suggesting a possible role for ETV7 in antiviral immunity.

The roles of ETV7 are still poorly understood and studied, partially because of the absence of *ETV7* gene in most rodent species, including mice [131]. However, several studies highlighted multiple roles for ETV7 in hematopoiesis. For examples, the over-expression of ETV7 in both human and mice hematopoietic stem cells (HSCs) could increase the proliferation and deplete HSCs [132]. Moreover, ETV7 over-expression in human U937 cells was shown to impede monocytic differentiation [122].

4.3 ETV7 roles in cancer

The human *ETV7* gene is located within the MHC cluster region at chromosome 6p21, a region that has been involved in a variety of different cancers, such as B-cell non-Hodgkin's lymphomas, cervical cancer, non-small cell lung carcinomas, ovarian and breast carcinomas [133]. However, the role of ETV7 in cancer has been poorly investigated.

Elevated ETV7 expression has been associated with several tumor types. In particular, the analysis of ETV7 expression in cancer revealed its up-regulation in 70% of ALL and AML

samples [134] and 48% of pediatric solid tumor xenografts [135]. Among solid tumors, ETV7 was shown to be 1 of the 10 most frequently up-regulated proteins in hepatocellular carcinoma [136] and was found to be up-regulated in 85% of medulloblastoma cases [137]. Recently, Piggin and colleagues reported an average higher level of ETV7 expression in tissues from all the breast cancer subtypes compared to normal breast tissues, with a correlation of ETV7 expression and breast cancer aggressiveness [138].

ETV7 was shown to cooperate with Eμ-MYC in promoting B-lymphomagenesis and Myc-induced apoptosis inhibition and exhibited pro-proliferative and anti-differentiation functions in myeloid and lymphoid cells [139]. Moreover, forced expression of ETV7 in mouse bone marrow was shown to cause myeloproliferative diseases, even if with a long latency, and the treatment with DNA-damaging agents greatly accelerated the tumor development, suggesting *TEL2* as a bona fide oncogene [134]. Besides, the crossing of the latest established ETV7 transgenic mouse model with an established leukemic mouse model revealed a remarkable acceleration in $Pten^{-/-}$ leukemogenesis [140].

Further evidence supporting ETV7 pro-tumorigenic functions comes from the recent identification of a transcriptional-independent activity of ETV7, which was shown to physically interact with mTOR into the cytoplasm generating a novel complex called mTORC3, which contributes to resistance to rapamycin, an mTOR-targeting anti-cancer agent [137].

In contrast, ETV7 was shown to act as tumor suppressor in nasopharyngeal carcinoma by repression of SERPINE1 gene expression [141], and its down-regulation was observed in drug-resistant cancer cells [142].

In this work, we observed that the expression of ETV7 can affect the breast cancer stem-like cell plasticity and that this effect can be reverted by Interferon treatment. Moreover, we observed that ETV7 can mediate the repression of a signature of Interferon-stimulated genes (ISGs). Thus, being ETV7 an ISG itself, we speculate that ETV7 may play a role in the negative feedback regulation of the IFN response.

5. Interferon and interferon response

5.1 Interferon (IFN)

The Interferons (IFNs) are heterogeneous glycoproteins with an antiviral activity which are secreted by cells in response to different stimuli [143]. IFNs were first recognized in 1957, when Isaacs and Lindenmann, studying the process known as viral interference, discovered a secreted factor able to protect the cells from viral infection, from which the name "Interferon" [144]. Viral interference refers to the fact that some cells, after being infected with a virus, can develop resistance to subsequent infections by the same or by similar viruses [145]. The discovery of IFNs also represented the first identification of cytokines; moreover, among these, IFNs were the first used therapeutically [146]. Indeed, given their ability to modulate the immune response, IFNs have been widely used for the treatment of viral infection, such as HCV and HBV infections [147].

IFNs are members of class II family of α-helical cytokines, and, based on the structure of their receptors, are classified into three types: type I IFN, type II IFN and the most recently identified type III IFN (or IFN-like proteins) [147].

Type I IFNs signal by binding to the dimeric IFN-α/β receptor called IFNAR, constituted by IFNAR1 and IFNAR2, and in humans comprise at least 12 IFN-α species (encoded by 14 genes), and a single species of IFN-β, IFN-κ, IFN-ω and IFN-ε [148].

Type II IFNs include a single known subtype, which is IFN-γ, that exerts its action by binding to the tetrameric IFN-γ receptor (IFNGR) composed by 2 subunits, IFNGR1 and 2 of IFNGR2 [149].

Type III IFNs include 4 known subtypes (IFN-λ1, -λ2, -λ3 and -λ4), which activate the IFN-λ receptor (IFNLR), a heterodimeric complex formed by IFNLR1 and IL10RB [150].

Despite, their common ability to inhibit virus replication of infected cells, the different IFNs types can exert distinct functions, which are mainly based on their (or their receptors') differential cell- and tissue-expression, and their different activation of signal transduction pathways, that drive the expression of different groups of Interferon-stimulated genes (ISGs) [149]. Indeed, IFNs and their receptors are not expressed by all the cell types. For example, plasmacytoid dendritic cells (pDCs) are the major producers of IFN-α in response to microbial infection [151], IFN-γ is produced by other cells of the immune

system (e.g., natural killer cells, natural killer T-cells, B-cells and antigen presenting cells) [150], IFN-ε is expressed in the female reproductive tract [152], IFNAR is ubiquitously expressed, whereas IFNLR subunits are produced mainly in cells of epithelial origins and hepatocytes [149,153]. Moreover, different IFNs types regulate the expression of different sets of ISGs, either through the activation of various intracellular signaling pathways by the different receptors or by the cell type-specific expression of additional transcription factors [149].

5.2 IFN signaling pathway

All the IFNs, by binding to their receptors on the cell surface membrane, transmit the signal into the cell through the JAK-STAT signaling pathway, finally resulting in ISGs transcription [154]. However, IFNs can bind with different affinity to their receptors, causing quantitative differences in the activation of the JAK-STAT pathway, which may partially explain the different biological outcomes observed [155].

In normal conditions, the cytoplasmic domains of IFN receptor chains are bound to inactive JAK proteins, but, when IFN binds to the receptor, the conformational changes of the receptor bring the cytoplasmic chains nearby, allowing JAKs trans-phosphorylation and activation [154]. Subsequently, JAKs can phosphorylate the IFN receptor chains causing the binding or repositioning of STAT proteins, which are then phosphorylated on conserved tyrosine residues by the receptor [156]. STATs phosphorylation causes conformational changes resulting in their release from the receptor, the formation of homo- or heterodimers and their translocation into the nucleus, where they can activate ISGs transcription [157,158].

Signal Transducers and Activators of Transcription (STAT) proteins include 7 members in mammals, all of which can play some functions in the innate immune response. However, STAT1 and STAT2 are the most important in the regulation of IFN signaling [154].

The binding to type II IFN receptor drives the phosphorylation of STAT1 on tyrosine 701, with subsequent homo-dimerization and nuclear translocation [159]. Once in the nucleus, STAT1 homo-dimers bind to gamma-activated sequence (GAS) elements upstream IFN-γ induced genes, activating their transcription [160].

On the other hand, type I and type III IFNs receptor activation causes the phosphorylation of both STAT1 and STAT2, which leads to their hetero-dimerization and interaction with

the IFN regulatory factor 9 (IRF9), forming a complex called ISGF3 [161]. ISGF3 can translocate to the nucleus where it binds to IFN-stimulated regulatory elements (ISREs) upstream type I or type III ISGs, inducing their transcription [162]. Alternatively, IFNs can induce the phosphorylation and homo-dimerization of STAT3, which can regulate the transcription of genes containing the enhancer sequence STAT3-binding element [147].

Additionally, IFNs can exert their activity via other members of the STAT family or by other pathways, such as the PI3K/AKT pathway, NF-κB pathway and the RAS/MAPK pathway [143].

The regulation of IFN signaling is tuned by many different mechanisms, such as post-translational modification (e.g., acetylation, methylation, SUMOylation or palmitoylation) and by the modulation of IFN receptors mRNA splice variants [149].

Moreover, negative feedback regulatory mechanisms are essential for attenuating the IFN response and are mainly mediated by two families of proteins: suppressor of cytokine signaling (SOCS) and protein inhibitors of activated STATs (PIAS). Furthermore, also the ubiquitin-proteasome pathway has been reported to negatively regulate STATs activity [143].

5.3 IFN biological activities and roles in cancer

The main and defining function of IFNs is the establishment of a state of resistance to viral infectivity in the target cells by blocking or impairing viral replication. This activity is achieved through the induction of proteins which can inhibit any stage of viral replication, including entry, transcription, RNA stability, translation, maturation, assembly and release [163].

Moreover, increased interest in IFN study was acquired when Gresser and colleagues showed that Interferon was able to suppress the growth of tumors *in vivo* [164]. Since then, many studies revealed that IFNs could play pleiotropic functions through the activation of ISGs. IFNs were shown to play a central role in innate and adaptive immunity, to regulate cell cycle, angiogenesis, hematopoiesis, to increase the expression of tumor-associated cell surface antigens and MHC class I and II antigens, to induce the expression of pro-apoptotic genes and proteins (e.g. BAK, BAX, Caspases, TRAIL), to repress anti-apoptotic proteins (e.g. BCL-2 and IAP) and to modulate the differentiation [148,165].

These functions make IFN a promising factor for the treatment of various diseases, including cancer; and its use has already been approved for the treatment of several cancer types, such as hairy cell leukemia, malignant melanoma, follicular lymphoma, bladder and renal cancer [165].

However, IFNs can play opposing functions in cancer, as it can be both immunostimulatory or immunosuppressive. The factors driving IFN activity towards the stimulation or suppression of immunity in cancer are still not completely understood. However, these factors include the type of cells targeted with IFNs (cancer cells vs. immune cells), the stimulus inducing IFN signaling, its timing and the ISGs expressed [166]. IFN signaling has also been involved in the resistance to cancer therapy, in which again it can play opposing activities. ISGs signatures related to IFN signaling are widely expressed in various human tumors, and have been shown to predict therapy response; however, different studies associated it with either good or poor response [167–171].

IFN plays a central role in the induction of immunogenic cell death (ICD), a type of death of tumor cells occurring when the therapy generates an immune-dependent response and immunological memory [172]. Recent evidence suggested that DNA damage can result in IFN-driven immune modulation, as DNA damage-associated single-stranded DNA can be sensed by cytoplasmic DNA sensors (e.g., cytosolic DNA sensor cyclic GMP-AMP synthase - cGAS), that activate STING, which can induce IFN production [173]. In this way, IFN activated by DNA damaging therapy can contribute to immune-recognition of cancer cells and their removal, reinforcing the therapy action.

On the other side, some studies showed that IFNs could also have detrimental effects, as they can promote tumor growth. For example, low dose or autocrine exposure to IFN-γ in melanoma and breast cancer cells were shown to enhance their metastatic ability and caused resistance to natural killer cells [174,175].

Despite the recognized central role of IFNs in the regulation of cell intrinsic, extrinsic and immune-mediated effects of tumor therapy response, the complexity of IFN functions in cancer still needs to be completely understood, and further studies are needed to better understand its opposing functions.

PREFACE

Preliminary work in the laboratory showed that the combined treatment with Doxorubicin and TNFα in the breast cancer cell line MCF7 was able to increase the migration capabilities of the cells and to induce the synergistic up-regulation of a signature of genes, which was shown to have prognostic value in breast cancer patients data [125]. Among the top synergistically up-regulated genes we identified ETV7, a poorly studied transcription factor with demonstrated pro-tumorigenic functions in hematological malignancies [134]. The synergistic effect of Doxorubicin and TNFα on ETV7 expression was further confirmed in various other breast and non-breast cancer cell lines and, along with LAMP3 (a lysosome-associated membrane protein), was one of the most conserved synergistically up-regulated genes tested. Moreover, ETV7 expression was recently shown to be higher in cancer tissues compared to normal tissues in breast cancer patients [138], suggesting a possible involvement of ETV7 in breast cancer pathogenesis.

Given these preliminary works, the few literature data regarding ETV7, and in particular the absence of studies focusing on its impact in breast cancer, we decided to explore the roles and functions of ETV7 in this cancer type.

Therefore, this work aims to characterize the effects of the increased ETV7 expression in breast cancer, particularly focusing on its pro-tumorigenic functions and its involvement in the resistance to cancer therapy.

RESULTS

This section of the thesis presents the results I obtained during my doctoral studies, and it is divided into three chapters.

In the first chapter, I will present my contribution to the published manuscript attached in Annex I (Alessandrini, Pezzè *et al.*, 2018), implemented with some unpublished data. In this study we uncovered a novel mechanism mediating the ETV7-dependent resistance to Doxorubicin in breast cancer cells; we suggested this effect involves the repression of *DNAJC15* gene.

In the second part of this project (manuscript in preparation), I will describe the impact of ETV7 increased expression on the resistance to other conventional treatments for breast cancer (i.e., 5-FU and radiotherapy) and its involvement in cancer stem cell-like plasticity in breast cancer. We also investigated genome-wide the pathways regulated by ETV7 and shortlisted a group of ETV7 targets possibly responsible for the observed effects.

In the last chapter, I will present some preliminary results regarding the role of ETV7 in the survival of breast cancer cells and the involvement of p53 in the cell death associated with reduced expression levels of ETV7.

1. ETV7 promotes the resistance to Doxorubicin via DNAJC15 repression

1.1 ETV7 is activated in response to Doxorubicin and other DNA damaging agents in MCF7 cells

Given the previously observed induction of ETV7 expression following Doxorubicin treatment in MCF7 cells [125], we first tested a panel of cytotoxic drugs in order to evaluate the differential expression of ETV7 in response to different stimuli in this breast cancer-derived cell line (Figure 1). We observed a significant induction of ETV7 expression with most of the drugs, especially the DNA damaging agents (Doxorubicin, 5-FU, Camptothecin,

and Etoposide), among which Doxorubicin was the most effective inducer of ETV7 expression. Also, the treatment with Paclitaxel (a mitotic inhibitor), and Nutlin-3a (a specific activator of p53) could trigger an increase in ETV7 levels, while Everolimus (an mTOR inhibitor), Imatinib (a tyrosine kinase inhibitor) and Tamoxifen (an estrogen modulator) had no significant effect on its mRNA expression.

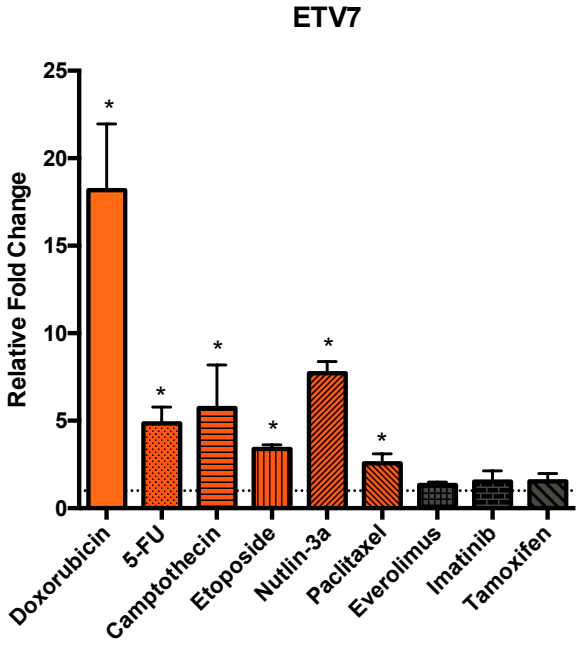

Figure 1. *The expression of ETV7 is induced by several DNA damaging agents.* RT-qPCR analysis of ETV7 expression in MCF7 cells treated with different chemotherapeutic agents for 24 hours. Bars represent average Fold Change relative to untreated control and standard deviations of at least three biological replicates. * = p-value < 0.01.

1.2 The over-expression of ETV7 induces increased resistance to Doxorubicin

In order to investigate the effects of ETV7 induction upon the treatment with chemotherapeutics, we tested whether the altered expression of ETV7 could affect the sensitivity of the cells to these drugs. In particular, in this first part of the work, we focused on Doxorubicin, which was the strongest inducer of ETV7 expression.

To accomplish this task, we first generated MCF7 cells stably over-expressing ETV7 by transfecting either the empty vector (pCMV6-Entry plasmid) or the vector carrying ETV7 cDNA (pCMV6-ETV7 plasmid). We thus obtained cells from now on referred to as “MCF7 Empty” and “MCF7 ETV7”, whose ETV7 expression was tested by western blot analysis (Figure 2A).

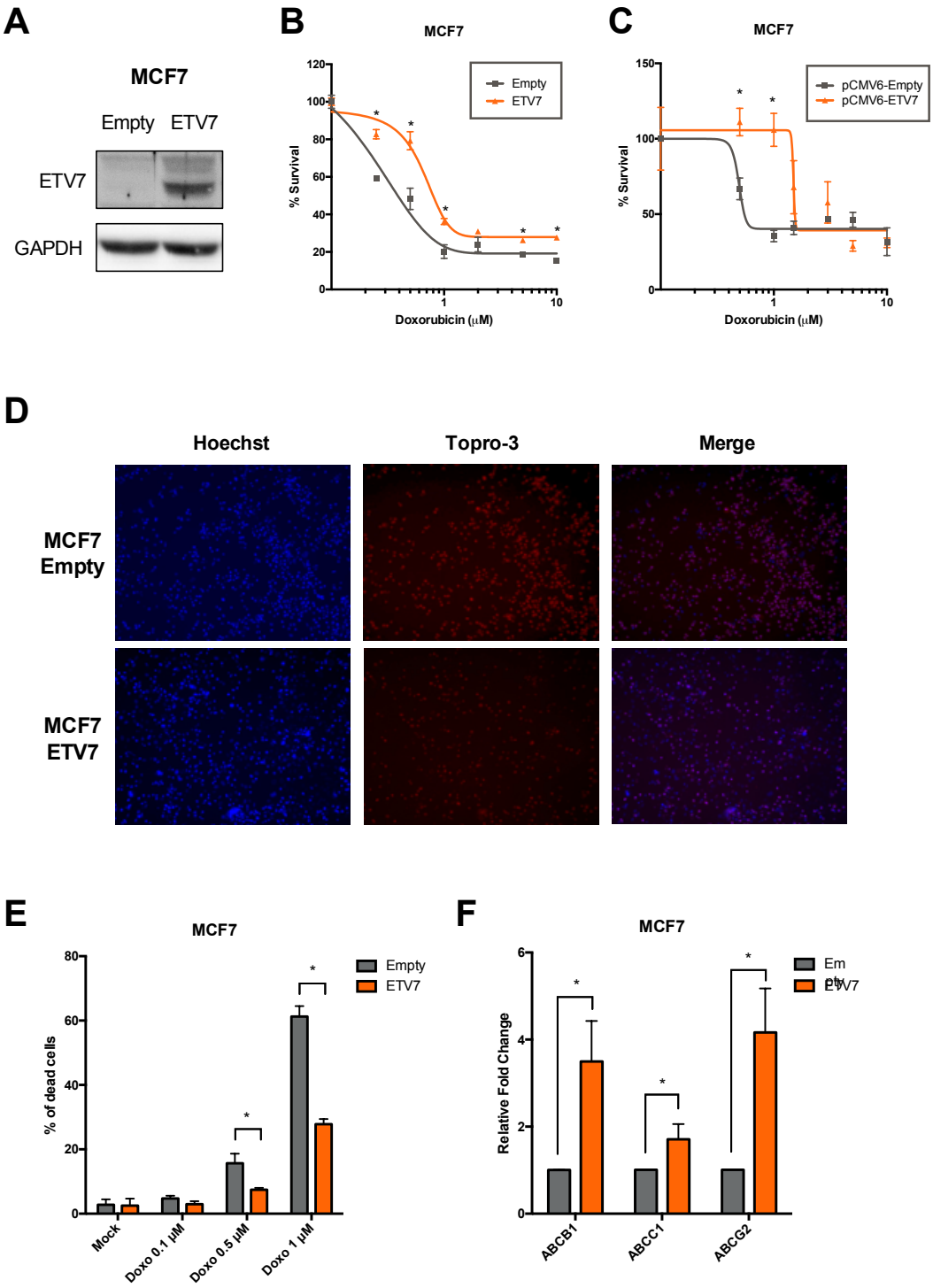

Figure 2. *ETV7 triggers breast cancer resistance to Doxorubicin*. A) Western blot analysis demonstrating the over-expression of ETV7 in MCF7 cells. B) MTT Assays for survival analysis upon Doxorubicin treatment in MCF7 cells over-expressing ETV7 and their empty control. Each dot corresponds to a. tested dose of Doxorubicin. C) MTT Assays for survival analysis upon Doxorubicin treatment in MCF7 cells transiently transfected with plasmid over-expressing ETV7 or their empty control. Each dot corresponds to a tested dose of Doxorubicin. D-E) Cell death analysis of Doxorubicin treated (three different doses) MCF7 Empty and ETV7 cells. A representative image of cells treated with Doxorubicin 0.5 μM is shown in panel D, and the percentage of dead cells (panel E) was obtained through fluorescence studies (at Operetta, Perkin Elmer) calculated as the ratio between the amount of Topro-3 positive cells (dead cells) and the total number of cells (Hoechst 33342 positive cells). A merged image with overlapping fluorescent signal is shown on the right. F) RT-qPCR analysis of ABCB1, ABCC1 and ABCG2 expression in MCF7 Empty and ETV7. Bars represent the average Fold Change relative to the untreated control and the standard deviations of at least three biological replicates. * = p-value < 0.01.

In the following step, we analyzed the sensitivity of these cells to Doxorubicin by measuring cell viability via MTT assay, showing that ETV7 over-expression could exert a protective role against Doxorubicin toxicity (Figure 2B). We then confirmed that the observed effect is truly dependent on ETV7 expression by testing the viability of MCF7 cells upon Doxorubicin treatment following transient transfection with ETV7 over-expressing plasmid and their relative control (Figure 2C). We further tested the effect of ETV7 expression on Doxorubicin-induced cell death by using the cell-impermeable dye Topro-3, which can permeate only in dying or dead cells. By image analysis of Topro-3 and Hoechst 33342 stained cells, we measured the percentage of cell death, and we confirmed that the over-expression of ETV7 remarkably reduced the sensitivity of MCF7 cells to Doxorubicin treatment (Figure 2D and 2E).

Since drug efflux mediated by ABC transporters is one of the most common mechanisms responsible for increased chemoresistance, we tested the expression of some of the ABC family members which are more commonly deregulated in chemoresistant breast cancers: ABCB1/PgP, ABCC1/MRP1, and ABCG2/BCRP. Noteworthy, we observed a significant up-regulation of the three ABC transporters at the transcript levels, with ABCB1 and ABCG2 induced more than 3-fold (Figure 2F), suggesting that ETV7-dependent resistance to Doxorubicin could be mediated by the regulation of ABC transporters.

1.3 DNAJC15 as a possible target for ETV7-mediated Doxorubicin resistance

In order to identify a possible mechanism by which the over-expression of ETV7 could decrease the sensitivity of the cells to Doxorubicin, we looked for its putative targets by analyzing the previously cited microarray data obtained in our lab on MCF7 cells treated with Doxorubicin [125]. Being ETV7 a transcriptional repressor, we focused our search on genes whose repression was already known to be involved in the resistance to Doxorubicin in breast cancer cells. In particular, we considered a short list of genes obtained from a recent study by Boettcher and colleagues [176], whose hyper-methylation, and subsequent repression correlated with Doxorubicin resistance in breast cancer, which included *BRCA1, ESR1, DNAJC15, CDH1, RAB6C,* and *SULF2*. Since Doxorubicin strongly activated the expression of ETV7, we expected to observe a significant down-regulation of ETV7 putative targets under the same treatment condition. Out of the six genes

mentioned above, three of them, DNAJC15, BRCA1, and ESR1 were down-regulated upon Doxorubicin treatment in MCF7 cells, whereas an induction or no significant effects were observed for CDH1 and RAB6C, and SULF2 (Figure 3A). Furthermore, we found that most of the DNAJC family members were down-regulated upon Doxorubicin treatment in MCF7 cells (Figure 3B). We then validated some of the highly down-regulated members of DNAJC family by RT-qPCR in Doxorubicin-treated MCF7 cells, and we confirmed the repression of DNAJC2, C7, C14, C15, and C17 upon Doxorubicin treatment (Figure 3C).

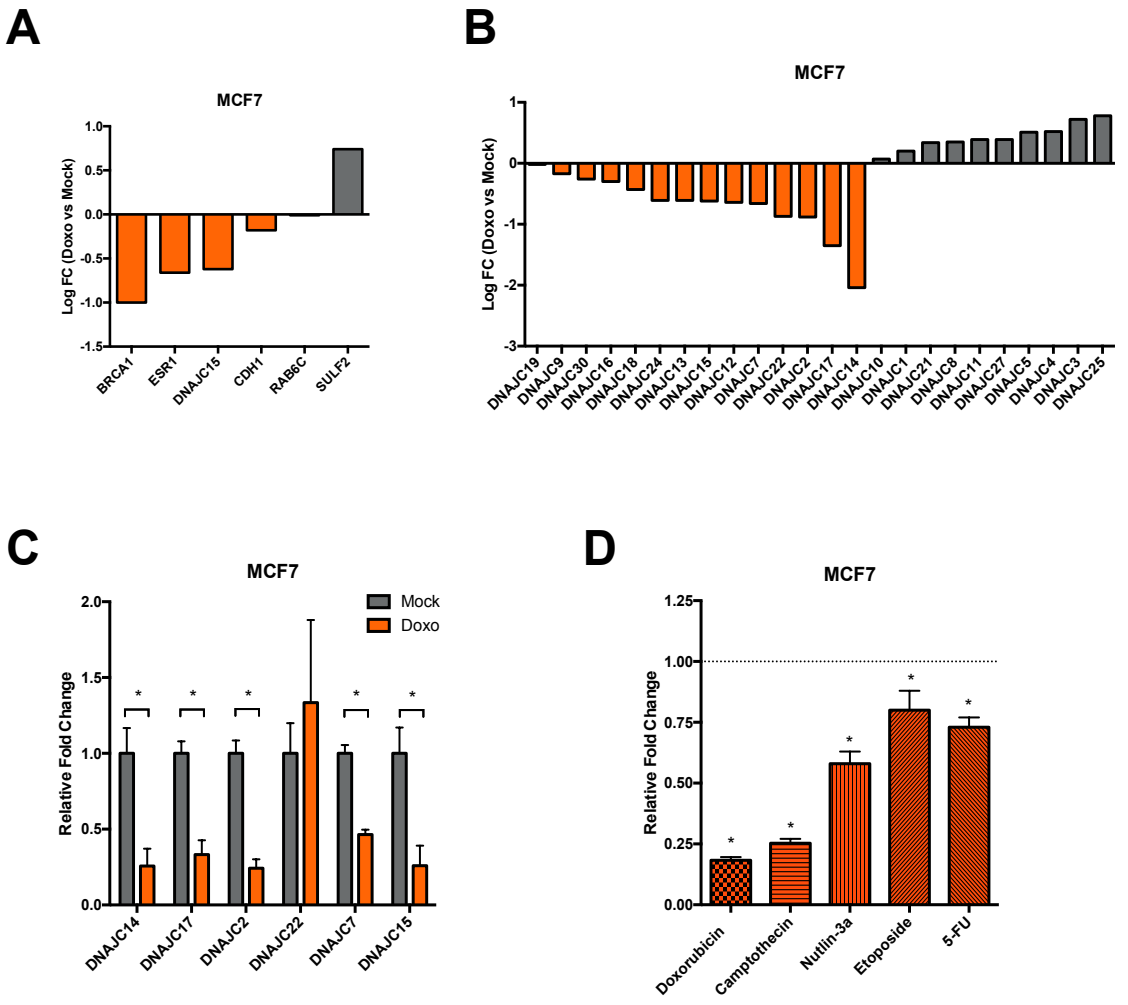

Figure 3. *Identification of DNAJC15 as a putative target of ETV7.* A-B) Expression values from microarray data previously obtained by our group from MCF7 cells treated with Doxorubicin (GSE24065) of the gene list studied by Boettcher and colleagues (A), and of the DNAJC family members (B). Results are presented as logarithm of Fold Change from Doxorubicin-treated samples calculated over Mock condition. C) RT-qPCR analysis of the expression of a selected group of DNAJC family members in MCF7 cells treated or untreated with Doxorubicin 1.5 μM for 24 hours. D) Expression analysis of DNAJC15 mRNA upon the treatment with different chemotherapeutics for 24 hours in breast cancer-derived MCF7 cells. Bars represent the averages Fold Changes relative to the untreated condition of at least three biological replicates and the standard deviations. * = p-value < 0.01.

Given these observations and the involvement of DNAJC15 in the negative regulation of ABCB1 transcription [177], we decided to focus our attention on DNAJC15 as a putative mediator of the ETV7-dependent resistance to Doxorubicin in breast cancer cells. *DNAJC15* is a tumor suppressor gene belonging to the HSP40/DNAJ family of co-chaperones, mainly contributing to ATP hydrolysis and the consequent activation of the HSP70 chaperone, thus helping in protein folding, trafficking, interaction, import, and export [178,179]. DNAJC15 down-regulation was associated with increased drug resistance in ovarian and breast cancer [180], and Hatle and colleagues showed that the expression of DNAJC15 in the Golgi was responsible for the degradation of some proteins, including the transcription factor c-JUN [181]. Therefore, the inhibition of DNAJC15 in Doxorubicin-resistant MCF7 clones resulted in increased levels of c-JUN protein, which was responsible for an enhanced transcription of the multidrug transporter ABCB1/MDR1 [181]. Other studies reported that DNAJC15 could control the respiratory chain and the production of ROS by localizing into the mitochondrial inner membrane [182].

Moreover, DNAJC15 could exert its tumor suppressor role also by promoting the release of pro-apoptotic molecules through the mitochondrial permeability transition pore complex [183]. We thus extended the analysis of DNAJC15 transcript expression levels to the other DNA damaging agents able to induce expression of ETV7 in MCF7 cells and verified the significant down-regulation of DNAJC15 in response to all of the analyzed agents (Figure 3D).

1.4 ETV7 downregulates the expression of DNAJC15

To test whether DNACJ15 could represent a novel target of ETV7 and whether it could mediate the enhancement in resistance to Doxorubicin in MCF7 cells, we first analyzed the mRNA expression of DNAJC15 in ETV7-over-expressing cells and we could appreciate a slight but significant repression of DNAJC15 in MCF7 ETV7 compared to the Empty control (Figure 4A). The transcriptional repression of DNAJC15 was further confirmed by gene reporter assay performed with a luciferase reporter vector in which a region of *DNAJC15* promoter containing two putative binding sites for ETV7 was cloned. We observed strong repression of luciferase activity in MCF7 ETV7, confirming the transcriptional repression of DNAJC15 (Figure 4B). We then performed site-directed

mutagenesis on the two putative ETV7 binding sites (BS1 and BS2), to test their contribution to the ETV7-dependent down-regulation of DNAJC15. The mutation of ETV7 binding site 1 (BS1 – chr.13: 43'597'329–43'597'335) did not affect the repression of luciferase activity in response to ETV7 over-expression, whereas the disruption of binding site 2 (BS2 – chr.13: 43'597'624–43'597'632) in the *DNAJC15* promoter was able to prevent the inhibition of the luciferase activity induced by ETV7 over-expression, demonstrating the importance of ETV7 binding to this site in the modulation of DNAJC15 transcriptional expression (Figure 4B).

Moreover, we demonstrated the direct binding of ETV7 to the BS2 region within *DNAJC15* promoter by chromatin immunoprecipitation (ChIP) analysis (Figure 4C).

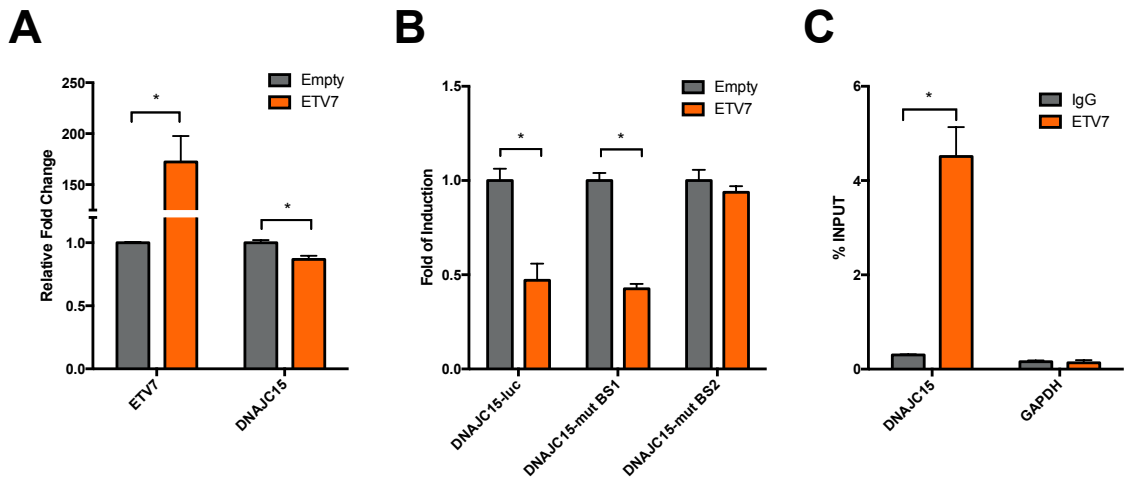

Figure 4. *DNAJC15 is a direct target of ETV7.* A) RT-qPCR analysis to measure the expression levels of ETV7 and DNAJC15 in MCF7 cells transfected with pCMV6-Entry or pCMV6-ETV7 plasmids. B) Gene reporter assay on MCF7 cells over-expressing pCMV6-Entry or pCMV6-ETV7 and transfected with pGL4.26-DNAJC15 reporter plasmid or the pGL4.26-DNAJC15-BS1 or -BS2 plasmids mutated in the putative ETV7 binding sites. Data are normalized using the pRL-SV40 plasmid and data are shown as fold of induction relative to the empty control. C) ChIP-PCR for DNAJC15 and GAPDH (control) promoter regions in MCF7 transfected with pCMV6-ETV7. Shown is the percentage of enrichment of ETV7 or control (IgG) bound to DNAJC15 promoter region in respect to INPUT DNA. For panels A-C, bars represent averages and standard deviations of at least three biological replicates. * = p-value < 0.01.

1.5 The ETV7-mediated repression of DNAJC15 is methylation-dependent

Since DNAJC15 expression is well-recognized for being methylation controlled, and its promoter methylation has been associated with chemoresistance [177], we investigated the methylation status of *DNAJC15* promoter in our context. Thus, we performed genomic DNA bisulfite conversion followed by PCR and sequencing for the analysis of the presence of methylated or un-methylated CpGs within a frequently hypermethylated region of the

DNAJC15 promoter which includes the newly identified ETV7 binding sites. We observed an increase in CpGs methylation of DNAJC15 promoter in response to Doxorubicin treatment, which was even more remarkable in ETV7-over-expressing cells (Figure 5A).

To test the dependency of ETV7-mediated DNAJC15 repression on DNA promoter hyper-methylation, we treated the cells with the DNA methyltransferase (DNMT) inhibitor 5-Aza-2'-deoxycytidine (5-Aza). The treatment with 5-Aza was not able to affect the repression of DNAJC15 expression caused by Doxorubicin treatment (Figure 5B), suggesting that the repression of DNAJC15 expression upon Doxorubicin is only partially dependent on hyper-methylation. The repression of DNAJC15 in ETV7 over-expressing cells was instead reversible by 5-Aza treatment, suggesting that the mechanism of DNAJC15 inhibition mediated by ETV7 involves methylation of the promoter (Figure 5C). Since DNMTs were shown to play key roles in Doxorubicin resistance [184], we hypothesized

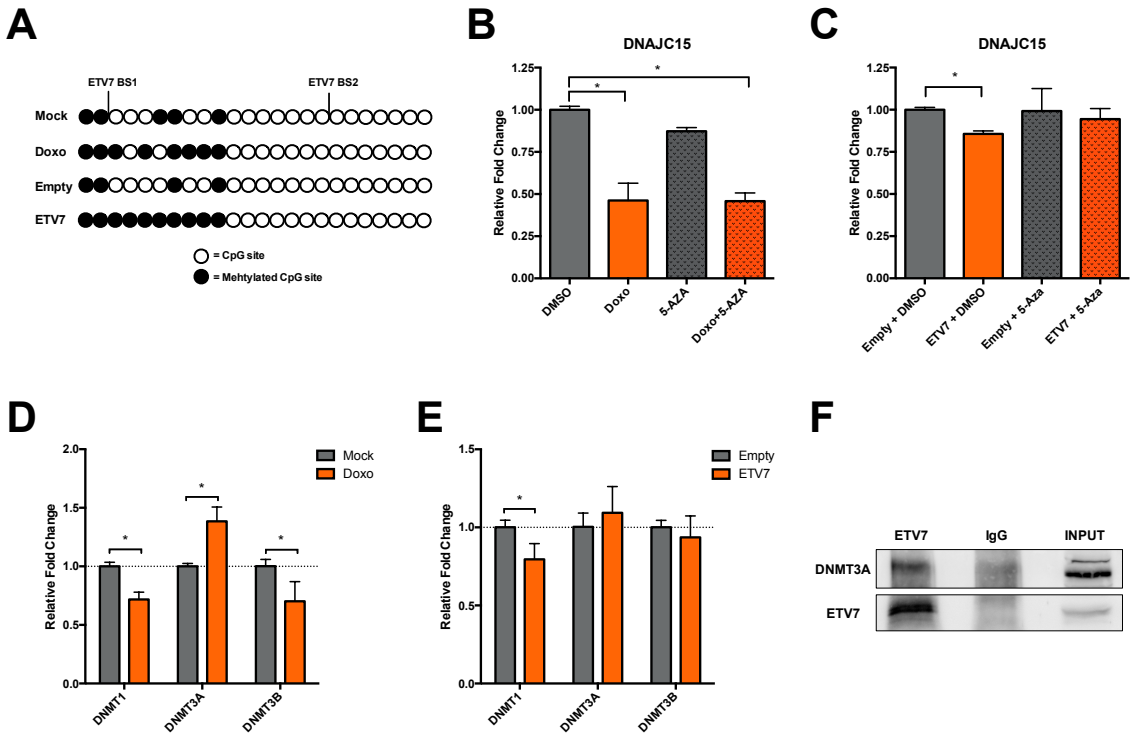

Figure 5. *ETV7 dependent repression of DNAJC15 involves DNA methylation*. A) Methylation status of CpGs within DNAJC15 promoter analyzed by bisulfite conversion followed by PCR and direct sequencing in MCF7 untreated, treated with Doxorubicin for 24 hours or transiently transfected with pCMV6-Entry or pCMV6-ETV7 plasmids for 48 hours. Methylated CpGs are shown as black dots, whereas unmethylated CpGs as white dots. B) RT-qPCR analysis of DNAJC15 expression in MCF7 treated with Doxorubicin for 24 hours and/or DMSO or 5-Aza-2'-deoxycytidine for 48 hours. C) RT-qPCR analysis of DNAJC15 expression in MCF7 transfected with pCMV6-Entry-Empty or pCMV6-Entry-ETV7 and treated with DMSO or 5-Aza-2'-deoxycytidine for 48 hours. D) RT-qPCR analysis of DNMT1, DNMT3A and DNMT3B expression in MCF7 treated with Doxorubicin for 16 hours. E) RT-qPCR analysis of DNMT1, DNMT3A and DNMT3B expression in MCF7 Empty and MCF7 ETV7. F) Western blot of DNMT3A and ETV7 on the immunoprecipitation with an antibody against ETV7 or normal IgG as control and on INPUT lysates in MCF7 transfected with pCMV6-ETV7 plasmid. * = p-value < 0.01

that ETV7 could mediate the repression of the *DNAJC15* promoter by recruiting specific DNMTs responsible for the observed hyper-methylation in ETV7 over-expressing cells. To demonstrate this, we tested whether ETV7 and DNMTs could possibly physically interact. We first analyzed the expression of DNMT1, DNMT3A and DNMT3B genes in Doxorubicin-treated MCF7 cells by RT-qPCR, revealing the up-regulation of the only DNMT3A among these DNMTs, while both DNMT1 and DNMT3B were down-regulated in response to the treatment (Figure 5D). We observed a similar trend for DNMTs expression upon ETV7 over-expression in MCF7 cells, even if only for DNMT1 we could appreciate statistically significant alterations (Figure 5E). Therefore, we hypothesized that DNMT3A might cooperate with ETV7 in DNAJC15 repression. Thus, we tested their putative interaction by immunoprecipitation of ETV7 and we found in ETV7 over-expressing cells that DNMT3A and ETV7 can directly interact (Figure 5F).

1.6 The over-expression of DNAJC15 can partially rescue the ETV7-mediated resistance to Doxorubicin

To finally confirm that the ETV7-mediated Doxorubicin resistance mechanism is, at least partially, dependent on DNAJC15 repression, we over-expressed DNAJC15 in MCF7 ETV7 cells and we analyzed the sensitivity of the cells to Doxorubicin using the MTT assay

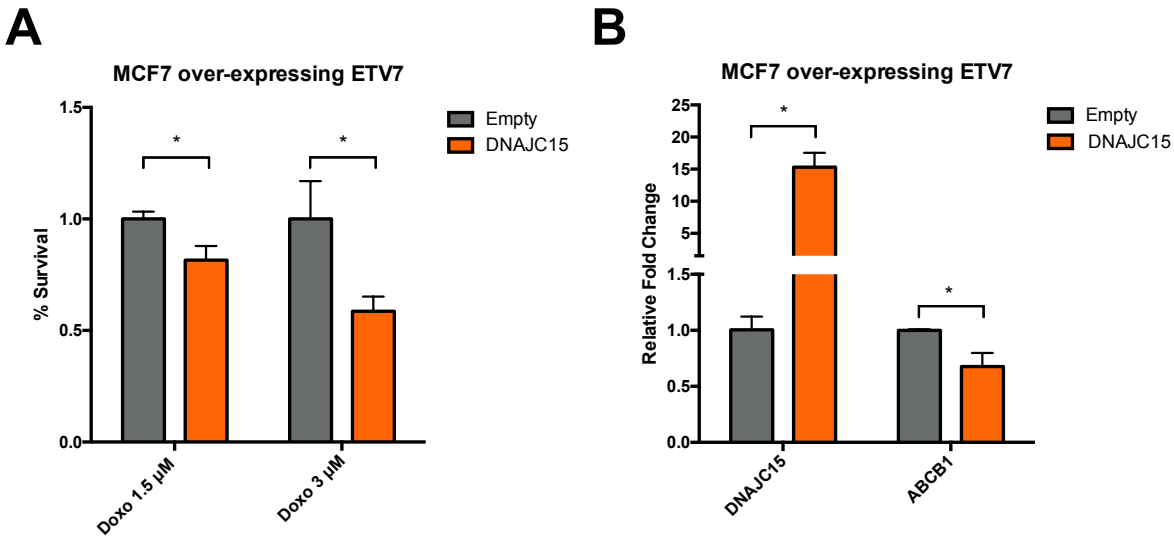

Figure 6. *DNAJC15 over-expression can partially rescue Doxorubicin sensitivity in ETV7-over-expressing cells*. A) MTT Assay in ETV7-over-expressing MCF7 cells transiently transfected with pCMV6-Entry or pCMV6-DNAJC15 plasmids and treated with Doxorubicin 1.5 µM or 3 µM for 72 hours. B) RT-qPCR analysis to measure the expression levels of DNAJC15 and ABCB1 expression in ETV7-over-expressing MCF7 cells transiently transfected with pCMV6-Entry or pCMV6-DNAJC15 plasmids. Bars represent averages and standard deviations of at least three biological replicates. * = p-value < 0.01.

(Figure 6A). Despite the over-expression of ETV7, cells further over-expressing DNAJC15 became more sensitive to Doxorubicin-mediated toxicity, supporting the idea that DNAJC15 repression is exploited by ETV7 as a mechanism of resistance to Doxorubicin. Moreover, the over-expression of DNAJC15 was also able to down-regulate the expression of ABCB1 in MCF7 cells over-expressing ETV7, in agreement with its reported negative role in ABCB1 expression (Figure 6B).

2. ETV7 regulates BCSC-like plasticity by the repression of IFN response genes

2.1 ETV7 regulates the resistance to 5-FU and radiotherapy

Given the observed effects of ETV7 on Doxorubicin resistance in MCF7 cells, we decided to test whether ETV7 could confer increased resistance to other therapeutic agents and whether these effects could be conserved in other breast cancer cell lines.

2.1.1 The over-expression of ETV7 induces an increased resistance to 5-FU

We first generated different breast cancer cell lines stably over-expressing ETV7 through lentiviral transduction of a plasmid carrying the *ETV7* gene (pAIP-ETV7) or the empty counterpart (pAIP). After selection with Puromycin, we obtained two cell lines stably over-expressing ETV7: MCF7 and T47D (Figure 7A and 7B). We chose to use these cell lines because they are representative for the luminal breast cancer subtypes, thus belonging to poorly aggressive subtypes of breast cancer, which usually express low levels of ETV7 [138] in order to appreciate its pro-tumorigenic potential.

We thus tested the sensitivity of breast cancer cells over-expressing ETV7 to 5-FU, which, similarly, to Doxorubicin, is commonly used for breast cancer treatment and it is also able to induce the expression of ETV7 (Figure 1). We analyzed the sensitivity of these cells using the Cell Titer Glo Assay, and we observed that T47D cells were much more resistant to 5-FU treatment compared to MCF7 cells. Furthermore, we obtained a significant increase in cell viability in ETV7 over-expressing cells, both for MCF7 and T47D (Figure 7C and 7D). To

further confirm this increased resistance, we tested the induction of cell death, and in particular of apoptosis, in response to 5-FU treatment by the staining with Annexin V-FITC/PI staining and flow cytometry analysis. ETV7 over-expressing MCF7 cells showed a significant decrease in the rate of cell death and apoptosis compared to the empty control (Figure 7E, 7F, and 7G), suggesting that the over-expression of ETV7 can decrease the sensitivity of BC cells to 5-FU as well.

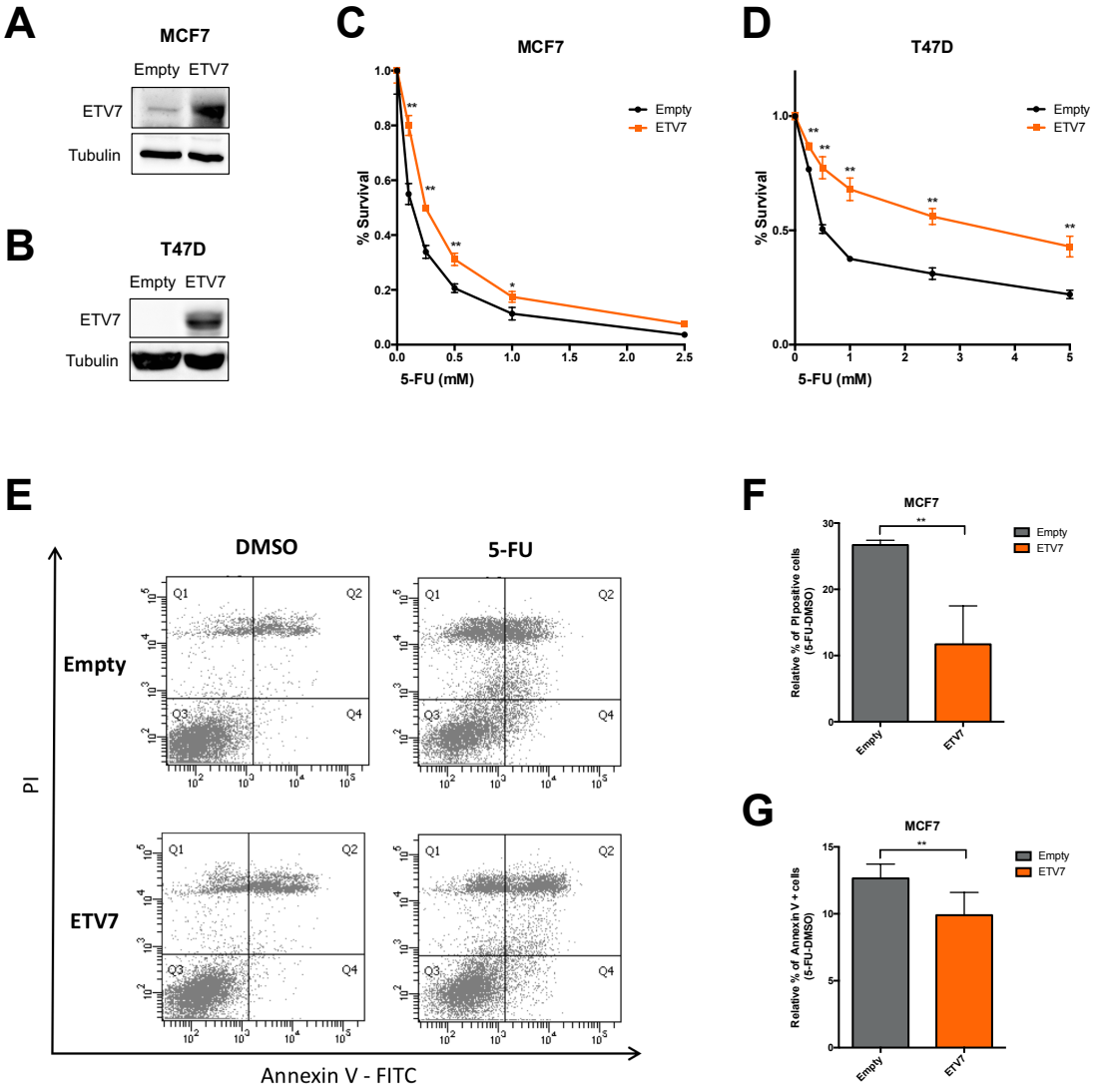

Figure 7. *ETV7 over-expression increases 5-FU resistance in MCF7 and T47D.* A-B) Western blot analysis of MCF7 (A) and T47D (B) cells over-expressing ETV7. C-D) Cell Titer Glo Assay for survival analysis upon 5-FU treatment in MCF7 (C) and T47D (D) cells over-expressing ETV7 and their empty control. E-F-G) Annexin V-FITC/PI staining of MCF7 Empty and MCF7 ETV7 cells treated with 5-FU 200 μM for 72 hours. E) Representative dotplot of flow cytometry analysis. F) Relative percentage of PI positive cells calculated as difference of 5-FU and DMSO treated cells. G) Relative percentage of Annexin V positive cells calculated as difference of 5-FU and DMSO treated cells. Bars represent the averages and standard deviations of at least three biological replicates. * = p-value < 0.05; ** = p-value < 0.01

2.1.2 The over-expression of ETV7 induces increased resistance to radiotherapy

We then tested the sensitivity of the cells to another commonly therapeutic option for the treatment of breast cancer: radiotherapy. In order to assess the viability of the cells in response to radiotherapy, we measured the percentage of viable cells in response to different doses of radiation (from 2 to 10 Gy) (Figure 8A and 8B). By this analysis we found that T47D cells are more sensitive to radiation compared to MCF7 cells, thus showing an opposite behavior compared to the one observed in response to 5-FU. However, also in this case, the cells over-expressing ETV7 showed reduced sensitivity to the treatment in both the analyzed cell lines.

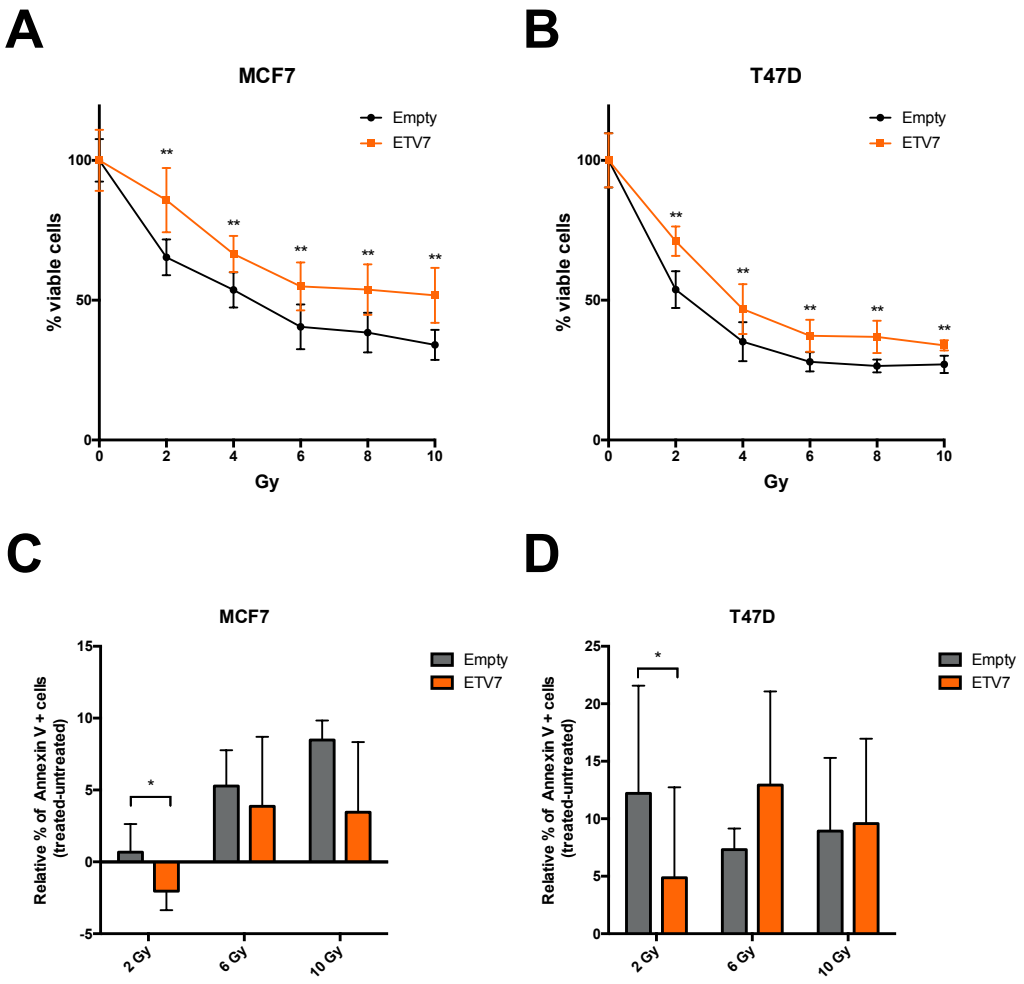

Figure 8. *ETV7 expression affects the sensitivity of breast cancer cells to radiotherapy*. A-B) ViCell Assay for survival analysis upon radiotherapy treatment in MCF7 (A) and T47D (B) cells over-expressing ETV7 and their empty control. C-D) Annexin V-FITC/PI staining of MCF7 (C) and T47D (D) Empty or over-expressing ETV7 treated with radiotherapy with 2-6-10 Gy for 72 hours. Relative percentage of Annexin V positive cells calculated as difference of treated and untreated cells. Bars represent the averages and standard deviations of at least four biological replicates. * = p-value < 0.05; ** = p-value < 0.01

We then measured the induction of apoptosis in response to radiotherapy following different doses of radiation. ETV7 over-expressing cells showed a significant decrease in the percentage of apoptosis in response to radiotherapy at the lowest dose used (2Gy), whereas no significant differences could be observed with higher doses in both the cell lines tested (Figure 8C and 8D). These results suggest that the increased expression of ETV7 can affect the sensitivity of breast cancer cells to several different therapeutic agents, including chemotherapy (i.e. Doxorubicin and 5-FU) and radiotherapy. However, the mechanism of resistance to radiotherapy seems to involve only partially the apoptotic response, and further investigations are needed to better explain the contribution of ETV7 to this mechanism.

2.1.3 ETV7 over-expressing cells present drug resistance-related properties

We showed that the over-expression of ETV7 could increase the resistance to Doxorubicin, 5-FU, and radiotherapy; however, the upregulation of ABC transporters (Figure 2D) can only partially explain the resistance to chemotherapy, but this is not sufficient to explain the resistance to radiotherapy. We thus investigated some of the properties that can confer resistance to the cells. Notably, we could appreciate a strong increase in the expression of the anti-apoptotic proteins BCL-2 and Survivin (Figure 9A), which can explain the decreased rate of apoptosis observed in ETV7 over-expressing cells upon the treatment with 5-FU or radiotherapy. Since both 5-FU and radiotherapy exert their action when the cells divide, their activity is strongly dependent on the proliferative rate of the cells. Thus, we analyzed their proliferative capacity by measuring their doubling time by the ViCell instrument. We observed a significant increase in the doubling time of MCF7 ETV7 compared to MCF7 Empty cells, demonstrating that cell proliferation was much slower in cells over-expressing ETV7 compared to the empty control (Figure 9B). In T47D cells, this increase in the doubling time was instead slight and not significant (Figure 9C). We then tested the colony formation potential of ETV7 over-expressing cells by clonogenic assay, and we could appreciate a significant decrease in the capacity of ETV7 over-expressing cells to form colonies when grown on plastic in both MCF7 and T47D cells (Figure 9D and 9E). Thus, the decreased proliferative rate of the cells could also contribute to the increased resistance to 5-FU and radiotherapy, together with the increased

expression of anti-apoptotic proteins and ABC transporters.

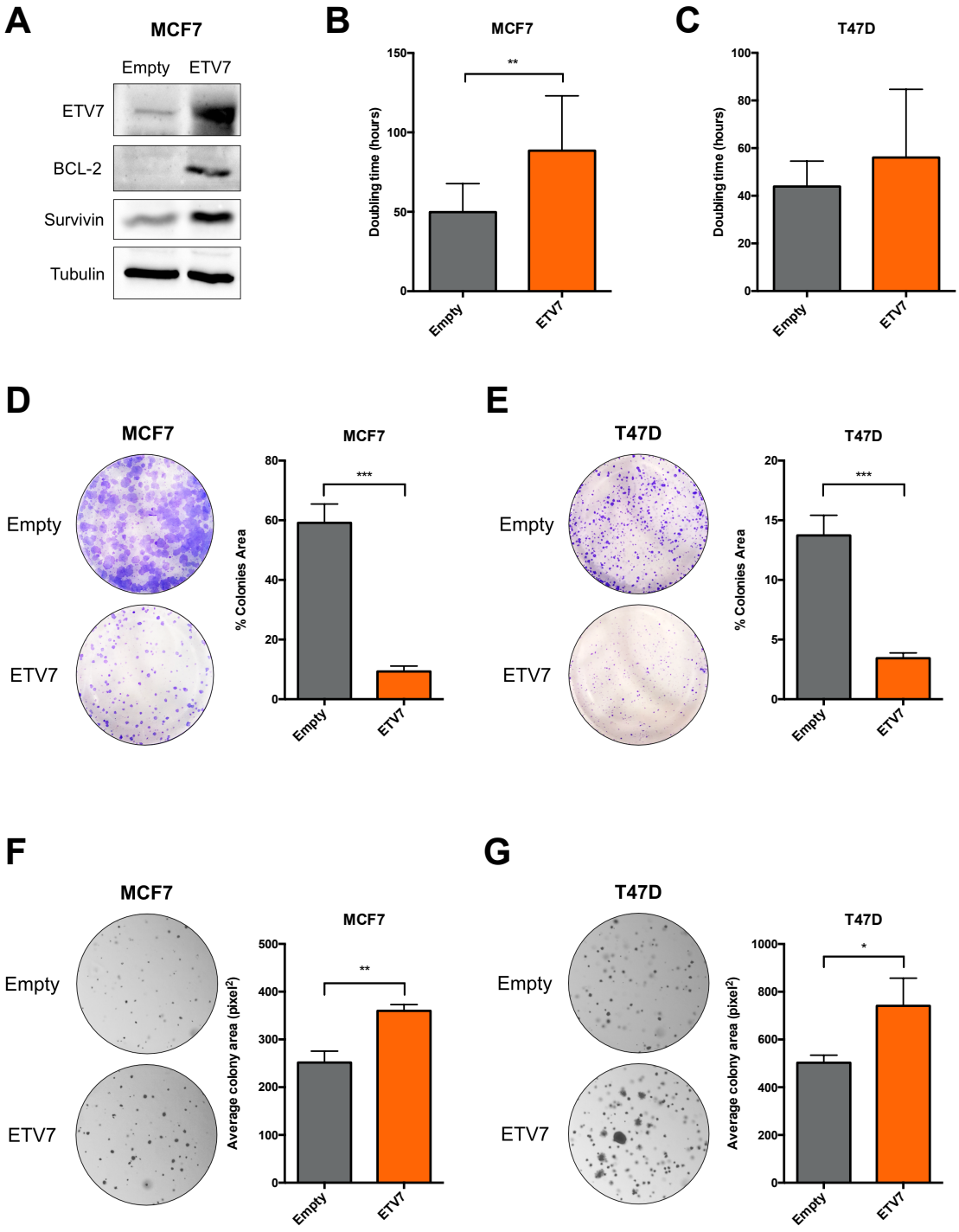

Figure 9. *ETV7 over-expressing BC cells express high levels of anti-apoptotic proteins and display different proliferative potential*. A) Western Blot analysis of the anti-apoptotic BCL-2 and Survivin protein expression in MCF7 Empty and MCF7 ETV7. B-C) Doubling time of MCF7 (B) and T47D (C) Empty and ETV7 cells calculated by cell count at ViCell instrument. D-E) Colony formation/clonogenic assay of MCF7 (D) and T47D (E) Empty and ETV7 cells after 3 weeks of growth. On the left a representative image and on the right the total colonies area calculated with the ImageJ software. F-G) Soft agar colony formation assay of MCF7 (F) and T47D (G) Empty and ETV7 cells after 3 weeks of growth. On the left a representative image and on the right the average colony area calculated with the ImageJ software. Bars represent the averages and standard deviations of at least three biological replicates. * = p-value < 0.05; ** = p-value < 0.01; *** = p-value < 0.001

Surprisingly, when we analyzed the colony formation capacity of the cells in an anchorage-independent system with the soft agar assay, we observed an opposite proliferative behavior. Both MCF7 and T47D cells over-expressing ETV7 formed more abundant and larger colonies when grown in soft agar compared to plastic (Figure 9F and 9G). Despite these apparently contradictory data, the anchorage-independent growth is commonly considered a pro-tumorigenic feature; thus, these results might suggest that cells over-expressing ETV7 can switch to different proliferative behaviors based on the environmental conditions.

2.2 ETV7 affects BCSC-like plasticity

We observed that the over-expression of ETV7 could determine an increased resistance to standard anti-cancer therapies (i.e. Doxorubicin, 5-FU, and radiotherapy), which is accompanied by i) an increase in ABC transporter expression, ii) higher anti-apoptotic protein expression and iii) a differential switchable proliferative rate.

Given these observations, and data from the literature reporting the involvement of ETV7 in cell differentiation [139], we hypothesized that ETV7 could play a role in breast cancer stemness.

2.2.1 The expression of ETV7 affects BCSCs markers expression

To test this hypothesis we first analysed some of the most commonly used markers for breast cancer stem cells, including CD44 and CD24 expression and ALDH activity. We analysed the percentage of $CD44^+$ and $CD24^-$ cells (representing the BCSCs population according to most of the researchers) in MCF7 and T47D cells over-expressing ETV7 or their relative control. Both the parental cell lines present a very low or almost absent population of $CD44^+/CD24^-$ cells; however, we could appreciate an impressive increase in this population in both the cell lines tested upon ETV7 over-expression (Figure 10A and 10B). Importantly, this increase in breast cancer stem cells population was not due solely on alterations in either CD44 or CD24 expression, but the over-expression of ETV7 could stimulate both an increase in CD44 expression and a decrease in CD24 expression on the plasma membrane of the cells.

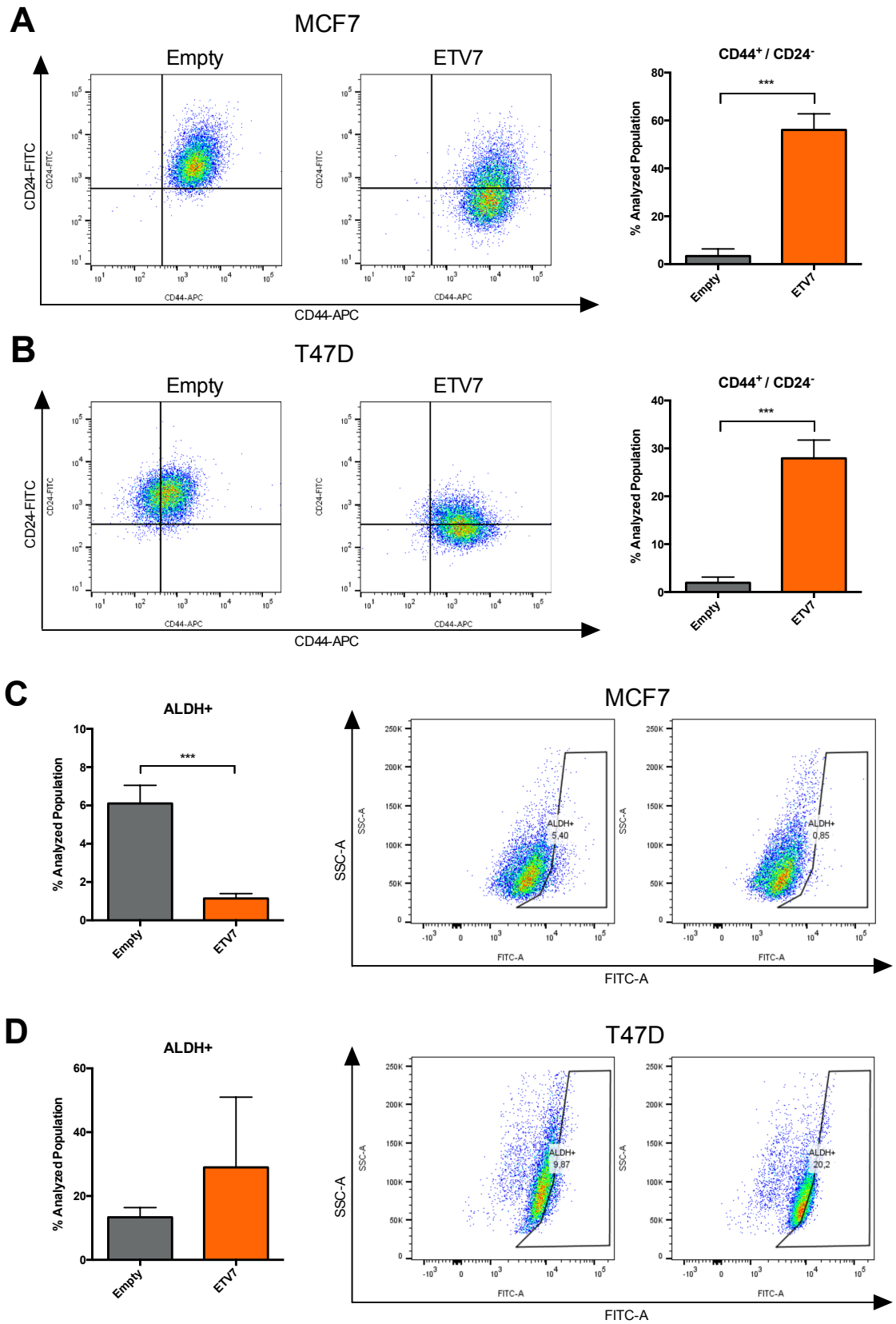

Figure 10. *The over-expression of ETV7 influences the expression of BCSCs markers.* A-B) CD44-APC and CD24-FITC staining and flow cytometry analysis in MCF7 (A) and T47D (B) Empty and ETV7 cells. On the left a representative dot plot of the results obtained at FACS Canto A; the histogram on the right summarizes the percentage of CD44+/CD24- cells in Empty and ETV7 over-expressing cells. C-D) ALDEFLUOR analysis in MCF7 (C) and T47D (D) Empty and ETV7 cells. The histogram on the left summarizes the percentage of ALDH positive cells in Empty and ETV7 over-expressing cells; on the right a representative dot plot of the results obtained at FACS Canto II. Bars represent the averages and standard deviations of at least three biological replicates. *** = p-value < 0.001

We then analysed the activity of ALDH via ALDEFLUOR kit in our models. Here again, the population of ALDH+ cells was very low in the parental cell lines, but, either a decrease in this already small population or no significant differences were observed in response to ETV7 over-expression in MCF7 (Figure 10C) and T47D (Figure 10D) cells respectively. Therefore, ETV7 over-expression seems to drive a strong polarization of the analysed breast cancer cells toward a more cancer stem cell-like phenotype, which is mainly represented by the $CD44^{+}/CD24^{-}$ population.

To further confirm these results, we tested whether modulating the expression of ETV7 in the opposite direction could also affect the population of $CD44^{+}/CD24^{-}$ cells. In order to detect whether the knock-down of ETV7 could decrease the population of BCSC-like cells, we tested ETV7 silencing in the aggressive triple negative BC cell line MDA-MB-231, which is known from the literature to present almost exclusively $CD44^{+}/CD24^{-}$ cells. We knocked-down ETV7 expression using 2 different siRNAs against ETV7 (siETV7#1 and siETV7#2) and we confirmed their activity by RT-qPCR analysis (Figure 11A). Importantly, in both MDA-MB-231 samples silenced for ETV7, it was possible to observe a population of cells with decreased CD44 membrane expression compared to the scramble control, suggesting that tuning the expression of ETV7 can bi-directionally affect the population of $CD44^{+}/CD24^{-}$ cells (Figure 11B).

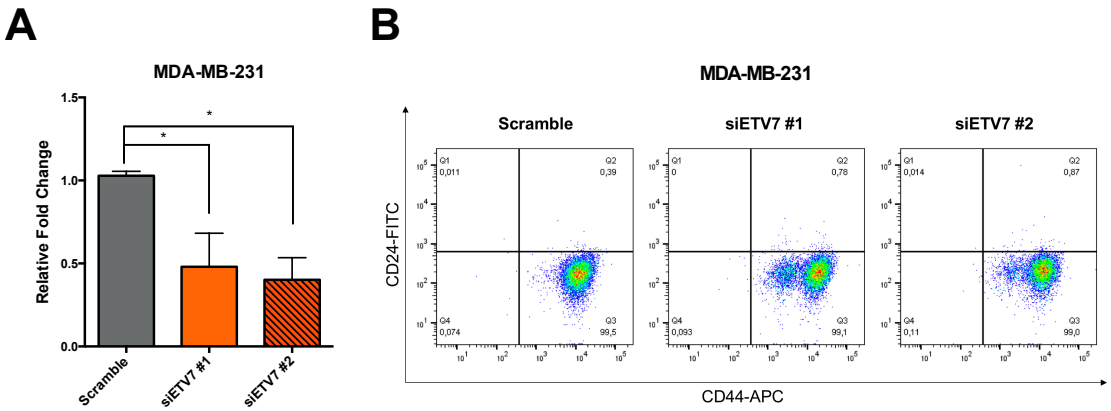

Figure 11. *The silencing of ETV7 decreases CD44 membrane expression in MDA-MB-231 cells*. A) RT-qPCR analysis of ETV7 expression in MDA-MB-231 transfected with siRNA against ETV7 (siETV7 #1 and #2) and the relative scramble control for 72 hours. Bars represent the averages and standard deviations of at least three biological replicates. * = p-value < 0.05. B) Representative dot plot of CD44-APC and CD24-FITC staining and flow cytometry analysis in MDA-MB-231 cells transfected with siRNA against ETV7 (siETV7 #1 and #2) and the relative scramble control for 72 hours.

2.2.2 ETV7 expression affects the potential to form mammospheres

Given the conflicting literature data on the use of markers for the detection of breast cancer stem cells, we tested another common well-accepted feature of cancer stem cells by measuring their potential to form spheres when grown in non-differentiating and non-adherent conditions. We measured the mammosphere formation efficiency (MFE) of MCF7 Empty and MCF7 ETV7 cells and we could observe a significant increase in the mammosphere formation efficiency of MCF7 cells over-expressing ETV7 compared to the control (Figure 12A and 12B). We then tested the propagation potential of mammospheres by passaging them in culture, and we could appreciate the ability of cells over-expressing ETV7 to generate second, third and fourth generation mammospheres

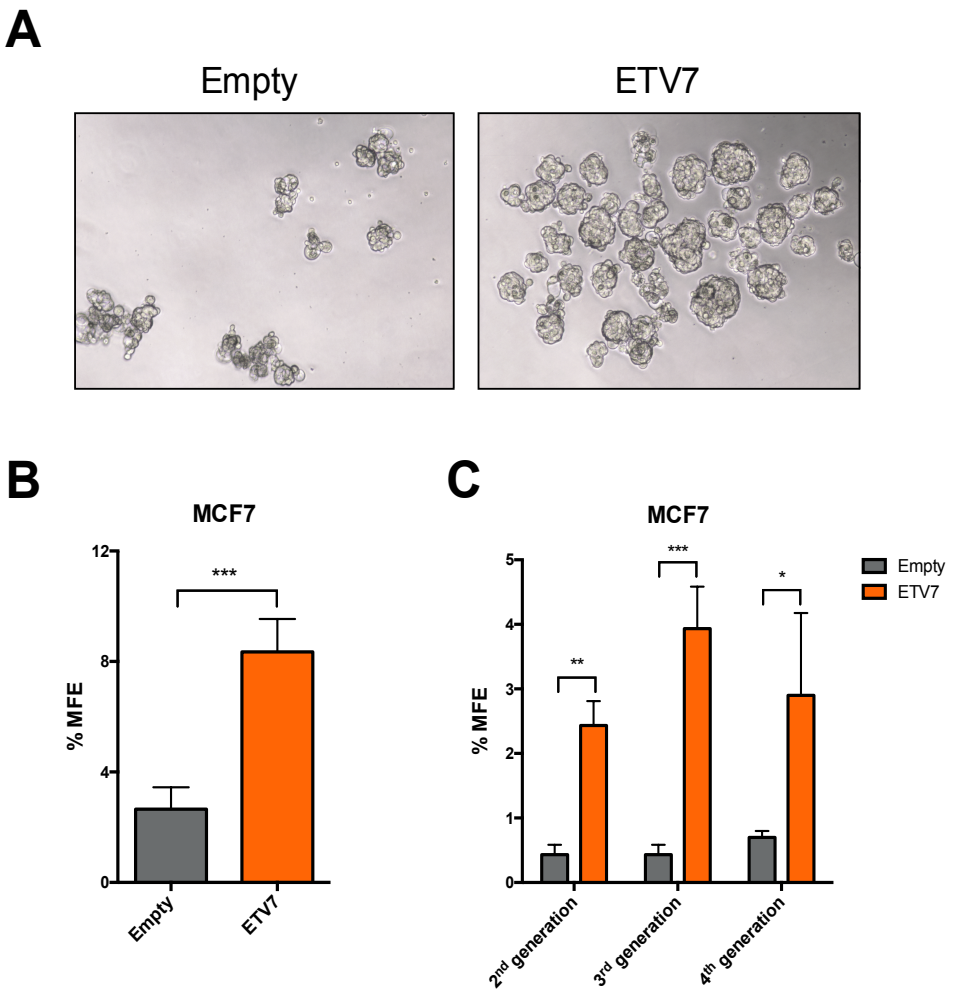

Figure 12. *ETV7 over-expression enhances the mammospheres formation potential of MCF7 cells*. A) A representative image of first generation mammospheres obtained from MCF7 Empty and MCF7 ETV7 cells. B) The percentage of mammosphere formation efficiency (%MFE) in MCF7 Empty and ETV7 calculated as number of mammospheres per well/number of cells seeded per well X 100. C) % MFE in second, third and fourth generation mammospheres obtained by passing the mammosphere once a week. Bars represent the averages and standard deviations of at least three biological replicates. * = p-value < 0.05; ** = p-value < 0.01; *** = p-value < 0.001.

(Figure 12C). These data confirmed that the over-expression of ETV7 in breast cancer cells can enhance the cancer stem cell-like properties and thus suggest a role for ETV7 in breast cancer stem cell-like plasticity.

We also tested the mammosphere formation potential in T47D cells; however, when grown in non-adherent and non-differentiating conditions, T47D cells were forming only aggregates of cells with unorganized structures, that cannot be defined as mammospheres (data not shown).

2.2.3 Metabolic alterations in ETV7 over-expressing cells

Since we observed a plastic and adaptable proliferative rate in ETV7 over-expressing cells, and an increase in CSC-like cells, which are usually characterized by differences in the metabolic phenotype [185], we investigated whether the over-expression of ETV7 could affect the energetic phenotype of breast cancer cells.

We first performed an analysis of the cell energetic phenotype by using the specifically designed kit for Seahorse XFp instrument, which measures the oxygen consumption rate (OCR), a measure of the rate of cellular mitochondrial respiration, and the extracellular acidification rate (ECAR), which is instead a measure of the glycolysis rate of the cells. By the addition of two stressor compounds, Oligomycin and FCCP (Carbonyl cyanide-4-(trifluoromethoxy)phenylhydrazone), it is possible to measure the metabolic potential of the cells, which measures the ability of the cells to meet an energetic demand via respiration and glycolysis. Indeed, Oligomycin is an inhibitor of ATP synthase, which stops ATP production by the mitochondria, causing an increase in compensatory glycolysis, whereas FCCP is a mitochondrial uncoupling agent that depolarizes the mitochondrial membrane driving an increase in OCR, as mitochondria attempt to restore their membrane potential. By this analysis, we could observe that cells over-expressing ETV7 presented a significant higher OCR compared to their relative control already in basal condition, which are also maintained in stressed condition in both MCF7 and T47D cells (Figure 13A and 13D), whereas there were no significant differences in the ECAR measurements (Figure 13B and 13E). However, the metabolic potential of the cells was partially different only in MCF7 cells, in which the over-expression of ETV7 could stimulate an increase in the glycolytic metabolic potential of the cells, which was not confirmed in

T47D cells (Figure 13C and 13F).

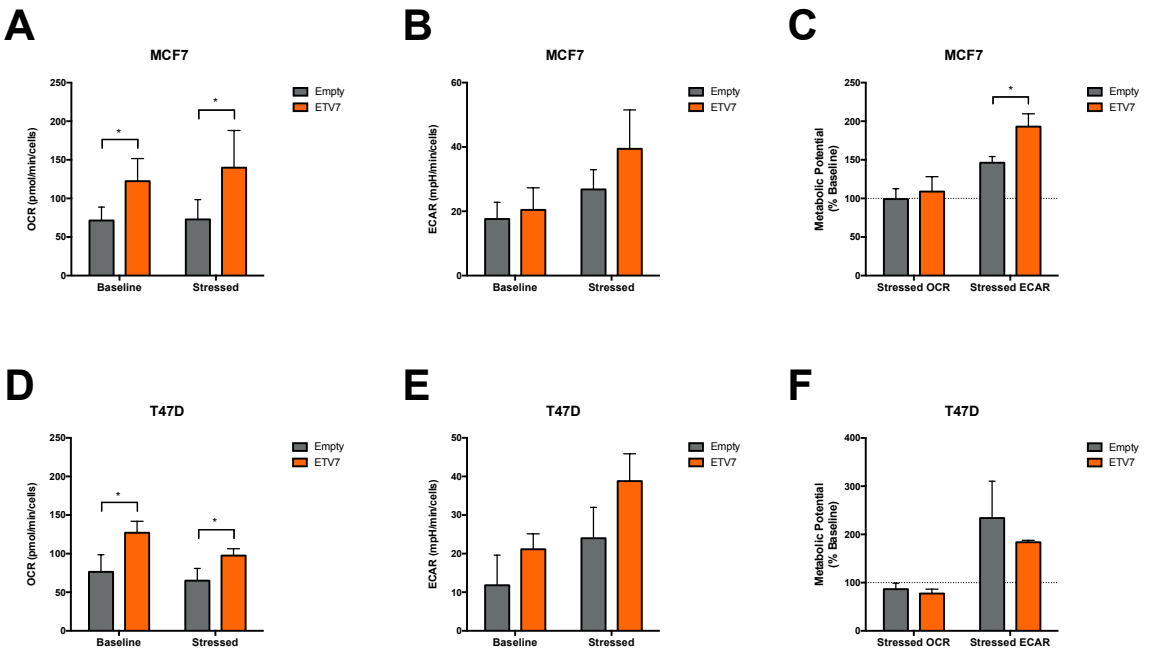

Figure 13. *ETV7 over-expression affects the energetic phenotype of the cells*. Cell energy phenotype analysis of MCF7 (A-C) and T47D (D-E) Empty and ETV7 cells performed with the Seahorse XFp instrument and Cell Energy Phenotype Test kit. A and D) Measure of Oxygen Consumption Rate (OCR) at starting condition (Baseline) and in the presence of stressor compunds (i.e. Oligomycin+FCCP) in MCF7 (A) and T47D (D) Empty and ETV7 cells. B and E) Measure of Extracellular Acidification Rated (ECAR) at starting condition (Baseline) and in the presence of stressor compounds (Stressed) in MCF7 (B) and T47D (E) Empty and ETV7 cells. C and F) Measure of Metabolic Potential, calculated as the percentage of the increase of stressed OCR or ECAR over baseline OCR or ECAR respectively, in MCF7 (C) and T47D (F) Empty and ETV7 cells. Bars represent the averages and standard deviations of at least three biological replicates. * = p-value < 0.05.

Given the observed increase in the OCR of ETV7 over-expressing cells in basal condition, we analyzed more in-depth the mitochondrial respiration parameters of the cells using the Cell Mito Stress Test kit at the Seahorse XFp instrument (Figure 14E). Interestingly, MCF7 cells over-expressing ETV7 showed a significant increase in most of the mitochondrial parameters analyzed (i.e. basal respiration, maximal respiration, ATP production, and spare respiratory capacity), showing a general increase in the oxygen consumption rate (Figure 14A and 14B). Moreover, MCF7 ETV7 cells showed a significant increase also in non-mitochondrial oxygen consumption, suggesting that this increased OCR was not solely dependent on mitochondria contribution. Similar behavior was also observed in T47D cells, with a significant increase in basal and maximal respiration in ETV7 over-expressing cells (Figure 14C and 14D). However, T47D cells presented a different mitochondrial energetic profile compared to MCF7 cells, as displayed by the OCR measurements over time, since they have increased proton leak and almost absent spare

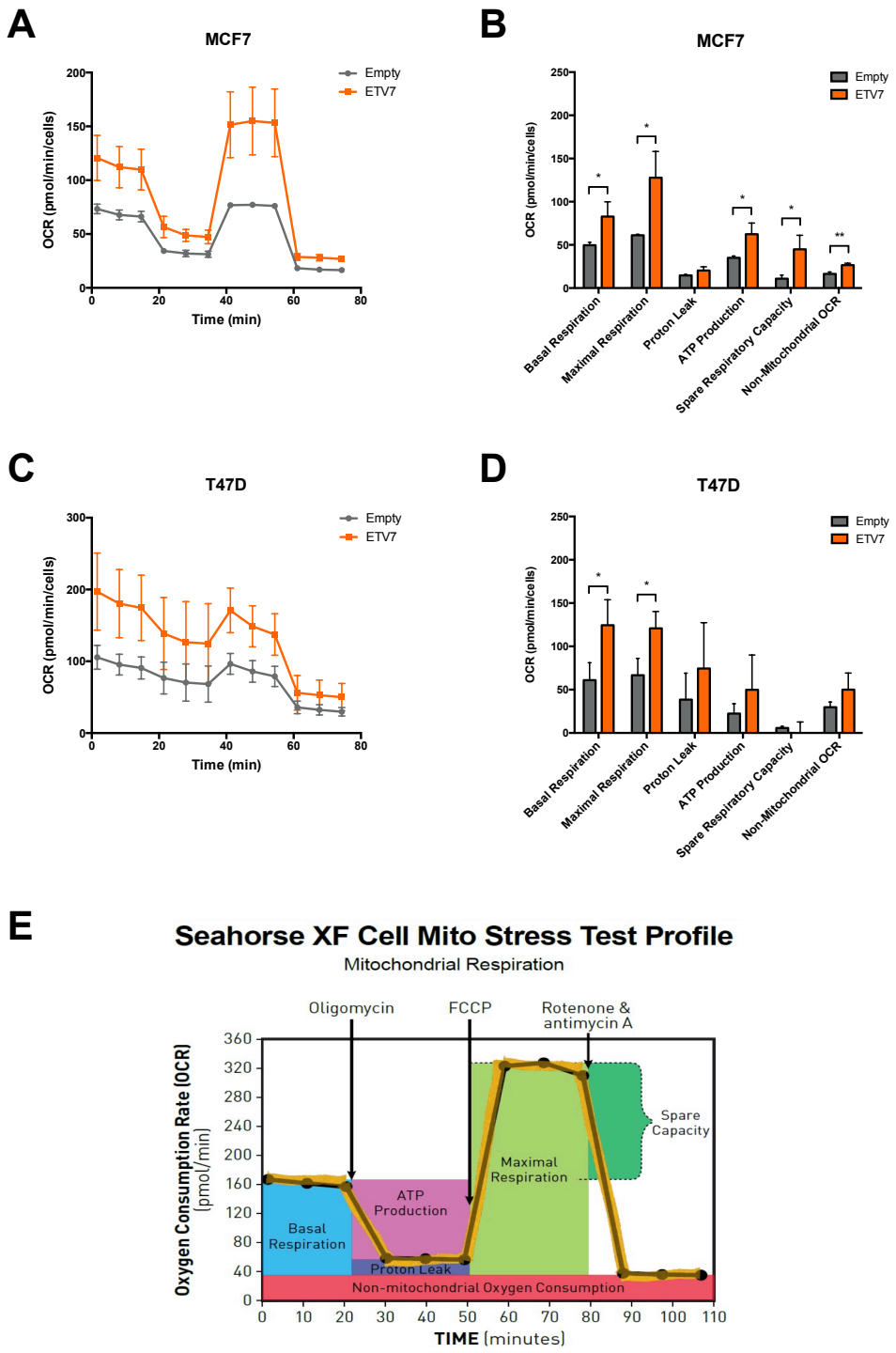

Figure 14. *ETV7 over-expression affects the mitochondrial respiration in breast cancer cells.* Mitochondrial respiration analysis of MCF7 (A-B) and T47D (C-D) Empty and ETV7 cells performed with the Seahorse XFp instrument and Cell Mito Stress Test kit. A and C) Measure of Oxygen Consumption Rate (OCR) during time in MCF7 (A) and T47D (C) Empty and ETV7 cells. B and D) Data extrapolated from the OCR measurement over time following different stressors administration in MCF7 (B) and T47D (D) cells. E) A schematic representation of the protocol and the way used to extrapolate data from OCR measurements over time. Non-mitochondrial oxygen consumption (OCR) is the minimum rate of OCR after the last (Rotenone/antimycin A) injection. Basal respiration represents the difference between the last OCR measurement before the first stressor (Oligomycin) injection (20 minutes after the start) and Non-Mitochondrial Oxygen consumption. Maximal Respiration is the difference between the maximum rate measurement after second stressor (FCCP) injection 50 min after the start and the Non-mitochondrial OCR. Proton leak is the difference between the minimum rate measurement after Oligomycin injection and non-mitochondrial OCR. ATP production is calculated as the difference between the last measurement before Oligomycin injection and the minimum rate measurement after Oligomycin injection. Spare Respiratory Capacity is the difference between the Maximal respiration and basal respiration. Bars represent the averages and standard deviations of at least three biological replicates. * = p-value < 0.05. ** = p-value < 0.01.

respiratory capacity. These results suggest that the over-expression of ETV7 in breast cancer cell lines can drive a different metabolic profile, with an increased oxygen consumption rate, mainly due to augmented basal and maximal mitochondrial respiration, which is in agreement with the increasing observations reporting that CSCs preferentially rely on mitochondrial respiration and oxidative metabolism rather than to the glycolytic phenotype, a condition more frequently characterizing the non-CSCs [186].

2.2.4 ETV7 over-expression influences the migration potential

Cancer stem cells plasticity has frequently been associated with epithelial to mesenchymal transition (EMT). Thus, we tested some EMT properties in MCF7 cells over-

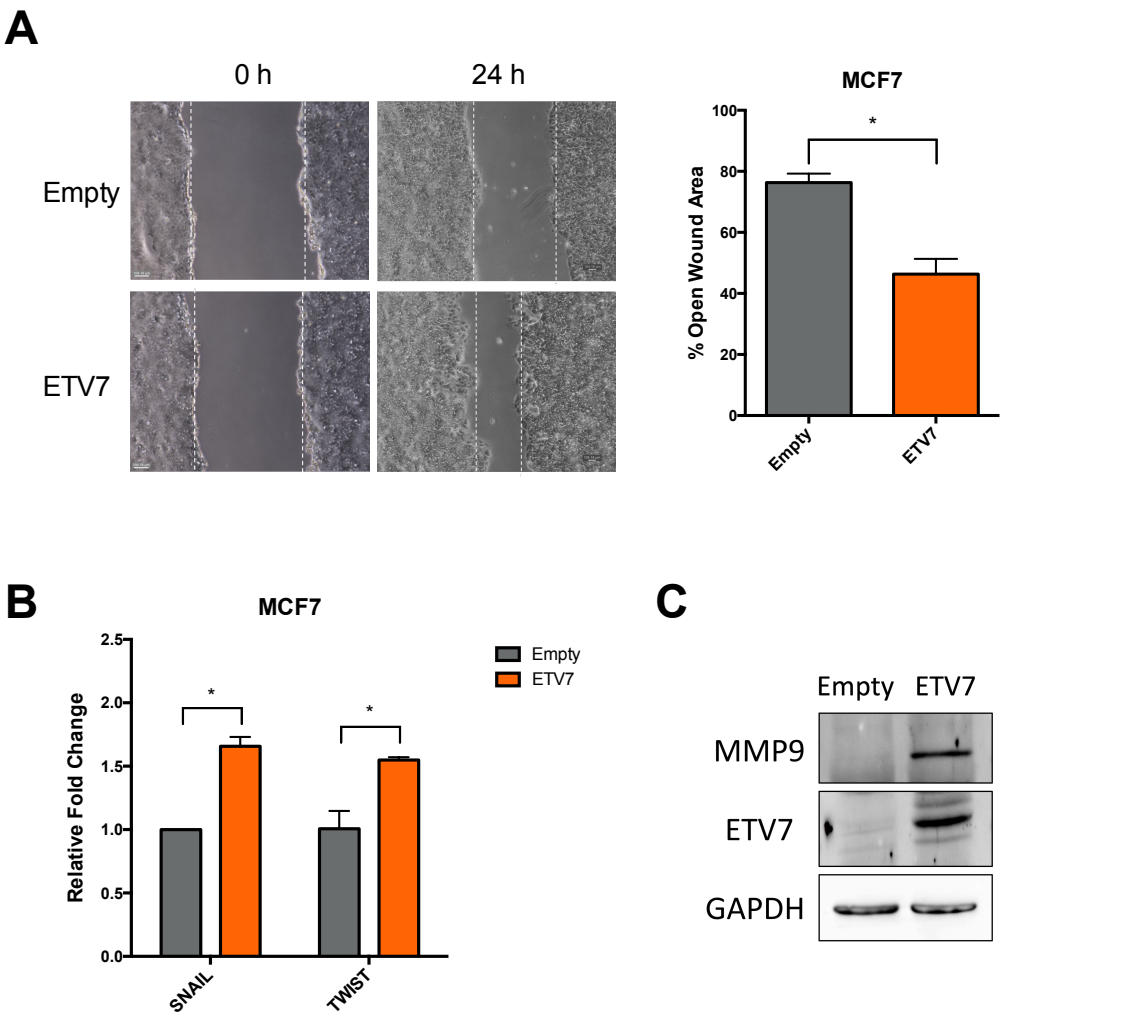

Figure 15. *MCF7 cells over-expressing ETV7 present increased motility*. A) Scratch Assay measuring the motility of MCF7 Empty and ETV7 cells. On the left a representative image and on the right the average percentage of open wound area calculated with the TScratch software[221]. B) RT-qPCR analysis of SNAIL and TWIST gene expression in MCF7 cells -over-expressing ETV7. C) Western Blot analysis to measure MMP9 protein expression in MCF7 cells over-expressing ETV7; GAPDH served as reference protein. Bars represent the averages and standard deviations of at least three biological replicates. * = p-value < 0.05.

expressing ETV7. We first measured the motility ability of the cells by wound healing assay (also known as scratch assay) and we could observe a significant increase in the motility potential of the cells over-expressing ETV7 (Figure 15A). We then analyzed the expression of some mesenchymal markers associated with increased migration and invasion capacity. Interestingly, in cells over-expressing ETV7 we observed a significant increase in the expression of the EMT master regulators SNAIL and TWIST (Figure 15B), as well as an increase in MMP9 expression (Figure 15C), which is often associated with increased invasive capacity.

2.2.5 Testing the ETV7 pro-tumorigenic potential in vivo

In order to test the pro-tumorigenic functions of ETV7 *in vivo*, we decided to perform xenotransplantations of our breast cancer cell lines over-expressing ETV7. We chose to use the zebrafish embryo model given its easy manipulation, fast reproduction, and transparency, which allow following the transplanted cells during time. In particular, we used either the transparent Casper model [187] or the SCID Prkdc$^{-/-}$ model [188]. We first generated cellular clones stably expressing a nuclear eGFP by viral transduction with PGK-H2BeGFP and isolation by FACS sorting in order to visualize the transplanted cells within the embryos.

We then injected the MCF7 and T47D Empty and ETV7 fluorescent cells into either the yolk sac or the Duct of Cuvier of 2 days post-fertilization zebrafish embryos (0 days post-injection, dpi), and followed the cell fluorescence over time until 3 days post-injection (maximum time allowed by the Italian Ministry of Health for working with zebrafish embryos) (Figure 16A). Cells injected into the Duct of Cuvier were usually not able to survive 3 days after injection (data not shown), whereas cells injected into the yolk could survive. Despite their ability to survive, injected cells were not able to proliferate in the first 3 days after the transplantation. Furthermore, we could not appreciate any difference in the relative number of transplanted cells at 3 dpi compared to the cells injected, both for cells over-expressing ETV7 and their relative control in either MCF7 (Figure 16B) or T47D (Figure 16C). This result may be due to the slow proliferative potential of MCF7 and T47D cells given the low aggressiveness of the luminal breast cancer subtypes, for which the 3 days allowed for the experiment might not be sufficient to observe differences.

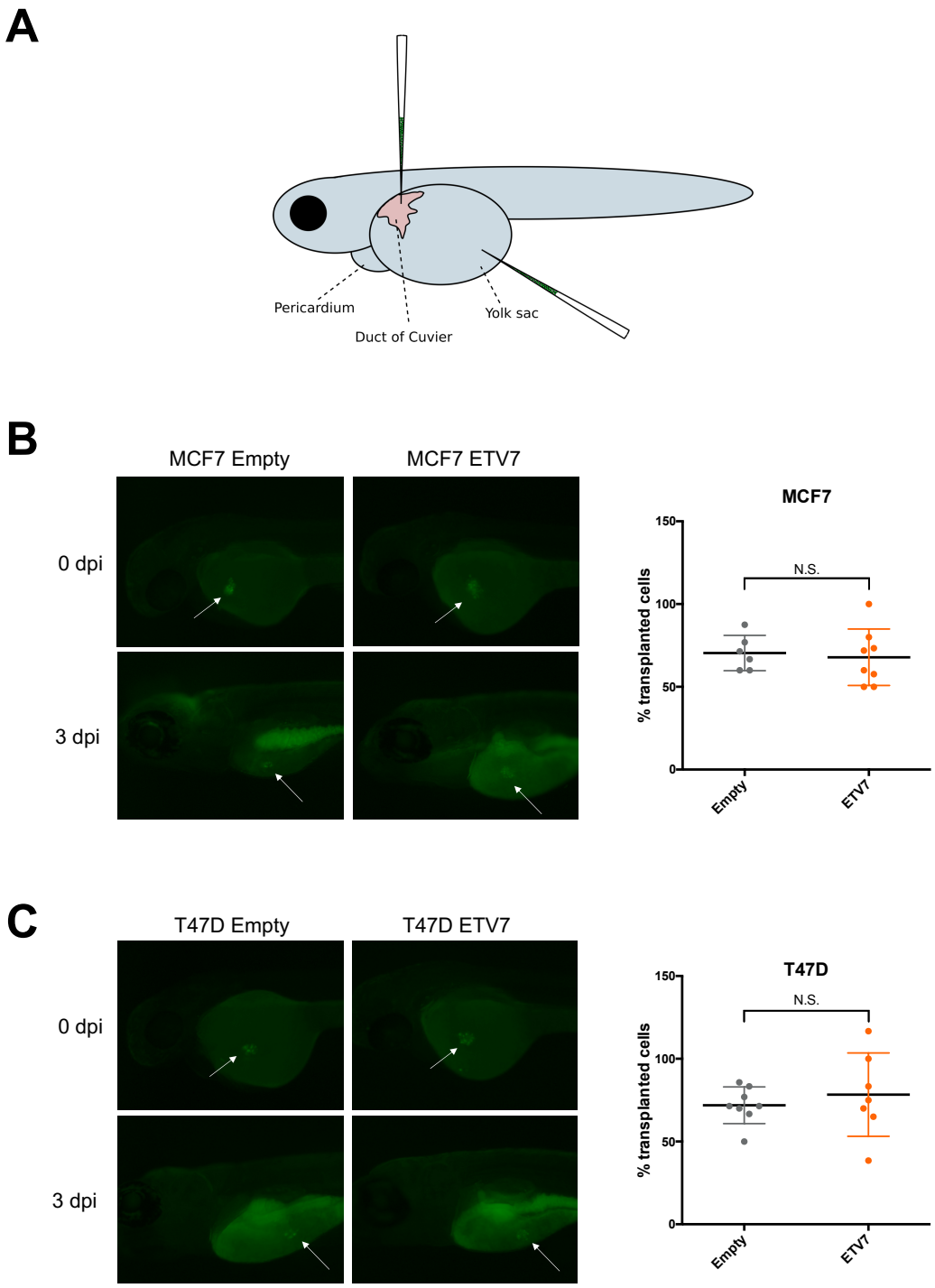

Figure 16. *Xenotransplantation of fluorescent cells over-expressing ETV7 into PRDKC-/- zebrafish embryos*. A) Schematic representation of a zebrafish embryo with the preferred sites of injection, which include the yolk, which is re-absorbed during development and the Duct of Cuvier, which facilitates the entering of the cells into the blood stream. B-C) Image analysis of MCF7 (B) and T47D (C) cells transplantation within the yolk of 2 days PRDKC-/- zebrafish embryos. On the left a representative image of cells injected at 0 or 3 days post injections (dpi), with a white arrow to pinpoint the fluorescent cells. On the right, the percentage of transplanted cells calculated as the number of cells 3 dpi relative to the number of cells injected at 0 dpi X 100. Images were obtained with a stereomicroscope. The same experiment was performed in Casper embryos and gave similar results. Number of embryos injected per group>6. N.S.: not statistically significant.

2.3 Molecular mechanisms regulated by ETV7

We showed that the over-expression of ETV7 in breast cancer cells was able to induce increased chemoresistance as well as modulate breast CSCs plasticity; however, the down-regulation of DNAJC15 could only partially explain some of these effects. In order to investigate the molecular mediators of the biological effects observed at the genome scale, we performed an analysis of the transcriptome on MCF7 and T47D cells over-expressing ETV7 or the relative empty plasmid by RNA-seq. In fact, being ETV7 a transcription factor, we expect that most of its effects could be explained by the genes it regulates at the transcriptional level.

2.3.1 ETV7 is responsible for the repression of a set of Interferon response genes

The analysis of the genes differentially expressed (DEGs) in cells over-expressing ETV7 compared to the empty control identified 5,387 genes for MCF7 and 1,883 genes for T47D cells. The higher number of DEGs in MCF7 cells can be possibly explained by the method of generation of stable ETV7 over-expression in the two cell lines: MCF7 cells were in fact obtained by single cell clone expansion, thus it may account for intrinsic clones diversity, whereas T47D cells were grown from the selected pool of transduced cells.

Through the separation of the up- and down-regulated genes, it was possible to observe a similar number of genes in the two clusters, which was conserved in the two cell lines (Figure 15A). By comparing the list of DEGs from two cell lines, it was possible to identify a reasonable amount of genes which were commonly regulated in the two cellular systems (427 commonly down-regulated and 294 commonly up-regulated genes), with a lower number of genes which were inversely regulated in MCF7 and T47D cells (Figure 17A). Given that most of the biological effects previously observed in cells over-expressing ETV7 were common to both the cell lines, we focused our subsequent analyses on the common DEGs. Particularly, being ETV7 known as a transcriptional repressor, we focused on the commonly down-regulated genes, which might be more directly regulated by ETV7. Interestingly, the most significant terms obtained by the gene ontology analysis of common down-regulated genes were involved in the innate immune response and inflammatory response, with several terms referred to the pathogen/viral entry into the

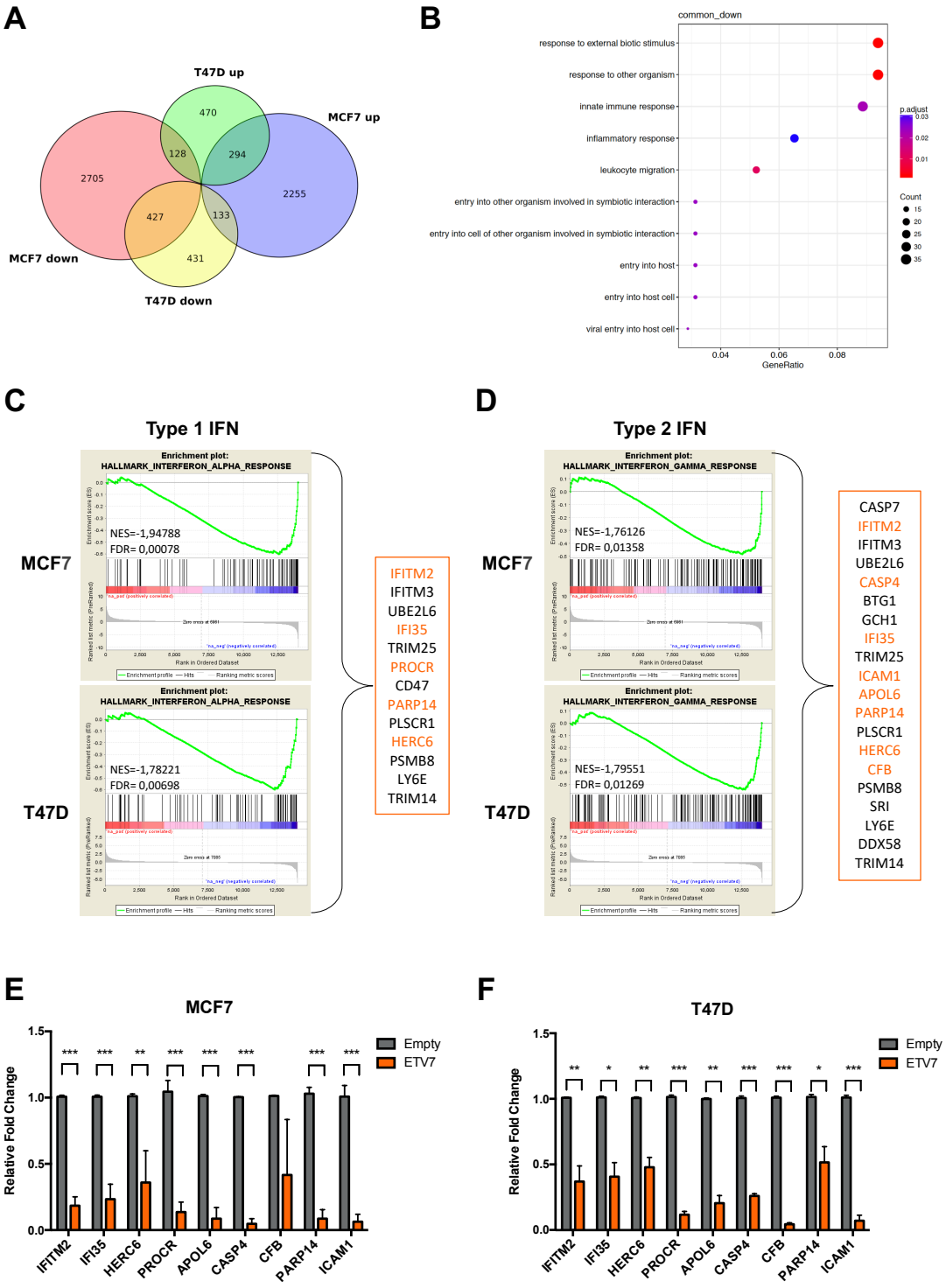

Figure 17. *RNA-seq analysis reveals a repression of a set of Interferon response genes in ETV7 over-expressing cells*. A) A Venn diagram of differential expression summary with the secific number of DEGs (ETV7 vs. Empty) in MCF7 and T47D Empty and ETV7 with a False Discovery Rate (FDR) < 0.05. B) Gene ontology analysis of commonly downregulated DEGs (orange area in panel A) in MCF7 and T47D cells(ETV7 vs. Empty). In the image are shown the top 10 significant terms. C-D) Gene Set Enrichment Analysis (GSEA) of down-regulated genes in MCF7 and T47D cells (ETV7 vs. Empty). Enrichment plots for Type 1 Interferon response (C) and Type 2 Interferon response (D) were obtained using the Hallmark Collection. Common gene lists obtained from GSEA is shown on the right of the enrichment plots from which they were retrieved. In orange the genes with an FDR < 0.05 and a Fold Change (FC) < -2 in both the cell lines, which were chosen for validation. E-F) RT-qPCR for validation of genes obtained from the lists in panel C and D in MCF7 (E) and T47D (F) Empty and ETV7 cells. Bars represent the averages and standard deviations of at least three biological replicates. * = p-value < 0.05; ** = p-value < 0.01; *** = p-value < 0.001.

host (Figure 17B). We thus performed a gene set enrichment analysis (GSEA) using the Hallmark collection, from which the only commonly significant gene sets enriched were "Interferon_alpha_response" and "Interferon_gamma_response", which refer to the genes that have been involved in the response to type I or type II Interferons (Figure 17C and 17D). From these analyses, we then obtained two short lists of genes significantly down-regulated (FDR < 0.05) in both the cell lines. Notably, most of the genes were common to both the lists, as genes responsive to one type of Interferon are often responsive to other types as well. We next selected for validation by RT-qPCR the genes of the lists whose Fold Change was lower than -2 in both the cell lines, and we were able to confirm the repression of all of them in ETV7 over-expressing MCF7 (Figure 17E) and T47D (Figure 17F) cells over-expressing ETV7, except for CFB gene, whose repression could be proved only in T47D cells.

2.3.2 The genes regulated by ETV7 are differentially responsive to type I-type II IFNs

We then tested the induction of the selected genes upon type I and type II IFN treatment in MCF7 cells, to verify whether these genes can respond differently to the IFN types. In particular, we chose to use IFN-β as type I IFN, given the previous literature data suggesting a role for this IFN in breast cancer stemness [189], and IFN-γ as type II IFN, being the only member of this subfamily. Since ETV7 itself is a well-recognized Interferon-stimulated gene (ISG), we first checked how its expression could be regulated during time in response to IFN-β and IFN-γ in MCF7 cells. We could observe a robust and significant induction of the expression of ETV7 in

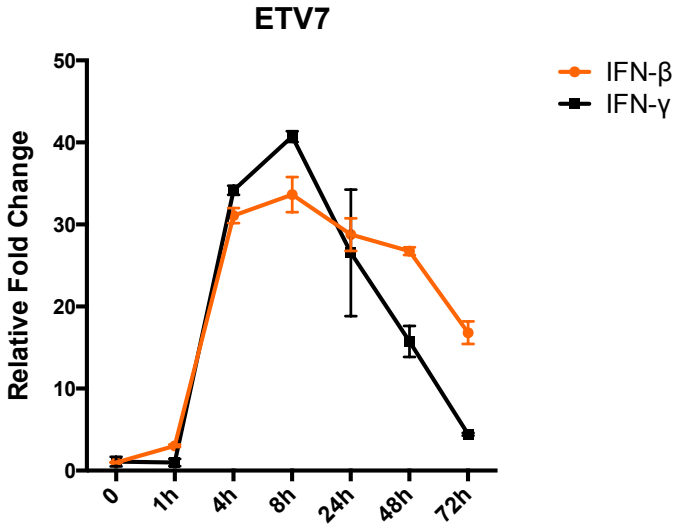

Figure 18. *ETV7 expression is induced in response to IFN-β and IFN-γ in MCF7 cells*. RT-qPCR analysis of normalized ETV7 expression relative to untreated control in MCF7 cells treated with IFN-β (orange) or IFN-γ (black) 5ng/ml at different time points. Bars represent the averages and standard deviations of at least three biological replicates.

response to both types of IFNs, with a peak of induction at 8 hours, confirming that IFN is a strong inducer of ETV7 expression also in breast cancer-derived MCF7 cells (Figure 18). We then analyzed the expression of the genes regulated by ETV7 chosen for validation in response to IFN-β and IFN-γ. Importantly, all the analyzed genes, except for ICAM1, were more strongly induced by IFN-β than by IFN-γ (Figure 19), although some of these genes (i.e. CASP4, APOL6, and CFB) were identified by GSEA as type II, but not type I, Interferon-stimulated genes. Moreover, the kinetics of the response to IFN types was slightly different, with IFN-β inducing the expression of the genes with a peak at 8 hours, whereas IFN-γ stimulated a delayed and more transient induction with a peak at 24 hours.

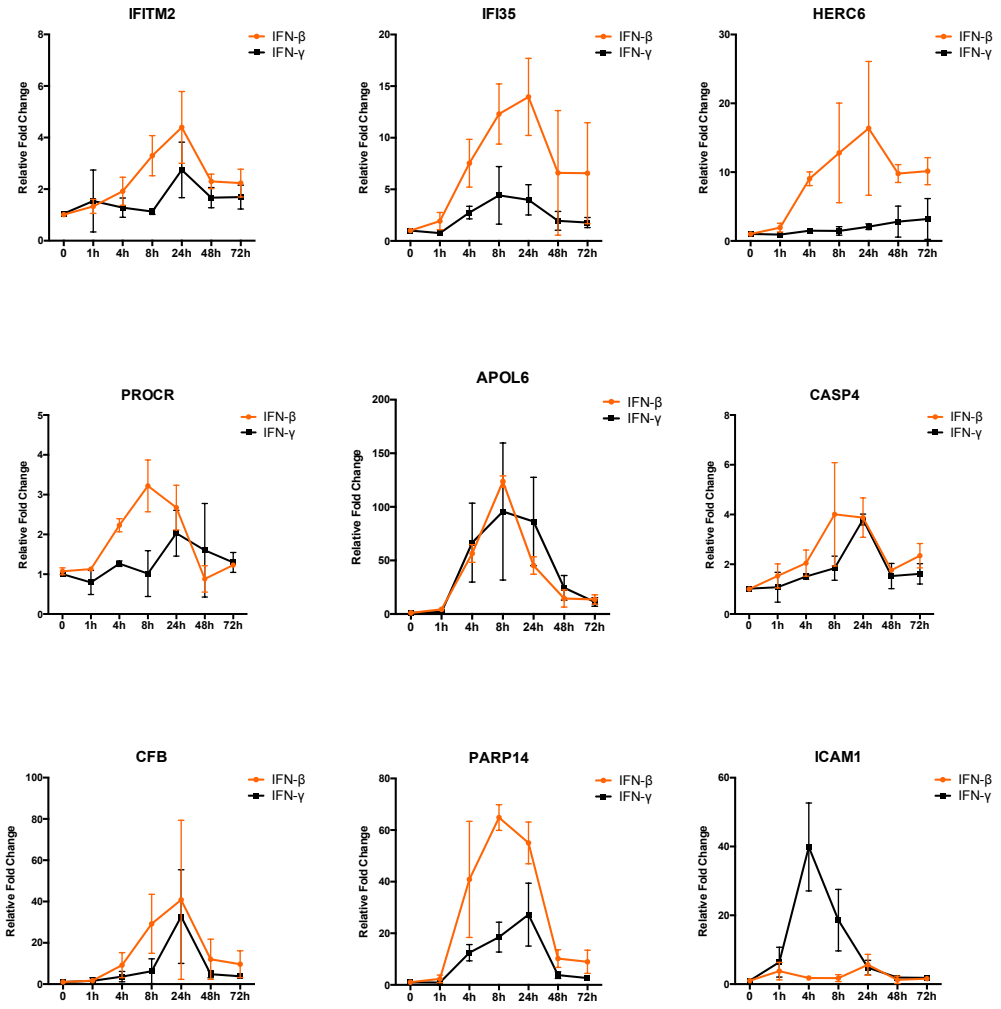

Figure 19. *The genes regulated by ETV7 can respond differently to IFN-β and IFN-γ.* RT-qPCR analysis of the normalized expression of the genes regulated by ETV7 (IFITM2, IFI25, HERC6, PROCR, APOL6, CASP4, CFB, PARP14 and iCAM1) in MCF7 treated with IFN-β (orange) or IFN-γ (black) 5ng/ml at different time points. Bars represent the averages and standard deviations of at least three biological replicates.

2.3.3 IFN treatment partially rescues ETV7-repressed genes expression

We then tested whether the treatment with IFN-β and IFN-γ could rescue the repression determined by ETV7 on the ISGs. We, therefore, treated both MCF7 Empty and MCF7 ETV7 cells with either IFN-β or IFN-γ and checked the expression levels of the ISGs repressed in cells over-expressing ETV7. In ETV7 over-expressing cells the expression of most of the genes (IFI35, HERC6, APOL6, CFB, and PARP14) could still be induced and rescued at the level obtained with Empty cells by treatment with IFN-β, whereas IFN-γ treatment, whose induction of these genes was more transient, could only partially

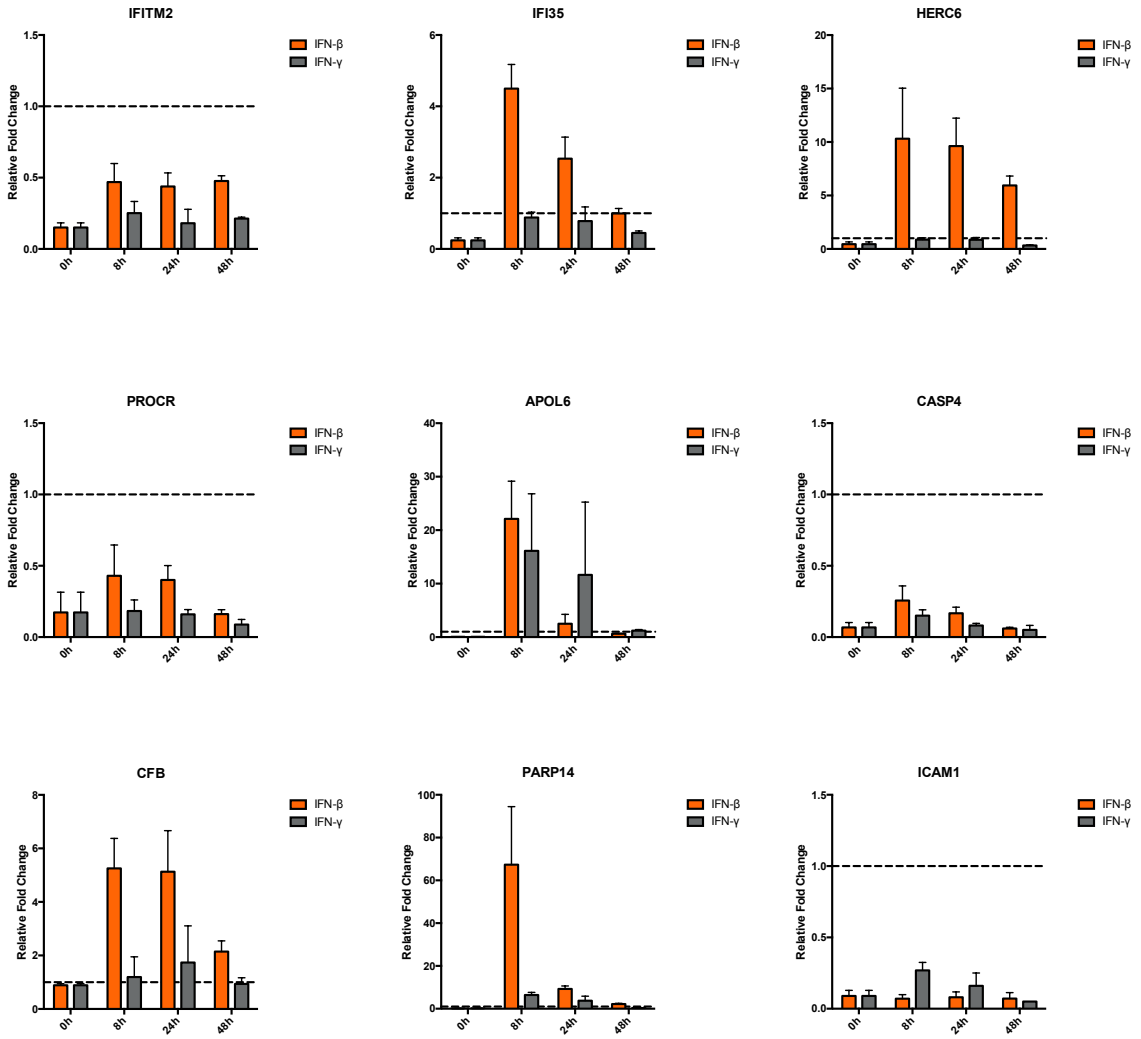

Figure 20. *IFN treatment partially rescues the endogenous expression levels of genes repressed by ETV7 in ETV7 over-expressing cells*. RT-qPCR analysis of ISGs repressed by ETV7 in MCF7 cells over-expressing ETV7 treated with IFN-β and IFN-γ 5ng/ml at different time points. The expression is normalized on housekeeping genes and relative to the expression levels of untreated MCF7 Empty cells (dotted line). Bars represent theaverages and standard deviations of at least three biological replicates.

restore the expression of APOL6, CFB, and PARP14, which were again repressed 48 hours after the treatment (Figure 20).

2.3.4 ETV7 does not alter the STAT1 activation induced by Interferon

STAT1 is well-recognized as an essential component of IFN signalling that, in response to IFN, can bind to the promoter of ISGs and regulate their expression [190].

Given the repression of a set of ISGs in cells over-expressing ETV7, we tested whether this repression might be related to an altered induction of STAT1 expression or its activation. Thus, we analysed the expression of STAT1 protein and its phosphorylation (a modification which mediates its activation and translocation into the nucleus) in MCF7 Empty and ETV7 cells upon IFN-β and IFN-γ treatment. As previously observed [189], a single dose of IFN could cause a rapid and transient induction of phosphorylated STAT1 (p-STAT1), followed by sustained induction of unphosphorylated STAT1 expression (Figure 21). Importantly, the same kinetics and levels of expression were observed in both MCF7 Empty and ETV7 treated with either IFN-β or IFN-γ. This observation suggests that ETV7 over-expression does not alter STAT1 activation, and supports the concept that ETV7 over-expressing cells maintain the responsiveness to IFN-β and IFN-γ, at least for what regards STAT1 activation, possibly indicating that the ETV7-dependent regulation of the previously identified ISGs involves a STAT1-independent mechanism.

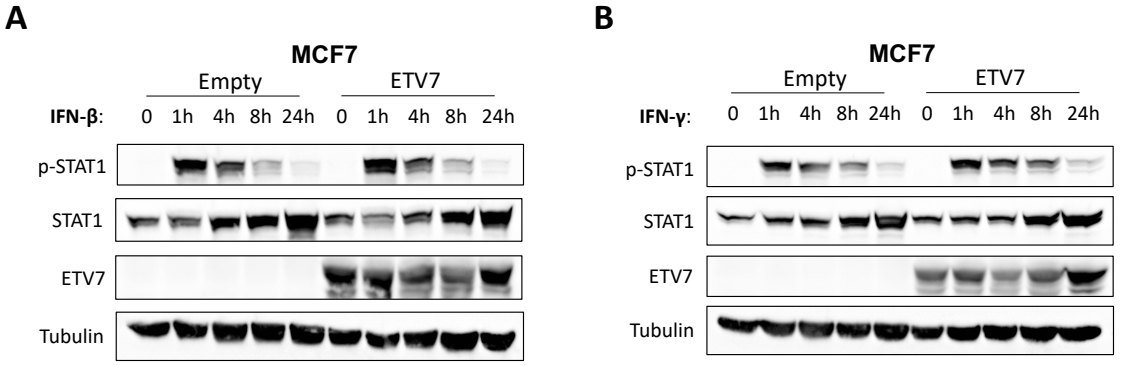

Figure 21. *Activation of STAT1 in response to IFN-β and IFN-γ is not altered in cells over-expressing ETV7*. A-B) Western Blot analysis of phosphorylated and un-phosphorylated levels of STAT1 in MCF7 Empty and ETV7 cells in response to IFN-β (A) and IFN-γ (B) 5ng/ml at different time points. Tubulin served as reference protein.

2.3.5 *IFN-β can revert ETV7-dependent BCSC-like plasticity*

We observed that the over-expression of ETV7 can modulate BCSC-like plasticity in both MCF7 and T47D cells and that the most significant conserved effect at the transcriptional level is represented by the strong repression of a set of IFN-stimulated genes. Therefore, we hypothesized that the repression of these genes might be at least partially responsible

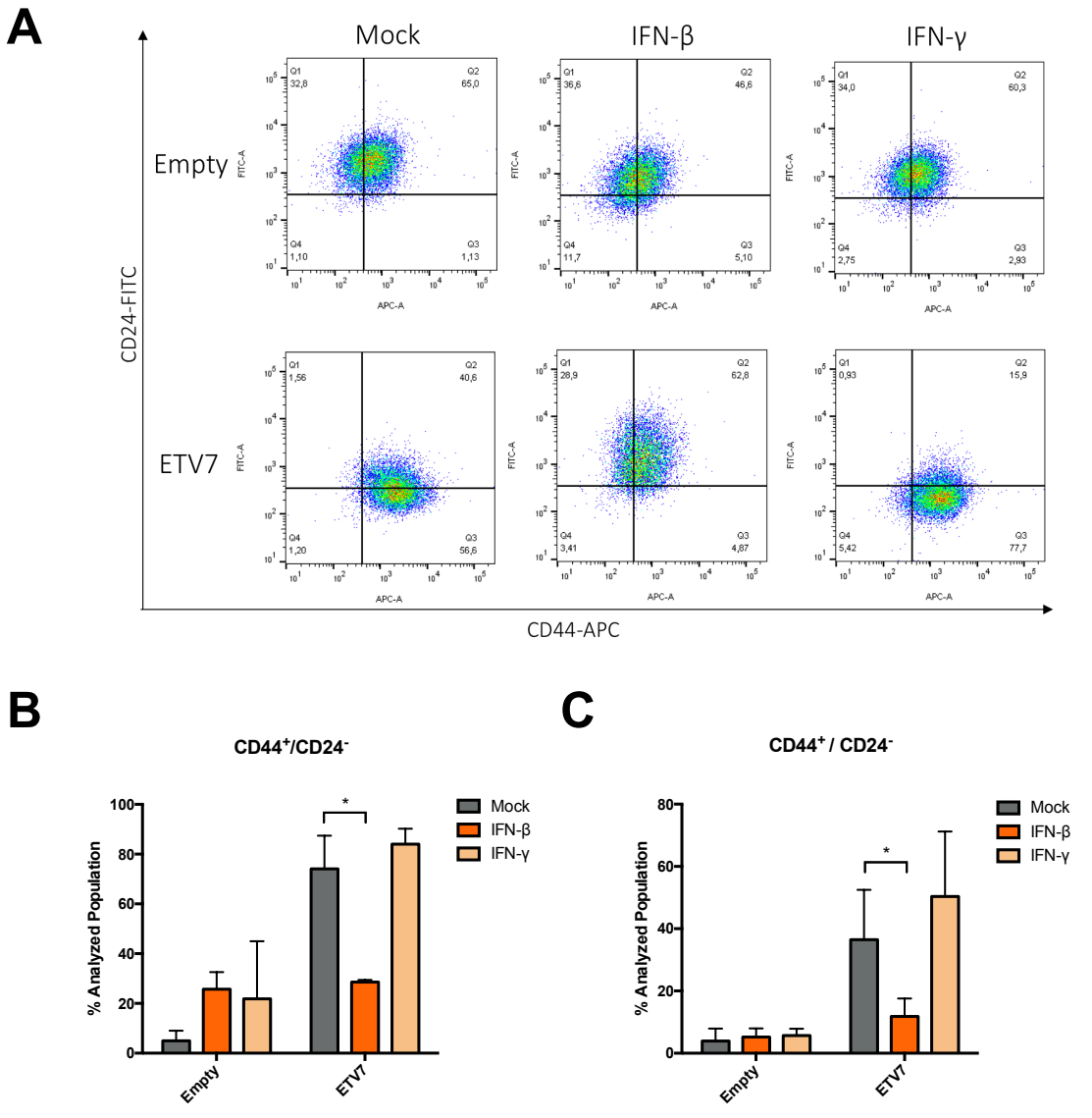

Figure 22. *IFN-β treatment decreases the population of CD44⁺/CD24⁻ cells in MCF7 and T47D cells over-expressing ETV7.* A-C) CD44-APC and CD24-FITC staining and flow cytometry analysis in MCF7 (B) and T47D (A,C) Empty and ETV7 cells treated with IFN-β and IFN-γ 5ng/ml for 2 weeks. A) A representative dot plot of the results obtained at FACS Canto A in T47D. B-C) Histograms summarizing the percentage of CD44⁺/CD24⁻ cells in MCF7 (B) and T47D (C) Empty and ETV7 over-expressing cells. Bars represent the averages and standard deviations of at least three biological replicates. * = p-value < 0.05

for the effects on breast cancer cells stemness. Since we observed that ETV7 over-expressing cells are still responsive to IFN-β and IFN-γ and that the treatment with these cytokines can rescue, at least in part, the expression of the repressed ISGs, we speculated that the treatment with IFN-β and IFN-γ could revert the effects of ETV7 on BCSC-like plasticity.

Thus, we analyzed by flow cytometry the membrane expression of CD44 and CD24 protein in MCF7 and T47D Empty or ETV7 cells treated with IFN-β and IFN-γ for 2 weeks. Notably, IFN-β treatment could significantly revert the increase of $CD44^{+}/CD24^{-}$ cells population observed in ETV7 over-expressing cells, whereas IFN-γ treatment did not influence the abundance of this population (Figure 22).

We then tested the effects of these cytokines on the mammosphere potential of MCF7 Empty and ETV7 cells, and on their ability to be maintained across different passages in culture (Figure 23A and 23B). Again, IFN-β, but not IFN-γ, exerted a potent inhibition of the mammosphere formation ability of MCF7 cells over-expressing ETV7. Moreover, this effect was even more pronounced in the following passages, where IFN-β treatment could completely inhibit the formation of mammospheres (Figure 23C, 23D, and 23E).

In the light of these results, we propose a novel role for ETV7 as a regulator of breast cancer stem cell-like plasticity, which is mediated by the repression of IFN-stimulated genes and that can be reverted by the stimulation of IFN response with IFN-β.

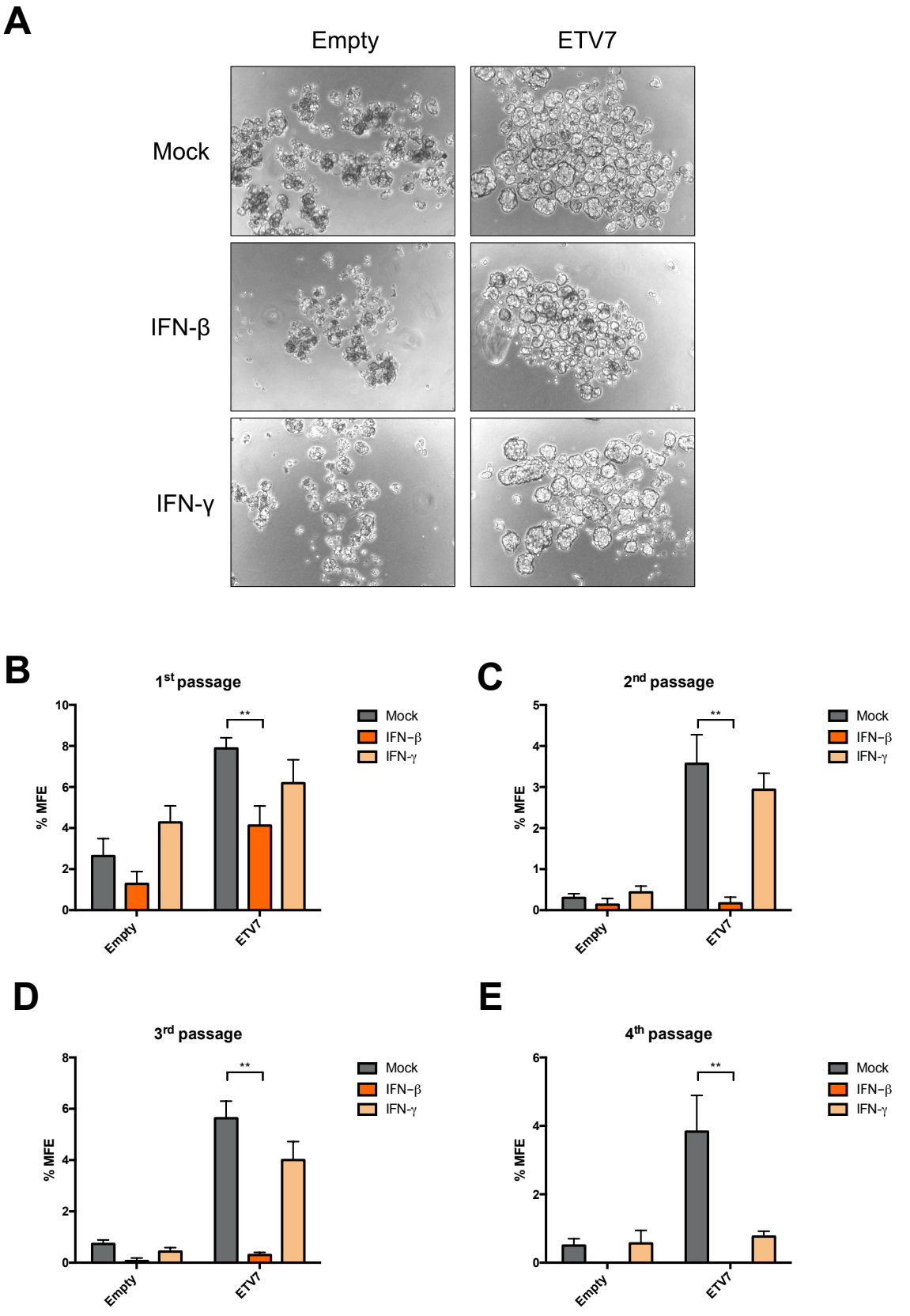

Figure 23. The treatment with *IFN-β inhibits mammosphere formation potential of MCF7 cells over-expressing ETV7*. A) A representative image of first generation mammospheres obtained from MCF7 Empty or MCF7 ETV7 cells in response to the treatment with IFN-β or IFN-γ 5ng/ml. B-E) Percentage of first (B), second (C), third (D) and fourth (E) generation mammosphere formation efficiency (%MFE) in MCF7 Empty and ETV7 cells in response to IFN-β or IFN-γ 5ng/ml calculated as number of mammospheres per well/number of cells seeded per well X 100. Bars represent the averages and standard deviations of at least three biological replicates. ** = p-value < 0.01.

3. ETV7 knock-down induces p53-dependent apoptosis

In this last part of the study, we analyzed the effects of ETV7 knock-down on cell viability using siRNAs targeting ETV7 expression. The following experiments here presented are still preliminary and might pave the way for subsequent studies focusing on ETV7 targetability in breast cancer.

3.1 The knock-down of ETV7 in MCF7 cells results in apoptotic cell death

Given the observed effects of the over-expression of ETV7 on chemo- and radio-sensitivity of breast cancer cells, and on breast cancer stem-like cells population, we decided to investigate the effects of ETV7 knock-down in breast cancer cells. If the over-expression of ETV7 is able to confer the cells some pro-tumorigenic features (i.e. survival to therapy and stemness-like features), its targeting might possibly represent a therapeutic approach

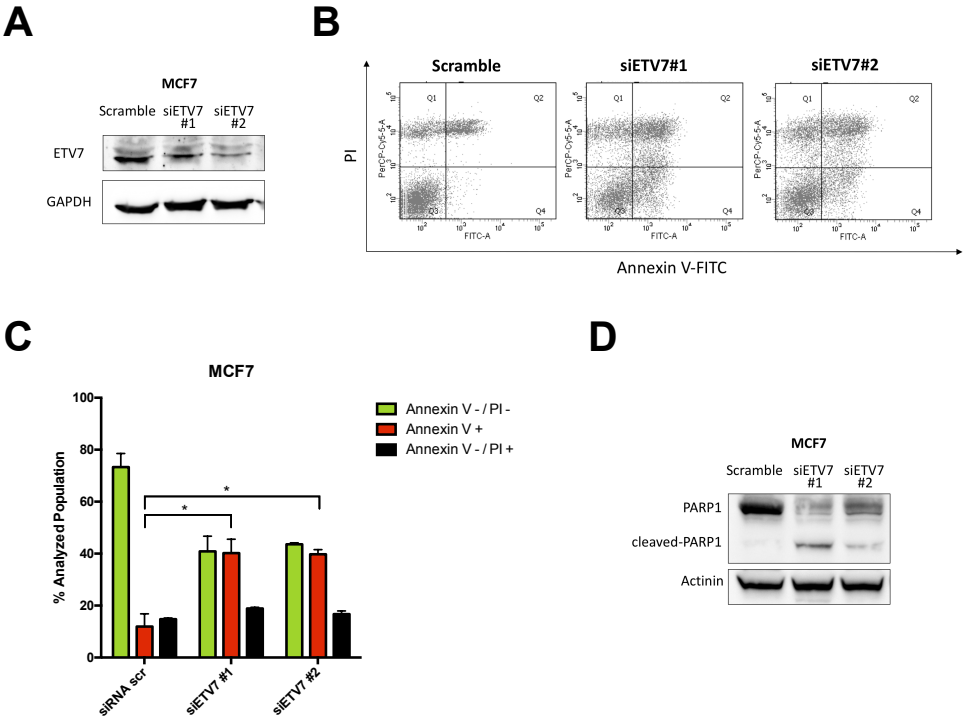

Figure 24. *ETV7 knock-down induces strong apoptosis in MCF7 cells*. A) Western Blot analysis of ETV7 expression in MCF7 cells transfected with siRNAs against ETV7 (siETV7#1 and siETV7#2) or the relative Scramble control for 72 hours. B and C) AnnexinV-FITC/PI staining and flow cytometry analysis of MCF7 transfected with siRNA against ETV7 (siETV7#1 and siETV7#2) or the relative Scramble control for 72 hours. B) Representative dotplots of the flow cytometry analysis. C) Quantification of the flow cytometry experiments represented in panel B. D) Western Blot analysis of PARP cleavage in MCF7 cells transfected with siRNAs against ETV7 (siETV7#1 and siETV7#2) or the relative Scramble control for 72 hours. Bars represent the averages and standard deviations of at least three biological replicates. * = p-value < 0.05.

for breast cancer. Thus, we performed a knock-down experiment in MCF7 cells with two differently designed siRNAs targeting ETV7. We first confirmed their efficacy by analyzing the protein expression of ETV7 (Figure 24A), and we then tested their effect on cell viability. Interestingly, the knock-down of ETV7 induced massive apoptosis in MCF7 cells, which could be confirmed both by Annexin V/PI analysis at FACS (Figure 24B and 24C) and PARP cleavage detection by western blot (Figure 24D).

3.2 The knock-down of ETV7 does not induce apoptosis in MDA-MB-231 cells

We, therefore, tested whether the same effect could be reproduced in a more aggressive breast cancer cell line, such as MDA-MB-231 triple negative BC-derived cells. However, ETV7 knock-down did not affect the viability of the cells in this cell line, which showed no increase in the number of apoptotic cells (Figure 25). Similar results could also be obtained in T47D and SK-BR-3 cells, whose viability was not affected by ETV7 silencing (data not shown).

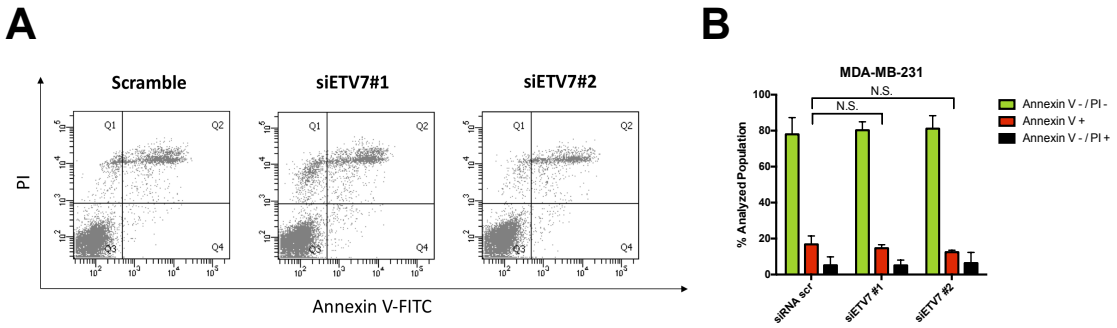

Figure 25. *ETV7 knock down does not induce apoptosis in MDA-MB-231 cells*. A-B) AnnexinV-FITC/PI staining and flow cytometry analysis of MDA-MB-231 cells transfected with siRNAs against ETV7 (siETV7#1 and siETV7#2) or the relative Scramble control for 72 hours. A) Representative dotplot of flow cytometry analysis. B) Quantification of the flow cytometry experiments represented in panel A. Bars represent the averages and standard deviations of at least three biological replicates. N.S. = not statistically significant.

3.3 The induction of apoptosis caused by ETV7 knock-down in MCF7 cells is p53-dependent

Since only MCF7 cells, among the BC-derived cell lines tested, were undergoing apoptosis upon the silencing of ETV7, we looked for genetic differences among the cell lines that might be responsible for this cell line-specific apoptosis. Since MCF7 cells expressed a wild type p53, whereas the other cell lines were p53 mutated, we hypothesized that the

apoptosis caused by ETV7 knock-down might be p53-dependent. Indeed, one of the most important functions of p53 is its ability to control the induction of apoptosis [191].

We first checked whether the silencing of ETV7 in MCF7 cells affected p53 expression, and we observed a strong p53 accumulation in response to ETV7 silencing in MCF7 cells (Figure 26A). Therefore, we tested whether p53 was responsible for the observed induction of apoptosis. We thus double-transfected MCF7 cells with a siRNA against p53 first, and siRNAs against ETV7 later or their relative Scramble controls and checked for the induction of apoptosis. We first confirmed the partial silencing of p53 (Figure 26B), and we then tested the induction of apoptosis by Annexin V/PI analysis. Interestingly, we observed that, knocking down p53 before ETV7 was able to inhibit the induction of apoptosis caused by ETV7 deficiency in MCF7 cells (Figure 26C and 26D), suggesting that the expression of ETV7 is needed for cell survival only in a p53 wild type context. However, further experiments using other BC, and non-BC, cell lines will be required to confirm these

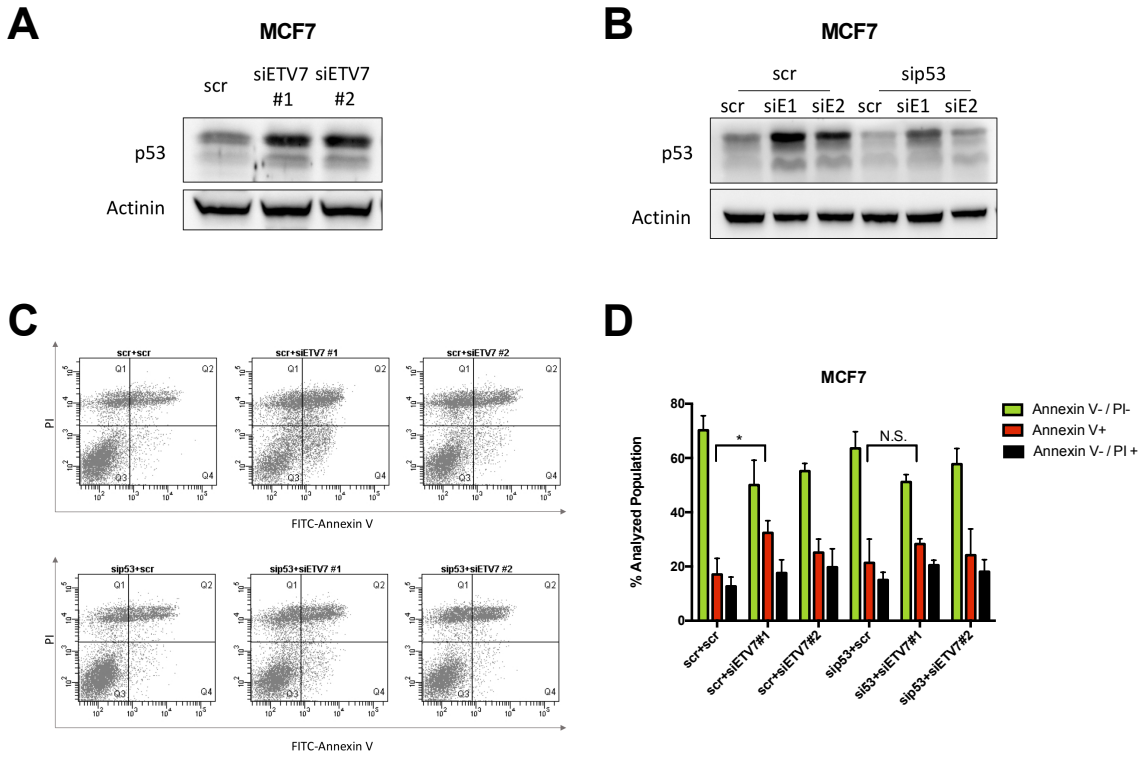

Figure 26. *Apoptosis induced by ETV7 knock-down in MCF7 cells is p53 dependent*. A) Western Blot analysis of p53 expression in MCF7 cells transfected with siRNA against ETV7 (siETV7#1 and siETV7#2) or the relative Scramble control for 72 hours. B) Western Blot analysis of p53 expression in MCF7 cells co-transfected with siRNA against p53 or relative Scramble control for 96 hours and against ETV7 (siETV7#1 and siETV7#2) or the relative Scramble control for 72 hours. C-D) AnnexinV-FITC/PI staining and flow cytometry analysis of MCF7 transfected with siRNA against p53 (sip53) or ETV7 (siETV7#1 and siETV7#2) or the relative Scramble controls for 96 and 72 hours respectively. C) Representative dotplot of flow cytometry analysis. D) Average replicates analysis of flow cytometry experiments Bars represent the averages and standard deviations of at least three biological replicates. N.S. = not statistically significant; * = p-value < 0.05.

observations. Moreover, the mechanisms by which ETV7 knock-down causes p53 activation are still to be elucidated.

DISCUSSION

ETV7 is a poorly studied transcriptional repressor of the ETS family of transcription factors, which is mainly considered as an oncoprotein [134,192]. ETV7 is well-recognized as Interferon (IFN)-stimulated gene (ISG) [126,127], and it was previously showed that its expression could be synergistically induced by the combined treatment with the chemotherapeutic drug Doxorubicin and the inflammatory cytokine TNFα in the breast cancer-derived cell line MCF7 [125]. Recently, it was shown that the expression of ETV7 is significantly higher in breast cancer tissues compared to normal breast [138], suggesting a possible role for ETV7 in breast cancer pathogenesis; however, the functions and impact of ETV7 expression in breast cancer were still to be elucidated.
In this work, we studied the effects of altered ETV7 expression on breast cancer progression and resistance to conventional anti-cancer drugs.

In the first part of this project, we showed that the increased expression of ETV7 in MCF7 cells can decrease the sensitivity of the cells to Doxorubicin, and we identified DNAJC15 as a novel target of ETV7 partially responsible for this effect. Firstly, we observed that ETV7 expression could be induced by different stimuli, in particular by the treatment with chemotherapeutic drugs able to cause DNA damage, whereas its expression was not affected by other types of anti-cancer agents treatments, such as Tamoxifen (estrogen antagonist), Imatinib (tyrosine kinase inhibitor) or Everolimus (mTOR inhibitor) (Figure 1). This observation is in accordance with previous data showing that p53 is a direct regulator of ETV7 expression [125], as all of the drugs inducing the expression of ETV7 are also known to activate p53 in the p53 wild-type MCF7 cell line. However, the expression of ETV7 could still be induced upon the same treatments, even if less strongly, also in the MDA-MB-231 breast cancer-derived cell line, which expresses a mutated form of p53 [193]; thus, other pathways may be involved in ETV7 induction. Since ETV7 is known to be an Interferon-stimulated gene, and we showed that its expression is strongly induced by Interferon

treatments in MCF7 cells, we may speculate that its activation in response to the chemotherapeutic treatments mentioned above may be due to the production of type I IFN, which is well known to be induced upon DNA damage [173,194]; however, further investigations would be needed to determine the contribution of IFN signaling to the chemotherapy-dependent induction of ETV7 expression.

We then demonstrated that the stable over-expression of ETV7 in MCF7 cells was able to decrease the sensitivity of the cells to Doxorubicin, the most potent inducer of ETV7 expression among the ones tested, and that it was accompanied by an increase in the expression of some ABC transporters frequently responsible for chemoresistance in breast cancer (i.e. ABCB1, ABCC1, and ABCG2) (Figure 2). We then investigated the possible mechanism responsible for ETV7-dependent resistance to Doxorubicin. Being ETV7 known as a transcription factor, we looked for putative ETV7 targets that could mediate the increased resistance, and we identified DNAJC15, a co-chaperone protein whose repression was previously associated with drug resistance and ABCB1 increased expression in breast cancer [180] (Figure 3). We pinpointed the binding site of ETV7 within *DNAJC15* promoter, located at +377 bp from the TSS, and we demonstrated its direct binding (Figure 4). Furthermore, we identified DNA methylation as a putative mechanism of transcriptional repression exerted by ETV7 on the *DNAJC15* promoter.

Since DNAJC15 was reported to be frequently repressed through hyper-methylation of the promoter in cancer [180], we investigated whether the repression of DNAJC15 driven by ETV7 could involve the same mechanism. Therefore, we mapped the methylation status of the CpGs localized near the ETV7 binding site within *DNAJC15* promoter, and we observed a slight increase in methylation upon Doxorubicin treatment while a stronger hyper-methylation was observed in ETV7 over-expressing cells (Figure 5). Moreover, we confirmed the methylation dependency of the ETV7-mediated repression of DNAJC15 with the DNA Methyltransferase (DNMT) inhibitor (5-Aza) treatment, which was able to revert the inhibition of DNAJC15 expression. Furthermore, we propose that this hyper-methylation might be due to the recruitment of DNMT3A on the *DNAJC15* promoter, given the observed physical interaction between ETV7 and DNMT3A (Figure 5).

We finally confirmed the contribution of DNAJC15 to the ETV7-mediated resistance to Doxorubicin by performing a rescue experiment in which we over-expressed DNAJC15 in

ETV7 over-expressing cells, and we showed the partial rescue of Doxorubicin sensitivity in these cells (Figure 6).

We thus propose a model for this new mechanism of Doxorubicin resistance in breast cancer, in which ETV7 plays a major role. According to our model, the increased expression of ETV7, which is itself driven by Doxorubicin treatment, can negatively regulate the expression of DNAJC15, which results in the increased resistance to Doxorubicin. The proposed mechanism of repression involves the direct binding of ETV7 to *DNAJC15* promoter, where ETV7 can recruit DNMT3A, which enhances the promoter methylation, thereby resulting in transcriptional repression (Figure 27).

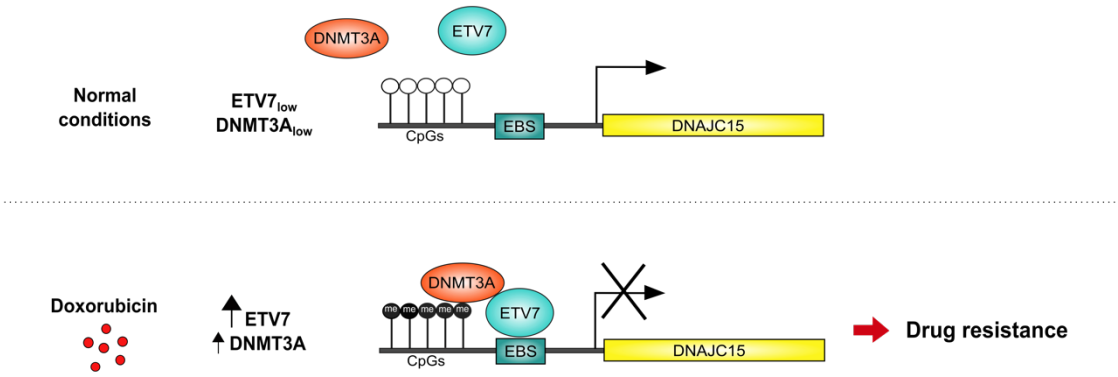

Figure 27. *Schematic representation of the proposed model for ETV7-dependent resistance to Dpxorubicin in breast cancer cells* [193]. Under normal conditions, ETV7 and DNMT3A are kept at basal levels and DNAJC15 is regularly expressed. Upon Doxorubicin treatment, the expression of ETV7 is strongly induced, with DNMT3A slightly increasing as well. ETV7 can then bind to chromatin in the region of the *DNAJC15* promoter, where it recruits, through direct interactions with putative additional cofactors, DNMT3A, that is in turn responsible for the CpGs methylation. This process results in DNAJC15 repression and ultimately leads to the resistance to Doxorubicin. EBS: ETV7 Binding Site. Methylated CpGs are shown as black-filled circles, whereas unmethylated CpGs as white-empty circles.

In the light of our findings, we uncovered a novel molecular mechanism that might explain the acquired resistance to the standard-of-care treatment for breast cancer Doxorubicin, which involves ETV7, DNMT3A, and DNAJC15, all of which have the potential for pharmacological targeting. Furthermore, our data provided the first evidence for a role of ETV7 in the resistance to a chemotherapeutic drug in BC cells.

In the second part of this study, we observed that the decreased drug sensitivity observed in MCF7 cells over-expressing ETV7 is not limited to Doxorubicin, but is also valid for 5-FU treatment. We confirmed the increased resistance to 5-FU also in another luminal breast cancer model using the T47D cell line, and we observed a decreased rate of apoptosis in

ETV7 over-expressing cells treated with 5-FU compared to the empty control (Figure 7). Notably, similar results could be obtained by treating the cells with a different anti-cancer therapy: radiotherapy (Figure 8). This enhanced resistance to chemo- and radiotherapy can be partially explained by the increased expression of the anti-apoptotic proteins BCL-2 and Survivin, and by the decreased proliferative potential observed in ETV7 over-expressing cells, since both 5-FU and radiotherapy efficacy depend on cell division (Figure 9). Indeed, the observed increase in the expression of ABC transporters and anti-apoptotic proteins, together with the decreased cell proliferation, are common drug resistance-associated properties [60,65,68].

Interestingly, we observed that the proliferation rate of the cells underwent a switch when the cells were grown in an anchorage-independent manner. In fact, the soft agar colony formation potential of the cells was significantly higher in ETV7 over-expressing cells compared to the empty counterpart, whereas the opposite behavior was observed when the colony formation efficiency was measured on plastic-support (Figure 9). This observation suggests a flexible behavior of the cells over-expressing ETV7, which can adapt their proliferative potential to the environmental conditions. Moreover, anchorage-independent growth is a pro-tumorigenic feature [195], suggesting that the over-expression of ETV7 may drive pro-tumorigenic effects in breast cancer cells.

Given these observations in ETV7 over-expressing cells, and the literature data reporting anti-differentiation roles for ETV7 [139], we hypothesized that the altered expression of ETV7 could affect the breast cancer stem cells population.

Indeed, cancer stem cells (CSCs) are known to be chemo- and radioresistant [196], and usually present all the features we observed in ETV7 over-expressing cells. Thus, we analyzed some of the commonly used markers for breast CSCs detection, which can be represented by $CD44^{+}/CD24^{low}$ population and/or cells with enhanced activity of ALDH protein. We found that ETV7 expression could exert a remarkable effect on breast cancer stem-like cells, with a massive increase in $CD44^{+}/CD24^{low}$ population in both MCF7 and T47D cells over-expressing ETV7 (Figure 10). Importantly, we observed that the ETV7-dependent effect on this population was true in both directions, as knocking-down ETV7 expression in the triple negative breast cancer cell line MDA-MB-231 was able to decrease the membrane expression levels of CD44 (Figure 11). Thus, tuning the expression levels of ETV7 can modulate the content of $CD44^{+}/CD24^{low}$ cells in breast cancer cells, suggesting a

novel role for ETV7 in breast cancer stem cells plasticity. Given the debated reliability of CD44 and CD24 as BCSCs markers [197], we measured another commonly recognized property of BCSCs: the ability to grow as spheres (called mammospheres) when grown in non-adherent and non-differentiating conditions. Also with this method, we could observe a substantial increase in the mammosphere formation efficiency of MCF7 cells over-expressing ETV7, which was further supported by the ability to propagate mammospheres by sequential passages in culture (Figure 12).

We then analyzed the metabolic phenotype of ETV7 over-expressing cells, as several publications reported an increase of the OXPHOS dependency in cancer stem cells [198–207]. Interestingly, we could observe an increase in the oxygen consumption rate (a measure related mainly to the mitochondrial respiration) in ETV7 over-expressing cells, whereas no significant differences could be observed in the extracellular acidification rate (glycolytic rate) of the cells under basal condition (Figure 13). A deeper investigation of the mitochondrial parameters affected revealed that ETV7 over-expressing cells present significantly higher basal and maximal respiration compared to the parental cells (Figure 14), suggesting that cells over-expressing ETV7 may rely more on OXPHOS compared to the relative control. These data are in agreement with previous literature data which observed the same phenotype in breast cancer stem cells [198–207], even though few publications reported an increased glycolytic rate in cancer stem cells [208–210]. Nevertheless, these contradictory data can possibly support the idea of cancer stem cells behavior as plastic and adaptable to external conditions, and further studies are needed to fully explain the relation of cancer stem cells and metabolism. Therefore, a more in-depth investigation of the metabolic alterations observed in ETV7 over-expressing cells might provide a rationale for targeting the ETV7 network in cancer cells.

Breast cancer stem-like cells are also frequently characterized by increased migratory and invasive potential [211]. We thus analyzed the motility of ETV7 over-expressing cells, and we could appreciate a significant increase in their migratory ability in MCF7 cells, which was accompanied by the slight, but significant, enhanced expression of the mesenchymal markers SNAIL and TWIST, together with a strong increase in the invasive marker MMP9 (Figure 15).

To test whether ETV7 could have pro-tumorigenic potential also *in vivo,* we generated ETV7 over-expressing MCF7 and T47D cells stably expressing a nuclear GFP and injected

them into the yolk of zebrafish embryos. However, the limited time available for the experiment was not sufficient to appreciate any difference in the number of cells, as, possibly, the proliferation of the cells was too slow (Figure 16). To appreciate any possible difference, further experiments with longer cell tracking time would be needed. Moreover, to confirm the self-renew capacity *in vivo*, we should perform a serial transplantation experiment. However, the use of immunocompromised mouse models would be more appropriate for this type of experiments.

In the meantime, in order to investigate genome-wide the mechanisms responsible for the effects of ETV7 observed in culture, we performed an RNA-seq analysis on MCF7 and T47D cells over-expressing ETV7 and the relative controls. In fact, ETV7 is mainly known for its functions as a transcription factor, and we thus expect it to mediate the observed biological effects by transcriptional regulation, even though Harwood and colleagues have recently shown a novel function of ETV7 exerted in the cytoplasm, which is independent on its transcriptional activity [137]. Since ETV7 is known to act as a transcriptional repressor, we focused our analysis mainly on the commonly down-regulated genes in MCF7 and T47D cells over-expressing ETV7. Interestingly, the enrichment analysis revealed significant repression of a signature of Interferon-stimulated genes (ISGs) (Figure 17).

Therefore, we hypothesized that, if ETV7 exerts its effect on breast cancer stem cell plasticity via the repression of IFN response genes, stimulating the re-expression of these genes in the cells might possibly revert the observed effects. We thus selected IFN-β and IFN-γ as representative of type I and type II IFN respectively, and tested the responsiveness of the obtained signature of ISGs in MCF7 cells. Interestingly, despite the fact that several genes were classified by GSEA as type II ISGs, almost all of the analyzed genes were more responsive to IFN-β than to IFN-γ (Figure 19), and IFN-β treatment could rescue the parental expression levels of most of the tested genes (Figure 20). Since ETV7 is also known to be an ISG, we examined its activation in response to IFN-β and IFN-γ in MCF7 cells, and we confirmed its robust induction upon both the treatments (Figure 18), suggesting that ETV7 could play a role in the IFN response as a negative feedback regulator of this pathway. However, ETV7 expression did not affect STAT1 induction in response to IFN treatment, suggesting that the repression of the ISGs may act independently, or possibly downstream, on STAT1 activation (Figure 21). Interestingly, other ETS family members, among which the ETV7-closely related ETV6, were previously shown to

physically interact with protein members of the Interferon regulatory factors (IRF) family and play a role in the regulation of Interferon-responsive genes [212,213]. Thus, another possible mechanism by which ETV7 regulates the transcription of interferon stimulated genes, might involve the binding to their transcriptional regulatory regions, or the binding to other proteins which regulate their transcription. However, further experiments would be needed to test these hypothesis.

Finally, we tested the effects of IFN-β and IFN-γ treatment on the CSC-like population. Interestingly, we showed that the prolonged treatment of the cells with IFN-β, but not with IFN-γ, was able to rescue the effects on CSCs content analyzed by CD44 and CD24 membrane expression (Figure 22). Moreover, IFN-β treatment was also able to revert the first and subsequent generations mammospheres formation ability of MCF7 cells over-expressing ETV7 (Figure 23). The fact that IFN treatment, and in particular IFN-β, but not IFN-γ, can revert the observed effects on CSC plasticity, supports the hypothesis that ETV7 mediates its functions via the repression of ISGs, as IFN-β is a stronger inducer of the ETV7-repressed genes compared to IFN-γ. Our results support the observations made in previous studies, which showed that immune-repressed triple-negative breast cancers lacking endogenous IFN signaling were highly recurrent, therapy-resistant and characterized by CSC-like features [171,214]. Moreover, Doherty and colleagues, recently showed that the treatment with IFN-β, which was able to restore the IFN signaling, could revert the CSCs properties observed in transformed mammary epithelial cells, suggesting it as a potential therapeutic approach for TNBC treatment [189]. Our data strengthen the validity of these data and provide a novel role for ETV7 in breast cancer stem-like cell plasticity.

Given these results, we finally investigated the possibility of ETV7 targeting in breast cancer cells. We tested the effects of ETV7 knock-down in MCF7 cells, and we observed a strong induction of apoptosis (Figure 24). However, the same effect was not observed in the other BC cell lines tested (Figure 25). We finally showed that the induction of apoptosis following ETV7 knock-down was dependent on p53 activity, as silencing p53 could revert the induction of apoptosis (Figure 26).

These preliminary results suggest that ETV7 is fundamental for survival in MCF7 cells, when p53 is active, whereas it is not required for survival when p53 is mutated. Since the mutation of p53 is a frequent event in breast cancer patients [215], whereas it is usually not occurring in normal breast tissue, we might speculate that the direct targeting of ETV7 may not be a suitable option for breast cancer treatment, as it might affect the viability of normal mammary epithelial cells as well and be less efficient on p53 mutated BCs. However, further investigation is needed to test this concept.

CONCLUSION AND FUTURE PERSPECTIVES

Taken collectively, our data revealed that the altered expression of ETV7 can affect the sensitivity of BC cells to some anti-cancer agents (i.e. Doxorubicin, 5-FU, and radiotherapy) and that it may accomplish this task by modulating the breast cancer stem cells plasticity. Particularly, by transcriptomic analysis, we identified the molecular mechanism that mediates this effect in the repression of a signature of Interferon-stimulated genes. Being ETV7 itself an ISG, we also uncovered a novel putative negative feedback regulatory mechanism of the Interferon signaling. Since timing is a crucial factor in the IFN response signaling, ETV7 might normally act in this signaling pathway to attenuate the IFN response. However, when the expression of ETV7 is not due to a transient IFN stimulation, but it is maintained high (a condition frequently observed in some cancer tissues), this may cause the prolonged repression of the ISGs that it regulates, which can result in the induction of a CSC-like status in breast cancer cells. We finally showed that the re-induction of these ISGs by prolonged treatment with IFN-β could revert this status. Therefore, we propose a novel role for ETV7 in breast cancer stem cell plasticity, which involves the regulation of IFN response genes. Finally, we showed that ETV7, which is usually expressed at low levels, is necessary for cells survival in p53 wild type MCF7 cells since its silencing can induce tremendous apoptosis. However, the viability of p53 mutated cell lines is not affected by ETV7 knock-down. Since T47D is a p53 mutated BC cell lines, whereas MCF7 is a p53 wild type cell lines, the effects observed in ETV7 over-expressing cells on chemotherapy resistance, on BCSC-like plasticity, and on ISGs regulation seem to be independent on the p53 status, as they can be reproduced in both the cellular systems. Thus, targeting the molecular pathways activated by ETV7, such as IFN signaling, may represent a better option compared to a direct ETV7 targeting.

In conclusion, this work provided evidence for a novel role of ETV7 in resistance to chemotherapy and breast cancer stem-like cells plasticity.

Nevertheless, several further experiments could be performed for a more comprehensive understanding of the phenomenon observed.

Firstly, the cancer stem-like cells properties acquired by BC cells over-expressing ETV7 should be confirmed also *in vivo*. As previously mentioned, a serial transplantation experiment in immunocompromised mice might be needed to demonstrate the self-renew capacity of the BCSC-like cells. Moreover, we showed that the ETV7 knock-down can affect the membrane expression of CD44 in MDA-MB-231 cells; however, this mechanism needs further investigations. Since prolonged ETV7 repression should be more efficient in affecting BCSC-like plasticity, we might generate ETV7 knock-out or stable knock-down cells and perform other experiments to characterize them, such as mammosphere formation efficiency, expression of ABC transporters, anti-apoptotic proteins, as well as *in vivo* transplantation experiments.

Furthermore, the molecular mechanism by which ETV7 can repress the signature of ISGs needs further investigation. In fact, ETV7 might repress the ISGs in a direct way, by acting as a transcriptional repressor, or it may affect their transcriptional regulation indirectly. We observed no differences in STAT1 induction upon IFN treatments in ETV7 over-expressing cells; however, ETV7 may regulate its activity or may affect the expression or the activity of other IFN signaling mediators, such as other STAT proteins or other pathways, such as PI3K/AKT or NF-κB.

We also showed that long term treatment with IFN-β, but not IFN-γ, could reduce the population of $CD44^{+}/CD24^{low}$ cells and the mammosphere formation efficiency. This may suggest the use of IFN-β as a therapeutic approach for breast cancer treatment. We showed that IFN-β was a stronger inducer of the tested ISGs repressed by ETV7 compared to IFN-γ, however, other types of IFNs may be even more efficient, and should, therefore, be tested. A global analysis of the effects of all the IFN subtypes on ETV7 over-expressing cells could thus allow the identification of putative treatment options for breast cancer. In addition, since the over-expression of ETV7 could induce the resistance to treatment, a possible combinatorial approach of Doxorubicin, 5-FU, radiotherapy or other treatments with IFN-β could be tested to target ETV7 over-expressing cells.

Finally, we uncovered a novel role for ETV7 in IFN response regulation, in which it can act as a negative feedback regulator. Given the central role of IFN response in the immune

regulation, ETV7 may play a role in immunity as well. Thus, exploring how ETV7 over-expression affects the immune-recognition of cancer cells, may represent a possible future direction inspired by this work. Moreover, it would be interesting to analyze the effects of ETV7 over-expression also in immune cells, to test whether the repression of ISGs expression could be conserved in this cell type and to study its effects.

In addition, IFN signaling plays its defining functions in antiviral response, and ETV7 was already shown to be up-regulated following HCV infection in hESCs-derived hepatocytes [130]. Given the observed effects of ETV7 in the negative feedback regulation of IFN signaling, its increased expression may represent an advantage for viruses infecting cells. However, a better understanding of the role of ETV7 in the IFN response and studying the effects of host cells' altered ETV7 expression on viral infectivity may elucidate the role of ETV7 in the antiviral response.

Finally, since ETV7 shares several structural and functional similarities with the other ETS family members, it could be interesting to understand whether the biological and molecular effects of ETV7 may be regulated by a crosstalk with other ETS proteins. The ETS family proteins have been mainly studied in prostate cancer and hematological malignancies, but some family members are emerging to play a crucial role in breast cancer tumorigenesis as well. In particular, similarly to ETV7, ETS1 was found to be involved in breast cancer tumorigenesis, promoting EMT and invasiveness [104,216] and ETV4 has been suggested as a breast cancer therapeutic target, given its involvement in tumor aggressiveness, motility and invasiveness [217–219]. Moreover, as previously mentioned, other ETS proteins have already been shown to regulate the transcriptional activity of interferon stimulated genes through protein-protein interaction or DNA binding [212,213]. Given their shared structural domains and similar DNA binding motifs, the investigation of the involvement of other ETS proteins in ETV7 functions and target genes regulation might be of particular interest.

In conclusion, this work supports the value of a better characterization of ETV7 and the other ETS family members in breast cancer.

METHODS

Cell lines and culture conditions

MCF7 cells were obtained from Interlab Cell Line Collection bank (Genoa, Italy), T47D cells were received from Dr. U. Pfeffer (National Institute for Cancer Research, Genoa, Italy), HEK293T cells were a gift from Prof. J. Borlak (Hanover Medical School, Germany), while MDA-MB-231 cells were a gift from Prof. A. Provenzani (CIBIO, University of Trento, Italy). MCF7, T47D, and HEK293T cells were grown in DMEM medium (Gibco, Thermo Fisher Scientific, Milan Italy) supplemented with 10% FBS (Gibco), 2mM L-Glutamine (Gibco) and a mixture of 100U/ml Penicillin / 100μg/ml Streptomycin (Gibco). MDA-MB-231 cells were cultured in the same medium with the addition of 1% Non-Essential Amino acids. Cells were grown at 37°C with 5% CO_2 in a humidified atmosphere.

Treatments

Doxorubicin (Sigma-Aldrich, Milan, Italy) and 5-FluoroUracil (5FU) were used at different concentrations and for different times based on the experiment. Treatments with the following drugs were performed for 24 hours: Etoposide 50μM (Enzo Life Science, Rome, Italy), Nutlin-3a 10μM, Camptothecin 0.5μM, Everolimus 50 nM, Paclitaxel 1 μM (Selleckchem, Aurogene, Rome, Italy), Tamoxifen 1μM, Imatinib 3μM (Selleckchem). 5-Aza-2'-deoxycytidine treatment was performed for 48 hours at the concentration of 5 μM. Recombinant human IFN-β and IFN-γ (Peprotech, Tebu-Bio, Milan, Italy) were used at different concentrations and for different times based on the experiment. Compounds were purchased from Sigma-Aldrich when not specifically indicated. Radiation treatment was performed using a linear accelerator (Elekta) for different doses and times.

Plasmids

The expression vectors pCMV6-Entry-Empty, pCMV6-Entry-ETV7, and pCMV6-Entry-DNAJC15 C-terminally tagged with DDK-Myc tags were purchased from Origene (Tema

Ricerca, Bologna, Italy). The pGL4.26-DNAJC15 reporter was obtained by cloning the promoter region of *DNAJC15* (-299 to +512 bp from TSS according to the Eukaryotic Promoter Database, http://epd.vital-it.ch/) upstream the *Photinus pyralis* luciferase gene into the pGL4.26 reporter vector (Promega, Milan, Italy). The pRL-SV40 (Promega) vector constitutively expressing the *Renilla reniformis* luciferase cDNA was used as transfection efficiency control for gene reporter assays. The lentiviral vector pAIP-ETV7 was obtained by cloning using the following primers to amplify the ETV7 gene from pCMV6-Entry-ETV7 and inserting it into the pAIP plasmid:

Fw: aggttaacATGCAGGAGGGAGAATTGGCTA

Rv: gagaattcTTAAACCTTATCGTCGTCATCC

pAIP was a gift from Jeremy Luban (Addgene plasmid # 74171 ; http://n2t.net/addgene:74171 ; RRID:Addgene_74171, Watertown, MA, USA).

Purified PCR product was inserted into pAIP backbone using HpaI and EcoRI restriction endonucleases (New England Biolabs; Euroclone, Milan, Italy). Cloning was checked by restriction analysis and direct sequencing (Eurofins Genomics, Ebersberg, Germany).

PGK-H2BeGFP was a gift from Mark Mercola (Addgene plasmid # 21210 ; http://n2t.net/addgene:21210 ; RRID:Addgene_21210).

Generation of stable pCVM6-Entry-ETV7 and Empty MCF7 cells

In order to get MCF7 cells stably over-expressing ETV7 and the empty control, cells were seeded in 6-well plates and subsequently transfected for 48 hours with 1 µg of pCMV6-Entry-Empty or pCMV6-Entry-ETV7 (Origene) using Lipofectamine LTX and Plus Reagent (Life Technologies, Thermo Fisher Scientific). Afterward, cells were split, and Geneticin (Life Technologies) was added at a concentration of 600 µg/ml; each 3 days medium was replaced, and after 4 cycles of selection, single cell cloning was performed according to the Corning protocol for cell cloning by Serial dilution in 96-well plates. During the single cell cloning procedure Geneticin concentration was gradually reduced to 300 µg/ml.

Generation of stable pAIP-ETV7 and Empty MCF7 and T47D cells

To obtain cell lines having a stable over-expression of the ETV7 gene, MCF7 and T47D cells were transduced with the lentiviral vector pAIP Empty and with the lentiviral vector for

the expression of the heterologous gene ETV7, pAIP ETV7. After 72 hours, cells were split, and Puromycin (Life Technologies) was added at a concentration of 1.5 and 2.5 µg/ml respectively for MCF7 and T47D cells. Each 3 days medium was replaced, and after 4 cycles of selection, single cell cloning was performed for MCF7 cells according to the Corning protocol for cell cloning by Serial dilution in 96-well plates. During the single cell cloning procedure Puromycin concentration was gradually reduced to 0.75 µg/ml. T47D did not undergo serial dilution but were kept as the pooled population under Puromycin selection (1.5 µg/ml).

For zebrafish transplantation experiments, cells were subsequently transduced with lentiviral vectors for expression of nuclear eGFP produced using the pGK-H2B-eGFP plasmid. 1 week after transduction, eGFP positive cells were selected by cell sorting. Sorting experiment was conducted at the CIBIO Cell Analysis and Separation Core Facility using the FACS Aria instrument (BD Biosciences, Milan, Italy).

Viral vectors production in HEK293T

To obtain viral particles, HEK293T packaging cells were seeded into P150 dishes and transfected with a mix containing 17.5 µg pCMV-Δ8.9 plasmid (expression *GAG* and *POL* viral genes), 7.5 µg pCMV-VSVg plasmid (expressing the ENV protein from VSVg virus), 25 µg lentiviral vector containing the gene of interest and 112.5 µl PEI 2X transfection solution (Sigma-Aldrich). After 48 hours, viral vectors containing the plasmid of interest were collected in the supernatant and filtered through a 0.45 µm filter. Vectors yield was quantified with PERT (product-enhanced reverse transcriptase) assay.

RNA interference

Silencing of target RNAs was performed using small interfering RNAs (siRNAs) and the transfection reagent INTERFERin® (Polyplus-Transfection, Euroclone). Scramble siRNA was used as control. Scramble and ETV7 targeting siRNA were purchased from Integrated DNA Technologies (IDT, Tema Ricerca).

Cells were seeded in 6-well plates 24 hours prior transfection in order to get 40-50% confluence and were then transfected with 10 nM siRNA and 8 µl INTERFERin reagent respectively, diluted in 200 µl of OptiMEM (Life Technologies). The mix was vortexed 10

seconds, then incubated 10 minutes at room temperature and finally added to the wells. Analyses were performed 48 or 72 hours post-transfection.

RNA isolation and RT-qPCR

Total RNA was extracted using the Illustra RNA spin Mini Kit (GE Healthcare, Milan, Italy), converted into cDNA with the RevertAid First Strand cDNA Synthesis Kit following manufacturer's recommendations (Thermo Fisher Scientific) and RT-qPCR was performed with 25 ng of template cDNA into 384-well plates (BioRad, Milan, Italy) using the Kapa Sybr Fast qPCR Master Mix (Kapa Biosystems, Resnova, Ancona, Italy) or the qPCRBIO SyGreen 2X (PCR Biosystems, Resnova) and the CFX384 Detection System (BioRad). YWHAZ and GAPDH genes were used as housekeeping genes to obtain the relative fold change with the ΔΔCt method [220]. Primer sequences were designed using Primer-BLAST designing tool (https://www.ncbi.nlm.nih.gov/tools/primerblast/), checked for specificity and efficiency, and are listed in Table 1 (Eurofins Genomics).

Table 1: List of primers used for RT-qPCR

ETV7-FW	CAAGATCTTCCGAGTTGTGGA
ETV7-RV	GTTCACCCGGTTCTTGTGAT
YWHAZ-FW	CAACACATCCTATCAGACTGGG
YWHAZ-RV	AATGTATCAAGTTCAGCAATGGC
GAPDH-FW	TCCAAAATCAAGTGGGGCGA
GAPDH-RV	AGTAGAGGCAGGGATGATGT
DNAJC22-FW	AGGACAGCTTGGGTTGGATG
DNAJC22-RV	CGCTCCTATCTGTAGTGCTCAA
DNAJC17-FW	CTAGGCATTGAGGAGAAGGCA
DNAJC17-RV	AGAGTTCAGCTGCTCTGGGATT
DNAJC2-FW	GGCTCGGAGTGAGAGGTAGA
DNAJC2-RV	GAGTGTAGAGGCAGAGGTCAG
DNAJC7-FW	CGGAGCTGCTCTATGCTCCA
DNAJC7-RV	AAAGTCTCTGCTTCCCTCTTCG
DNAJC14-FW	GTAGCTAGTGGGCGCTACTG
DNAJC14-RV	GCTGCTCGCAAAACCTTGAA
DNAJC15-FW	TGGTGTCATCGCTCCAGTTG
DNAJC15-RV	ATGCGTAGCGACCTGCAAAT
ABCB1-FW	TGCCTATGGAGACAACAGCC
ABCB1-RV	TGAAGGCATGTATGTTGGCCT
ABCC1-FW	CCCGCTCTGGGACTGGAA
ABCC1-RV	GTAGAAGGGGAAACAGGCCC
ABCG2-FW	TCAGCTGGTTATCACTGTGAGG
ABCG2-RV	GGCTCTATGATCTCTGTGGCT
DNMT1-FW	ACATCCTGGACAAGCACCG

DNMT1-RV	TTTAGCTGAGGCACTCTCTCG
DNMT3A-FW	GTGTCTTGGTGGATGACGGG
DNMT3A-RV	CGGCATCAGCTTCTCAACAC
DNMT3B-FW	TAAGTCGAAGGTGCGTCGTG
DNMT3B-RV	CGTCTTCGAGTCTTGTTCTCGTA
IFITM2-FW	CGCGTACTCCGTGAAGTCTA
IFITM2-RV	ACGACCAACACTGGGATGAT
IFI35-FW	TGAGAGAGACCACAGCCCTT
IFI35-RV	GGAGGGCGGCATCCAGT
HERC6-FW	GGAGCTGCCAGAACCAATTC
HERC6-RV	AAGACCCTTCCTTTGTGGCA
PROCR-FW	CTCGGTATGAACTGCGGGAA
PROCR-RV	TTGTTTGGCTCCCTTTCGTG
APOL6-FW	TTTCTCCAGCCCAGACACTC
APOL6-RV	TCAAATGATTTTCTTCTCTCCACGG
CASP4-FW	CTGTTCCCTATGGCAGAAGGC
CASP4-RV	TCTGCCATGACCCGAACTTT
CFB-FW	GACACGAGAGCTGTATGGGG
CFB-RV	CTTCTCCCCTCCTACGCTGA
PARP14-FW	TGCCAAGAATGGCCAGACAA
PARP14-RV	TATGCCACAGCATTCTTTCCG
ICAM1-FW	ATGGCAACGACTCCTTCTCG
ICAM1-RV	GCCGGAAAGCTGTAGATGGT

Western Blot

Total protein extracts were obtained by lysing the cells in RIPA buffer (150mM Sodium Chloride, 1.0% NP-40, 0.5% Sodium Deoxycholate, 0.1% SDS, and 50mM TrisHCl pH 8.0) and proteins were quantified with the BCA method (Pierce, Thermo Fisher Scientific); 20-50 µg of protein extracts were loaded on appropriate 7.5%, 10% or 12% polyacrylamide gels and SDS-PAGE was performed. Proteins were then transferred on Nitrocellulose membranes, which were probed over-night at 4°C with specific antibodies diluted in 1% non-fat skim milk-PBS-T solution: GAPDH (6C5, sc-32233), ETV7/TEL2 (E-1, sc-374478), ETV7/TEL2 (H-88, sc-292509), α-Actinin (H-2, sc-17829), β-Tubulin (3F3-G2, sc-53140), DNMT3A (GTX129125, GeneTex, Prodotti Gianni, Milan, Italy), STAT1 (D1K9Y, 14994S, Cell Signaling Technology, Euroclone), p-STAT1(Y701) (#7649S, Cell Signaling Technology), MMP9 (D603, 13667P, Cell Signaling Technology), BCL-2 (100, sc-509), Survivin (D-8, sc-17779), PARP (GTX628838). Antibodies were obtained from Santa Cruz Biotechnologies (Milan, Italy) when not explicitly indicated. Detection was performed with ECL Select reagent (GE Healthcare) using the UVITec Alliance LD2 (UVITec Cambridge, UK) imaging system.

Site-directed mutagenesis

Site-directed mutagenesis was performed using the GENEART Site-Directed Mutagenesis kit (Life Technologies) according to manufacturer's instructions. In order to mutate ETV7 binding sites within pGL4.26-DNAJC15 (substituting the GGA conserved bases with ATC random sequence), the reporter plasmid was first methylated and then amplified with AccuPrime Pfx DNA Polymerase (InVitrogen, Life Technologies) in a mutagenesis reaction with the following primers (Eurofins Genomics):

BS1_Fw: GGGAAGAAAGGCTGCCCatcAGGGGGTCAGGAAAGC;

BS1_Rv: GCTTTCCTGACCCCCTgatGGGCAGCCTTTCTTCCC;

BS2_Fw: GGTGAGAAGGGTATCTgatGGGAACCTCGCCTTTAA;

BS2_Rv: TTAAAGGCGAGGTTCCCatcAGATACCCTTCTCACC.

Mutagenesis was then followed by an in vitro recombination reaction to enhance efficiency and colony yield. Mutated plasmids (pGL4.26-DNAJC15-BS1 and -BS2) were subsequently transformed into DH5α-T1R *E. coli* competent cells, which circularize the linear mutated DNA and exploit McrBC endonuclease activity to digest methylated DNA. Complete and correct mutagenesis was verified by direct sequencing (Eurofins Genomics).

Gene reporter Assay

24 hours prior transfection, 7 x 10^4 MCF7 cells were seeded in 24-well plates. Cells were transfected with Lipofectamine LTX and Plus Reagent (Thermo Fisher Scientific) along with 250 ng pGL4.26-DNAJC15 reporter, 250 ng pCMV6-Entry-Empty or pCMV6-Entry-ETV7 vectors, and 50 ng pRL-SV40 for each well. After 48 hours, cells were washed once in PBS and lysed in 1X PLB buffer (Promega), and luciferase activity was measured using the Dual-Luciferase Reporter Assay System (Promega) following manufacturer's instructions and detected using the Infinite M200 plate reader (Tecan, Milan, Italy). Renilla luciferase activity was used as an indicator of transfection efficiency and used to obtain the Relative Light Unit (RLU) values.

MTT Viability Assay

Cells were seeded in 96-well plates and treated with different concentrations of Doxorubicin for 72 hours. 10 µl of 5ng/ml MTT reagent (Sigma-Aldrich) was added to 100 µl of culture medium and left in incubation for 3 hours. Afterward, medium was accurately removed and cells were lysed in 100 µl of DMSO (Sigma-Aldrich), and a colorimetric measure was performed at the Infinite M200 plate reader (Tecan). Viability was calculated as a % ratio of viable cells treated with the indicated drug respect to an untreated control.

Cell Death Analysis (Operetta)

$6x10^3$ MCF7 cells were seeded in 96-well plates and 24 hours after seeding cells were treated with different concentrations of Doxorubicin. 72 hours after treatment cells were incubated with Hoechst 33342 2µg/ml (Life Technologies) for 30 min (to stain nuclei of both viable and dead cells) and Topro-3 0.1µM (Life Technologies) for 15 minutes (to visualize dead cells). Fluorescent images were obtained with the Operetta High Content Imaging System (Perkin Elmer) at CIBIO HTS Facility. The Topro-3 and Hoechst 33342 positive objects were detected using the Harmony 4.1 PhenoLOGIC software (Perkin Elmer); subsequently, the relative ratio of Topro-3 positive objects on the total number of objects (Hoechst 33342 positive) was calculated.

Cell Titer Glo Viability Assay

Viability assay was performed using the Cell Titer-Glo Luminescent cell viability assay (Promega) according to the manufacturer's instructions. Cells were seeded in white flat 96-well plates and treated with different concentrations of 5-FU for 72 hours. Afterward, the plates were equilibrated at room temperature for 30 minutes; then, 100 µl of Cell Titer-Glo reagent was added to 100 µl of medium and left in incubation for 2 minutes on an orbital shaker. Then, a luminescence measure was performed at the Infinite M200 plate reader (Tecan). Viability was calculated as a % ratio of viable cells treated with the indicated drug respect to DMSO control.

Vi-CELL Viability Assay and doubling time calculation

The cell viability after radiotherapy treatment was measured using the Vi-CELL viability analyzer (Beckman Coulter), which performs trypan blue dye exclusion method with an automated system. Cells were seeded in 6-well plates for 24 hours and then treated with different radiation doses (2 to 10 Gy) and incubated for 72 hours. Afterward, cells were harvested using trypsin and re-suspended in PBS. Vi-CELL performed the automated count of viable cells in the sample, allowing for viability measurement. The viability was calculated as the percentage of viable cells respect to the untreated control.

Doubling time was calculated with the following formula:

Doubling time (hours) = time in culture (hours) x ln(2)/ln(# cells harvested/# cells seeded)

Chromatin Immunoprecipitation (ChIP) Assay

MCF7 cells were seeded in P150 dishes and transiently transfected with 10µg of pCMV6-Entry- Empty or -ETV7 vectors using Lipofectamine LTX and Plus Reagent (Thermo Fisher Scientific) for 48 hours. ChIP was performed following a revised version of Myers Lab protocol [193]. 5 µg of anti-ETV7/TEL2 antibody (H-88, sc-292509) and normal rabbit IgG (sc-2027, Santa Cruz Biotechnologies) were used for immunoprecipitation with the aid of Dynabeads protein A magnetic beads (Life Technologies). 2 µl of purified immmunoprecipitated DNA was then used for qPCR analysis and calculation was performed using the ΔCt method in respect to non-immunoprecipitated DNA (% of input). A genomic region within GAPDH gene was used as a negative control. The qPCR on purified immunoprecipitated DNAs was performed as indicated above using the following primers:

DNAJC15-ChIP-Fw: TGCGAACAGAAGTTGAGAGTGG

DNAJC15-ChIp-Rv: AGTAAGCTCGGAGTCTAGCTGT

GAPDH-ChIP-Fw: AAAAGCGGGGAGAAAGTAGG

GAPDH-ChIP-Rv: CTAGCCTCCCGGGTTTCTCT.

Co-Immunoprecipitation

MCF7 were seeded in P150 dishes and transiently transfected with pCMV6-Entry-ETV7 as above. 48 hours post-transfection cells were lysed in CHAPS buffer and then incubated

overnight with 2μg of an anti-ETV7 antibody (H-88, sc-292509) or normal rabbit IgG (sc-2027) previously bound to Dynabeads protein A magnetic beads (Life Technologies). Beads were then washed, and the immunoprecipitated lysate was eluted and loaded on a polyacrylamide gel for SDS-PAGE.

Bisulfite-conversion

Genomic DNA was extracted from MCF7 cells left untreated, treated with Doxorubicin or over-expressing pCMV6-Entry-Empty or -ETV7 vectors. DNA and RNA extractions were obtained from the same samples using the AllPrep DNA/RNA/Protein Mini Kit (Qiagen, Milan Italy). Purified DNA was then denaturated and subjected to bisulfite conversion with the EZ DNA Methylation-Lightning™ Kit (Zymo Research, Euroclone) according to manufacturer's recommendations. The resulting product was subsequently PCR amplified and sequenced using the following bisulfite-specific primers (Eurofins Genomics):

Fw: TTGGTAGGATTTATTAGTTTTTGTTGG

Rv: CACCCAACTAATCTTTATATTTTTAATAAA.

Annexin V-FITC/PI staining and flow cytometry analysis

Apoptosis was measured using the FITC Annexin V Apoptosis Detection Kit I (BD Biosciences). Cells were stained with Annexin V conjugated to FITC fluorochrome together with the vital dye propidium iodide (PI), which can permeate only the membranes of dead or damaged cells; this combination of dyes allows for the identification of various stages of apoptosis.

After the appropriate treatment, cells were harvested in tubes and counted. Cells were then washed twice with cold PBS and re-suspended in 1X Annexin V Binding Buffer at the concentration of $1.5x10^6$ cells/ml.

100 μl of the cell suspension was then incubated with 2.5 μl of FITC Annexin V and 5 μl of PI for 15 minutes at room temperature in the dark. Subsequently, 400 μl of 1X Annexin V Binding Buffer was added to each tube and samples were then analyzed. Flow cytometry analysis was conducted at the CIBIO Cell Analysis and Separation Core Facility using a FACS Canto A instrument (BD Biosciences). Thresholds and gates were set by the analysis of the

following controls: unstained cells, cells stained only with FITC Annexin V and cells stained with PI only.

CD44/CD24 staining and flow cytometry analysis

The membrane expression of CD44 and CD24 cell surface markers was measured by double staining with antibodies conjugated with fluorophores and flow cytometry analysis. Cells were seeded in 6-well plate or T25 flasks and, after the appropriate treatments, were harvested, washed with PBS, and counted. $3x10^3$ cells were re-suspended in 30 µl PBS + 0.1% BSA and incubated with APC mouse anti-human CD44 (cat.no 559942, BD Bioscience) and FITC mouse anti-human CD24 (cat.no 555427, BD Bioscience) antibodies or with their isotype controls (FITC mouse IgG2a, k isotype -cat.no 556652, BD Bioscience – and APC mouse IgG2b, k isotype – cat.no 555745, BD Bioscience) in ice for 30 minutes. After incubation cells were washed three times with PBS and finally re-suspended in 300 µl PBS. Flow cytometry analysis was performed at the CIBIO Cell Analysis and Separation Core Facility using a FACS Canto A instrument (BD Biosciences). Thresholds and gates were set by the analysis of the following controls: unstained cells, cells stained with an isotype mix.

ALDEFLUOR analysis

ALDEFLUOR kit (STEMCELL Technologies, Cologne, Germany) was used to identify cells expressing high levels of ALDH enzyme. Experiments were performed following the manufacturer's instructions. Briefly, cells were harvested and re-suspended in ALDEFLUOR Assay Buffer at the concentration of $3x10^5$ cells/ml. Then, 5 µl of activated ALDEFLUOR reagent was added to the cells and mixed. 500 µl of the cell suspension and reagent mixture was immediately moved to the control tube containing 5 µl of DEAB (diethylaminobenzaldehyde) reagent, a specific inhibitor of ALDH activity. Samples and controls were incubated for 45 minutes at 37°C. After the incubation, cells were centrifuged and re-suspended in ALDEFLUOR Assay Buffer. Flow cytometry analysis was performed at the Tyrolean Cancer Research Institute using a FACS Canto II instrument (BD Biosciences). Thresholds and gates were set by the analysis of the following controls: unstained cells, DEAB control.

Colony formation assays

The clonogenic assay was performed seeding single cell suspension with $2x10^3$ MCF7 or $4x10^3$ T47D cells in 6-well plates in complete growth medium. Cells were let grow for 3 weeks changing the medium twice a week. After 3 weeks, the cell colonies were gently washed with PBS and stained by the incubation with 0.1% Crystal Violet solution in 20% methanol for 20 minutes. Excess staining was removed, and colonies were washed twice in PBS. Image analysis was performed with the Image J software in order to calculate the percentage of well's area occupied by colonies.

To characterize the capability of transformed cells to grow independently from a solid surface (anchorage-independent growth), we performed soft agar colony formation assay.

The wells of 6-well plates were prepared with a layer of base agar (0.7% agarose in DMEM complete medium + 10% FBS). After the solidification of the base, single cell suspension containing $1.5x10^4$ (MCF7) or $2x10^4$ (T47D) cells/well was rapidly mixed to the soft agar solution (0.35% agarose in DMEM complete medium) and disposed of as a layer over the previously prepared base agar. Finally, 1 ml of growing medium was added on the top. Cells were let grow for 3 weeks changing the top medium twice a week. Afterward, cells were stained with of 0.1% Crystal Violet solution in 20% methanol and washed several times with PBS 1X to remove the excess of Crystal Violet solution. Image analysis was performed with the Image J software in order to calculate the average size of the colonies.

Mammospheres culturing

To generate primary mammospheres, cells were harvested with trypsin, centrifuged and re-suspended in mammosphere medium (DMEM/F12 supplemented with 2mM L-Glutamine, 100U/ml penicillin, 100μg/ml streptomycin with the addition of 20ng/ml recombinant human Epidermal Growth Factor (EGF), 10ng/ml recombinant human basic Fibroblast Growth Factor (bFGF) and 1x B27 supplement. Cells were then counted and passed through a 25G needle to obtain a single cell suspension. Then, 10^3 cells/well were seeded in ultra-low attachment 24-well plates (Corning, Rome, Italy) in 800 μl of mammosphere medium. Plates were incubated at 37°C for one week, and images were

obtained at DM IL LED Inverted Microsocope (Leica). Mammospheres were split by harvesting the mammospheres with PBS, centrifuging and re-suspending with TrypLE Express Reagent (Thermo Fischer) as an alternative to trypsin. The single cell suspension was then again counted, and seeded at the same starting concentration in mammosphere medium.

After 1 week, mammospheres were counted and it was possible to calculate the Mammosphere Forming Efficiency (%) using the following equation:

MFE(%) = (# of mammospheres per well) / (# of cells seeded per well) x 100

Metabolic Assays

Metabolic assays were performed using the Agilent Seahorse XFp instrument (Agilent Technologies, Mila, Italy) with standard miniplates. The metabolic phenotype of the cells was determined using the Cell Energy Phenotype Test (Agilent Technologies).

The mitochondrial respiratory ability of the cells was determined using the Agilent Seahorse XF Mito Stress Test (Agilent Technologies).

For both the tests, $1x10^4$ (MCF7) or $1.5x10^4$ (T47D) cells were plated in the Agilent Seahorse XFp culture miniplates with complete growth medium the day prior to the assay and incubated at 37°C. The day of the assay, the medium was substituted with 180 µl of assay medium/well (Agilent Seahorse XF Base Medium supplemented with 1mM Pyruvate, 2mM L-Glutamine, 10 mM Glucose) and the plates were incubated for 1 hour at 37°C into a non-CO_2 incubator.

For Cell Energy Phenotype Test, oxygen consumption rate (OCR) and extracellular acidification rates (ECAR) were measured by Seahorse XFp extracellular flux analyzer (Agilent Technologies) before and after the injection with a mix of 1µM Oligomycin and 1µM FCCP.

For Mito Stress Test, oxygen consumption rate (OCR) was measured by Seahorse XFp extracellular flux analyzer (Agilent Technologies) with sequential injection 1µM Oligomycin, 1µM FCCP and 0.5µM Rotenone/Antimycin A. Data were analyzed with the Seahorse Wave Desktop software.

Wound healing migration assay

For wound healing assay, cells were seeded 24 hours prior treatment in order to get to 80-90% confluence. Then, a scratch was introduced using a 10 µl tip, and cells were rinsed twice with PBS to remove detached cells. Culture medium was re-added, and wound closure was followed for 48 hours. Images were obtained with DM IL LED Inverted Microscope (Leica) and quantified with the software TScratch (CSE Lab, ETH, Zurich, Switzerland) [221]. The software expresses the results as the percentage of Open Wound area, namely the area of the wound generated that remains non-colonized by the cells.

Xenografts into zebrafish embryos

Xenografts were performed 2 days post-fertilization on Casper or PRKDC$^{-/-}$ embryos. Few minutes before the transplant, fluorescent cells were harvested, counted, and re-suspended at a concentration of 1x10^{7} cells/ml in 2% PVP (Polyvinylpyrrolidone) solution in E3 medium. Dechorionated embryos were then anaesthetized using 1X Tricaine Methane Sulfonate in E3 medium and disposed on a previously prepared 1.5% agarose dish. 10 µl of cell suspension was then loaded into the needle previously prepared using borosilicate capillary without filaments. The loaded needle was then inserted into a micromanipulator and injections were performed into the yolk or the duct of Cuvier of the embryos. The micromanipulator was set with the following parameters in order to inject about 50 cells/embryo: pressure of injection ~ 3-4 PSI, time of injection: 0.1-0.2 s. Images were obtained at a Leica MZ10F stereo microscope by loading the embryos on 3% methylcellulose (Sigma Aldrich). After transplant and image acquisition, embryos were maintained in E3 medium at 32°C for 3 days.

RNA-seq

RNA from three independent biological samples for MCF7 and T47D cells stably transduced with pAIP and pAIP-ETV7 was converted into cDNA libraries according to the Illumina TruSeq Stranded mRNA Sample Preparation Guide (Illumina) following manufacturer's instructions. Pair-end reads (2x75 bp) were generated from the libraries using the Illumina HiSeq2500 sequencer at CIBIO NGS Core Facility according to the

standard Illumina protocol. The entire analysis of RNA-seq data was performed by Dr. Mattia Forcato and Prof. Silvio Bicciato (Center for Genome Research, University of Modena and Reggio Emilia, Italy).

Statistical analysis

Statistical analyses were performed using the GraphPad Prism version 6.0 software. When appropriate, unpaired t-test was applied for statistical significance. We selected throughout this study the two-sample Student's t-test for unequal variance, given that we generally compared two conditions (i.e., treated vs. untreated samples, or over-expression of ETV7 vs. Empty control).

REFERENCES

1. Akram, M., Iqbal, M., Daniyal, M. & Khan, A. U. Awareness and current knowledge of breast cancer. *Biol. Res.* **50**, 33 (2017).
2. Ferlay J, Soerjomataram I, Ervik M, Dikshit R, Eser S, Mathers C, Rebelo M, Parkin DM, Forman D, Bray, F. GLOBOCAN 2012 v1.0, Cancer Incidence and Mortality Worldwide: *IARC CancerBase No. 11 [Internet]. Lyon, Fr. Int. Agency Res. Cancer; 2013.* (2013). doi:https://doi.org/10.1002/ijc.29210
3. Howlader N, Noone AM, Krapcho M, Miller D, Bishop K, Altekruse SF, Kosary CL, Yu M, Ruhl J, Tatalovich Z, Mariotto A, Lewis DR, Chen HS, Feuer EJ, C. K. (eds). SEER Cancer Statistics Review 1975-2013 National Cancer Institute SEER Cancer Statistics Review 1975-2013 National Cancer Institute. *SEER Cancer Stat. Rev. 1975-2013, Natl. Cancer Institute. Bethesda, MD, http//seer.cancer.gov/csr/1975_2013/, based Novemb. 2015 SEER data submission, posted to SEER web site, April 2016.* (2016). doi:https://seer.cancer.gov/csr/1975_2014/
4. DeSantis, C., Ma, J., Bryan, L. & Jemal, A. Breast cancer statistics, 2013. *CA. Cancer J. Clin.* (2014). doi:10.1039/b614914f
5. Taherian-Fard, A., Srihari, S. & Ragan, M. A. Breast cancer classification: Linking molecular mechanisms to disease prognosis. *Brief. Bioinform.* **16**, 461–474 (2014).
6. Malhotra, G. K., Zhao, X., Band, H. & Band, V. Histological, molecular and functional subtypes of breast cancers. *Cancer Biol. Ther.* **10**, 955–960 (2010).
7. Viale, G. The current state of breast cancer classification. *Ann. Oncol.* **23**, (2012).
8. Perou, C. M. *et al.* Molecular portraits of human breast tumours [In Process Citation]. *Nature* (2000).
9. Sorlie, T. *et al.* Gene expression patterns of breast carcinomas distinguish tumor subclasses with clinical implications. *Proc. Natl. Acad. Sci.* (2001). doi:10.1073/pnas.191367098
10. Sorlie, T. *et al.* Repeated observation of breast tumor subtypes in independent gene

expression data sets. *Proc. Natl. Acad. Sci.* (2003). doi:10.1073/pnas.0932692100

11. Rouzier, R. *et al.* Breast cancer molecular subtypes respond differently to preoperative chemotherapy. *Clin. Cancer Res.* (2005). doi:10.1158/1078-0432.CCR-04-2421
12. Parker, J. S. *et al.* Supervised Risk Predictor of Breast Cancer Based on Intrinsic Subtypes. *J. Clin. Oncol.* **27**, 1160–1167 (2009).
13. Hugh, J. *et al.* Breast cancer subtypes and response to docetaxel in node-positive breast cancer: Use of an immunohistochemical definition in the BCIRG 001 trial. *J. Clin. Oncol.* (2009). doi:10.1200/JCO.2008.18.1024
14. Dai, X. *et al.* Breast cancer intrinsic subtype classification, clinical use and future trends. *Am. J. Cancer Res.* **5**, 2929–2943 (2015).
15. Eliyatkin, N., Yalcin, E., Zengel, B., Aktaş, S. & Vardar, E. Molecular Classification of Breast Carcinoma: From Traditional, Old-Fashioned Way to A New Age, and A New Way. *J. Breast Heal.* (2015). doi:10.5152/tjbh.2015.1669
16. Lakhani, S. R. *et al.* Multifactorial analysis of differences between sporadic breast cancers and cancers involving BRCA1 and BRCA2 mutations. *J. Natl. Cancer Inst.* (1998). doi:10.1093/jnci/90.15.1138
17. Rakha, E. A. *et al.* Basal phenotype identifies a poor prognostic subgroup of breast cancer of clinical importance. *Eur. J. Cancer* (2006). doi:10.1016/j.ejca.2006.08.015
18. Lehmann, B. D. *et al.* Identification of human triple-negative breast cancer subtypes and preclinical models for selection of targeted therapies. *J. Clin. Invest.* (2011). doi:10.1172/JCI45014
19. Nounou, M. I. *et al.* Breast Cancer: Conventional Diagnosis and Treatment Modalities and Recent Patents and Technologies. *Breast Cancer (Auckl).* **9**, 17–34 (2015).
20. Papademetriou, K., Ardavanis, A. & Kountourakis, P. Neoadjuvant therapy for locally advanced breast cancer: Focus on chemotherapy and biological targeted treatments' armamentarium. *Journal of Thoracic Disease* (2010). doi:10.3978/j.issn.2072-1439.2010.02.03.8
21. Goldhirsch, A. *et al.* Personalizing the treatment of women with early breast cancer: Highlights of the st gallen international expert consensus on the primary therapy of early breast Cancer 2013. *Ann. Oncol.* (2013). doi:10.1093/annonc/mdt303

22. Dhankhar, R. *et al.* Advances in novel drug delivery strategies for breast cancer therapy. *Artificial Cells, Blood Substitutes, and Biotechnology* (2010). doi:10.3109/10731199.2010.494578

23. Albain, K. *et al.* Comparisons between different polychemotherapy regimens for early breast cancer: Meta-analyses of long-term outcome among 100 000 women in 123 randomised trials. *The Lancet* (2012). doi:10.1016/S0140-6736(11)61625-5

24. Shepherd, G. M. Hypersensitivity reactions to chemotherapeutic drugs. *Clin. Rev. Allergy Immunol.* (2003). doi:10.1385/CRIAI:24:3:253

25. Wood, A. J. J., Shapiro, C. L. & Recht, A. Side Effects of Adjuvant Treatment of Breast Cancer. *N. Engl. J. Med.* (2001). doi:10.1056/NEJM200106283442607

26. Shao, N. *et al.* Sequential versus concurrent anthracyclines and taxanes as adjuvant chemotherapy of early breast cancer: A meta-analysis of phase III randomized control trials. *Breast* (2012). doi:10.1016/j.breast.2012.03.011

27. Arcamone, F. *et al.* Adriamycin, 14-hydroxydaunomycin, a new antitumor antibiotic from S. peucetius var. caesius. *Biotechnol. Bioeng.* (2000). doi:10.1002/(SICI)1097-0290(20000320)67:6<704::AID-BIT8>3.0.CO;2-L

28. Cagel, M., Grotz, E., Bernabeu, E., Moretton, M. A. & Chiappetta, D. A. Doxorubicin: nanotechnological overviews from bench to bedside. *Drug Discovery Today* (2017). doi:10.1016/j.drudis.2016.11.005

29. Hilmer, S. N., Cogger, V. C., Muller, M. & Le Couteur, D. G. The hepatic pharmacokinetics of doxorubicin and liposomal doxorubicin. *Drug Metab. Dispos.* (2004). doi:10.1124/dmd.32.8.794

30. Buchholz, T. A. *et al.* Global Gene Expression Changes during Neoadjuvant Chemothera... : The Cancer Journal. *Cancer J.* (2002).

31. Gewirtz, D. A. A critical evaluation of the mechanisms of action proposed for the antitumor effects of the anthracycline antibiotics adriamycin and daunorubicin. *Biochemical Pharmacology* (1999). doi:10.1016/S0006-2952(98)00307-4

32. Tacar, O., Sriamornsak, P. & Dass, C. R. Doxorubicin: An update on anticancer molecular action, toxicity and novel drug delivery systems. *Journal of Pharmacy and Pharmacology* (2013). doi:10.1111/j.2042-7158.2012.01567.x

33. Heidelberger, C. *et al.* Fluorinated pyrimidines, a new class of tumour-inhibitory compounds. *Nature* (1957). doi:10.1038/179663a0

34. Rutman, R. J., Cantarow, A. & Paschkis, K. E. Studies in 2-Acetylaminofluorene Carcinogenesis: III. The Utilization of Uracil-2-C14 by Preneoplastic Rat Liver and Rat Hepatoma. *Cancer Res.* (1954). doi:10.1088/0370-1328/82/6/315
35. Longley, D. B., Harkin, D. P. & Johnston, P. G. 5-Fluorouracil: Mechanisms of action and clinical strategies. *Nature Reviews Cancer* (2003). doi:10.1038/nrc1074
36. Ceilley, R. I. Mechanisms of action of topical 5-fluorouracil: Review and implications for the treatment of dermatological disorders. *Journal of Dermatological Treatment* (2012). doi:10.3109/09546634.2010.507704
37. Ghoshal, K. & Jacob, S. T. Specific Inhibition of Pre-Ribosomal RNA Processing in Extracts from the Lymphosarcoma Cells Treated with 5-Fluorouracil. *Cancer Res.* (1994).
38. Parker, W. B. & Cheng, Y. C. Metabolism and mechanism of action of 5-fluorouracil. *Pharmacology and Therapeutics* (1990). doi:10.1016/0163-7258(90)90056-8
39. Patton, J. R. Ribonucleoprotein Particle Assembly and Modification of U2 Small Nuclear RNA Containing 5-Fluorouridine. *Biochemistry* (1993). doi:10.1021/bi00085a027
40. Doong, S. L. & Dolnick, B. J. 5-Fluorouracil substitution alters pre-mRNA splicing in vitro. *J. Biol. Chem.* (1988).
41. Grubbé, E. H. Priority in the Therapeutic Use of X-rays. *Radiology* (1933). doi:10.1148/21.2.156
42. Darby, S. *et al.* Effect of radiotherapy after breast-conserving surgery on 10-year recurrence and 15-year breast cancer death: Meta-analysis of individual patient data for 10 801 women in 17 randomised trials. *Lancet* (2011). doi:10.1016/S0140-6736(11)61629-2
43. Mameghan, H. Recent developments in radiotherapy. *Med. J. Aust.* **156**, 3–4 (1992).
44. Baskar, R., Dai, J., Wenlong, N., Yeo, R. & Yeoh, K.-W. Biological response of cancer cells to radiation treatment. *Front. Mol. Biosci.* **1**, 1–9 (2014).
45. Knight, R. D., Parshad, R., Price, F. M., Tarone, R. E. & Sanford, K. K. X-ray-induced chromatid damage in relation to dna repair and cancer incidence in family members. *Int. J. Cancer* (1993). doi:10.1002/ijc.2910540412
46. Shahidi, M., Mozdarani, H. & Bryant, P. E. Radiation sensitivity of leukocytes from healthy individuals and breast cancer patients as measured by the alkaline and

neutral comet assay. *Cancer Lett.* (2007). doi:10.1016/j.canlet.2007.08.002

47. Baskar, R., Balajee, A. S., Geard, C. R. & Hande, M. P. Isoform-specific activation of protein kinase c in irradiated human fibroblasts and their bystander cells. *Int. J. Biochem. Cell Biol.* (2008). doi:10.1016/j.biocel.2007.07.002
48. Luqmani, Y. A. Mechanisms of drug resistance in cancer chemotherapy. *Med. Princ. Pract.* **14**, 35–48 (2005).
49. Johnstone, R. W., Ruefli, A. A. & Lowe, S. W. Apoptosis: A link between cancer genetics and chemotherapy. *Cell* (2002). doi:10.1016/S0092-8674(02)00625-6
50. Senthebane, D. A. *et al.* The role of tumor microenvironment in chemoresistance: To survive, keep your enemies closer. *Int. J. Mol. Sci.* **18**, (2017).
51. Zheng, H.-C. The molecular mechanisms of chemoresistance in cancers. *Oncotarget* **8**, 59950–59964 (2017).
52. Fletcher, J. I., Haber, M., Henderson, M. J. & Norris, M. D. ABC transporters in cancer: More than just drug efflux pumps. *Nature Reviews Cancer* (2010). doi:10.1038/nrc2789
53. Glavinas, H., Krajcsi, P., Cserepes, J. & Sarkadi, B. The Role of ABC Transporters in Drug Resistance, Metabolism and Toxicity. *Curr. Drug Deliv.* (2004). doi:10.2174/1567201043480036
54. Kast, C. & Grost, P. Topology mapping of the amino-terminal half of multidrug resistance- associated protein by epitope insertion and immunofluorescence. *J. Biol. Chem.* (1997). doi:10.1074/jbc.272.42.26479
55. Kast, C. & Gros, P. Epitope insertion favors a six transmembrane domain model for the carboxy-terminal portion of the multidrug resistance-associated protein. *Biochemistry* (1998). doi:10.1021/bi972332v
56. Jiang, Z. S., Sun, Y. Z., Wang, S. M. & Ruan, J. S. Epithelial-mesenchymal transition: Potential regulator of ABC transporters in tumor progression. *Journal of Cancer* (2017). doi:10.7150/jca.19079
57. Gamcsik, M. P., Dubay, G. R. & Cox, B. R. Increased rate of glutathione synthesis from cystine in drug-resistant MCF-7 cells. *Biochem. Pharmacol.* (2002). doi:10.1016/S0006-2952(01)00931-5
58. Deng, H. B., Parekh, H. K., Chow, K. C. & Simpkins, H. Increased expression of dihydrodiol dehydrogenase induces resistance to cisplatin in human ovarian

carcinoma cells. *J. Biol. Chem.* (2002). doi:10.1074/jbc.M112028200

59. Dumontet, C. *et al.* Common resistance mechanisms to deoxynucleoside analogues in variants of the human erythroleukaemic line K562. *Br. J. Haematol.* (1999). doi:10.1046/j.1365-2141.1999.01509.x

60. Igney, F. H. & Krammer, P. H. DEATH AND ANTI-DEATH: TUMOUR RESISTANCE TO APOPTOSIS. *Nat. Rev. Cancer* (2002). doi:10.1038/nrc776

61. Guerra, F., Arbini, A. A. & Moro, L. Mitochondria and cancer chemoresistance. *Biochim. Biophys. Acta - Bioenerg.* **1858**, 686–699 (2017).

62. Li, W. & Melton, D. W. Cisplatin regulates the MAPK kinase pathway to induce increased expression of DNA repair gene ERCC1 and increase melanoma chemoresistance. *Oncogene* (2012). doi:10.1038/onc.2011.426

63. Wickström, M. *et al.* Wnt/β-catenin pathway regulates MGMT gene expression in cancer and inhibition of Wnt signalling prevents chemoresistance. *Nat. Commun.* (2015). doi:10.1038/ncomms9904

64. Miller, W. R. Biological rationale for endocrine therapy in breast cancer. *Best Practice and Research: Clinical Endocrinology and Metabolism* (2004). doi:10.1016/S1521-690X(03)00044-7

65. Luqmani, Y. A. Mechanisms of drug resistance in cancer chemotherapy. in *Medical Principles and Practice* (2005). doi:10.1159/000086183

66. Steel, G. G. *et al.* The 5Rs of Radiobiology. *Med. J. Aust.* **156**, 216–222 (2017).

67. Shiloh, Y. ATM and related protein kinases: Safeguarding genome integrity. *Nature Reviews Cancer* (2003). doi:10.1038/nrc1011

68. Pawlik, T. M. & Keyomarsi, K. Role of cell cycle in mediating sensitivity to radiotherapy. *International Journal of Radiation Oncology Biology Physics* (2004). doi:10.1016/j.ijrobp.2004.03.005

69. Pajonk, F., Vlashi, E. & McBride, W. H. Radiation resistance of cancer stem cells: The 4 R's of radiobiology revisited. *Stem Cells* (2010). doi:10.1002/stem.318

70. Thomlinson, R. H. & Gray, L. H. The Histological Structure of Some Human Lung Cancers and the Possible Implications for Radiotherapy. *Br. J. Cancer* **9**, 539–549 (1955).

71. Hockel M *et al.* Association between tumor hypoxia and malignant progression in advanced cancer of the uterine cervix. *Cancer Res.* (1996).

72. Brizel, D. M. *et al.* Tumor oxygenation predicts for the likelihood of distant metastases in human soft tissue sarcoma. *Cancer Res.* (1996). doi:8640781

73. Hall, E. J. & Cox, J. D. *Physical and Biologic Basis of Radiation Therapy*. *Radiation Oncology* (2016). doi:10.1016/B978-0-323-04971-9.00001-9

74. Wang, T. *et al.* Cancer stem cell targeted therapy: progress amid controversies. *Oncotarget* (2015). doi:10.18632/oncotarget.6176

75. Ito, T., Zimdahl, B. & Reya, T. ASIRTing Control over Cancer Stem Cells. *Cancer Cell* (2012). doi:10.1016/j.ccr.2012.01.014

76. Wicha, M. S., Liu, S. & Dontu, G. Cancer stem cells: An old idea - A paradigm shift. *Cancer Research* (2006). doi:10.1158/0008-5472.CAN-05-3153

77. Virchow, R. Die Cellularpathologie in ihrer Begründung auf physiologische and pathologische Gewebelehre. *Verlag von August Hirschfeld, Berlin.* (1858).

78. Pierce, G. B. & Wallace, C. Differentiation of malignant to benign cells. *Cancer Res.* **31**, 127–134 (1971).

79. Fialkow, P. J. Stem cell origin of human myeloid blood cell neoplasms. *Verh Dtsch Ges Pathol* (1990).

80. Lapidot, T. *et al.* A cell initiating human acute myeloid leukaemia after transplantation into SCID mice. *Nature* (1994). doi:10.1038/367645a0

81. Lobo, N. A., Shimono, Y., Qian, D. & Clarke, M. F. The Biology of Cancer Stem Cells. *Annu. Rev. Cell Dev. Biol.* (2007). doi:10.1146/annurev.cellbio.22.010305.104154

82. Ajani, J. A., Song, S., Hochster, H. S. & Steinberg, I. B. Cancer stem cells: The promise and the potential. *Semin. Oncol.* (2015). doi:10.1053/j.seminoncol.2015.01.001

83. Clarke, M. F. *et al.* Cancer stem cells - Perspectives on current status and future directions: AACR workshop on cancer stem cells. in *Cancer Research* (2006). doi:10.1158/0008-5472.CAN-06-3126

84. Yu, Z., Pestell, T. G., Lisanti, M. P. & Pestell, R. G. Cancer stem cells. *Int. J. Biochem. Cell Biol.* **44**, 2144–2151 (2012).

85. Venezia, T. A. *et al.* Molecular signatures of proliferation and quiescence in hematopoietic stem cells. *PLoS Biol.* (2004). doi:10.1371/journal.pbio.0020301

86. Park, Y. & Gerson, S. L. DNA Repair Defects in Stem Cell Function and Aging. *Annu. Rev. Med.* (2005). doi:10.1146/annurev.med.56.082103.104546

87. Cairns, J. Somatic stem cells and the kinetics of mutagenesis and carcinogenesis.

Proc. Natl. Acad. Sci. (2002). doi:10.1073/pnas.162369899

88. Potten, C. S., Owen, G. & Booth, D. Intestinal stem cells protect their genome by selective segregation of template DNA strands. *J. Cell Sci.* (2002).

89. Rambhatla, L., Ram-Mohan, S., Cheng, J. J. & Sherley, J. L. Immortal DNA strand cosegregation requires p53/IMPDH-dependent asymmetric self-renewal associated with adult stem cells. *Cancer Res.* (2005). doi:10.1158/0008-5472.CAN-04-3161

90. Wang, S., Yang, D. & Lippman, M. E. Targeting Bcl-2 and Bcl-XLwith Nonpeptidic Small-Molecule Antagonists. in *Seminars in Oncology* (2003). doi:10.1053/j.seminoncol.2003.08.015

91. DeGorter, M. K., Xia, C. Q., Yang, J. J. & Kim, R. B. Drug Transporters in Drug Efficacy and Toxicity. *Annu. Rev. Pharmacol. Toxicol.* (2012). doi:10.1021/acs.inorgchem.8b00616

92. Cabrera, M. C., Hollingsworth, R. E. & Hurt, E. M. Cancer stem cell plasticity and tumor hierarchy. *World J. Stem Cells* **7**, 27 (2015).

93. Place, A. E., Jin Huh, S. & Polyak, K. The microenvironment in breast cancer progression: Biology and implications for treatment. *Breast Cancer Research* (2011). doi:10.1186/bcr2912

94. Brooks, M. D. & Wicha, M. S. Tumor twitter: Cellular communication in the breast cancer stem cell niche. *Cancer Discov.* **5**, 469–471 (2015).

95. Gupta, P. B. *et al.* Stochastic state transitions give rise to phenotypic equilibrium in populations of cancer cells. *Cell* (2011). doi:10.1016/j.cell.2011.07.026

96. Doherty, M. R., Smigiel, J. M., Junk, D. J. & Jackson, M. W. Cancer stem cell plasticity drives therapeutic resistance. *Cancers* (2016). doi:10.3390/cancers8010008

97. Al-Hajj, M., Wicha, M. S., Benito-Hernandez, A., Morrison, S. J. & Clarke, M. F. Prospective identification of tumorigenic breast cancer cells. *Proc. Natl. Acad. Sci.* (2003). doi:10.1073/pnas.0530291100

98. Luo, M. *et al.* Breast cancer stem cells: Current advances and clinical implications. *Methods Mol. Biol.* (2015). doi:10.1007/978-1-4939-2519-3_1

99. Bozorgi, A., Khazaei, M. & Khazaei, M. R. New Findings on Breast Cancer Stem Cells: A Review. *J. Breast Cancer* **18**, 303 (2015).

100. Herrera-Gayol, A. & Jothy, S. Adhesion proteins in the biology of breast cancer:

Contribution of CD44. *Experimental and Molecular Pathology* (1999). doi:10.1006/exmp.1999.2251

101. Götte, M. & Yip, G. W. Heparanase, hyaluronan, and CD44 in cancers: A breast carcinoma perspective. *Cancer Research* (2006). doi:10.1158/0008-5472.CAN-06-1464
102. Suzuki, T. *et al.* CD24 Induces Apoptosis in Human B Cells Via the Glycolipid-Enriched Membrane Domains/Rafts-Mediated Signaling System. *J. Immunol.* (2001). doi:10.4049/jimmunol.166.9.5567
103. Balicki, D. Moving Forward in Human Mammary Stem Cell Biology and Breast Cancer Prognostication Using ALDH1. *Cell Stem Cell* (2007). doi:10.1016/j.stem.2007.10.015
104. Dittmer, J. Breast cancer stem cells: Features, key drivers and treatment options. *Semin. Cancer Biol.* **53**, 59–74 (2018).
105. Liu, S. *et al.* Breast cancer stem cells transition between epithelial and mesenchymal states reflective of their normal counterparts. *Stem Cell Reports* (2014). doi:10.1016/j.stemcr.2013.11.009
106. Mani, S. A. *et al.* The Epithelial-Mesenchymal Transition Generates Cells with Properties of Stem Cells. *Cell* (2008). doi:10.1016/j.cell.2008.03.027
107. Tsuji, T., Ibaragi, S. & Hu, G. F. Epithelial-mesenchymal transition and cell cooperativity in metastasis. *Cancer Research* (2009). doi:10.1158/0008-5472.CAN-09-1618
108. Dontu, G. *et al.* In vitro propagation and transcriptional profiling of human mammary stem/progenitor cells. *Genes Dev.* (2003). doi:10.1101/gad.1061803
109. Ben-Porath, I. *et al.* An embryonic stem cell-like gene expression signature in poorly differentiated aggressive human tumors. *Nat. Genet.* (2008). doi:10.1038/ng.127
110. Kar, A. & Gutierrez-Hartmann, A. Molecular mechanisms of ETS transcription factor-mediated tumorigenesis. *Critical Reviews in Biochemistry and Molecular Biology* (2013). doi:10.3109/10409238.2013.838202
111. Jedlicka, P., Sui, X. & Gutierrez-Hartmann, A. The Ets dominant repressor En/Erm enhances intestinal epithelial tumorigenesis in ApcMin mice. *BMC Cancer* (2009). doi:10.1186/1471-2407-9-197
112. Seth, A. & Watson, D. K. ETS transcription factors and their emerging roles in human

cancer. *European Journal of Cancer* (2005). doi:10.1016/j.ejca.2005.08.013

113. Sizemore, G. M., Pitarresi, J. R., Balakrishnan, S. & Ostrowski, M. C. The ETS family of oncogenic transcription factors in solid tumours. *Nat. Rev. Cancer* **17**, 337 (2017).
114. Prescott, J. D., Koto, K. S., Singh, M. & Gutierrez-Hartmann, A. The ETS transcription factor ESE-1 transforms MCF-12A human mammary epithelial cells via a novel cytoplasmic mechanism. *Mol. Cell. Biol.* (2004). doi:10.1128/MCB.24.12.5548-5564.2004
115. Tynan, J. A., Wen, F., Muller, W. J. & Oshima, R. G. Ets2-dependent microenvironmental support of mouse mammary tumors. *Oncogene* (2005). doi:10.1038/sj.onc.1208856
116. Vinagre, J. *et al.* Frequency of TERT promoter mutations in human cancers. *Nat. Commun.* (2013). doi:10.1038/ncomms3185
117. Gutierrez-Hartmann, A., Duval, D. L. & Bradford, A. P. ETS transcription factors in endocrine systems. *Trends in Endocrinology and Metabolism* (2007). doi:10.1016/j.tem.2007.03.002
118. Wei, G. H. *et al.* Genome-wide analysis of ETS-family DNA-binding in vitro and in vivo. *EMBO J.* (2010). doi:10.1038/emboj.2010.106
119. Rasighaemi, P. & Ward, A. C. ETV6 and ETV7: Siblings in hematopoiesis and its disruption in disease. *Crit. Rev. Oncol. Hematol.* **116**, 106–115 (2017).
120. Kim, C. A. *et al.* Polymerization of the SAM domain of TEL in leukemogenesis and transcriptional repression. *EMBO J.* (2001). doi:10.1093/emboj/20.15.4173
121. Poirel, H. *et al.* Characterization of a novel ETS gene, TELB, encoding a protein structurally and functionaly related to TEL. *Oncogene* (2000). doi:10.1038/sj.onc.1203830
122. Kawagoe, H., Potter, M., Ellis, J. & Grosveld, G. C. TEL2, an ETS factor expressed in human leukemia, regulates monocytic differentiation of U937 cells and blocks the inhibitory effect of TEL1 on Ras-induced cellular transformation. *Cancer Res.* **64**, 6091–6100 (2004).
123. Potter, M. D., Buijs, A., Kreider, B., van Rompaey, L. & Grosveld, G. C. Identification and characterization of a new human ETS-family transcription factor, TEL2, that is expressed in hematopoietic tissues and can associate with TEL1/ETV6. *Blood* (2000).

124. Gu, X. *et al.* Tel-2 is a Novel Transcriptional Repressor Related to the Ets Factor Tel/ETV-6. *J. Biol. Chem.* (2001). doi:10.1074/jbc.M010070200

125. Bisio, A. *et al.* Cooperative interactions between p53 and NFκB enhance cell plasticity. *Oncotarget* **5**, (2014).

126. Matz, M. *et al.* The regulation of interferon type I pathway-related genes RSAD2 and ETV7 specifically indicates antibody-mediated rejection after kidney transplantation. *Clin. Transplant.* e13429 (2018). doi:10.1111/ctr.13429

127. Minutti, C. M. *et al.* Surfactant Protein A Prevents IFN-γ/IFN-γ Receptor Interaction and Attenuates Classical Activation of Human Alveolar Macrophages. *J. Immunol.* **197**, 590–598 (2016).

128. Qiao, Y., Kang, K., Giannopoulou, E., Fang, C. & Ivashkiv, L. B. IFN-γ Induces Histone 3 Lysine 27 Trimethylation in a Small Subset of Promoters to Stably Silence Gene Expression in Human Macrophages. *Cell Rep.* **16**, 3121–3129 (2016).

129. Pervolaraki, K. *et al.* Differential induction of interferon stimulated genes between type I and type III interferons is independent of interferon receptor abundance. *PLOS Pathog.* **14**, e1007420 (2018).

130. Ignatius Irudayam, J. *et al.* Characterization of type I interferon pathway during hepatic differentiation of human pluripotent stem cells and hepatitis C virus infection. *Stem Cell Res.* **15**, 354–364 (2015).

131. Quintana, A. M., Picchione, F., Klein Geltink, R. I., Taylor, M. R. & Grosveld, G. C. Zebrafish etv7 regulates red blood cell development through the cholesterol synthesis pathway. *Dis. Model. Mech.* (2014). doi:10.1242/dmm.012526

132. Numata, M., Geltink, R. K. & Grosveld, G. The ETS transcription factor ETV7 exhausts hematopoietic stem cells by enhancing the cell cycle entry and cell proliferation. *Blood* **122**, 733 (2013).

133. Santos, G. C., Zielenska, M., Prasad, M. & Squire, J. A. Chromosome 6p amplification and cancer progression. *Journal of Clinical Pathology* (2007). doi:10.1136/jcp.2005.034389

134. Carella, C. *et al.* The ETS factor TEL2 is a hematopoietic oncoprotein. *Blood* **107**, 1124–1132 (2006).

135. Neale, G. *et al.* Molecular characterization of the pediatric preclinical testing panel. *Clin. Cancer Res.* (2008). doi:10.1158/1078-0432.CCR-07-5090

136. Matos, J. M., Witzmann, F. A., Cummings, O. W. & Schmidt, C. M. A Pilot Study of Proteomic Profiles of Human Hepatocellular Carcinoma in the United States. *J. Surg. Res.* (2009). doi:10.1016/j.jss.2008.06.008

137. Harwood, F. C. *et al.* ETV7 is an essential component of a rapamycin-insensitive mTOR complex in cancer. *Sci. Adv.* **4**, (2018).

138. Piggin, C. L. *et al.* ELF5 isoform expression is tissue-specific and significantly altered in cancer. *Breast Cancer Res.* **18**, 1–18 (2016).

139. Cardone, M. *et al.* The novel ETS factor TEL2 cooperates with Myc in B lymphomagenesis. *Mol Cell Biol* (2005). doi:10.1128/MCB.25.6.2395-2405.2005

140. Numata, M., Klein Geltink, R. I. & Grosveld, G. C. Establishment of a transgenic mouse to model ETV7 expressing human tumors. *Transgenic Res.* **0123456789**, (2018).

141. Sang, Y. *et al.* TEL2 suppresses metastasis by down-regulating SERPINE1 in nasopharyngeal carcinoma. *Oncotarget* **6**, (2015).

142. Maeda, O. *et al.* Alteration of gene expression and DNA methylation in drug-resistant gastric cancer. *Oncol. Rep.* (2014). doi:10.3892/or.2014.3014

143. Pestka, S., Krause, C. D. & Walter, M. R. Interferons, interferon-like cytokines, and their receptors. *Immunol. Rev.* **202**, 8–32 (2004).

144. Isaacs, A. & Lindenmann, J. Virus Interference: I. The Interferon. *CA. Cancer J. Clin.* (1988). doi:10.3322/canjclin.38.5.280

145. Hoskins, M. A Protective Action of Neurotropic Against Viscerotropic Yellow Fever Virus in Macacus Rhesus. *Am. J. Trop. Med. Hyg.* (1935). doi:DOI: https://doi.org/10.4269/ajtmh.1935.s1-15.675

146. Stark, G. R., Kerr, I. M., Williams, B. R. G., Silverman, R. H. & Schreiber, R. D. How Cells Respond to interferons. *Annu. Rev. Biochem.* 227–264 (1998). doi:0066-4154

147. Lin, F. & Young, H. A. Interferons: Success in anti-viral immunotherapy. *Cytokine Growth Factor Rev.* **25**, 369–376 (2014).

148. Capobianchi, M. R., Uleri, E., Caglioti, C. & Dolei, A. Type I IFN family members: Similarity, differences and interaction. *Cytokine Growth Factor Rev.* (2015). doi:10.1016/j.cytogfr.2014.10.011

149. Fensterl, V., Chattopadhyay, S. & Sen, G. C. No Love Lost Between Viruses and Interferons. *Annu. Rev. Virol.* **2**, 549–572 (2015).

150. De Weerd, N. A. & Nguyen, T. The interferons and their receptors-distribution and regulation. *Immunology and Cell Biology* (2012). doi:10.1038/icb.2012.9

151. Fitzgerald-Bocarsly, P., Dai, J. & Singh, S. Plasmacytoid dendritic cells and type I IFN: 50 years of convergent history. *Cytokine Growth Factor Rev.* (2008). doi:10.1016/j.cytogfr.2007.10.006

152. Fung, K. Y. *et al.* Interferon-ε protects the female reproductive tract from viral and bacterial infection. *Science* (2013). doi:10.1126/science.1233321

153. Sommereyns, C., Paul, S., Staeheli, P. & Michiels, T. IFN-lambda (IFN-λ) is expressed in a tissue-dependent fashion and primarily acts on epithelial cells in vivo. *PLoS Pathog.* (2008). doi:10.1371/journal.ppat.1000017

154. Schneider, W. M., Chevillotte, M. D. & Rice, C. M. Interferon-Stimulated Genes: A Complex Web of Host Defenses. *Annu. Rev. Immunol.* (2014). doi:10.1146/annurev-immunol-032713-120231

155. van Boxel-Dezaire, A. H. H., Rani, M. R. S. & Stark, G. R. Complex Modulation of Cell Type-Specific Signaling in Response to Type I Interferons. *Immunity* (2006). doi:10.1016/j.immuni.2006.08.014

156. Heim, M. H., Kerr, I. M., Stark, G. R. & Darnell, J. E. Contribution of STAT SH2 groups to specific interferon signaling by the Jak-STAT pathway. *Science (80-.).* (1995). doi:10.1126/science.7871432

157. Shuai, K., Schindler, C., Prezioso, V. & Darnell, J. Activation of transcription by IFN-gamma: tyrosine phosphorylation of a 91-kD DNA binding protein. *Science (80-.).* (1992). doi:10.1126/science.1281555

158. Greenlund, A. C. *et al.* Stat recruitment by tyrosine-phosphorylated cytokine receptors: An ordered reversible affinity-driven process. *Immunity* (1995). doi:10.1016/1074-7613(95)90012-8

159. Shuai, K., Stark, G. R., Kerr, I. M. & Darnell, J. E. A single phosphotyrosine residue of Stat91 required for gene activation by interferon-γ. *Science (80-.).* (1993). doi:10.1126/science.7690989

160. Decker, T., Kovarik, P. & Meinke, A. GAS elements: a few nucleotides with a major impact on cytokine-induced gene expression. *J. Interf. Cytokine Res.* (1997). doi:10.1089/jir.1997.17.121

161. Fu, X. Y., Kessler, D. S., Veals, S. A., Levy, D. E. & Darnell, J. E. ISGF3, the

transcriptional activator induced by interferon alpha, consists of multiple interacting polypeptide chains. *Proc. Natl. Acad. Sci.* (1990). doi:10.1073/pnas.87.21.8555

162. Levy, D. E., Larner, A., Chaudhuri, A., Babiss, L. E. & Darnell, J. E. Interferon-stimulated transcription: isolation of an inducible gene and identification of its regulatory region. *Proc. Natl. Acad. Sci. U. S. A.* (1986). doi:PMC387047
163. Chelbi-Alix, M. K. & Wietzerbin, J. Interferon, a growing cytokine family: 50 years of interferon research. *Biochimie* **89**, 713–718 (2007).
164. Gresser, I. *et al.* Interferon and murine leukaemia. III: Efficacy of interferon preparations administered after inoculation of friend virus [28]. *Nature* (1967). doi:10.1038/215174a0
165. Pestka, S. The interferons: 50 Years after their discovery, there is much more to learn. *J. Biol. Chem.* **282**, 20047–20051 (2007).
166. Minn, A. J. Interferons and the Immunogenic Effects of Cancer Therapy. *Trends in Immunology* (2015). doi:10.1016/j.it.2015.09.007
167. Weichselbaum, R. R. *et al.* An interferon-related gene signature for DNA damage resistance is a predictive marker for chemotherapy and radiation for breast cancer. *Proc. Natl. Acad. Sci.* (2008). doi:10.1073/pnas.0809242105
168. Ulloa-Montoya, F. *et al.* Predictive gene signature in MAGE-A3 antigen-specific cancer immunotherapy. *J. Clin. Oncol.* (2013). doi:10.1200/JCO.2012.44.3762
169. Gajewski, T. F., Fuertes, M., Spaapen, R., Zheng, Y. & Kline, J. Molecular profiling to identify relevant immune resistance mechanisms in the tumor microenvironment. *Current Opinion in Immunology* (2011). doi:10.1016/j.coi.2010.11.013
170. Wilson, E. B. *et al.* Blockade of chronic type I interferon signaling to control persistent LCMV infection. *Science (80-.).* (2013). doi:10.1126/science.1235208
171. Sistigu, A. *et al.* Cancer cell-autonomous contribution of type I interferon signaling to the efficacy of chemotherapy. *Nat. Med.* **20**, 1301–1309 (2014).
172. Kroemer, G., Galluzzi, L., Kepp, O. & Zitvogel, L. Immunogenic Cell Death in Cancer Therapy. *Annu. Rev. Immunol.* (2013). doi:10.1146/annurev-immunol-032712-100008
173. Härtlova, A. *et al.* DNA Damage Primes the Type I Interferon System via the Cytosolic DNA Sensor STING to Promote Anti-Microbial Innate Immunity. *Immunity*

(2015). doi:10.1016/j.immuni.2015.01.012

174. Taniguchi, K. *et al.* Interferon gamma induces lung colonization by intravenously inoculated B16 melanoma cells in parallel with enhanced expression of class I major histocompatibility complex antigens. *Proc. Natl. Acad. Sci.* (1987). doi:10.1073/pnas.84.10.3405

175. Lollini, P. -L *et al.* Inhibition of tumor growth and enhancement of metastasis after transfection of the γ-interferon gene. *Int. J. Cancer* (1993). doi:10.1002/ijc.2910550224

176. Boettcher, M., Kischkel, F. & Hoheise, J. D. High-definition DNA methylation profiles from breast and ovarian carcinoma cell lines with differing doxorubicin resistance. *PLoS One* (2010). doi:10.1371/journal.pone.0011002

177. Hatle, K. M. *et al.* Methylation-Controlled J Protein Promotes c-Jun Degradation To Prevent ABCB1 Transporter Expression. *Mol. Cell. Biol.* **27**, 2952–2966 (2007).

178. Kuang, Y. Q. *et al.* Dopamine receptor-interacting protein 78 acts as a molecular chaperone for CCR5 chemokine receptor signaling complex organization. *PLoS One* **7**, (2012).

179. Mitra, A., Shevde, L. A. & Samant, R. S. Multi-faceted role of HSP40 in cancer. *Clin. Exp. Metastasis* **26**, 559–567 (2009).

180. Fernández-Cabezudo, M. J. *et al.* Deficiency of mitochondrial modulator MCJ promotes chemoresistance in breast cancer. *JCI Insight* **1**, 1–15 (2016).

181. Hatle, K. M. *et al.* Methylation-Controlled J Protein Promotes c-Jun Degradation To Prevent ABCB1 Transporter Expression. *Mol. Cell. Biol.* (2007). doi:10.1128/MCB.01804-06

182. Hatle, K. M. *et al.* MCJ/DnaJC15, an Endogenous Mitochondrial Repressor of the Respiratory Chain That Controls Metabolic Alterations. *Mol. Cell. Biol.* **33**, 2302–2314 (2013).

183. Sinha, D., Srivastava, S., Krishna, L. & D'Silva, P. Unraveling the Intricate Organization of Mammalian Mitochondrial Presequence Translocases: Existence of Multiple Translocases for Maintenance of Mitochondrial Function. *Mol. Cell. Biol.* (2014). doi:10.1128/MCB.01527-13

184. Segura-Pacheco, B. *et al.* Global DNA hypermethylation-associated cancer chemotherapy resistance and its reversion with the demethylating agent

hydralazine. *J. Transl. Med.* (2006). doi:10.1186/1479-5876-4-32

185. Snyder, V., Reed-Newman, T. C., Arnold, L., Thomas, S. M. & Anant, S. Cancer Stem Cell Metabolism and Potential Therapeutic Targets. *Front. Oncol.* (2018). doi:10.3389/fonc.2018.00203

186. De Francesco, E. M., Sotgia, F. & Lisanti, M. P. Cancer stem cells (CSCs): metabolic strategies for their identification and eradication. *Biochem. J.* (2018). doi:10.1042/BCJ20170164

187. White, R. M. *et al.* Transparent Adult Zebrafish as a Tool for In Vivo Transplantation Analysis. *Cell Stem Cell* (2008). doi:10.1016/j.stem.2007.11.002

188. Jung, I. H. *et al.* Impaired Lymphocytes Development and Xenotransplantation of Gastrointestinal Tumor Cells in Prkdc-Null SCID Zebrafish Model. *Neoplasia (United States)* (2016). doi:10.1016/j.neo.2016.06.007

189. Doherty, M. R. *et al.* Interferon-beta represses cancer stem cell properties in triple-negative breast cancer. *Proc. Natl. Acad. Sci.* **114**, 13792–13797 (2017).

190. Meissl, K., Macho-Maschler, S., Müller, M. & Strobl, B. The good and the bad faces of STAT1 in solid tumours. *Cytokine* (2017). doi:10.1016/j.cyto.2015.11.011

191. Fridman, J. S. & Lowe, S. W. Control of apoptosis by p53. *Oncogene* (2003). doi:10.1038/sj.onc.1207116

192. Rasighaemi, P. & Ward, A. C. ETV6 and ETV7: Siblings in hematopoiesis and its disruption in disease. *Crit. Rev. Oncol. Hematol.* **116**, 106–115 (2017).

193. Alessandrini, F., Pezzè, L., Menendez, D., Resnick, M. A. & Ciribilli, Y. ETV7-Mediated DNAJC15 Repression Leads to Doxorubicin Resistance in Breast Cancer Cells. *Neoplasia* **20**, 857–870 (2018).

194. Brzostek-Racine, S., Gordon, C., Van Scoy, S. & Reich, N. C. The DNA Damage Response Induces IFN. *J. Immunol.* (2011). doi:10.1007/BF01422808

195. Schwartz, M. A. Integrins, oncogenes, and anchorage independence. *Journal of Cell Biology* (1997). doi:10.1083/jcb.139.3.575

196. Prieto-Vila, M., Takahashi, R. U., Usuba, W., Kohama, I. & Ochiya, T. Drug resistance driven by cancer stem cells and their niche. *Int. J. Mol. Sci.* **18**, (2017).

197. Li, W. *et al.* Unraveling the roles of CD44/CD24 and ALDH1 as cancer stem cell markers in tumorigenesis and metastasis. *Sci. Rep.* (2017). doi:10.1038/s41598-017-14364-2

198. Pastò, A. *et al.* Cancer stem cells from epithelial ovarian cancer patients privilege oxidative phosphorylation, and resist glucose deprivation. *Oncotarget* (2014). doi:10.18632/oncotarget.2010

199. Sato, M. *et al.* Spheroid cancer stem cells display reprogrammed metabolism and obtain energy by actively running the tricarboxylic acid (TCA) cycle. *Oncotarget* (2016). doi:10.18632/oncotarget.8947

200. Gao, C., Shen, Y., Jin, F., Miao, Y. & Qiu, X. Cancer stem cells in small cell lung cancer cell line H446: Higher dependency on oxidative phosphorylation and mitochondrial substrate-level phosphorylation than non-stem cancer cells. *PLoS One* (2016). doi:10.1371/journal.pone.0154576

201. De Luca, A. *et al.* Mitochondrial biogenesis is required for the anchorage-independent survival and propagation of stem-like cancer cells. *Oncotarget* (2015). doi:10.18632/oncotarget.4401

202. Lamb, R. *et al.* Mitochondria as new therapeutic targets for eradicating cancer stem cells: Quantitative proteomics and functional validation via MCT1/2 inhibition. *Oncotarget* (2014). doi:10.18632/oncotarget.2789

203. Sancho, P. *et al.* MYC/PGC-1α balance determines the metabolic phenotype and plasticity of pancreatic cancer stem cells. *Cell Metab.* (2015). doi:10.1016/j.cmet.2015.08.015

204. Vlashi, E. *et al.* Metabolic differences in breast cancer stem cells and differentiated progeny. *Breast Cancer Res. Treat.* (2014). doi:10.1007/s10549-014-3051-2

205. Farnie, G., Sotgia, F. & Lisanti, M. P. High mitochondrial mass identifies a sub-population of stem-like cancer cells that are chemo-resistant. *Oncotarget* (2015). doi:10.18632/oncotarget.5401

206. Vazquez, F. *et al.* PGC1α Expression Defines a Subset of Human Melanoma Tumors with Increased Mitochondrial Capacity and Resistance to Oxidative Stress. *Cancer Cell* (2013). doi:10.1016/j.ccr.2012.11.020

207. Katajisto, P. *et al.* Asymmetric apportioning of aged mitochondria between daughter cells is required for stemness. *Science (80-.).* (2015). doi:10.1126/science.1260384

208. Liu, P. P. *et al.* Metabolic regulation of cancer cell side population by glucose through activation of the Akt pathway. *Cell Death Differ.* (2014).

doi:10.1038/cdd.2013.131

209. Palorini, R. *et al.* Energy metabolism characterization of a novel cancer stem cell-like line 3AB-OS. *J. Cell. Biochem.* (2014). doi:10.1002/jcb.24671

210. Shen, Y.-A., Wang, C.-Y., Hsieh, Y.-T., Chen, Y.-J. & Wei, Y.-H. Metabolic reprogramming orchestrates cancer stem cell properties in nasopharyngeal carcinoma. *CELL CYCLE* (2015). doi:10.4161/15384101.2014.974419

211. Scheel, C. & Weinberg, R. A. Cancer stem cells and epithelial-mesenchymal transition: Concepts and molecular links. *Seminars in Cancer Biology* (2012). doi:10.1016/j.semcancer.2012.04.001

212. Kuwata, T. *et al.* Gamma Interferon Triggers Interaction between ICSBP (IRF-8) and TEL, Recruiting the Histone Deacetylase HDAC3 to the Interferon-Responsive Element. *Mol. Cell. Biol.* (2002). doi:10.1128/mcb.22.21.7439-7448.2002

213. Brass, A. L., Kehrli, E., Eisenbeis, C. F., Storb, U. & Singh, H. Pip, a lymphoid-restricted IRF, contains a regulatory domain that is important for autoinhibition and ternary complex formation with the Ets factor PU.1. *Genes Dev.* (1996). doi:10.1101/gad.10.18.2335

214. Burstein, M. D. *et al.* Comprehensive genomic analysis identifies novel subtypes and targets of triple-negative breast cancer. *Clin. Cancer Res.* (2015). doi:10.1158/1078-0432.CCR-14-0432

215. Gasco, M., Shami, S. & Crook, T. The p53 pathway in breast cancer. *Breast Cancer Res.* (2002). doi:10.1186/bcr426

216. Furlan, A. *et al.* Ets-1 controls breast cancer cell balance between invasion and growth. *Int. J. Cancer* (2014). doi:10.1002/ijc.28881

217. Kinoshita, J. *et al.* Clinical significance of PEA3 in human breast cancer. *Surgery* (2002). doi:10.1067/msy.2002.119792

218. Bièche, I. *et al.* Expression of PEA3/E1AF/ETV4, an Ets-related transcription factor, in breast tumors: Positive links MMP2, NRG1 and CGB expression. *Carcinogenesis* (2004). doi:10.1093/carcin/bgh024

219. Hsing, M., Wang, Y., Rennie, P. S., Cox, M. E. & Cherkasov, A. ETS transcription factors as emerging drug targets in cancer. *Med. Res. Rev.* med.21575 (2019). doi:10.1002/med.21575

220. Pfaffl, M. W. A new mathematical model for relative quantification in real-time RT-

PCR. *Nucleic Acids Res.* (2001). doi:10.1093/nar/29.9.e45

221. Gebäck, T., Schulz, M. M. P., Koumoutsakos, P. & Detmar, M. TScratch: A novel and simple software tool for automated analysis of monolayer wound healing assays. *Biotechniques* (2009). doi:10.2144/000113083

DECLARATION OF ORIGINAL AUTHORSHIP

I, Laura Pezzè, confirm that this is my own work and the use of all material from other sources has been properly and fully acknowledged.

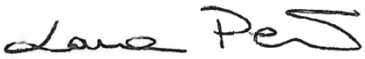

ANNEX: PUBLICATIONS

In this section are collected the publications I contributed to (* = these authors equally contributed to the work):

- Alessandrini F*, **Pezzè L***, Menendez D, Resnick MA, Ciribilli Y; ETV7-mediated DNAJC15 repression leads to Doxorubicin resistance in breast cancer cells. *Neoplasia.* 2018 Jul 16;20(8):857-870. doi: 10.1016/j.neo.2018.06.008. → *This paper contains all the results I described in the first chapter of the results section. The article is hereby attached (Annex I).*
- Alessandrini F*, **Pezzè L***, Ciribilli Y; LAMPs: shedding light on cancer biology. *Seminars in Oncology*. 2017 Aug;44(4):239-253. doi: 10.1053/j.seminoncol.2017.10.013. → *This review article focus on the family of Lysosomal Associated Membrane Proteins (LAMP) and their role in cancer biology. Here I contributed to the description of LAMP3, CD68 and BAD-LAMP family members, to the design of figures 2, 3, 4 and 5, to part of the introduction and discussion and to revision of the manuscript. The article is hereby attached (Annex II).*
- Pinazza M, Ghisi M, Minuzzo S, Agnusdei V, Fossati G, Ciminale V, **Pezzè L**, Ciribilli Y, Pilotto G, Venturoli C, Amadori A, Indraccolo S; Histone Deacetylase 6 controls Notch3 trafficking and degradation in T-cell Acute Lymphoblastic Leukemia Cells. *Oncogene*. 2018 Apr 12. doi: 10.1038/s41388-018-0234-z. → *Here I performed the subcellular fractionation and western blot analysis of DND41 cells treated with TSA to demonstrate Notch3-FL enrichment in the lysosomal fraction upon TSA treatment (Figure 3D and 3E). The article is hereby attached (Annex III).*
- Knezović Florijan M, Ozretić P, Bujak M, **Pezzè L**, Ciribilli Y, Kaštelan Z, Slade N, Hudolin T; The role of p53 isoforms' expression and p53 mutation status in renal cell cancer prognosis. *Urologic Oncology*. 2019 Apr 1. pii: S1078-1439(19)30100-0. doi: 10.1016/j.urolonc.2019.03.007. [Epub ahead of print] → *Here I performed the*

functional analysis of separate allele in yeast (FASAY) to identify the p53 status of 41 renal cell carcinoma patients (Table 1). The article is hereby attached (Annex IV)

- Agnusdei V, Minuzzo S, Pinazza M, Gasparini A, **Pezzè L**, Amaro AA, Pasqualini L, Del Bianco P, Palumbo P, Ciribilli Y, Pfeffer U, Carella M, Amadori A, Indraccolo S; Dissecting molecular mechanisms of resistance to Notch1-targeted therapy in T-ALL xenografts. Under revision → *Here I performed the subcellular fractionation and western blot analysis of PD19TALL cells to Notch1-FL decrease in the plasma membrane lysate fraction in OMP52M51-resistant cells compared to the control cells (Figure 5B).*

NEOPLASIA
www.neoplasia.com

Volume 20 Number 8 August 2018 pp. 857–870 857

ETV7-Mediated DNAJC15 Repression Leads to Doxorubicin Resistance in Breast Cancer Cells[1]

Federica Alessandrini[*,2], Laura Pezzè[*,2], Daniel Menendez[†], Michael A. Resnick[†] and Yari Ciribilli[*]

[*]Laboratory of Molecular Cancer Genetics, Centre for Integrative Biology (CIBIO), University of Trento, Via Sommarive 9, 38123, Povo (TN), Italy; [†]Genome Integrity and Structural Biology Laboratory, National Institute of Environmental Health Sciences (NIHES), NIH, Research Triangle Park, NC 27709, USA

Abstract

Breast cancer treatment often includes Doxorubicin as adjuvant as well as neoadjuvant chemotherapy. Despite its cytotoxicity, cells can develop drug resistance to Doxorubicin. Uncovering pathways and mechanisms involved in drug resistance is an urgent and critical aim for breast cancer research oriented to improve treatment efficacy. Here we show that Doxorubicin and other chemotherapeutic drugs induce the expression of ETV7, a transcriptional repressor member of ETS family of transcription factors. The ETV7 expression led to DNAJC15 down-regulation, a co-chaperone protein whose low expression was previously associated with drug resistance in breast and ovarian cancer. There was a corresponding reduction in Doxorubicin sensitivity of MCF7 and MDA-MB-231 breast cancer cells. We identified the binding site for ETV7 within *DNAJC15* promoter and we also found that DNA methylation may be a factor in ETV7-mediated DNAJC15 transcriptional repression. These findings of an inverse correlation between ETV7 and DNAJC15 expression in MCF7 cells in terms of Doxorubicin resistance, correlated well with treatment responses of breast cancer patients with recurrent disease, based on our analyses of reported genome-wide expression arrays. Moreover, we demonstrated that ETV7-mediated Doxorubicin-resistance involves increased Doxorubicin efflux via nuclear pumps, which could be rescued in part by DNAJC15 up-regulation. With this study, we propose a novel role for ETV7 in breast cancer, and we identify DNAJC15 as a new target gene responsible for ETV7-mediated Doxorubicin-resistance. A better understanding of the opposing impacts of Doxorubicin could improve the design of combinatorial adjuvant regimens with the aim of avoiding resistance and relapse.

Neoplasia (2018) 20, 857–14

Introduction

Chemotherapy is commonly adopted for the pre- and post-surgical treatment of many solid tumors, including breast cancer, and it is still the only therapeutic option for most cases of metastatic spread. Among the drugs used in different regimens, Doxorubicin is often employed and is one of the most effective [1]. This drug is an anthracyclin intercalator that poisons topoisomerase II, thereby causing DNA damage and subsequent cytotoxicity [2]. As for most chemotherapeutic agents, several unwanted side-effects have been reported and, unfortunately, Doxorubicin is also known for late-onset cardiotoxicity determined by a complex cascade of events [3]. Despite the efficacy of Doxorubicin and other chemotherapeutic drugs, cancer

Abbreviations: ETV7, Ets Variant Gene 7; ETS, E26 Transformation-Specific; DNAJC15, DNAJ Heat Shock Protein family (Hsp40) member C15; ABCB1, ATP Binding Cassette subfamily B member 1; DNMT3A, DNA Methyl-Transferase 3A; 5-Aza, 5-Aza-2′-deoxycytidine; TNBC, Triple Negative Breast Cancer; ADR, Adriamycin.

Address all correspondence to: Federica Alessandrini or Yari Ciribilli, Laboratory of Molecular Cancer Genetics, Centre for Integrative Biology (CIBIO), University of Trento, Via Sommarive 9, 38123, Povo (TN), Italy.
E-mails: f.alessandrini@unitn.it, yari.ciribilli@unitn.it

[1] Disclosure of Potential Conflicts of Interest: the authors declare no potential conflicts of interest.

[2] These authors contributed equally to this work.

Received 1 May 2018; Revised 26 June 2018; Accepted 26 June 2018

1476-5586/18
https://doi.org/10.1016/j.neo.2018.06.008

cells may develop chemoresistance, resulting in treatment failure and recurrence. Indeed, there are many survival strategies available to cancer cells and some of them can even be activated by chemotherapy itself. Some activation mechanisms can lay the groundwork for unwanted future resistance to treatment, which can be driven or stimulated by the activation of pro-survival or pro-tumorigenic transcription factors, such as NF-κB [4,5] and FOXM1 [6,7]. Moreover, Doxorubicin can lead to an increased expression of drug efflux pumps such as MRP1 in breast cancer [8] and to the activation of the anti-apoptotic cascade HER3-PI3K-AKT in ovarian cancer [9].

ETV7 (Ets Variant Gene 7) is a transcription factor belonging to the ETS (E26 transformation-specific) family of transcriptional regulators. Various ETS factors, such as ETS1, ETS2, PU1, FLI1, and ERG, are distinguished for their pro-tumorigenic functions and are involved in chromosomal translocations often associated with Ewing's sarcoma and prostate cancer [10]. ETV7 is a poorly characterized protein that can act as a transcriptional repressor, which presents an 85-amino acid ETS domain responsible for binding a purine-rich GGAA core motif in the regulatory regions of target genes. The protein also has a conserved pointed (PNT) protein–protein interaction domain, required for the formation of homo–/hetero-dimers and oligomers and involved in transcriptional repression [11,12]. Given the presence of the PNT domain, ETV7 can either self-associate or form heterodimers/oligomers with ETV6/TEL, a highly related ETS family member with tumor suppressor functions that also acts as transcriptional repressor [13]. In contrast, ETV7 is generally acknowledged to be an oncoprotein, and some of its pro-tumorigenic functions result from its ability to directly bind and inhibit ETV6-mediated gene repression [14].

Deregulated high ETV7 expression levels has been linked to hepatocellular carcinoma [15] and to leukemia [10,16]. Over-expressed ETV7 can also cooperate with Eμ-MYC in promoting lymphomagenesis and blocking Myc-induced apoptosis [17]. Furthermore, ETV7 is able to enhance the Ras-driven transformation in fibroblasts and shows pro-proliferative and anti-differentiation roles observed in myeloid and lymphoid cells [10,17]. In contrast, ETV7 can act as a tumor suppressor in nasopharyngeal carcinoma through binding *SERPINE1* promoter and decreasing its expression [18]. Further, ETV7 down-regulation has been reported in drug-resistant gastric cancer cells [19].

We recently observed in human breast cancer cells that *ETV7* can be transcriptionally activated upon Doxorubicin treatment and synergistically induced by the combined treatment with Doxorubicin and TNFα. Among the possible activators of its transcription, we identified tumor suppressor p53 and NFκB (p65) as transcription factors able to directly bind to *ETV7* promoter [20].

Interestingly, ETV7 and DNAJC15 expression appear to inversely correlate upon Doxorubicin treatment and also upon interferon gamma expression. ETV7 is recognized as an interferon-stimulated gene, whereas down-regulation of DNAJC15 has been reported in interferon gamma treated macrophages [21]. DNAJC15 plays an intriguing role among the tumor suppressor genes whose repression is associated with tumor aggressiveness and chemoresistance. It belongs to the HSP40/DNAJ family of co-chaperones, mostly involved in helping ATP hydrolysis and thus the activation of the HSP70 chaperone with its roles in protein folding, trafficking, interaction, import and export [22,23].

DNAJC15 is often hyper-methylated and repressed in malignant pediatric tumors [24], neuroblastoma [25], Wilm's tumor and melanoma [26]. Furthermore, its down-regulation associates with increased drug resistance in ovarian and breast cancer [27,28]. Using MCF7 breast cancer cells, Hatle and colleagues observed that in Doxorubicin-resistant clones, the low expression of DNAJC15 in the Golgi network was responsible for the degradation of some proteins including the transcription factor c-JUN [29]. Therefore, inhibition of DNAJC15 resulted in increased levels of c-JUN protein, which was ultimately responsible for increased transcription of the multidrug transporter ABCB1/MDR1 [29]. Other studies have reported the localization of DNAJC15 inside the mitochondrial inner membrane where it can control the respiratory chain and thus the production of ROS [30]. Inside the mitochondria, it can also help mitochondrial import of proteins by favoring the ATP hydrolysis of a chaperone member of the TIMP23 translocase [26]. DNAJC15 exerts its tumor suppressor role also by promoting the release of pro-apoptotic molecules through the mitochondrial permeability transition pore complex [31].

In this study, we identify a novel circuitry for Doxorubicin resistance in breast cancer cells where ETV7 acts as a major player. Given the pro-tumorigenic roles of ETV7, its activation upon Doxorubicin treatment represents one of the unwanted side-effects that could possibly unleash a drug resistance mechanism. In particular, ETV7 appears to trigger the activation of a resistance circuitry by directly binding and, therefore, repressing the transcription of some tumor suppressor genes. Specifically, we demonstrate that ETV7 can repress DNAJC15 in a methylation-dependent manner. We propose a novel drug resistance mechanism directly driven by Doxorubicin whereby Doxorubicin itself induces the up-regulation of ETV7 that, in turn, down-regulates DNAJC15 expression giving rise to Doxorubicin resistance in breast cancer cells.

Materials and Methods

Cell Culture Conditions and Treatments

MCF7 cells were obtained from Interlab Cell Line Collection bank (Genoa, Italy). A549 and U2OS cell lines were from ATCC (Manassas, VA, USA), while A375M and MDA-MB-231 cells were a gift from, respectively, Dr. D. Bergamaschi (Centre for Cell Biology and Cutaneous Research, Blizard Institute, Barts and The London School of Medicine & Dentistry, UK) and Prof. A. Provenzani (Laboratory of Genomic Screening, CIBIO, University of Trento, Italy). MCF7 and U2OS cells were grown in DMEM medium supplemented with 10% FBS, 2 mM L-Glutamine and 2 mM of Penicillin/Streptomycin; MDA-MB-231 cells in the same medium with the addition of 1% Non-Essential Amino acids. A549 and A375M cells were cultured in RPMI medium +10% FBS, 2 mM L-Glutamine and 2 mM of Penicillin/Streptomycin. BJ1-hTERT cells (immortalized normal fibroblasts) were obtained from Dr. K. Lobachev (Georgia Institute of Technology, GA, USA) and were grown in MEM medium supplemented with 10% FBS, 2 mM L-Glutamine, 2 mM of Penicillin/Streptomycin and Puromycin. MCF10A cells (immortalized normal mammary epithelial cells) were received from Dr. S. Soddu (Unit of Cellular Networks and Molecular Therapeutic Targets, Regina Elena National Cancer Institute-IRCCS, Rome, Italy) and cultivated in DMEM/F12 1:1 medium supplemented with 5% Horse Serum, 17 ng/ml human epidermal growth factor (hEGF), 10% Mammary Epithelial Growth Supplement (MEGS: 0.4% bovine pituitary extract; 1 μg/ml recombinant human insulin-like

growth factor 1; 0.5 μg/ml hydrocortisone, 3 ng/ml hEGF), 100 ng/ml cholera toxin (Sigma-Aldrich, Milan, Italy). When not explicitly stated, cell culture reagents were obtained from Gibco (Life Technologies, Thermo Fisher Scientific, Milan, Italy).

When needed cells were authenticated from the DNA Diagnostic Center (DDC, Fairfield, OH, USA) or Eurofins Genomics (Ebersberg, Germany). Mycoplasma test was done monthly as scheduled by our CIBIO Cell Technology Facility (PlasmoTest™ — Mycoplasma Detection Kit, InvivoGen, Toulouse, France). Experiments were performed within one month from the thawing procedure.

Human lymphocytes were isolated and cultured from the blood of healthy donors as previously described, in accordance with an NIEHS IRB-approved protocol IRB#10-E-0063 and in compliance with the Helsinki Declaration. Prior to participation in the study, subjects were informed of the procedures and potential risks and each signed a statement of informed consent [32].

Doxorubicin (Sigma-Aldrich) was used at the concentration of 1.5 μM (for all cells except for U2OS and BJ1-hTERT cells, which were treated with 0.5 μM Doxorubicin) for 16 hours treatment in the case of qPCR analysis and western blotting and at different concentrations for 72 hours for MTT viability assays.

Twenty-four-hour treatments were performed with the following drugs and concentrations: Etoposide 50 μM (Enzo Life Science, Rome, Italy), Nutlin-3a 10 μM, 5-FluoroUracil (5FU) 375 μM, Camptothecin 0.5 μM, Everolimus 50 nM, Tamoxifen 1 μM, Imatinib 3 μM (Selleckchem, Aurogene, Rome, Italy). Compounds were purchased from Sigma-Aldrich when not specifically indicated.

5-Aza-2′-deoxycytidine (Sigma-Aldrich) treatment was performed for 48 hours at the concentration of 5 μM.

Quercetin and Genistein were purchased from Extrasynthese (Genay, Lyon, France), and treatments were performed for 16 hours at the concentration of 50μM for Quercetin and 30μM for Genistein.

Plasmids

The expression vectors pCMV6-Entry-Empty, pCMV6-Entry-ETV7 and pCMV6-Entry-DNAJC15 C-terminally tagged with DDK-Myc tags were purchased from Origene (Tema Ricerca, Bologna, Italy).

pGL4.26-DNAJC15 reporter was obtained by cloning the promoter region of DNAJC15 (−299 to +512 bp from TSS according to the Eukaryotic Promoter Database, http://epd.vital-it.ch/) amplified with Q5 High Fidelity DNA Polymerase (New England Biolabs, Euroclone, Milan, Italy) and the following primers (Eurofins Genomics): Fw: GCCTCGAGCAGCACAAACTCATTTGAGGG and Rv: GCAAGCTTAGGCGGCCCGGAGACTCAAG. Purified PCR product was inserted into pGL4.26 backbone using Xho I and Hind III restriction endonucleases. Cloning was checked by restriction analysis and direct sequencing (Eurofins Genomics). For site-directed mutagenesis of this vector please refer to the section below. The pRL-SV40 (Promega) vector constitutively expressing the *Renilla reniformis* luciferase cDNA was used as transfection efficiency control for gene reporter assays.

Generation of Stable pCVM6-Entry-ETV7 and Empty MCF7 and MDA-MB-231 Cells

In order to get MCF7, MDA-MB-231 and U2OS cells stably over-expressing ETV7 and the empty control, cells were seeded in 6-well plates and subsequently transfected for 48 hours with 1 μg of pCMV6-Entry-Empty or pCMV6-Entry-ETV7 (Origene) using Lipofectamine LTX and Plus Reagent (Life Technologies) or FuGene HD (Promega, Milan, Italy) respectively for MCF7 or MDA-MB-231 and U2OS cells. Afterwards, cells were split and Geneticin (Life Technologies) was added at a concentration of 600 and 800 μg/ml respectively for MCF7 or MDA-MB-231 and U2OS cells; each 3 days medium was replaced and after 4 cycles of selection, single cell cloning was performed according to the Corning protocol for cell cloning by Serial dilution in 96 well plates. During the single cell cloning procedure Geneticin concentration was gradually reduced to 300 (MCF7) and 400 μg/ml (MDA-MB-231 and U2OS).

RNA Isolation and RT-qPCR

Total RNA was extracted using the Illustra RNA spin Mini Kit (GE Healthcare, Milan, Italy), converted to cDNA with the RevertAid First Strand cDNA Synthesis Kit (Thermo Fisher Scientific) and RT-qPCR was performed with 25 ng of template cDNA in 384 wells-plate (BioRad, Milan, Italy) using the Kapa Sybr Fast qPCR Master Mix (Kapa Biosystems, Resnova, Ancona, Italy) and the CFX384 Detection System (BioRad). YWHAZ and B2M genes were used as housekeeping genes to obtain the relative fold change by the ΔΔCt method as previously described [33]. Primer sequences were designed using Primer-BLAST designing tool (https://www.ncbi.nlm.nih.gov/tools/primer-blast/), checked for specificity and efficiency, and are listed in Supplementary Table 1 (Eurofins Genomics).

Western Blot

Total protein extracts were obtained by lysing the cells in RIPA buffer and proteins were quantified by the BCA method (Pierce, Thermo Fisher Scientific); 20 to 50 μg of protein extracts were loaded on 7.5% and 12% polyacrylamide gels, and western blotting was performed as previously described [34]. Transferred proteins were probed over-night at 4°C with specific antibodies diluted in 1% non-fat skim milk-PBS-T solution: GAPDH (6C5, sc-32,233), ETV7/TEL2 (F-8, sc-376,137X), ETV7/TEL2 (H-88, sc-292,509), Histone H3 (FL-136, sc-10,809), α-Actinin (H-2, sc-17,829), DNMT3A (GTX129125, GeneTex, Prodotti Gianni, Milan, Italy). Antibodies were obtained from Santa Cruz Biotechnologies (Milan, Italy) when not specifically indicated. Detection was performed with ECL Select reagent (GE Healthcare) using a ChemiDoc XRS+ (BioRad) or UVITec Alliance LD2 (UVITec Cambridge, UK) imaging systems.

In order to separate cytoplasmic and nuclear fractions of proteins, MCF7 cells were seeded in p150 dishes and treated with Doxorubicin for either 6 or 16 hours. Cytoplasmic proteins were extracted following the instructions of NE-PER kit (Thermo Fisher Scientific). Alternatively, in order to enrich the nuclear extracts for chromatin-associated proteins, pellets remaining from cytoplasmic extraction were directly resuspended in 1x Loading Buffer and boiled. Approximately, 150 μg of nuclear protein extracts and 50 μg of cytoplasmic protein extracts were loaded on a polyacrylamide gel, blotted and detected as described above. Histone H3 and GAPDH were used respectively as controls for nuclear and for cytoplasmic extracts.

Gene Reporter Assay

24 hours prior to transfection, 7×10^4 MCF7 cells were seeded in 24 well-plate. Cells were transfected with Lipofectamine LTX and

Plus Reagent (Thermo Fisher Scientific) along with 250 ng pGL4.26-DNAJC15 reporter, 250 ng pCMV6-Entry-Empty or pCMV6-Entry-ETV7 vectors, and 50 ng pRL-SV40 for each well. After 48 hours, cells were washed once in PBS and lysed in 1X PLB buffer and luciferase activity measurements were performed using the Dual-Luciferase Reporter Assay System (Promega) as previously described [35,36] and detected using the Infinite M200 plate reader (Tecan, Milan, Italy). Renilla luciferase activity was used as an indicator of transfection efficiency and used to obtain the Relative Light Unit (RLU) measure.

Site-Directed Mutagenesis

Site-directed mutagenesis was performed using GENEART Site-Directed Mutagenesis kit (Life Technologies) according to manufacturer's instructions. In order to mutate ETV7 binding sites within pGL4.26-DNAJC15 (substituting the GGA conserved bases with ATC random sequence), the reporter plasmid was first methylated and then amplified with AccuPrime *Pfx* DNA Polymerase (InVitrogen, Life Technologies) in a mutagenesis reaction with the following primers (Eurofins Genomics):

BS1_Fw: GGGAAGAAAGGCTGCCCatcAGGGGGTCAGGAAAGC;
BS1_Rv: GCTTTCCTGACCCCCTgatGGGCAGCCTTTCTTCCC;
BS2_Fw: GGTGAGAAGGGTATCTgatGGGAACCTCGCCTTTAA;
BS2_Rv: TTAAAGGCGAGGTTCCCatcAGATACCCTTCTCACC.

Mutagenesis was then followed by an in vitro recombination reaction to enhance efficiency and colony yield. Mutated plasmids (pGL4.26-DNAJC15-BS1 and -BS2) were subsequently transformed into DH5α-T1^{R} *E. coli* competent cells, which circularize the linear mutated DNA and exploits McrBC endonuclease activity to digest methylated DNA. Complete and correct mutagenesis was verified by direct sequencing (Eurofins Genomics).

Bisulfite-Conversion

Genomic DNA was extracted from MCF7 cells left untreated, treated with Doxorubicin or over-expressing pCMV6-Entry-Empty or -ETV7 vectors. DNA and RNA extractions were obtained from the same samples using the AllPrep DNA/RNA/Protein Mini Kit (Qiagen, Milan Italy).

Purified DNA was then denaturated and subjected to bisulfite conversion with the EZ DNA Methylation-Lightning™ Kit (Zymo Research, Euroclone) according to manufacturer's recommendations. The resulting product was subsequently PCR amplified and sequenced using the following bisulfite-specific primers (Eurofins Genomics): Fw: TTGGTAGGATTTATTAGTTTTTGTTGG; Rv: CACCCAACTAATCTTTATATTTTTAATAAA.

Doxorubicin Efflux Analysis

1.5 x 10^4 MDA-MB-231 cells were seeded in a 96 well-plate; the subsequent day, 10 or 20 μM Doxorubicin was added for 3 hours and cells were analyzed with the Operetta High Content Imaging System (Perkin Elmer, Milan, Italy) at CIBIO High Throughput Screening (HTS) Facility exploiting the intrinsic fluorescence of Doxorubicin. By using the Harmony 4.1 PhenoLOGIC software (Perkin Elmer) nuclear and cytoplasmic regions were detected; successively, the relative ratio of nuclear respect to cytoplasmic fraction from Doxorubicin signal was calculated. To measure the Doxorubicin efflux area, the Doxorubicin spot area into the cytoplasm was measured (see Suppl. Figure S2*A* for details).

Viability Assay

Cells were seeded in a 96 well-plate and treated with different concentrations of Doxorubicin for 72 hours. Medium was removed and wells were washed with 1X PBS to avoid possible reduction effects of the added compound with MTT reagent (Sigma-Aldrich). Ten μl of MTT (5 mg/ml solution in 1X PBS) was added to 100 μl of fresh medium and left in incubation for 3 hours. Afterwards, medium was accurately removed and cells were lysed in 100 μl of DMSO (Sigma-Aldrich), and a colorimetric measure was performed at the Infinite M200 plate reader (Tecan). Viability was calculated as a % ratio of viable cells treated with the indicated drug respect to an untreated control.

Cell Death Analysis

6 × 10^3 MCF7 cells were seeded in a 96 well-plate; 24 hours after seeding, cells were treated with different concentrations of Doxorubicin; 72 hours after treatment cells were incubated with Hoechst 33,342 2 μg/ml (Life Technologies) for 30 min (to stain nuclei, therefore both viable and dead cells) and Topro-3 0.1 μM (Life Technologies) for 15 minutes (to visualize dead cells). Fluorescent images were obtained with the Operetta High Content Imaging System (Perkin Elmer) at CIBIO HTS Facility. The Topro-3 and Hoechst 33,342 positive objects were detected using the Harmony 4.1 PhenoLOGIC software (Perkin Elmer); subsequently, the relative ratio of Topro-3 positive objects on the total number of objects (Hoechst 33,342 positive) was calculated.

Chromatin Immunoprecipitation Assay

MDA-MB-231-ETV7 and MDA-MB-231-Empty cells were seeded in p150 dishes (four dishes each condition) and ChIP-PCR was performed following a revised version of Myers Lab protocol. Mouse monoclonal anti-ETV7/TEL2 antibody (F-8, sc-376,137X, Santa Cruz Biotechnologies) and normal mouse IgG (sc-2025, Santa Cruz Biotechnologies) were used for immunoprecipitation. Two μl of purified immmunoprecipitated DNA was then used for qPCR analysis and calculation was performed using the ΔCt method in respect to non-immunoprecipitated DNA (% of input) as previously detailed described [37]. A genomic region within GTF2H5 gene was used a negative control. A list of the primers sequences that were used for ChIP-PCR analysis is presented in Supplementary Table 1 (Integrated DNA Technologies, Coralville, IA, USA and Eurofins Genomics).

MCF7 cells were seeded in p150 dishes and transiently transfected with 10 μg of pCMV6-Entry-Empty or -ETV7 vectors using Lipofectamine LTX and Plus Reagent (Thermo Fisher Scientific) for 48 hours. ChIP was performed using the same protocol used for MDA-MB-231 using anti-ETV7/TEL2 (H-88, sc-292,509) and normal rabbit IgG (sc-2027, Santa Cruz Biotechnologies) for immunoprecipitation. qPCR on purified immunoprecipitated DNAs was performed as indicated above.

Co-Immunoprecipitation

MCF7 were seeded in p150 dishes and transiently transfected with pCMV6-Entry-ETV7 as above (Origene). 48 hours post-transfection

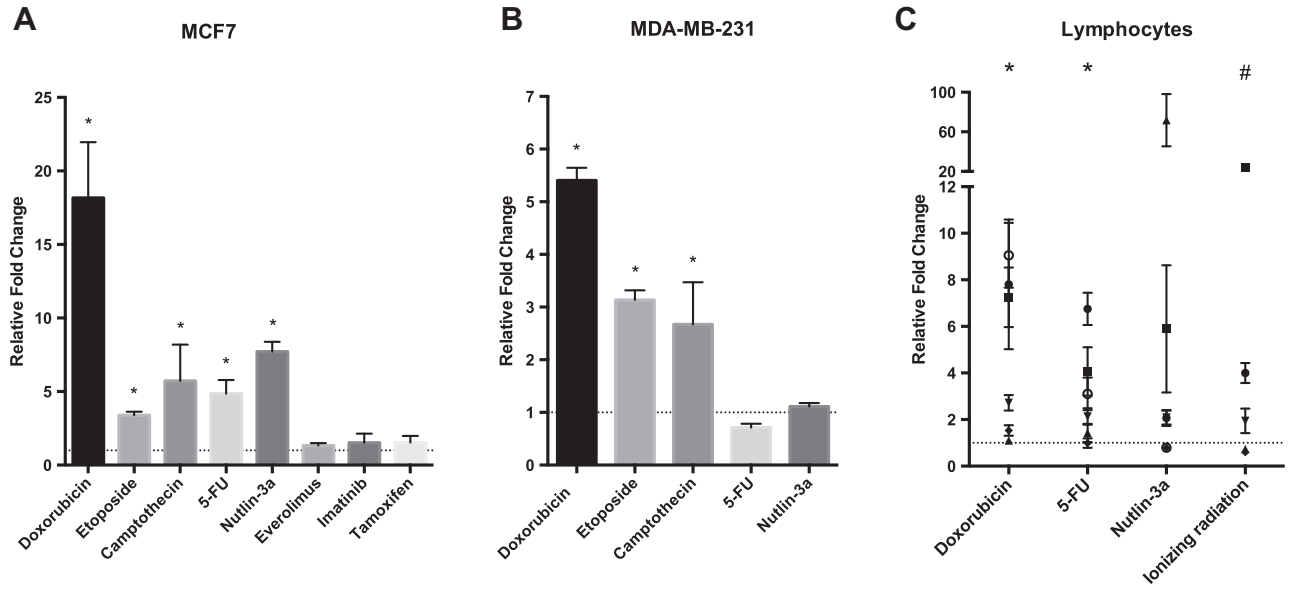

Figure 1. DNA damaging drugs promote ETV7 transcriptional activation. RT-qPCR analysis of ETV7 expression upon different chemotherapeutics treatment in breast cancer-derived MCF7 (A) and MDA-MB-231 cells (B), and in healthy donor-derived lymphocytes (C). Bars represent average Fold Changes relative to the untreated condition and standard deviations of at least three biological replicates. * = *P*-value <0.01.

cells were lysed in CHAPS buffer and then incubated over-night with an anti-ETV7 antibody (H-88, sc-292,509) or normal rabbit IgG (sc-2027) previously bound to Dynabeads protein A magnetic beads (Life Technologies). Beads were then washed and the immunoprecipitated lysate was eluted and loaded on a polyacrylamide gel for SDS-PAGE.

Analysis of Genome-Wide Data

Available expression arrays from our group (GSE24065, Agilent-014850 Whole Human Genome Microarray 4x44K G4112F) were analyzed for the specific genes of interest as previously described [20,38].

Expression data of MCF7 cells resistant to Adriamycin -MCF7/ADR- (e.g. Doxorubicin) were obtained from Affymetrix Human Genome U133 Plus 2.0 Array platform and downloaded from GEO (GSE76540). Two transcripts for each gene of interest (ETV7, DNAJC15, and ABCB1) were available and expression averages were calculated.

Expression levels of ETV7 and DNAJC15 were obtained from microarray data of Triple Negative Breast Cancer patients who underwent neoadjuvant chemotherapy protocols (GSE43502, Affymetrix Human Genome U133 Plus 2.0 Array). The study included 25 patients (out of 47) showing recurrence.

Statistical Analysis

When appropriate, Student's t-test was applied for statistical significance. We selected throughout the manuscript the two-sample Student's t-test for unequal variance.

Results

ETV7 is Activated by Doxorubicin and other DNA Damaging Drugs in Cancer and Normal Cells

To investigate the differential expression of ETV7 in response to various stimuli in breast cancer cells we tested a panel of cytotoxic drugs in MCF7 cells. We observed a substantial induction of ETV7 expression with many of the treatments, especially DNA damaging drugs, among which Doxorubicin was the most effective inducer of ETV7 expression in comparison with 5FU, Camptothecin, and Etoposide (Figure 1*A*). The treatment with Nutlin-3a, a p53 specific activator [39] also triggered an increment in ETV7 mRNA levels while Everolimus (mTOR inhibitor), Imatinib (tyrosine kinase inhibitor) and Tamoxifen (estrogen modulator) had no effect (Figure 1*A*). Moreover, ETV7 transcriptional activation by Doxorubicin in MCF7 cells was reflected by an increase in protein levels in the nuclear compartment (Suppl. Figure S1*A*), highlighting its role as a transcriptional regulator.

We extended the analysis to the breast cancer cell line MDA-MB-231 and confirmed the induction of ETV7 upon treatments with DNA damaging agents, especially Doxorubicin (Figure 1*B*). Nevertheless, the levels of ETV7 induction in this cell line were not as high as in MCF7. The reduced level might be explained by the presence of a mutant nonfunctional form of p53 in MDA-MB-231 since p53 is an activator of ETV7 transcription [20]. Doxorubicin treatment also induced ETV7 in other cancer-derived cell lines: lung adenocarcinoma (A549) and osteosarcoma (U2OS) and melanoma (A375M) (Suppl. Figure S1*B*). Given the activation in the various cancer cell lines, we investigated the ETV7 expression in normal cells. Therefore, we treated lymphocytes obtained from healthy donors and two non-cancerous cell lines (immortalized normal fibroblasts, BJ1-hTERT, and immortalized normal mammary cells, MCF10A). These results along with those from cancer cell lines establish that ETV7 induction is a conserved response to DNA damaging treatments (Figure 1*C* and Suppl. Figure S1*B*).

ETV7 Can Promote Resistance to Doxorubicin in Breast Cancer Cells

Given the observation that ETV7 is potently activated in response to Doxorubicin treatment, we hypothesized that it may be involved in drug resistance. To test this, we generated stable MCF7 and MDA-

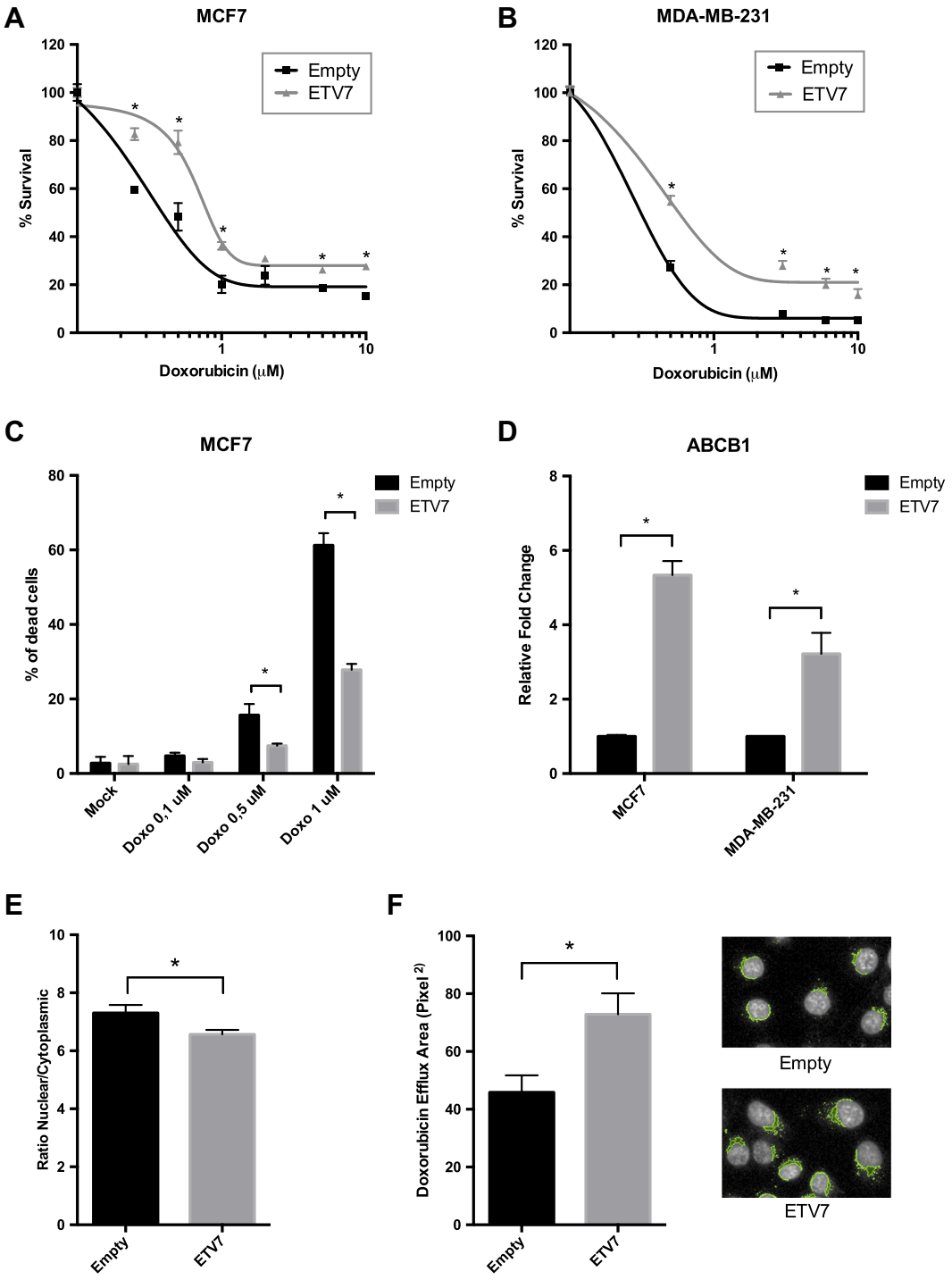

Figure 2. ETV7 can trigger breast cancer resistance to Doxorubicin. A-B) MTT Assays for survival analyses upon Doxorubicin treatment in MCF7 (A) and in MDA-MB-231 (B) cells over-expressing ETV7 with respect to their empty control. C) Cell death analysis on Doxorubicin-treated (three different doses) MCF7 cells over-expressing ETV7 in comparison to the ones stably transfected with an empty vector. Percentage of dead cells was obtained through fluorescence studies (at Operetta Perkin Elmer) calculated as a ratio between the amount of Topro-3 positive cells (dead cells) and the total number of cells (Hoechst 33,342 positive cells). D) RT-qPCR analysis of ABCB1 expression in MCF7 and MDA-MB-231 cells over-expressing ETV7. E) Analysis of the ratio between the nuclear and cytoplasmic intensity of Doxorubicin in MDA-MB-231 cells over-expressing ETV7 compared with their empty control, performed through Operetta Perkin Elmer Software. F) Analysis of the cytoplasmic area of Doxorubicin efflux in MDA-MB-231 cells over-expressing ETV7 in comparison to their empty counterpart. Images are reporting one representative analyzed by Operetta PerkinElmer Software. Experiments are done in quadruplicate. * = *P*-value <0.01.

MB-231 cell lines over-expressing this transcription factor (Suppl. Figure S2*A* and *B*, respectively) and evaluated whether this could influence the survival upon Doxorubicin treatment. Importantly, ETV7 over-expression exerted a protective role against Doxorubicin-induced cell viability in both cell lines (Figure 2*A-B*). Interestingly, this effect was also visible in non-breast cancer cells as shown for the

osteosarcoma U2OS cells stably over-expressing ETV7 (Suppl. Figure S2*C-D*). The effect of ETV7 over-expression on Doxorubicin-driven cell death was analyzed using the cell-impermeable dye Topro-3 (a representative image is presented in Supplementary Figure S2*E*). MCF7 cells over-expressing ETV7 resulted in a remarkably reduced sensitivity to Doxorubicin in comparison to cells stably transfected with an empty vector (Figure 2*C*). Since drug efflux is one of the most common mechanisms responsible for increased chemoresistance [40,41], we hypothesized that it could be affected by ETV7 expression. We therefore checked for the expression of ABCB1/PgP, an ABC transporter frequently over-expressed in doxorubicin-resistant cells [42–44], and we observed a significant up-regulation of ABCB1 upon ETV7 over-expression in both MCF7 and MDA-MB-231 cells (Figure 2*D*). To further verify the aforementioned hypothesis, we monitored the nuclear efflux of Doxorubicin exploiting its light emission property in the ETV7 over-expressing MDA-MB-231 cells relative to their empty-vector counterpart. By measuring the ratio of nuclear to cytoplasmic Doxorubicin and the area of Doxorubicin efflux from the nuclei, we found a statistically significant decrease of nuclear Doxorubicin in the MDA-MB-231 cells over-expressing ETV7 that corresponded to an increased nuclear efflux of Doxorubicin (Figure 2*E-F* and Suppl. Figure S2*F*, showing details regarding the selection of nuclear and cytoplasmic regions).

DNAJC15 is a Good Target for ETV7-Mediated Drug Resistance

To further understand how ETV7, as a transcriptional repressor, could influence drug resistance, we searched for its putative targets by restricting the analysis to genes whose silencing is already known to be involved in Doxorubicin resistance in breast cancer cells. In particular, we considered a list of six genes (*BRCA1, ESR1, DNAJC15, CDH1, RAB6C and SULF2)* whose hyper-methylation correlates with Doxorubicin resistance in breast cancer (Table 1 from Boettcher et al., 2010 [45] and available at the Archive of Functional Genomics Data, accession number #E-MEXP-2698, using the ArrayExpress tool). To restrict the search to the most promising ETV7 targets, we analyzed the expression of this group of genes in microarray data that we previously described with Doxorubicin treated MCF7 cells available (GSE24065, Gene Expression Omnibus, GEO, NCBI [20,38]). Given that Doxorubicin potently activated ETV7 expression, we expected to observe significant down-regulation of its targets upon the same treatment condition. Out of the six genes, three of them -DNAJC15, BRCA1, and ESR1- displayed a strong down-regulation pattern upon Doxorubicin treatment (Suppl. Figure S3*A*). No significant effects were observed for *CDH1* and *RAB6C*, while SULF2 was induced after Doxorubicin treatment. Moreover, most DNAJC family members were repressed upon Doxorubicin in MCF7 cells, based on the previously mentioned microarray data (Suppl. Figure S3*B*). Therefore, we validated some of the highly down-regulated members of DNAJC family with RT-qPCR experiments in Doxorubicin-treated MCF7 cells and confirmed the repression of DNAJC2, C7, C14, C15, and C17 in response to Doxorubicin treatment (Figure 3*A*). Furthermore, DNAJC15 has already been reported to be involved in the negative regulation of ABCB1 transcription, thereby potentially explaining the ETV7-mediated ABCB1 up-regulation and, at least partially, the drug resistance mechanism associated with ETV7 [29]. We decided to focus our attention on DNAJC15 as a putative mediator of the ETV7-dependent Doxorubicin resistance. We extended the analysis of DNAJC15 repression to other DNA damaging agents in MCF7, MDA-MB-231 cells and in lymphocytes (Figure 3*B*, *C,* and *D*, respectively), and verified DNAJC15 down-regulation in response to most of these agents.

ETV7 Transcriptionally Regulates DNAJC15 Expression

Since we observed that ETV7 and DNAJC15 expression were inversely correlated in response to several stimuli and given the presence of two putative ETV7 binding sites in the *DNAJC15* promoter, we investigated the possibility of direct ETV7 influence on DNAJC15 expression. First, we demonstrated that the modulation of ETV7 expression inversely affected the mRNA levels of DNAJC15. Specifically, ETV7 over-expression led to a small but significant, repression of DNAJC15 both in MCF7 (Figure 4*A*) and MDA-MB-231 (Suppl. Figure S4*A*) cells.

In order to assess whether transcriptional repression was associated with ETV7 binding to DNAJC15, we cloned a region of the *DNAJC15* promoter containing two putative binding sites for ETV7 into a pGL4.26 luciferase reporter vector. We found that ETV7 over-expression in MCF7 cells was able to decrease the expression of the luciferase reporter gene under the control of the DNAJC15 promoter (Figure 4*B*). We then performed site-directed mutagenesis to mutate the most conserved bases within the two putative ETV7-binding sites into the reporter vector in order to demonstrate the contribution of these two binding sites in DNAJC15 repression. The mutation of the binding site 1 (BS1 – chr.13:43′597’329–43′597’335) did not affect the ETV7-mediated down-regulation of luciferase activity. However, disruption of binding site 2 (BS2 – chr.13:43′597’624–43′597’632) prevented repression of the luciferase reporter induced by ETV7, demonstrating the importance of ETV7 binding to this site in the repression of DNAJC15 (Figure 4*B*).

Furthermore, we were able to demonstrate with chromatin immunoprecipitation the direct binding of ETV7 to the DNAJC15 promoter region (BS2) in both MCF7 and MDA-MB-231 cells (Figure 4*C* and Suppl. Figure S4*B*, respectively). In particular, in MDA-MB-231 cells over-expressing ETV7, the binding to the DNAJC15 promoter was markedly stimulated by Doxorubicin treatment. In order to better clarify this effect, we analyzed the distribution of ETV7 protein within the nucleus and found that upon Doxorubicin treatment the ETV7 protein was strongly enriched in the nuclear fraction especially in chromatin-associated structures (Suppl. Figure S4*C*).

DNAJC15 Over-Expression Partially Rescues ETV7-Mediated Drug Resistance

To address the idea that ETV7-mediated drug resistance is, at least partially, dependent on the repression of DNAJC15, we over-expressed DNAJC15 in MCF7 and MDA-MB-231 cells stably over-expressing ETV7 and analyzed cellular viability upon Doxorubicin treatment. Cells over-expressing DNAJC15 became more sensitive to Doxorubicin-mediated cell death, thus confirming this pathway as a mechanism exploited by ETV7 for drug resistance (Figure 4*D-E*). Furthermore, DNAJC15 over-expression was also able to down-regulate ABCB1 expression in MCF7 as well as MDA-MB-231 cells over-expressing ETV7, in accord with its reported negative role on ABCB1 levels (Suppl. Figure S5*A-B*).

ETV7 Represses DNAJC15 Expression by DNA Methylation

DNAJC15 is recognized to be a methylation-controlled gene, and its methylation-induced down-regulation has been associated with chemoresistance [29]. We investigated whether ETV7-mediated repression was dependent on DNA methylation. The methylation of CpGs in the promoter of DNAJC15 in MCF7 cells following ETV7 over-expression or Doxorubicin treatment was determined by

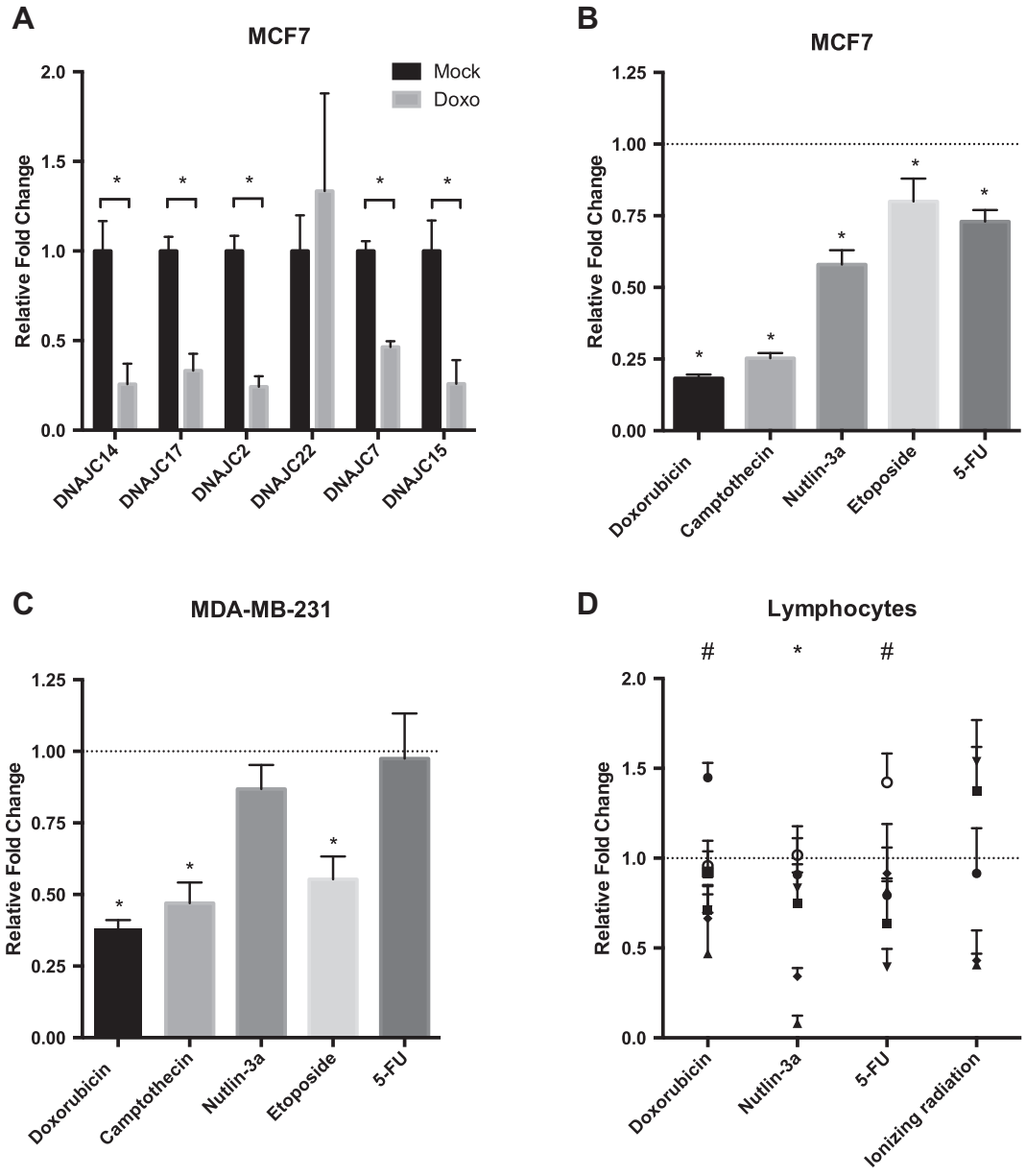

Figure 3. DNAJC15 expression is repressed by DNA damaging drugs. A) RT-qPCR analysis in MCF7 cells of the expression of a selected group of DNAJC family members repressed upon Doxorubicin treatment according to microarray analysis (GSE24065). B-C) Expression analysis of DNAJC15 mRNA upon different chemotherapeutics treatment in breast cancer-derived MCF7 (B) and MDA-MB-231 cells (C), and in healthy donor-derived lymphocytes (D). Bars represent averages Fold Changes relative to the untreated condition of at least three biological replicates and standard deviations. * = *P*-value <0.01.

bisulfite-conversion of genomic DNA followed by PCR and direct sequencing. In response to Doxorubicin, the promoter of DNAJC15 showed increased methylation of CpGs, which was even more evident upon ETV7 over-expression, as shown in Figure 5*A*. Moreover, ETV7-mediated effects on DNAJC15 transcript levels were abolished by treatment with the DNA methyltransferase (DNMT) inhibitor 5-Aza-2′-deoxycytidine (5-Aza) (Figure 5*B*), demonstrating that ETV7 repression of DNAJC15 expression is indeed methylation-dependent.

Given that DNMTs play key roles in Doxorubicin resistance as demonstrated for Adriamycin-resistant MCF7 cells [46], we hypothesized a possible direct interaction between ETV7 and DNMTs mediating the methylation and subsequent repression of the DNAJC15 promoter. Analysis of the expression of the *DNMT1, DNMT3A* and *DNMT3B* genes in our microarray data from Doxorubicin-treated MCF7 cells (GSE24065 [20,38]) (Suppl. Figure S6*A*) and validation by RT-qPCR (Figure 5*C*), revealed the up-regulation of only DNMT3A among these DNMTs. Conversely, both DNMT1 and DNMT3B were down-regulated in response to the treatment. Moreover, a similar trend could be observed for DNMTs expression in response to ETV7 over-expression in MCF7 cells, even if the only statistically significant alteration in expression was for DNMT1 (Suppl. Figure S6*B*). To test the putative interaction of ETV7 with DNMT3A as a candidate mediator of DNAJC15 repression, we performed immunoprecipitation of ETV7 and found the direct interaction of ETV7 with DNMT3A in MCF7 cells transiently over-expressing ETV7 (Figure 5*D*).

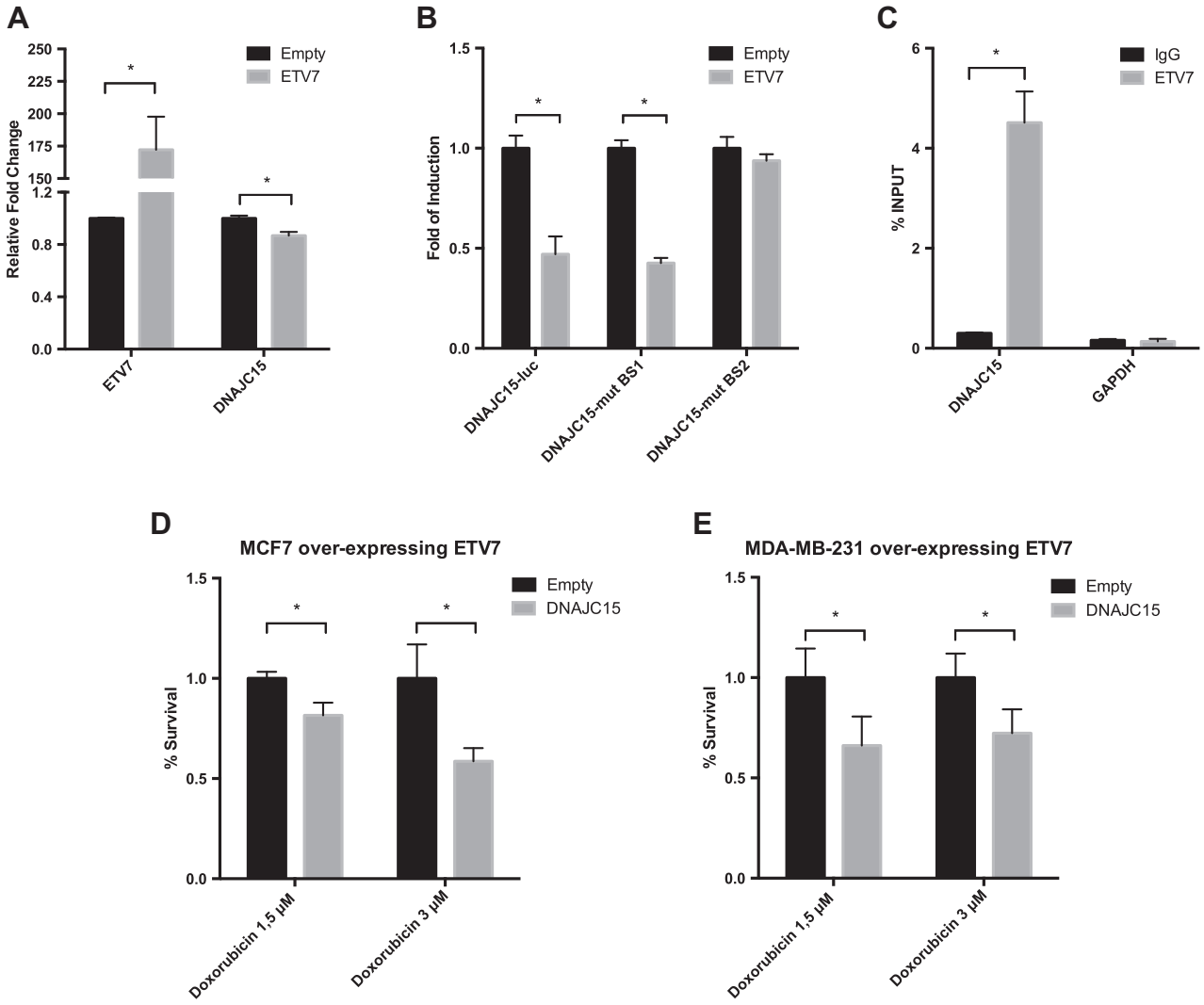

Figure 4. ETV7 can repress DNAJC15 expression at the transcriptional level and DNAJC15 over-expression can rescue Doxorubicin sensitivity. A) RT-qPCR analysis of ETV7 and DNAJC15 expression in MCF7 cells transfected with pCMV6-Entry-Empty or pCMV6-Entry-ETV7 plasmids. B) Gene reporter assay of MCF7 cells transiently over-expressing pCMV6-Entry-Empty or pCMV6-Entry-ETV7 along with pGL4.26-DNAJC15 reporter plasmid or the pGL4.26-DNAJC15-BS1 or -BS2 plasmids mutated in the putative ETV7 binding sites. Data are normalized using pRL-SV40 and are shown as fold of induction relative to the empty control. C) ChIP-PCR of DNAJC15 and GAPDH (control) promoter regions in MCF7 transfected with pCMV6-ETV7. Shown is the percentage of enrichment of ETV7 or control (IgG) bound to DNAJC15 promoter region in respect to INPUT DNA. For panels A-C, bars represent averages and standard deviations of at least three biological replicates. D-E) MTT Assay of ETV7-over-expressing MCF7 (D) and MDA-MB-231 (E) cells transiently transfected with pCMV6-Entry-Empty or pCMV6-Entry-DNAJC15 plasmids and treated with Doxorubicin 1.5 μM or 3 μM for 72 hours. Experiments are done in quadruplicate. * = *P*-value <0.01.

ETV7-DNAJC15 Clinical Relevance and Possible Therapeutic Strategy

We confirmed a dramatic decrease in DNAJC15 and a corresponding increase in ETV7 expression in reported microarray analysis performed with Adriamycin (i.e. Doxorubicin) resistant MCF7 cells (MCF7/ADR, GSE76540, [47]) as shown in Figure 6*A*. Moreover, this effect was associated with a large increase in ABCB1 expression in MCF7/ADR cells, an observation consistent with what is observed in MCF7 and MDA-MB-231 cells over-expressing ETV7 (Suppl. Figure S2*F-G*).

To address possible clinical relationships between ETV7, DNAJC15 and Doxorubicin treatment, we evaluated data obtained from 25 chemoresistant samples among 47 neoadjuvant chemotherapy-treated triple negative breast cancer (TNBC) patients (GSE43502, [48]). We found an inverse correlation between the expression levels of ETV7 and DNAJC15 in TNBC patients associated with recurrence. Specifically, despite not stringently significant, it is visible an increase in ETV7 expression in patients with a recurrent disease that correlated with a remarkable decrease in DNAJC15 expression. These data indicate that ETV7-mediated repression of DNAJC15 could be linked to a worse prognosis in breast cancer patients (Figure 6*B*).

Given that the over-expression of a particular gene is still a challenging approach for therapeutic purposes, we tried to overcome ETV7-mediated drug resistance using Quercetin, a flavonoid recently shown to both increase therapeutic efficacy of Doxorubicin [49–51] and to reduce its cardiotoxicity [52,53], and the isoflavone Genistein, which can inhibit topoisomerase II [54] and DNMTs [55] or act as a phytoestrogen [35]. The sensitizing action of

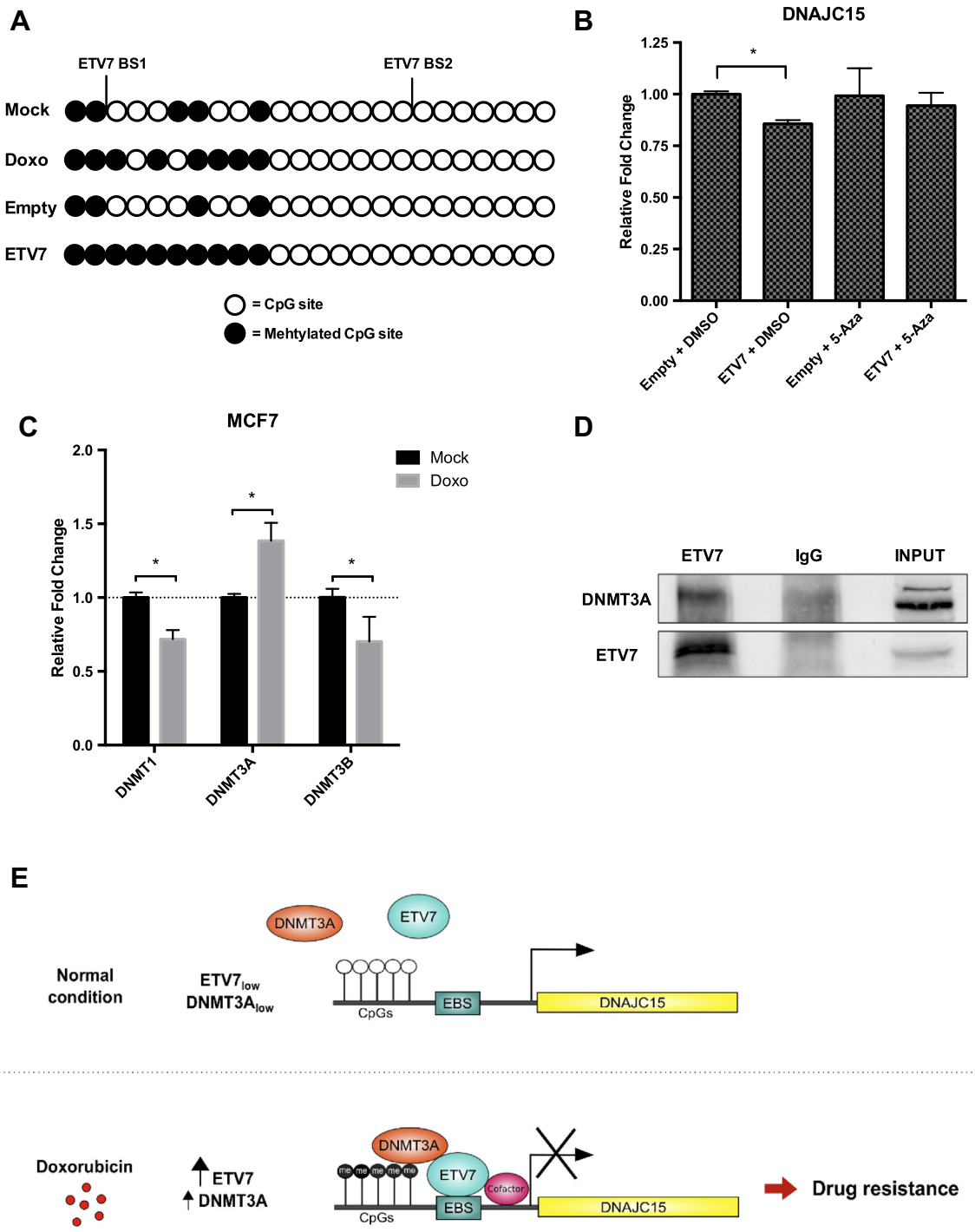

Figure 5. ETV7 can regulate DNAJC15 expression in a methylation-dependent manner. A) Methylation status of CpGs within DNAJC15 promoter analyzed by bisulfite conversion followed by PCR and direct sequencing in MCF7 untreated, treated with Doxorubicin for 16 hours or transfected with pCMV6-Entry-Empty or pCMV6-Entry-ETV7 plasmids. Methylated CpGs are shown as black dots, whereas unmethylated CpGs as white dots. B) RT-qPCR analysis of DNAJC15 expression in MCF7 transfected with pCMV6-Entry-Empty or pCMV6-Entry-ETV7 and treated with DMSO or 5-Aza-2′-deoxycytidine for 48 hours. C) RT-qPCR analysis of DNMT1, DNMT3A and DNMT3B expression in MCF7 treated with Doxorubicin for 16 hours. D) Western blot of DNMT3A and ETV7 on the immunoprecipitation with an antibody against ETV7 or normal IgG as control and on INPUT lysates in MCF7 transfected with pCMV6-Entry-ETV7 plasmid. * = *P*-value <0.01. E) A graphical model for ETV7-dependent Doxorubicin resistance in breast cancer cells. In normal conditions, ETV7 and DNMT3A are maintained at basal levels (particularly low in case of ETV7) and DNAJC15 can be regularly expressed. In response to Doxorubicin treatment, ETV7 levels get elevated and DNMT3A slightly increases as well. Induced ETV7 can then accumulate into the nucleus and specifically to chromatin-enriched regions. In the nucleus, ETV7 recruits DNMT3A (through direct interactions with putative additional cofactors) on target DNA (DNAJC15 promoter in this case) that in turn it is responsible for the methylation of CpGs. This will result in DNAJC15 repression and ultimately will lead to chemoresistance, partly through the exclusion of the drug from the nucleus. EBS: ETV7 Binding Site. Methylated CpGs are shown as filled circles, whereas unmethylated CpGs as empty circles.

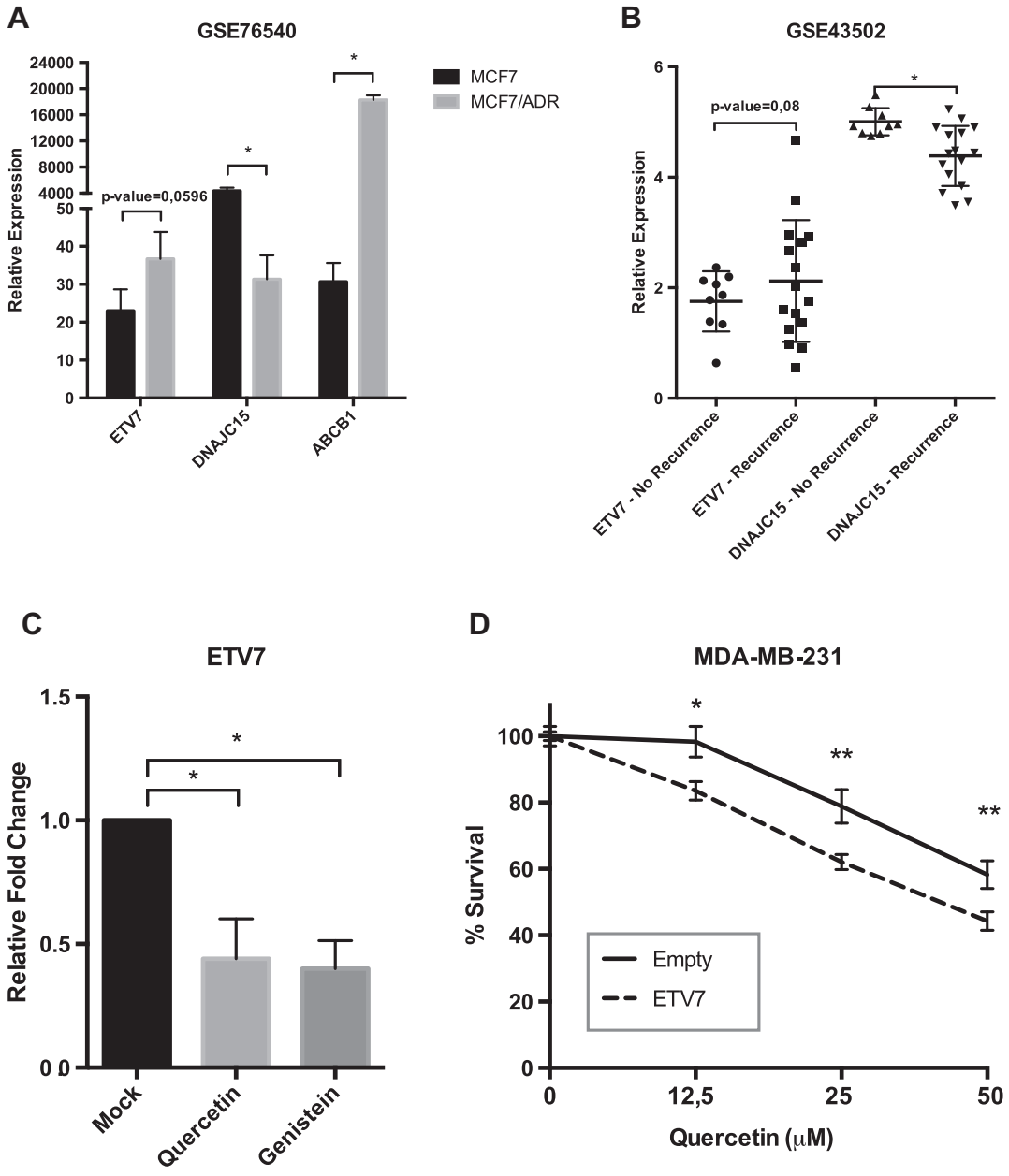

Figure 6. ETV7 and DNAJC15 levels inversely correlate with clinical status of breast cancer patients and ETV7 targeting could be exploited pharmacologically. A) ETV7, DNAJC15 and ABCB1 expression levels from microarray data (GSE76540) of MCF7 cells resistant to Adriamycin -MCF7/ADR- (e.g. Doxorubicin). Presented are the averages and standard deviations of at least three biological replicates. B) ETV7 and DNAJC15 expression levels from microarray data of Triple Negative Breast Cancer patients treated with neoadjuvant chemotherapy who were showing recurrence or not for the disease (GSE43502). C) ETV7 expression levels measured by RT-qPCR from MDA-MB-231 cells untreated (Mock) or treated with Quercetin 50μM or Genistein 30μM for 16 hours. Bars represent averages and standard deviations of at least three biological replicates. D) MTT assay in MDA-MB-231 cells over-expressing ETV7 or its empty vector and treated with increasing concentration of Quercetin. Experiments are done in quadruplicate. * = *P*-value <0.01.

flavonoids has not been fully elucidated yet, but it seems to involve the MDR transporter action. Surprisingly, we noticed that both flavonoids Quercetin and Genistein were able to reduce ETV7 expression in MDA-MB-231 cells, thereby suggesting a novel mechanism of sensitization for cancer cells (Figure 6*C*). Notably, MDA-MB-231 cells that over-express ETV7 were more sensitive to Quercetin relative to the empty counterpart, thereby unveiling a mechanism that could represent a promising target for ETV7-mediated resistance in cancer cells (Figure 6*D*).

Discussion

ETV7 has been recognized in the literature as an oncoprotein for blood cancers but its role in solid cancers is still poorly studied [10,17]. In this work, we showed that ETV7 is activated in response to different DNA damaging agents in breast cancer cells, but its expression is not affected by other types of anti-cancer treatments such as estrogen antagonists, tyrosine kinase or mTOR inhibitors (Figure 1). We observed that this transcriptional activation is conserved in different cancer cell types and normal cells including

lymphocytes obtained from healthy donors, thus highlighting its biological relevance. Moreover, we have demonstrated that ETV7 can directly promote resistance of breast cancer cells to standard-of-care chemotherapy, i.e. Doxorubicin (Figure 2). The ETV7-dependent mechanism of chemoresistance exploited by breast cancer cells involves the direct efflux of Doxorubicin from the nucleus of cells over-expressing ETV7 (Figure 2). This observation led us to hypothesize that the effect can be driven by membrane-associated transporters and, interestingly, we found that cells over-expressing ETV7 showed higher expression levels of ABCB1, a member of the family of ABC transporters (Figure 2). Despite being mainly expressed on the plasma membranes, ABCB1 protein has often been detected on nuclear membranes and Golgi compartments [56], possibly mediating the phenomenon of resistance to Doxorubicin observed in breast cancer cells in this study.

As a transcription factor, ETV7 can influence the expression of a complex range of targets that may result in the observed increased survival. Among the various possible ETV7 targets, we proposed DNAJC15, a co-chaperone member of the HSP40 family, reported to affect ABCB1 expression and anti-cancer drug efflux [29]. DNAJC15 has already been reported to be frequently hyper-methylated and repressed in breast cancer cells resistant to therapy [27,28]. However, which direct players were causing its transcriptional repression in breast cancer was not known. We confirmed the DNAJC15 repression triggered by Doxorubicin involves the direct binding of ETV7 on the *DNAJC15* promoter. We were also able to identify the precise promoter region that ETV7 uses to reduce the expression of DNAJC15 located at +377 bp from the TSS (Figures 3 and 4). Given reports of DNAJC15 hyper-methylation and decreased expression in cancer [28], we investigated whether ETV7 could modulate DNAJC15 expression through this mechanism. By mapping the CpG islands that are methylated in response to Doxorubicin and ETV7 over-expression in breast cancer cells, we demonstrated that ETV7-dependent DNAJC15 transcriptional repression is methylation-mediated (Figure 5). We speculate that this may be achieved through the direct recruitment of the DNA methyltransferase DNMT3A on chromatin mediated by ETV7 given our observation of physical interaction between the two proteins (Figure 5).

In Figure 5*E*, we propose a model for the novel mechanism of Doxorubicin resistance in breast cancer cells that includes a pivotal role for ETV7, which is directly activated by this chemotherapeutic drug. The induced ETV7 acts as a direct negative regulator of DNAJC15 expression through the DNA methylation of the promoter region via DNMT3A. DNAJC15 repression leads to the efflux of the drug from the nucleus, a process possibly driven by the loss of the DNAJC15-dependent repression of ABCB1.

A better knowledge of the transcriptional repressors that impact DNAJC15 expression could help inform clinical treatment strategies in order to avoid or minimize the activation of one of its direct repressors such as ETV7. A combinatorial treatment could disrupt this resistance circuitry driven by ETV7. Based on our findings, we suggest considering the combined treatment of Doxorubicin with Quercetin as a therapeutic strategy, given its protective role against Doxorubicin cardiotoxicity and its negative action on ETV7 expression (Figure 6).

Taken collectively, our results uncovered a novel molecular mechanism that underlies the resistance to a standard-of-care treatment for breast cancer (Doxorubicin), providing insights on the players that take part in this process: ETV7, DNMT3A, and DNAJC15 all of which have the potential for pharmacological targeting. Moreover, it is worth noting that our findings provide the first evidence for a role of ETV7 expression and function in the resistance to Doxorubicin in breast cancer cells. We propose that further analyses on additional ETV7 targets could help investigations for novel breast cancer prognostic markers.

In general, given the complex universe beyond chemoresistance in cancer cells, it is of paramount importance to search for downstream master regulators like transcription factors. Despite the difficulties beyond their targeting, understanding how to restrict their activation and activity could provide a more promising therapeutic strategy than simply targeting a specific resistance effector.

Conclusions

With this study, we have uncovered a novel mechanism of resistance to Doxorubicin where ETV7 plays a major role. We propose a novel role for ETV7 in breast cancer, and we identify DNAJC15 as a new target gene responsible for ETV7-mediated Doxorubicin-resistance. The described molecular mechanism involves the ETV7-dependent repression of DNAJC15 through promoter methylation, a process that results in the increased expression of ABCB1. Overall, these findings can help to better understand how resistance to conventional chemotherapy can be hindered and possibly tackled pharmacologically.

Acknowledgements

We thank Lia Pinto, Michael Pancher, Dr. Valentina Adami and CIBIO High Throughput Screening Facility for technical assistance. We are also thankful to Dr. Bergamaschi, Prof. Provenzani, Dr. Lobachev, and Dr. Soddu for sharing cell lines. We appreciated Prof. Alberto Inga's past and present group members for sharing reagents and helpful discussions. We thank the Clinical Research Unit of NIEHS for providing human lymphocytes from healthy donors. This work was supported by CIBIO Start-up funds (to YC) and by Intramural NIH Research Program NIEHS Z01-ES065079 (to MAR).

Appendix A. Supplementary data

Supplementary data to this article can be found online at https://doi.org/10.1016/j.neo.2018.06.008.

References

[1] Cagel M, Grotz E, Bernabeu E, Moretton MA, and Chiappetta DA (2017). Doxorubicin: nanotechnological overviews from bench to bedside. *Drug Discov Today* **22**(2), 270–281.

[2] Bodley A, Liu LF, Israel M, Seshadri R, Koseki Y, Giuliani FC, Kirschenbaum S, Silber R, and Potmesil M (1989). DNA topoisomerase II-mediated interaction of doxorubicin and daunorubicin congeners with DNA. *Cancer Res* **49**, 5969–5978.

[3] De Angelis A, Urbanek K, Cappetta D, Piegari E, Ciuffreda LP, Rivellino A, Russo R, Esposito G, Rossi F, and Berrino L (2016). Doxorubicin cardiotoxicity and target cells: a broader perspective. *Cardio-Oncol* **2**(1), 1–8.

[4] Bottero V, Busuttil V, Loubat A, Magne N, Fischel JL, Milano G, and Peyron JF (2001). Activation of nuclear factor kappaB through the IKK complex by the topoisomerase poisons SN38 and doxorubicin: a brake to apoptosis in HeLa human carcinoma cells. *Cancer Res* **61**, 7785–7791.

[5] Wang CY, Mayo MW, and Baldwin Jr AS (1996). TNF- and cancer therapy-induced apoptosis: potentiation by inhibition of NF-kappaB. *Science* **274**, 784–787.

[6] Koo CY, Muir KW, and Lam EW (2012). FOXM1: From cancer initiation to progression and treatment. *Biochim Biophys Acta* **1819**, 28–37.

[7] Zona S, Bella L, Burton MJ, Nestal de Moraes G, and Lam EW (2014). FOXM1: an emerging master regulator of DNA damage response and genotoxic agent resistance. *Biochim Biophys Acta* **1839**, 1316–1322.

[8] Kim B, Stephen SL, Hanby AM, Horgan K, Perry SL, Richardson J, Roundhill EA, Valleley EM, Verghese ET, and Williams BJ, et al (2015). Chemotherapy induces Notch1-dependent MRP1 up-regulation, inhibition of which sensitizes breast cancer cells to chemotherapy. *BMC Cancer* **15**, 635.

[9] Bezler M, Hengstler JG, and Ullrich A (2012). Inhibition of doxorubicin-induced HER3-PI3K-AKT signalling enhances apoptosis of ovarian cancer cells. *Mol Oncol* **6**, 516–529.

[10] Carella C, Potter M, Bonten J, Rehg JE, Neale G, and Grosveld GC (2006). The ETS factor TEL2 is a hematopoietic oncoprotein. *Blood* **107**, 1124–1132.

[11] Graves BJ and Petersen JM (1998). Specificity within the ets family of transcription factors. *Adv Cancer Res* **75**, 1–55.

[12] Kim CA, Phillips ML, Kim W, Gingery M, Tran HH, Robinson MA, Faham S, and Bowie JU (2001). Polymerization of the SAM domain of TEL in leukemogenesis and transcriptional repression. *EMBO J* **20**, 4173–4182.

[13] Potter MD, Buijs A, Kreider B, van Rompaey L, and Grosveld GC (2000). Identification and characterization of a new human ETS-family transcription factor, TEL2, that is expressed in hematopoietic tissues and can associate with TEL1/ETV6. *Blood* **95**, 3341–3348.

[14] Kawagoe H, Potter M, Ellis J, and Grosveld GC (2004). TEL2, an ETS factor expressed in human leukemia, regulates monocytic differentiation of U937 Cells and blocks the inhibitory effect of TEL1 on ras-induced cellular transformation. *Cancer Res* **64**, 6091–6100.

[15] Matos JM, Witzmann FA, Cummings OW, and Schmidt CM (2009). A pilot study of proteomic profiles of human hepatocellular carcinoma in the United States. *J Surg Res* **155**, 237–243.

[16] Quintana AM, Picchione F, Klein Geltink RI, Taylor MR, and Grosveld GC (2014). Zebrafish ETV7 regulates red blood cell development through the cholesterol synthesis pathway. *Dis Model Mech* **7**, 265–270.

[17] Cardone M, Kandilci A, Carella C, Nilsson JA, Brennan JA, Sirma S, Ozbek U, Boyd K, Cleveland JL, and Grosveld GC (2005). The novel ETS factor TEL2 cooperates with Myc in B lymphomagenesis. *Mol Cell Biol* **25**, 2395–2405.

[18] Sang Y, Chen MY, Luo D, Zhang RH, Wang L, Li M, Luo R, Qian CN, Shao JY, and Zeng YX, et al (2015). TEL2 suppresses metastasis by down-regulating SERPINE1 in nasopharyngeal carcinoma. *Oncotarget* **6**, 29240–29253.

[19] Maeda O, Ando T, Ohmiya N, Ishiguro K, Watanabe O, Miyahara R, Hibi Y, Nagai T, Yamada K, and Goto H (2014). Alteration of gene expression and DNA methylation in drug-resistant gastric cancer. *Oncol Rep* **31**, 1883–1890.

[20] Bisio A, Zamborszky J, Zaccara S, Lion M, Tebaldi T, Sharma V, Raimondi I, Alessandrini F, Ciribilli Y, and Inga A (2014). Cooperative interactions between p53 and NFkappaB enhance cell plasticity. *Oncotarget* **5**(23), 12111–12125.

[21] Navasa N, Martin I, Iglesias-Pedraz JM, Beraza N, Atondo E, Izadi H, Ayaz F, Fernandez-Alvarez S, Hatle K, and Som A, et al (2015). Regulation of oxidative stress by methylation-controlled J protein controls macrophage responses to inflammatory insults. *J Infect Dis* **211**, 135–145.

[22] Kuang YQ, Charette N, Frazer J, Holland PJ, Attwood KM, Dellaire G, and Dupre DJ (2012). Dopamine receptor-interacting protein 78 acts as a molecular chaperone for CCR5 chemokine receptor signaling complex organization. *PLoS One* **7**, e40522.

[23] Mitra A, Shevde LA, and Samant RS (2009). Multi-faceted role of HSP40 in cancer. *Clin Exp Metastasis* **26**, 559–567.

[24] Lindsey JC, Lusher ME, Strathdee G, Brown R, Gilbertson RJ, Bailey S, Ellison DW, and Clifford SC (2006). Epigenetic inactivation of MCJ (DNAJD1) in malignant paediatric brain tumours. *Int J Cancer* **118**, 346–352.

[25] Lau DT, Hesson LB, Norris MD, Marshall GM, Haber M, and Ashton LJ (2012). Prognostic significance of promoter DNA methylation in patients with childhood neuroblastoma. *Clin Cancer Res* **18**, 5690–5700.

[26] Schusdziarra C, Blamowska M, Azem A, and Hell K (2013). Methylation-controlled J-protein MCJ acts in the import of proteins into human mitochondria. *Hum Mol Genet* **22**, 1348–1357.

[27] Witham J, Vidot S, Agarwal R, Kaye SB, and Richardson A (2008). Transient ectopic expression as a method to detect genes conferring drug resistance. *Int J Cancer* **122**, 2641–2645.

[28] Fernandez-Cabezudo MJ, Faour I, Jones K, Champagne DP, Jaloudi MA, Mohamed YA, Bashir G, Almarzooqi S, Albawardi A, and Hashim MJ, et al (2016). Deficiency of mitochondrial modulator MCJ promotes chemoresistance in breast cancer. *JCI Insight* **1**(7), e86873.

[29] Hatle KM, Neveu W, Dienz O, Rymarchyk S, Barrantes R, Hale S, Farley N, Lounsbury KM, Bond JP, and Taatjes D, et al (2007). Methylation-controlled J protein promotes c-Jun degradation to prevent ABCB1 transporter expression. *Mol Cell Biol* **27**, 2952–2966.

[30] Hatle KM, Gummadidala P, Navasa N, Bernardo E, Dodge J, Silverstrim B, Fortner K, Burg E, Suratt BT, and Hammer J, et al (2013). MCJ/DnaJC15, an endogenous mitochondrial repressor of the respiratory chain that controls metabolic alterations. *Mol Cell Biol* **33**, 2302–2314.

[31] Sinha D, Srivastava S, Krishna L, and D'Silva P (2014). Unraveling the intricate organization of mammalian mitochondrial presequence translocases: existence of multiple translocases for maintenance of mitochondrial function. *Mol Cell Biol* **34**, 1757–1775.

[32] Menendez D, Shatz M, Azzam K, Garantziotis S, Fessler MB, and Resnick MA (2011). The Toll-like receptor gene family is integrated into human DNA damage and p53 networks. *PLoS Genet* **7**, e1001360.

[33] Ciribilli Y, Monti P, Bisio A, Nguyen HT, Ethayathulla AS, Ramos A, Foggetti G, Menichini P, Menendez D, and Resnick MA, et al (2013). Transactivation specificity is conserved among p53 family proteins and depends on a response element sequence code. *Nucleic Acids Res* **41**, 8637–8653.

[34] Monti P, Ciribilli Y, Bisio A, Foggetti G, Raimondi I, Campomenosi P, Menichini P, Fronza G, and Inga A (2014). N-P63alpha and TA-P63alpha exhibit intrinsic differences in transactivation specificities that depend on distinct features of DNA target sites. *Oncotarget* **5**, 2116–2130.

[35] Ciribilli Y, Andreotti V, Menendez D, Langen JS, Schoenfelder G, Resnick MA, and Inga A (2010). The coordinated p53 and estrogen receptor cis-regulation at an FLT1 promoter SNP is specific to genotoxic stress and estrogenic compound. *PLoS One* **5**, e10236.

[36] Monti P, Perfumo C, Bisio A, Ciribilli Y, Menichini P, Russo D, Umbach DM, Resnick MA, Inga A, and Fronza G (2011). Dominant-negative features of mutant TP53 in germline carriers have limited impact on cancer outcomes. *Mol Cancer Res* **9**, 271–279.

[37] Ciribilli Y, Singh P, Spanel R, Inga A, and Borlak J (2015). Decoding c-Myc networks of cell cycle and apoptosis regulated genes in a transgenic mouse model of papillary lung adenocarcinomas. *Oncotarget* **6**, 31569–31592.

[38] Lion M, Bisio A, Tebaldi T, De Sanctis V, Menendez D, Resnick MA, Ciribilli Y, and Inga A (2013). Interaction between p53 and estradiol pathways in transcriptional responses to chemotherapeutics. *Cell Cycle* **12**(8), 1211–1224.

[39] Vassilev LT, Vu BT, Graves B, Carvajal D, Podlaski F, Filipovic Z, Kong N, Kammlott U, Lukacs C, and Klein C, et al (2004). In vivo activation of the p53 pathway by small-molecule antagonists of MDM2. *Science* **303**, 844–848.

[40] Gottesman MM, Fojo T, and Bates SE (2002). Multidrug resistance in cancer: role of ATP-dependent transporters. *Nat Rev Cancer* **2**, 48–58.

[41] Longley DB and Johnston PG (2005). Molecular mechanisms of drug resistance. *J Pathol* **205**, 275–292.

[42] Tada Y, Wada M, Migita T, Nagayama J, Hinoshita E, Mochida Y, Maehara Y, Tsuneyoshi M, Kuwano M, and Naito S (2002). Increased expression of multidrug resistance-associated proteins in bladder cancer during clinical course and drug resistance to doxorubicin. *Int J Cancer* **98**, 630–635.

[43] Abolhoda A, Wilson AE, Ross H, Danenberg PV, Burt M, and Scotto KW (1999). Rapid activation of MDR1 gene expression in human metastatic sarcoma after in vivo exposure to doxorubicin. *Clin Cancer Res* **5**, 3352–3356.

[44] Cox J and Weinman S (2016). Mechanisms of doxorubicin resistance in hepatocellular carcinoma. *Hepat Oncol* **3**, 57–59.

[45] Boettcher M, Kischkel F, and Hoheisel JD (2010). High-definition DNA methylation profiles from breast and ovarian carcinoma cell lines with differing doxorubicin resistance. *PLoS One* **5**, e11002.

[46] Segura-Pacheco B, Perez-Cardenas E, Taja-Chayeb L, Chavez-Blanco A, Revilla-Vazquez A, Benitez-Bribiesca L, and Duenas-Gonzalez A (2006). Global DNA hypermethylation-associated cancer chemotherapy resistance and its reversion with the demethylating agent hydralazine. *J Transl Med* **4**(32).

[47] Wang C, Jin H, Wang N, Fan S, Wang Y, Zhang Y, Wei L, Tao X, Gu D, and Zhao F, et al (2016). Gas6/Axl Axis Contributes to Chemoresistance and Metastasis in Breast Cancer through Akt/GSK-3beta/beta-catenin Signaling. *Theranostics* **6**, 1205–1219.

[48] Yu KD, Zhu R, Zhan M, Rodriguez AA, Yang W, Wong S, Makris A, Lehmann BD, Chen X, and Mayer I, et al (2013). Identification of prognosis-relevant subgroups in patients with chemoresistant triple-negative breast cancer. *Clin Cancer Res* **19**, 2723–2733.

[49] Liu Z, Balasubramanian V, Bhat C, Vahermo M, Makila E, Kemell M, Fontana F, Janoniene A, Petrikaite V, and Salonen J, et al (2017). Quercetin-Based Modified Porous Silicon Nanoparticles for Enhanced Inhibition of Doxorubicin-Resistant Cancer Cells. *Adv Healthc Mater* **6**.

[50] Lv L, Liu C, Chen C, Yu X, Chen G, Shi Y, Qin F, Ou J, Qiu K, and Li G (2016). Quercetin and doxorubicin co-encapsulated biotin receptor-targeting nanoparticles for minimizing drug resistance in breast cancer. *Oncotarget* **7**, 32184–32199.

[51] Minaei A, Sabzichi M, Ramezani F, Hamishehkar H, and Samadi N (2016). Co-delivery with nano-quercetin enhances doxorubicin-mediated cytotoxicity against MCF-7 cells. *Mol Biol Rep* **43**, 99–105.

[52] Dong Q, Chen L, Lu Q, Sharma S, Li L, Morimoto S, and Wang G (2014). Quercetin attenuates doxorubicin cardiotoxicity by modulating Bmi-1 expression. *Br J Pharmacol* **171**, 4440–4454.

[53] Cote B, Carlson LJ, Rao DA, and Alani AW (2015). Combinatorial resveratrol and quercetin polymeric micelles mitigate doxorubicin induced cardiotoxicity in vitro and in vivo. *J Control Release* **213**, 128–133.

[54] Lopez-Lazaro M, Willmore E, and Austin CA (2007). Cells lacking DNA topoisomerase II beta are resistant to genistein. *J Nat Prod* **70**, 763–767.

[55] Fang M, Chen D, and Yang CS (2007). Dietary polyphenols may affect DNA methylation. *J Nutr* **137**, 223S–228S.

[56] Molinari A, Calcabrini A, Meschini S, Stringaro A, Crateri P, Toccacieli L, Marra M, Colone M, Cianfriglia M, and Arancia G (2002). Subcellular detection and localization of the drug transporter P-glycoprotein in cultured tumor cells. *Curr Protein Pept Sci* **3**, 653–670.

Seminars in Oncology 44 (2017) 239–253

Contents lists available at ScienceDirect

Seminars in Oncology

journal homepage: www.elsevier.com/locate/ysonc

LAMPs: Shedding light on cancer biology

Federica Alessandrini[1], Laura Pezzè[1], Yari Ciribilli*

Laboratory of Molecular Cancer Genetics, Centre for Integrative Biology (CIBIO), University of Trento, Povo (TN), Italy

ARTICLE INFO

Keywords:
LAMPs
Lysosomes
Cancer
Metastasis

ABSTRACT

Lysosomes are important cytoplasmic organelles whose critical functions in cells are increasingly being understood. In particular, despite the long-standing accepted concept about the role of lysosomes as cellular machineries solely assigned to degradation, it has been demonstrated that they play active roles in homeostasis and even in cancer biology. Indeed, it is now well documented that during the process of cellular transformation and cancer progression lysosomes are changing localization, composition, and volume and, through the release of their enzymes, lysosomes can also enhance cancer aggressiveness. LAMPs (lysosome associated membrane proteins) represent a family of glycosylated proteins present predominantly on the membrane of lysosomes whose expression can vary among different tissues, suggesting a separation of functions. In this review we focus on the functions and roles of the different LAMP family members, with a particular emphasis on cancer progression and metastatic spread. LAMP proteins are involved in many different aspects of cell biology and can influence cellular processes such as phagocytosis, autophagy, lipid transport, and aging. Interestingly, for all the five members identified so far (LAMP1, LAMP2, LAMP3, CD68/Macrosialin/LAMP4, and BAD-LAMP/LAMP5), a role in cancer has been suggested. While this is well documented for LAMP1 and LAMP2, the involvement of the other three proteins in cancer progression and aggressiveness has recently been proposed and remains to be elucidated. Here we present different examples about how LAMP proteins can influence and support tumor growth and metastatic spread, emphasizing the impact of each single member of the family.

1. Characteristics and functions of lysosomes

Lysosomes are eukaryotic acidic organelles originally thought to be exclusively involved in the degradation of intracellular and extracellular macromolecules into building blocks available for the cells. Lysosomes have only recently been recognized as crucial regulators of cell homeostasis and there is accumulating evidence of their involvement in different diseases such as neurodegenerative disorders, cardiovascular diseases, and cancer [1,2]. Lysosomes are single-membrane cytoplasmic organelles present in almost all eukaryotic cells. They exert several functions in the regulation of cell homeostasis, including lysosomal exocytosis, cholesterol homeostasis and, possibly more importantly, the degradation of macromolecules, such as lipids, nucleic acids, and proteins. This is achieved through the action of several hydrolases (more than 50 different lysosomal hydrolases have been described so far), among which cathepsins (proteases targeting either cysteine or aspartic acid residues) occupy a prominent place [3,4]. In particular, degradation of intracellular material is generally obtained via different forms of autophagy, whereas degradation of exogenous material occurs via endocytosis [1].

In the mid-twentieth century, de Duve referred to lysosomes as "suicide bags" because of the important role of these organelles in cell death signaling [5]. Indeed, lysosomes are implicated in three main distinct pathways of cell death: apoptosis, necrosis, and autophagy [6]. However, the recognition of autophagy as a cell death mechanism is still controversial, being a process aimed at survival during stress conditions that can also result is cell death [7]. Specifically, the autophagic process (sometimes reported as type II programmed cell death) represents an evolutionarily well-conserved pathway where entire organelles or part of the cytoplasm are recycled as a response to starvation or to remove damaged organelles. This multi-step process is mediated through the formation of the so-called autophagosome, a double-membrane vesicle that subsequently will fuse with the lysosomes forming the autolysosome for the final degradation step [8]. Lysosomes are the most critical components for a proper clearance of mature autophagosomes, which for instance can cause neurodegenerative disorders when they accumulate as a result of not being properly digested. Alternatively, the phenomenon of

*Corresponding author. Yari Ciribilli, Laboratory of Molecular Cancer Genetics, Centre for Integrative Biology (CIBIO), University of Trento, Via Sommarive 9, 38123, Povo (TN), Italy. Tel.: 0039461283173; fax.: 0039461283937.
E-mail address: yari.ciribilli@unitn.it (Y. Ciribilli).
[1]These authors contributed equally to this work.

https://doi.org/10.1053/j.seminoncol.2017.10.013
0093-7754/

lysosomal permeabilization and the consequent release of proteolytic enzymes into the cytosol have been recognized as a "lysosomal pathway for apoptosis." In this process lysosomes are not just passive bystanders, but rather play an active role that is tightly regulated. The factor considered a key determinant in the kind of cell death triggered by lysosomal enzymes, especially as regards apoptosis versus necrosis, is believed to be represented by the magnitude of lysosomal permeabilization, namely the amount of proteolytic enzymes released into the cytosol [9]. A complete collapse of the organelle itself with the release of high levels of lysosomal enzymes triggers unregulated necrosis, while selective lysosomes permeabilization results in the induction of apoptosis [10,11]. As soon as lysosomal hydrolases are released into the cytosol, they can take part in the execution of the apoptotic cascade by acting either in concert with the canonical caspase pathway or directly to actively cleave key cellular substrates [12,13]. However, the precise mechanisms by which lysosomes are involved in apoptosis are still poorly understood and currently under intense investigation.

The lysosomal surface has been identified as the subcellular site where mTORC1 (mammalian Target Of Rapamycin Complex 1) activation in response to amino acids occurs [14]. mTOR, the main catalytic component of mTORC1, is an atypical serine/threonine kinase reported as master regulator of cell growth, energy production, and protein synthesis [15]; its functions are often deregulated in different diseases and, in particular, in cancer [16]. These studies have demonstrated that amino acids trigger the translocation of the mTORC1 complex to the lysosomes where it gets activated by interacting with Rag GTPases, and Ragulator and Rheb, two proteins that are anchored to the lysosomes' membrane [14]. Active mTORC1 is responsible for the phosphorylation and the subsequent accumulation in the cytosol of TFEB, a nuclear transcription factor responsible for lysosomal biogenesis, thereby integrating signals from the lysosomes to the nucleus [17].

2. Role of lysosomes in cancer

During transformation and cancer progression lysosomes are changing localization, volume, and composition and, by releasing their enzymes, they can increase cancer aggressiveness [4,18]. For instance, several lysosomal enzymes, including cathepsins, are over-expressed in different cancer types, such as breast, prostate, and colon cancers [19,20], and there is data that their expression levels can be clinically significant [11]. Different reports have suggested that an increased production and subsequent secretion of these proteases via exocytosis can foster proliferation and invasion of cancer cells [19,21,22]. Therefore, this can enhance cancer progression and metastasis formation by promoting the degradation of the extracellular matrix and increasing the potential for angiogenesis [23]. Indeed, inhibition of cathepsin B by synthetic cysteine protease inhibitors has been shown to effectively reduce the invasiveness of glioblastoma [24] and breast cancer cells [25]. At the same time cancer cells are strongly dependent on lysosome function and are very sensitive to lysosome-mediated cell death [1,26]. Lastly, it has been demonstrated that lysosomal dysfunction can promote the inclusion of lysosomal materials (eg, proteins) to exosome cargo to simplify their elimination from cells (ie, neurons affected by Alzheimer disease) [27]. Exosomes are small vesicles (30–100 nm in diameter) derived from the endosomal system that can be released from cells and represent critical structures for different types of cellular communication, including the immune response [28]. Initially it was thought that the fusion of exosomes with lysosomes would serve exclusively for the removal of unnecessary exosomal materials [29]; however, because exosome materials can be shuttled to neighboring or even distant cells, secretion of unwanted material to the extracellular environment within exosomes may have either positive or negative effects on surrounding cells. Therefore, the interplay between exosomes and lysosomes may represent a novel layer of exploration for different pathologies including cancer.

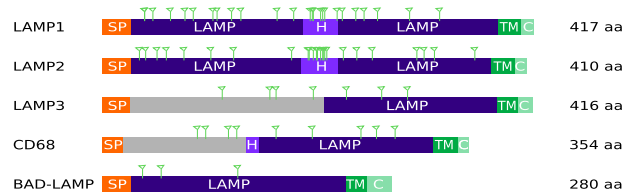

Fig. 1. Structural organization of the LAMP family members. Sequential boxes stand for domains, small flags indicate glycosylation residues and protein length is also provided for each depicted member. SP, signal peptide; LAMP, LAMP domain; H, hinge region; TM, transmembrane domain; C, cytoplasmic domain.

This review focuses on the role of a specific family of highly glycosylated membrane proteins usually found within lysosomal membranes known as lysosomal associated membrane proteins (LAMPs) and their involvement in cancer.

3. LAMP family of lysosomal proteins

The LAMP family is characterized by an evolutionary conserved membrane-proximal LAMP domain, composed of around 200 amino acids and containing several conserved cysteine residues that allow for the formation of two critical disulfide bonds [30]. Other common features in the family are represented by (i) a specific proline and two glycine residues in their single transmembrane region [30], (ii) the presence of several N-linked glycosylation sites within their luminal domain [31], and (iii) a short cytoplasmic tail harboring an endosomal and lysosomal sorting signal [32] (Fig. 1).

The LAMP family is composed of 5 known members: LAMP1/CD107a, LAMP2/CD107b, LAMP3/DC-LAMP, LAMP4/Macrosialin/CD68, and LAMP5/BAD-LAMP. LAMP1 and LAMP2 are ubiquitously expressed in human tissues and cell lines, whereas LAMP3, LAMP4/Macrosialin/CD68, and LAMP5/BAD-LAMP are cell-type specific proteins. LAMPs are involved in a variety of cellular processes including phagocytosis, autophagy, lipid transport, and aging [30]; moreover, growing evidence suggests an important role for LAMP family members in cancer (Tables 1–5 and Figs. 2 and 3).

3.1. LAMP1 and LAMP2

LAMP1 and LAMP2 represent the major constituents of the lysosomal membrane, are classified as type I transmembrane proteins, and share similar length and 37% amino acid sequence homology [30,33]. Their structure is characterized by a highly glycosylated luminal region forming a glycoprotein layer in the lysosomal lumen, a transmembrane region, and a short C-terminal cytosolic domain (Fig. 1). LAMP1 has only one transcript, whereas LAMP2 has three different splicing isoforms: LAMP2A, LAMP2B, and LAMP2C [30,33]. LAMP2 isoforms are expressed in a tissue specific manner and can exert opposing functions [34,35]. Specifically, the LAMP-2A isoform is recognized to be responsible for chaperone-mediated autophagy (CMA), a process that targets specific proteins to degradation by lysosomes via recognition of a specific motif within their amino acids sequence, and loss of the LAMP-2A isoform is associated with the formation of α-synuclein-positive aggregates in Parkinson's disease [36]. The LAMP-2B isoform is not involved in CMA, but mutations in exon 9 have been found in patients bearing a defective fusion process between

Table 1
Summary of cancer-associated functions for CD107a/LAMP1 (lysosome associated membrane protein-1).

Pro-tumorigenic roles	Evidence	Strength / Weakness of the Evidence
Early cancer progression [56]	• In OVCAR3 cells, LAMP1 was up-regulated 1.84-fold 24 h post-EGF treatment and down-regulated 48 h post-EGF exposure • Tissue microarray for LAMP1 positive in 35% of ovarian serous adenocarcinomas	• Although confirmatory studies not reported, observations are supported by GESA analysis using the TCGA database that revealed LAMP1 positively associated with EGFR-modulated molecular pathways ($P < .0060$)
Cancer cell survival [65]	• Screening identified anti-malarial agent mefloquine as compound selectively killing AML cells and stem cells • Genome-wide functional screen for mefloquine sensitizers in yeast, identified genes associated with yeast vacuole, the homolog of mammalian lysosome, and demonstrated mefloquine disrupts lysosomes by permeabilizing membranes and releasing cathepsins into cytosol	• Knockdown of LAMP1 and LAMP2 reduced AML cell viability, as did treatment with a lysosome disruptor, suggesting lysosomal disruption preferentially targets AML cells and progenitor cells, providing rationale for therapy. In support of this observation, artemisinins, artesunate, and dihydroartemisinin have been shown to be toxic to AML cells
Local tumor progression [55]	• LAMP1 detected in cytoplasm of tumor cells and in blood vessels in glioblastoma • Percentage of LAMP1+ tumor cells and staining intensities increased with tumor grade • LAMP1 and CD133, a putative marker of stemness, were co-expressed suggesting “cancer stem cells” contain LAMP1+ lysosomes	• Data do not fully support higher number of lysosomes in glioblastoma “cancer stem cells” • Despite increase in LAMP1+ tumor cells with tumor grade, association between LAMP1 expression and OS could not be found
Cancer development [57]	• LAMP1 was identified as a sialylated glycoprotein from metabolically oligosaccharide-engineered pancreatic cells • Immunohistochemistry showed preferential expression of LAMP1 in tumor cells but not in paired non-tumor pancreatic ductal cells	• At odds with previous studies showing longer survival after resection for patients whose pancreatic tumors expressed high levels of LAMP1 mRNA • Transfection of CAPAN-1 cells with LAMP1 decreased cell growth compared with non-transfected cells • Role for LAMP1 in cancer development remains uncertain
Adhesion of cancer cells to ECM, basement membrane and endothelium [45]; ECM remodeling [54]	• Flow cytometry showed LAMP1 expression on cell surface of A2058, HT1080, and CaCo-2 cells, increasing with 2 mM sodium butyrate treatment for 24–48 hr • FACS analysis proved interaction between LAMP1 expressing A2052 cells and Galectin-3 [45] • LAMP1 down-regulation using shRNA in B16F10 murine melanoma cells, decreases induction of MMP9 expression by p38 MAPK signaling, activated by Galectin-3 binding to the polyLacNAc present on LAMP1 [54]	• Data supported by studies showing increased LAMP1 expression on plasma membrane of highly metastatic compared with poorly metastatic cells • Associated with increased expression of carriers for polyLacNAc that can represent ligand structures to cell-adhesion molecules • However, role of LAMP1 in adhesion to the ECM and in ECM remodeling is indirect because it uses Galectin-3 as mediator, giving more importance to the role of LAMP1 as carrier of polyLacNAc rather than protein itself. Other proteins can also be carriers of these modifications, rendering role of LAMP1 in ECM regulation not exclusive [45,54]
Metastasis [50,53]	• Anti-LAMP1 antibodies proved to reduce lung metastasis of murine melanoma B16F10 cells in four mice	• Data supported by previous studies showing increased LAMP1 expression correlating with metastatic potential of human colon carcinoma and melanoma cells, and by silencing experiments linking LAMP1 expression with the metastatic potential • Absence of direct involvement diminishes possible therapeutic potential of LAMP1 targeting
Cancer cell migration [51,52]	• LAMP1 found as a BR96 antigen expressed on the cell surface domains responsible for locomotion [51] • FUT1 reported to be able to fucosylate LAMP1, thereby influencing lysosomes localization and promoting cell migration [52]	• The link between LAMP1 expression and migration is not direct, but controlled by LAMP1 polylactosamine modifications and fucosylation, responsible for the binding to key antigens for migration such as BR96 [51,52]
Drug resistance [66–68]	• Increased LAMP1 protein expression shown in RMS cells resistant to AS-DACA [66] and in renal and colorectal cancer cells resistant to TKIs [67] • Higher LAMP1 expression found in human sarcomas associated with relapse, and its direct role in increasing lysosomal exocytosis was found to be responsible for promoting invasion and doxorubicin-resistance in human sarcomas	• Increased LAMP1 protein expression used as a proxy for increased lysosomal capacity, without clearly stating the molecular mechanism involved in this process [66,67] • In contrast, detailed analysis of the role played by LAMP1 in lysosomal exocytosis is clearly stated [68]

Abbreviations: AML, acute myeloid leukemia; AS-DACA, N- [2-(Dimethylamino) ethyl] Acridine-4-CarboxAmide; ECM, extracellular matrix; EGF, epidermal growth factor; EGFR, epidermal growth factor receptor; GESA, gene-set enrichment analysis; OS, overall survival; polyLacNAc, poly-N-AcetylLactosamines; RMS, rhabdomyosarcoma; TCGA, The Cancer Genome Atlas; TKIs, tyrosine kinase Inhibitors.

Table 2
Summary of cancer-associated functions for CD107b/LAMP2 (lysosome associated membrane protein-2).

Pro-tumorigenic roles	Evidence	Strength / Weakness of the Evidence
Cancer pathogenesis [78,80]	• Increased LAMP2 protein expression reported in poorly differentiated human gastric adenocarcinoma relative to adjacent gastric mucosal tissues [78] • *LAMP2* gene is located in a region involved in BCL1/JH t(11;14)(q13;q32) translocation found in multiple myeloma patients [80]	• LAMP2 protein expression increase used as a proxy for autophagy-lysosome signaling with no clear indications on its specific role in the signaling • Conflicting data regarding role of autophagy-lysosome circuitry in cancer pathogenesis [78] • Functional studies supporting pathogenic significance of LAMP2 in multiple myeloma still missing [80]
Cancer cell migration [52,77]	• LAMP2 modification by FUT1 reported able to control localization of lysosomes, which often shift from perinuclear to peripheral compartment in invasive cancer [52] • LAMP2 protein highly expressed in invasive OVISE human ovarian clear cell adenocarcinoma cells, and ANXA4 knock-out decreased LAMP2 protein expression and migration [77]	• LAMP2 is not directly involved in the regulation of migration, but rather its modification by FUT1 plays a more important role [52]. • A direct LAMP2 knock-out experiment is needed to confirm its possible direct involvement in ovarian cancer cells migration [77]
Support early cancer growth [49]	• LAMP2 expression on plasma membrane supported early breast cancer progression by acting as protective shield against acidic extracellular microenvironment	• Relevance for a LAMP2 role in survival within acidic microenvironment supported by strong data from both breast cancer cell lines and patients • Exact molecular mechanisms involved in LAMP2 protective action not addressed in the reported study and are not yet discovered
Adhesion of cancer cells to ECM, basement membrane and endothelium [45]	• LAMP2 observed by flow cytometry on cell surface of A2058, HT1080 (human fibrosarcoma), and CaCo-2 (human colon adenocarcinoma) cells; and interaction with Galectin-3 reported	• Data supported by previous studies but the fact modifications of LAMP2 rather than their expression are reported as causal link with ECM adhesion diminishes the therapeutic potential of their targeting
Drug resistance [67]	• Increased protein expression of LAMP2 reported in renal and colorectal cancer cells resistant to TKIs [67]	• Study did not a provide data regarding mechanisms involved in lysosomal control exerted by LAMP2 and how this could lead to increased drug secretion
CMA activation [81,82]	• Ectopic expression of LAMP2A isoform, through its key action on CMA able to support cell survival upon oxidative stress; conversely, its inhibition promoted apoptosis and doxorubicin resistance in breast cancer cells [81] • Inhibition of LAMP2A blocked constitutive activation of CMA and led to the reduction of cell proliferation, the growth of pre-existing tumors and promoted metastatic potential of lung cancer cells [82]	• LAMP2A key role in cancer supported by high expression in patient-derived invasive carcinoma compared with adjacent tissues and in several cancer cell lines • Given its direct control on CMA, LAMP2A inhibition could represent a very promising strategy for sensitizing cancer cells to chemotherapy [81,82]

Abbreviations: CMA, chaperone-mediated autophagy; ECM, extracellular matrix; TKIs, tyrosine kinase inhibitors.

lysosomes and autophagosomes, suggesting a function for this isoform in macroautophagy [37]. Finally, LAMP-2C has been demonstrated to act as an inhibitor of CMA particularly in B cells, and to be capable of mediating the autophagy of nucleic acids by binding to RNA and DNA [38,39]. Many different mutations have been found in the LAMP2 gene and these are causative of Danon disease, a severe condition characterized by skeletal and cardiac myopathy and cognitive impairment [40–42]. Additionally, the loss of the LAMP-2B isoform could represent the phenotypic leading cause of Danon disease, probably given its putative role in macroautophagy [43]. A similar phenotype to Danon disease is observed in LAMP2 knockout mice, whereas LAMP1 single knockout mice are viable and fertile while LAMP1/LAMP2 double knockout mice show embryonic lethality, suggesting these two proteins play key and partially overlapping functions in cellular homeostasis [30]. LAMP2 deficiency has also been associated with pancreatitis, strengthening the importance of a correct lysosomal/autophagic compartment and its associated proteins for cell homeostasis [44].

Growing evidence of a role for lysosomes in different diseases has raised interest in deciphering the role of LAMP1 and LAMP2 in cancer progression. Examples of the roles of LAMP1 and LAMP2 in cancer are summarized in Tables 1 and 2 and depicted in Figs. 2 and 3. Reported roles for LAMP1 and LAMP2 as pro-invasive and pro-metastatic factors refer to their abnormal localization on the plasma membrane of cancer cells, as shown in human melanoma A2058 cells, human colon carcinoma CaCo-2 cells, and human fibrosarcoma HT1080 cells [45]. There is still no clear explanation on the way LAMP1 and LAMP2 translocate to plasma membrane but, possibly, this could be the result of plasma membrane damage leading to lysosome fusion and exocytosis as a membrane repair mechanism [46]. It has been proposed that a Rab3a-dependent complex or the tumor protein D52 could possibly mediate LAMP1 and LAMP2 trafficking to the plasma membrane [47,48]. *In vitro* studies have shown that the translocation of LAMP2 could be driven by an acidic microenvironment, which could support the thesis that plasma membrane damage recruits lysosomes and LAMPs to the plasma membrane [49]. Specifically, in the early phases of in situ breast carcinoma, progression, glycolytic metabolism, and the absence of vascularization generate an acidic microenvironment, which results in increased localization of LAMP2 on the plasma membrane serving as a protective shield, as shown in Fig. 4 [49]. In addition to protection, LAMP1 and LAMP2 expression on the plasma membrane provide binding to E-selectin through sialyl-Le^X residues and binding to galectin-3 through poly-N-acetyl-lactosamine (polyLacNAc)-substituted β1, 6 branched N-glycans. Thereby, LAMP1 and LAMP2 can promote both the adhesion of cancer cells to extracellular matrix, basement membrane, and endothelium and the migratory potential of cells during metastasis [45,50]. Both LAMP1 and LAMP2 can also be modified by the alpha1, 2-fucosyltransferases enzyme, FUT1,

Table 3
Summary of cancer-associated function for DC-LAMP/LAMP3 (lysosome associated membrane protein-3).

Pro-tumorigenic roles	Evidence	Strength / Weakness of the Evidence
Metastasis induction [95,106,112]	• Ectopic over-expression of LAMP3 in a uterine cervical cancer cell line (TCS), led to a higher migratory potential [106] • In SCID mice, 82% (9/11) of injected LAMP3 over-expressing TSC cells efficiently generated metastases (primarily to liver and lung) compared with 9% (1/11) of controls [106] • LAMP3 detection by RT-qPCR and IHC in lymph node metastases from cervical carcinoma patients revealed distant metastasis formation associated with higher expression levels of LAMP3 [106] • Increased migration potential of breast cancer-derived cells correlated with higher basal LAMP3 expression levels. LAMP3 knockdown resulted in decreased migration potential of MDA-MB-231 cells after exposure to 1% O_2. Moreover, MDA-MB-231-derived spheroids depleted of LAMP3 showed reduced migratory properties and lower invasion into collagen [95] • Patients with breast cancer with soft tissue metastases showed higher LAMP3 mRNA expression compared with those with non-soft tissue or bone metastases ($P = .034$) [112]	• Results obtained *in vitro* also supported by *in vivo* experiments. However, these results were based on over-expression experiments and therefore rely on excessive expression levels and need to be further validated. However, data were also confirmed by analyses on human patient samples [106] • A stronger migration potential of LAMP3-expressing cells also found in breast cancer-derived cell lines and spheroids, structures that represent a more physiologic model of the disease [95]
Lymph node metastasis [104,110]	• Despite variability among samples, high level of LAMP3 mRNA found in lymph node-positive breast cancer patients (n=183; $P = .019$) and ER/PR-negative tumors ($P < .001$) [104] • Loco-regional recurrences in patients with breast cancer who underwent lumpectomy and radiotherapy found more frequently in those whose tumors had higher LAMP3 mRNA levels [104] • IHC staining in biopsies from patients with HNSCC found high expression of LAMP3 restricted to normoxic regions of tumors and correlated with occurrence of lymph node metastasis [110]. Moreover, worse metastasis-free survival observed in patients whose tumors showed higher levels of LAMP3 [110]	• Data underline the relevant role of LAMP3 in tumor progression and metastatic spread, including patient-derived samples both from breast cancers [104] and HNSCC [110] • Surprisingly, same investigators reported controversial observation that while LAMP3 expression is associated with hypoxic regions in breast cancer tumors [104], it is limited to normoxic regions in HNSCC [110]
Poor overall survival of patients [105–108]	• TMA of gastric (n=750) and colorectal (n=479) tumors found LAMP3 expression significantly higher in tumors compared with normal or benign tissues. In both cancer types, significant association between high LAMP3 levels, tumor stage, and poorer OS with HR of 2.8 and 2.9, also confirmed with multivariate analysis (HR=2.8 and 2.6). • Study conducted on tumors from 24 patients with stage I or stage II cervical cancer who underwent radical hysterectomy reported high LAMP3 mRNA levels associated with poorer prognosis and higher mortality • TMA from 117 LSCC tumors found stronger LAMP3 signal associated with worse tumor stage ($P = .029$), bigger size ($P = .012$) and poorer prognosis (HR=5.706) • mRNA levels in 157 ESCC patients and 50 uninvolved normal tissues and protein level by IHC in 46 paired normal and cancerous tissues reported elevated LAMP3 levels correlated with OS (HR = 1.90) and DFS (HR = 1.80) • Increased expression of LAMP3 in cancer tissues correlated well with DNA Copy Number Amplification (observed in 35/50 cases).	• Remarkable association between high LAMP3 levels in tumors, clinical features and OS in patients with diagnosis of gastric as well as colorectal cancer • Relevance of results from patients with cervical cancer limited by smaller number of patients • Significant correlation between LAMP3 and TP53 expression was shown in LSCC, even if authors considered LAMP3 and TP53 as independent prognostic markers for LSCC • Taken collectively these studies, while relevant, reported retrospective analyses on human samples and the conclusions drawn might not apply to the general population. Moreover, there was not a direct impact on the therapeutic strategy used and the OS
Resistance to hormonal therapy [112]	• In MCF7 cells silencing of LAMP3 increased sensitivity to tamoxifen. Observation linked to activation of autophagy, a process associated with tamoxifen resistance. Indeed, tamoxifen induced LAMP3 mRNA levels, leading to resistance • LAMP3 mRNA levels 7-fold higher in tamoxifen-resistant MCF7 cells relative to tamoxifen-sensitive counterparts • In tumors of patients with advanced breast cancer treated with tamoxifen, higher LAMP3 expression associated with shorter PFS ($P = .003$) and post-relapse OS ($P = .040$)	• Inhibition of autophagy by silencing of associated genes such as MAP1LC3B, ATG5, and BECN1 resulted in enhanced sensitivity to tamoxifen, suggesting impact of LAMP3 on autophagy is crucial step in tamoxifen resistance • LAMP3 inhibition may be clinically relevant to hinder tamoxifen resistance in breast cancer
Resistance to radiation therapy [114]	• Silencing of LAMP3 (along with PERK and ATF4, two other members of UPR during hypoxia) sensitized MDA-MB-231 breast cancer cells to radiation therapy. This result seemed related to an attenuated DNA damage response during radiation when LAMP3 was down regulated by siRNA as measured by the quantification of γ-H2AX foci. Therefore, resistance to radiotherapy can be driven by up-regulation of LAMP3 (and PERK and ATF4) through UPR pathway and relies on an increase of DNA repair process • Effect more evident with MDA-MB-231 cells compared with MCF7 breast cancer cells with wild-type p53, suggesting presence of functional p53 may reduce effect of LAMP3 knock-down	• The specific mechanism underlying the LAMP3-dependent radio-resistance not completely elucidated and can rely on autophagy, as shown for resistance to hormonal therapy • Other evidence indicates MDA-MB-231 cells (but not HCT116) can be sensitized by treatment with the autophagy inhibitor chloroquine. Thus, these effects may be cancer type-dependent
Resistance to chemotherapy [115]	• Research suggests LAMP3 may be a direct target of miR-205, a miRNA down-regulated during EMT in prostate cancer • miR-205 impaired autophagy through reduction of lysosome-associated proteins LAMP3 and RAB27A, thus enhancing the cytotoxic effects of cisplatin in prostate cancer cells • Similar effects seen with silencing of LAMP3 with synthetic oligonucleotides, confirming putative role of LAMP3 expression in the resistance to cisplatin	• Effects on LAMP3 based on *in silico* predictions and indirect measurements, but did not provide direct evidence of miR-205 binding to LAMP3 mRNA • While miR-205 repression or loss in prostate cancer patients is well established, expression of LAMP3 in the same patients has not been evaluated

Abbreviations: DFS, disease-free survival; EMT, epithelial-to-mesenchymal transition; ER, estrogen receptor; ESCC, esophageal squamous cell carcinoma; HNSCC, head and neck squamous cell carcinoma; HR, hazard ratio; IHC, immunohistochemistry; LSCC, laryngeal squamous cell carcinoma; OS, overall survival; PFS, progression-free survival; PR, progesterone receptor; RT-qPCR, reverse transcription quantitative PCR; TMA, tissue microarray; UPR, unfolded protein response.

Table 4
Summary of cancer-associated functions for CD68/Macrosialin/LAMP4 (lysosome associated membrane protein-4).

Pro-tumorigenic roles	Evidence	Strength / Weakness of the Evidence
Marker for pro-tumorigenic TAMs in malignant uveal melanoma [135]	• CD68/Macrosialin/LAMP4+ tumor-infiltrating macrophages identified in 83% of 167 malignant uveal melanomas • Abundance of CD68/Macrosialin/LAMP4+ TAMs associated with parameters of known poorer prognosis, such as largest basal diameter (LBD), heavy pigmentation, and high microvascular density • Melanoma-specific mortality rate 10 years from diagnosis higher in patients with larger number of CD68/Macrosialin/LAMP4+ macrophages	• Evidence regarding enrichment of CD68/Macrosialin/LAMP4 macrophages in uveal melanoma and its association with aggressiveness is strong. However, as expected from functions identified thus far for CD68/Macrosialin/LAMP4 protein, there is not a direct role in cancer cells for CD68/Macrosialin/LAMP4, rather it is only relevant its impact on TAMs, where it represents one of the most used markers
Associated with TAMs in Hodgkin's lymphoma [137,140]	• CD68/Macrosialin/LAMP4 expression in TAMs analyzed by IHC on TMAs from lymph nodes of 166 patients with cHL, including 79 for whom treatment failed. Patients whose tumors were "enriched" with CD68/Macrosialin/LAMP4+ TAMs had at least eight times lower progression-free survival compared with patients whose tumors had very low levels of CD68/Macrosialin/LAMP4+ TAMs (< 5%) [137]. Moreover, CD68/Macrosialin/LAMP4 expression revealed to be more effective with respect to the conventional IPS value used for cHL samples [137] • In two series of advanced cHL patients (n=266 and n=103) CD68/Macrosialin/LAMP4 expression used as macrophage marker in IHC along with CD163, LYZ, and STAT1 • CD68/Macrosialin/LAMP4 the only marker associated with clinical features [140]	• At least two different studies from three independent patients' cohorts proved the prognostic value of CD68/Macrosialin/LAMP4 positivity within tumor tissues of cHL patients, suggesting effectiveness and value of this measurement. Weakness of the first observation is the reduced number of cHL cases with very low levels of CD68/Macrosialin/LAMP4+ TAMs and low-risk patients [137] • Interestingly, the fact that only CD68/Macrosialin/LAMP4 staining (among TAM markers) was significantly associated with clinical parameters underlies possibility CD68/Macrosialin/LAMP4 could be also expressed by cancer cells (see below)
Marker for TAMs in advanced thyroid cancer [138]	• CD68/Macrosialin/LAMP4 used as a marker for TAMs in thyroid cancers. Using TMAs observed that TAMs density increased with aggressiveness of thyroid cancer; specifically, from 27% in WDTC (n=33), to 54% in PDTC (n=37), and 95% in ATC (n=20)	• Remarkable correlation between CD68/Macrosialin/LAMP4+ status and tumor progression (increased grade, invasion property, and decreased survival) in thyroid cancers
Marker for TAMs in TNBCs [139]	• CD68/Macrosialin/LAMP4+ TAMs found in 71.5% of TNBCs • Increased presence of TAMs correlated with poorer prognosis and was associated with enhanced expression of IL-6 and CCL-5 diffusible factors	• Another report supporting association of high infiltration of TAMs (measured as CD68/Macrosialin/LAMP4+ cells) with cancer progression and poorer prognosis in TNBCs
Associated to poor prognosis [148]	• CD68/Macrosialin/LAMP4 immunostaining detected in histologic sections of 51 primary astrocytic tumors (11 benign astrocytomas, 40 malignant tumors) and eight relapses • CD68/Macrosialin/LAMP4 signal significantly higher in malignant tumors compared with benign ones ($P = .036$) • Higher staining score for CD68/Macrosialin/LAMP4 associated with a poorer OS for all the tumors analyzed ($P < .01$), with remarkable enrichment for anaplastic astrocytomas ($P = .021$)	• CD68/Macrosialin/LAMP4 can also be considered a marker for microglia and in gliomas the infiltration of macrophages and microglia has been established. This is in line with the characteristics mentioned above • Notably, authors showed presence of CD68/Macrosialin/LAMP4+ also on the surface of cancer cells, as well as in U87 glioblastoma-derived cell line

Abbreviations: ATC, anaplastic thyroid cancer; cHL, classical Hodgkin's lymphoma; IHC, Immunohistochemistry; IPS, International Prognostic Score; OS, overall survival; PDTC, poorly differentiated thyroid cancer; TAMs, tumor-associated macrophages; TMAs, tissue micro-arrays; TNBCs, triple negative breast cancers; WDTC, well-differentiated thyroid cancer.

which works by adding a fucose molecule to N-acetylglucosamine via α1, 3-linkage and generates Lewis Y (LeY) antigens. The presence of these modified LeY termini on LAMP1 is increased in breast cancer cells relative to their normal mammary counterpart and it has been associated with breast cancer cell migration [51,52]. The presence of this modification on both LAMP1 and LAMP2 is able to influence the localization of lysosomes and the autophagic flux because FUT1 down-regulation has been demonstrated to lead to an accumulation of lysosomes to perinuclear regions and to correlate with increased autophagy and decreased mTORC1 activity [52].

Despite the high expression of both LAMP1 and LAMP2 on the surface of some types of invasive cancer cells, only the surface translocation of LAMP1, but not LAMP2, has been shown to correlate with the metastatic potential of melanoma, non–small cell lung cancer (NSCLC), and laryngeal squamous cell carcinoma [50,53]. One well-described mechanism responsible for the LAMP1-mediated invasion in melanoma cells is the high expression of polyLacNAc bound to LAMP1 that activates the ERK and p38 pathways, thus leading to the secretion of matrix-metallo-protease-9 (MMP-9) and consequent extracellular membrane (ECM) remodeling [54]. In other types of cancer, specifically glioblastoma, pancreatic, and ovarian cancer, LAMP1 expression on the cell surface plays a role during early phases of cancer progression rather than in the metastatic process, thus suggesting different LAMP1 functions depend on the cancer type [55–57]. In these cases, the exact mechanism for LAMP1 tumor-promoting role is still poorly studied, but there are data reporting a regulation of the epidermal growth factor (EGF) pathway in some serous ovarian malignancies [56]. One possibility is that localization of LAMP1 to the plasma membrane could shape growth factor signaling, thereby modulating cancer development at various stages.

LAMP1 expression on the cell surface is also commonly found in some types of immune cells, such as natural killer cells (NK cells) and T cells, and is commonly used as a marker for degranulation and active cytotoxicity (Fig. 5) [58–63]. In particular, in NK cells LAMP1 is necessary for an efficient expression of perforin in lytic granules, and at the same time to protect NK cells from damage during exocytosis of cytotoxic granules [60,61]. LAMP1

Table 5
Summary of cancer-associated functions for BAD-LAMP/LAMP5 (lysosome associated membrane protein-5), C20orf103.

Pro-tumorigenic roles	Evidence	Strength / Weakness of the Evidence
Associated with poor prognosis [156]	• BAD-LAMP/LAMP5 identified through gene expression profiling with microarrays on FFPE samples along with seven other genes as part of the GCPS as a high-risk gene for recurrence in three different cohorts of stage II gastric cancer patients who underwent adjuvant chemo-radiotherapy • Higher expression of BAD-LAMP/LAMP5 associated with poorer prognosis	• The GCPS was validated in more than 700 stage II GC patients and proposed for routine use in the clinic. However, the increased BAD-LAMP/LAMP5 expression was significantly higher in stromal cells rather than in cancer cells, highlighting a more important role for BAD-LAMP/LAMP5 in the tumor microenvironment

Abbreviations: FFPE, formalin-fixed paraffin-embedded; GC, gastric cancer; GCPS, Gastric Cancer Prognostic Score.

expression on cancer cells could possibly recapitulate the role carried out in immune cells, thus protecting cancer cells from lytic granules and immune mediated destruction. Similarly, both LAMP1 and LAMP2 expression have been associated with the ability of leukocytes to adhere to the endothelium and to migrate, and in this way favoring the migration of cancer cells [64].

LAMP1 over-expression can also influence cancer progression from its normal localization inside the lysosomal membrane. In particular, increased expression of LAMP1 can influence lysosomal biogenesis and cancer cell viability: its knockdown in acute myeloid leukemia cells leads to diminished cancer cell viability through lysosome disruption [65]. In the lysosomal membrane, LAMP1 can also promote drug resistance by increasing lysosomal size and lysosomal exocytosis as it has been shown in rhabdomyosarcoma, soft tissue sarcomas, and renal and colorectal cancers. This ultimately leads to drug sequestration in lysosomes and drug release via exocytosis, thereby causing drug resistance [66,67]. Increased lysosomal exocytosis is also responsible for increased invasiveness of aggressive soft tissue sarcomas [68]. However, reduced expression of LAMP1 and LAMP2 have been reported in ovarian carcinoma cells resistant to cisplatin, suggesting their role in drug resistance could either be drug specific or cancer cell-type specific [69]. Tissue and type specificity effect of LAMP1 could also explain some conflicting evidence regarding a tumor-suppressing role of LAMP1 reported in pancreatic carcinoma and ovarian carcinoma cells exposed to ascites. Indeed, LAMP1 expression correlates with prolonged survival in pancreatic carcinoma, whereas ascites-mediated up-regulation of LAMP1 expression in ovarian carcinoma cells is responsible for a decreased cancer cell migration [70,71].

Increased expression of LAMP1 could be driven by the activation of specific cancer signaling pathways (such as STAT3, ETS1, and p65), or could be a result of a gene amplification as seen in chronic lymphocytic leukemia and in a number of p53 null and basal-like breast cancers (ENCODE database [72,73]). In the latter case, LAMP1 was seen to be over-expressed compared with normal

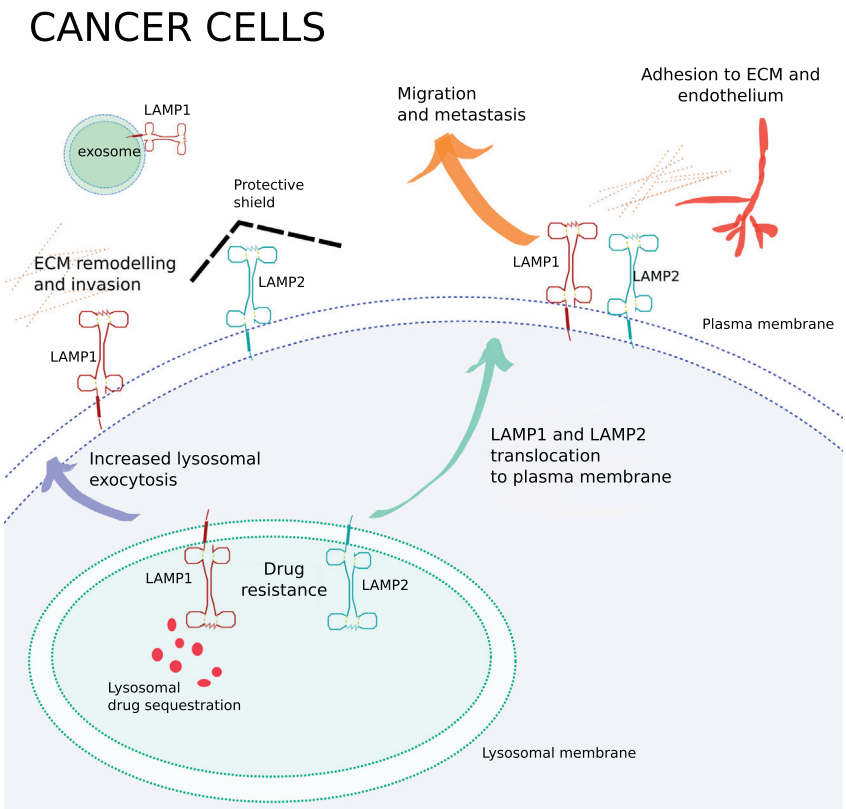

Fig. 2. LAMP1-LAMP2 subcellular localization and their roles in cancer. LAMP1 and LAMP2 can influence cancer biology in different ways depending on their localization. On the plasma membrane they promote adhesion to the endothelium and the extracellular membrane (ECM), migration and metastasis; whereas on the lysosomal membrane they promote drug resistance by increasing lysosomal drug sequestration and lysosomal exocytosis. LAMP1 expression on the plasma membrane can also play a role in ECM remodeling and invasion, whereas LAMP2 can act as a protective shield. LAMP1 is often found expressed in tumor-derived exosomes but its role in exosome biology it is still unknown.

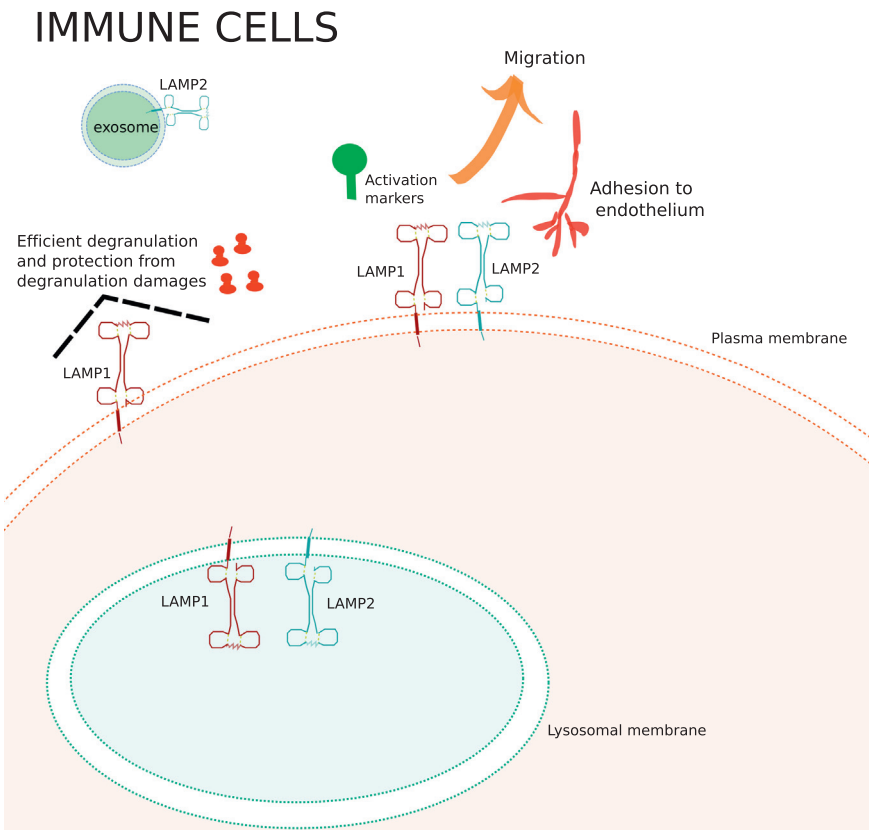

Fig. 3. LAMP1-LAMP2 subcellular localization and their roles in immune cells. LAMP1 and LAMP2 in immune cells can act as activation markers when expressed on the plasma membrane and they can promote adhesion to endothelium and migration. LAMP1 specifically has a crucial role in the degranulation process, whereas LAMP2 is expressed in immune cancer cells-derived exosomes.

mammary epithelium as a result of gene amplification, although this phenomenon alone did not correlate with survival [72,73]; while, a homozygous deletion of the LAMP1 gene has been found in some cases of gastric carcinoma, demonstrating again the opposing roles of LAMP1 in cancer progression [74]. Finally, LAMP1 is also commonly found expressed on the membrane of exosomes secreted by different types of tumors [28,75]. The exact role for LAMP1 expression on secreted exosomes is still unknown. However, it could be involved in the different effects of exosomes on the immune system by either promoting recognition of cancer antigens or inducing immune tolerance to cancer cells [75,76].

LAMP2 has fewer reports on its involvement in cancer progression than LAMP1, but similarly to it, some contradictory functions are also reported. LAMP2 may regulate migration of ovarian clear cell adenocarcinoma, possibly through ANXA4 (Annexin A4), whose knockout in the OVISE cell line resulted in a reduced expression of LAMP2 and was associated with a loss of migration and invasion capability [77]. Compared with normal tissues, LAMP2 is also highly expressed in poorly differentiated human gastric adenocarcinoma, hepatocellular carcinoma, salivary adenoid cystic carcinoma, and in the broncho-alveolar lavage fluid of patients with lung adenocarcinoma, representing one novel molecular marker for these cancer types [78,79]. It may be involved in the pathogenesis of patients whose multiple myeloma harbor a specific BCL1/JH t(11;14)(q13;q32) translocation and could be used as a prognostic marker or therapeutic target [80]. The LAMP2A isoform has shown increased expression in breast tumor tissues and prognostic value in NSCLC. Indeed, LAMP2A inhibition or genetic knockdown resulted in the sensitization of tumor cells to doxorubicin and radiation therapy [81–83]. Another important role reported for the LAMP2A isoform in cancer refers to its involvement in immunogenic cell death, a type of apoptosis that stimulates anti-cancer immune response [84]. In particular, the LAMP2A isoform can induce the expression of calreticulin and the secretion of ATP upon mitoxantrone- and hypericin-based photodynamic therapy, thus leading to immunogenic cell death, thereby suggesting opposing roles for this isoform in cancer [84].

Another reported tumor-suppressor role for LAMP2 stands on its ability to induce cell death upon depletion of the VEGF-NRP2 axis in prostate cancer cells. The up-regulation of LAMP2 and WDFY1 resulting from autophagy blockade caused by VEGF-NRP2 axis inhibition leads to increased cell death [85]. Similar oncosuppressive effects have been observed in neuroblastoma cells cultured under hyperoxia, which causes up-regulation of LAMP2 and LC3-II, macro-autophagy, and ultimately induces apoptosis [86]. A protective role of LAMP2 in drug resistance has been reported in lung cancer, where it is directly targeted by miR-487b-5p, a microRNA often found over-expressed in temozolomide-resistant lung cancer cells [87]. Finally, LAMP2 is often found expressed on the membrane of exosomes secreted from immune cells, but its role is still largely unknown; however, there could be a possible role for both LAMP1 and LAMP2 exosomal expression in shaping the immune system response (Fig. 3) [28].

3.2. *LAMP3/DC-LAMP*

Lysosomal-associated membrane protein 3 (LAMP3) is a 44-kDa protein and, unlike LAMP1 and LAMP2, which are ubiquitously expressed, LAMP3 is expressed only in specific conditions and tissues. To avoid ambiguity, it is worth noting that the LAMP3 gene/protein name can also be wrongly referred to as CD63, which, despite being a protein enriched in late endosomal and lysosomal compartment, belongs to the tetraspanin family [88]. In this review, we always refer to LAMP3 as a member of the LAMP family.

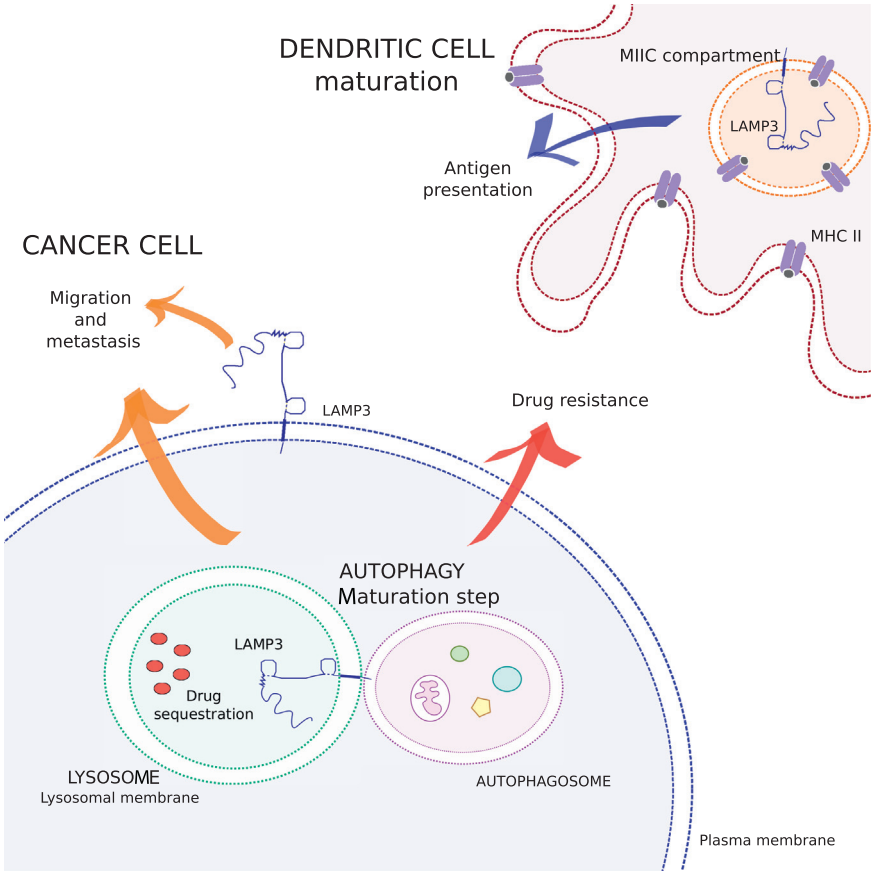

Fig. 4. LAMP3 subcellular localization and its roles in cancer and immune cells. LAMP3 can localize to different cellular compartments and can therefore exert different functions. LAMP3 can be bound to the lysosomal membrane or to the plasma membrane and regulate migration, metastasis, and drug resistance in cancer cells. Moreover, its cytoplasmic tail plays a role in the process of fusion of the lysosome with the autophagosome, thereby modulating the autophagic process, which can also mediate its pro-tumorigenic functions. LAMP3 is also a marker for mature dendritic cells, in which it is progressively expressed during maturation. During this process LAMP3 co-localizes with MHC class II molecules (MHCII) within the MHC class II compartment (MIIC), suggesting a possible role for LAMP3 in the antigen presentation process.

LAMP3 is also called DC-LAMP, because it was firstly shown to be induced progressively upon maturation of human dendritic cells (DCs), where it transiently co-localizes with major histocompatibility complex (MHC) class II molecules at the limiting membrane of specific intracellular compartments (ie, MHC class II compartment, MIIC), and is thus considered as a marker of mature DCs in humans [89]. In the same year of this observation, LAMP3 was independently characterized as a gene specifically expressed in lung tissue, and designated as TSC403 transcript [90]. Indeed, LAMP3 is highly expressed in a specific cell type in mammals, normal and transformed type II pneumocytes (PnIIs) [91], which are specialized pulmonary cells important for the repopulation of lung tissue during normal homeostasis and injury, and responsible for surfactant synthesis, secretion, and recycling [92,93]. However, the expression of LAMP3 in time and space is significantly different between human DCs and type II pneumocytes. LAMP3 is transiently expressed in the MIIC compartment (responsible for the exposure of MHC class II/peptide complexes on the plasma membrane) during the maturation of DCs and it then accumulates in perinuclear lysosomes without localizing to the plasma membrane [89]. Conversely, LAMP3 is constitutively expressed at the limiting membrane of PnII lamellar bodies (responsible for secretion of surfactant proteins, and also containing MHC class II molecules), and low levels of the protein can also be detected at the cell surface membrane in these cells [91]. Functional similarity between MIIC in DCs and lamellar bodies in PnIIs suggests a possible role for LAMP3 in the regulation of the exocytosis of these lysosomes, and particularly in MHC class II-restricted antigen presentation, which is a characteristic of both mature DCs and PnIIs [94].

LAMP3 expression is induced by the unfolded protein response (UPR) activated by hypoxic condition [95] and this induction is mediated by the PERK/eIF2α arm of UPR [96]. Further, proteasome inhibition induces LAMP3 expression in an ATF4 (a UPR transcription factor)-dependent manner. Increased expression of LAMP3 is able to trigger autophagy, whereas preventing LAMP3 induction enhanced apoptotic cell death, thereby demonstrating that LAMP3 regulation is important for proteasomal degradation and cell survival during proteasome dysfunction [97]. Furthermore, a recent meta-analysis of genome-wide association studies in Parkinson disease has identified the MCCC1/LAMP3 genetic locus associated with Parkinson disease risk [98,99]. LAMP3 expression is also driven by IFN-α during DC maturation [100], and it has been shown to regulate the expression of antiviral genes in cervical cancer [101]. LAMP3 expression is also induced in an interferon-dependent manner upon influenza A and hepatitis C virus infection and may play a role in the regulation of virus replication and infection at the post-entry stages [102,103].

Growing evidence has shown that LAMP3 is over-expressed in various human tumors, where it correlates with poor prognosis (LAMP3 functions in cancer are summarized in Table 3 and Figs. 4 and 6) [104,105]. Studies have revealed that LAMP3 might be important in tumor metastasis and resistance to therapies, suggesting LAMP3 could become a molecular marker for the prognosis of various cancers [106,107]. Indeed, LAMP3 expression has been shown to be higher in several primary cancers compared with normal tissues, including cancers of the esophagus, colon, fallopian tube, ovary, uterus, breast, and liver [90,108]. Moreover, the 3q27 region where the LAMP3 gene is located is often

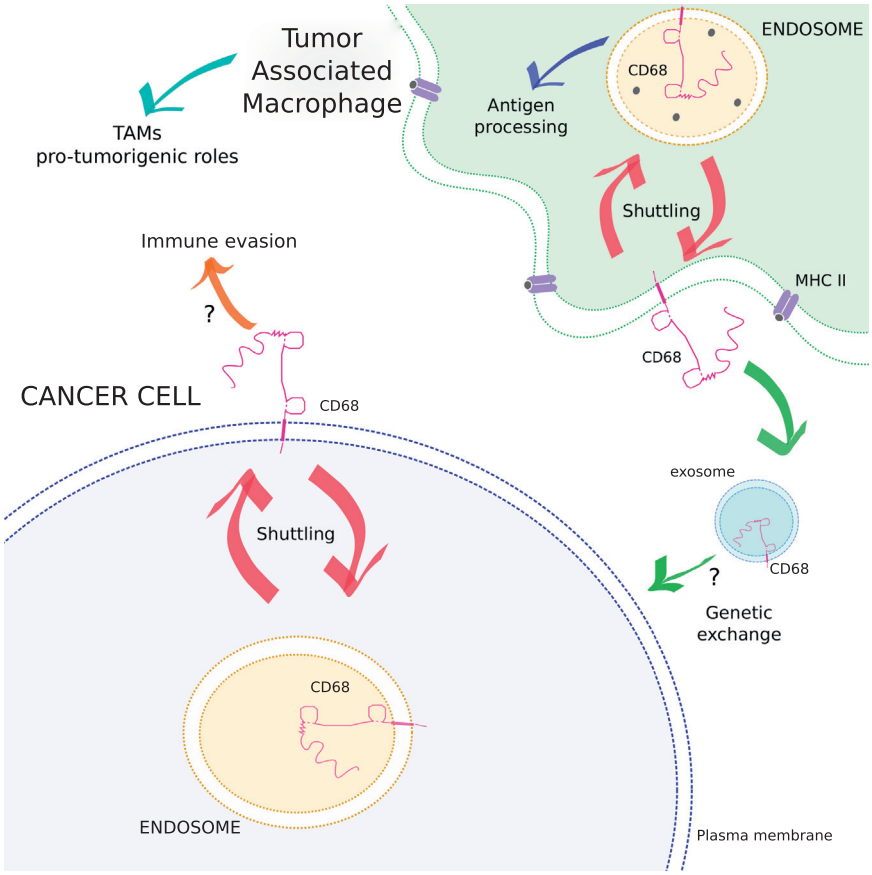

Fig. 5. CD68/Macrosialin/LAMP4 subcellular localization and its roles in cancer and immune cells. CD68/Macrosialin/LAMP4 represents a marker for tumor-associated macrophages, where it can rapidly shuttle between the endosomal compartment and the plasma membrane. Recent observations suggest that CD68/Macrosialin/LAMP4 may also have a negative role in the antigen presentation process. CD68/Macrosialin/LAMP4 has recently been found to also be expressed by some cancer cells, where it is associated with increased malignancy, possibly caused by immune evasion mechanisms. Expression of this immune-cell marker by cancer cells could be explained by genetic exchange between macrophages and cancer cells, which is supported by the recent detection of CD68/Macrosialin/LAMP4 in macrophages-derived exosomes.

amplified in various types of cancers, in particular squamous cell carcinomas and penile carcinomas [109].

LAMP3 over-expression in uterine cervical cancer cell lines is able to promote metastasis *in vitro* and *in vivo* [106], and its expression has been associated with lymph node metastasis [104,110] and increased migration in breast cancer cells [95], suggesting a role for LAMP3 in the metastatic process [106]. However, the mechanism whereby it might promote metastases has not been completely elucidated. Conversely, similarly to LAMP1 and LAMP2, its exposure on the plasma membrane could allow cancer cells to interact with endothelial cells. Nevertheless, LAMP3 expression on the cellular plasma membrane could be detected only in specific circumstances on cancer cells, such as upon Influenza A virus infections in HeLa cells [102], whereas it could not be detected on the plasma membrane of other cancer cell lines, for example MDA-MB-231 [95]. Another possible mechanism by which LAMP3 expression can increase the metastatic potential of cancer cells is through the modulation of the autophagic flux, which is known to play key roles in cancer metastasis [111]. Particularly, the cytoplasmic tail of LAMP3 seems to be required for the fusion of the autophagosome with the lysosome (ie, maturation step), a process inhibited in cancer cells when LAMP3 is knocked down [112].

LAMP3 expression has also been correlated with poor overall survival in head and neck squamous cell carcinomas [107,108], uterine cervical cancer [106], and gastric and colorectal cancers [105], whereas its expression levels, together with the expression of other pneumocyte-specific genes, has been associated with increased survival in the adenocarcinoma subgroup of NSCLC [113]. These conflicting data could be attributed to the high levels of LAMP3 expression in lung normal tissue, where LAMP3 could play a specific role that could be compromised during cancer development.

LAMP3 has also been implicated in drug resistance with up-regulation of LAMP3 associated with resistance to chemotherapy and radiotherapy in breast cancer [112,114], and its down-regulation possibly increasing cisplatin sensitivity in prostate cancer cells [115]. LAMP3 expression could decrease the sensitivity of cancer cells to chemotherapy by modulating autophagy, a process whose ability to influence drug resistance has been extensively studied [116]. LAMP3-mediated radiotherapy resistance has conversely been attributed to its ability to positively regulate the

Fig. 6. Roles of LAMP family members in cancer progression. All the LAMP proteins are involved in cancer progression; LAMP1, LAMP2 and LAMP3 are also implicated in migration and stress or drug resistance. LAMP1 and LAMP2 also promote adhesion to the extracellular matrix (ECM) or remodeling whereas LAMP1 and LAMP3 can induce metastasis formation. CD68/Macrosialin/LAMP4 is often expressed on tumor-associated macrophages (TAMs).

response to DNA damage [114]. Finally, induction of LAMP3 among a subset of genes, following combined treatment with the chemotherapeutic drug doxorubicin and the inflammatory cytokine TNF-α in breast cancer cells, suggests a possible involvement of LAMP3 in cancer-related inflammation [117].

Given that LAMP3 is highly expressed in DCs, it is essential to distinguish between its contribution to cancer when expressed by cancer cells or by DCs infiltrating the tumor. For example, it has been observed that infiltration of LAMP3$^+$ DCs in the sentinel lymph nodes of melanoma patients was correlated with the absence of metastasis in downstream lymph nodes [118].

3.3. CD68/Macrosialin/LAMP4

CD68, the human homologue to murine Macrosialin, is a heavily glycosylated transmembrane glycoprotein mainly localized in the endosomal/lysosomal compartment of macrophages showing a distinctive structure corresponding to the LAMP signature, with highest homology to LAMP3 [119,120]. Similarly to LAMP3, CD68 contains only a single LAMP-like domain and a mucin-like domain (Fig. 1) [119]; but, unlike LAMP3, which is mainly located within lysosomes, CD68 is found in endosomes and can rapidly shuttle to the plasma membrane [121].

CD68/Macrosialin/LAMP4 has been extensively used as a histologic marker of macrophage lineage cells because it is preferentially expressed by resident macrophages of multiple tissues, including macroglia in the brain, Kupffer cells in the liver, and bone marrow macrophages [122–124]. Although initially classified as a group D scavenger receptor because of its ability to bind oxidized low-density lipoproteins [125], CD68 silencing and knockout experiments failed to affect oxidized low-density lipoprotein binding and uptake to macrophages [126,127]. Beyond the use of CD68/Macrosialin/LAMP4 as a histologic marker to identify macrophages, the apparent specificity of the expression of CD68/Macrosialin/LAMP4 has led some to propose the use of CD68 transcriptional regulatory sequences to specifically drive *in vitro* and *in vivo* transgene expression, as well as for gene therapy approaches [89,128,129]. However, recent studies show that a high expression of CD68/Macrosialin/LAMP4 is not limited to cells of macrophage lineage, but is also observed in other hematopoietic and non-hematopoietic cells [130,131]; therefore, CD68/Macrosialin/LAMP4 should be considered a non-specific marker of macrophages.

Although a role for CD68/Macrosialin/LAMP4 in antigen processing is unknown, studies have shown enhanced capacity of antigen presentation to CD4$^+$ T cells by CD68$^{-/-}$ mononuclear phagocytes, suggesting CD68/Macrosialin/LAMP4 may have negative regulatory functions in MHC class II trafficking or antigen uptake and loading [127]. Interestingly, CD68 is also expressed in immature DCs, and its expression progressively disappears during maturation at the same time that LAMP3 accumulates in the lysosomes [89], suggesting a putative competing role in the antigen presentation process.

Immunohistochemical staining of bone specimens has identified CD68/Macrosialin/LAMP4 expression in osteoclasts [124], multi-nucleated cells responsible for bone reabsorption during normal bone remodeling or pathologic conditions [132], and genetic ablation of CD68/Macrosialin/LAMP4 resulted in morphologic alteration and functional defects in osteoclasts and increased bone in mice [133]. Importantly, infiltration of CD68/Macrosialin/LAMP4$^+$ cells is a marker for both inflammation and tumor progression (see Table 4 and Figs. 5 and 6) [134,135]. A population-based cohort study of malignant uveal melanoma observed diffuse infiltration of CD68/Macrosialin/LAMP4$^+$ macrophages in 83% of analyzed tumors, and the number of macrophages has been associated with the largest basal tumor diameter, presence of epithelioid cells, and high microvessel density in areas of high vascularization [135], which represent independent high-risk indicators for metastasis in uveal melanoma [135,136].

Tumor-associated macrophages (TAMs), for which CD68 represents one of the most recognized markers [137], are one of the most abundant population of normal cells in the tumor microenvironment. There is accumulating evidence for TAMs' pivotal role in driving pro-tumorigenic phenotype. Indeed, density of CD68$^+$ TAMs is increased in poorly differentiated thyroid cancers, and a high density of these cells correlates with invasion and decreased cancer-related survival in these advanced thyroid cancers [138]. Furthermore, increased expression of CD68$^+$ macrophages in the tumor stroma of patients with a diagnosis of triple-negative breast cancer and of patients with classic Hodgkin's lymphoma correlates with a poor prognosis [139,140]. In contrast, a high density of CD68/Macrosialin/LAMP4$^+$ macrophages correlates with increased overall survival in NSCLC and esophageal squamous cell carcinoma [141,142]. This discrepancy in the predictive power of CD68/Macrosialin/LAMP4 for tumor prognosis could be because of several factors, including technical variability, specificity of the antibodies, and differences in the case series [143]. We have reported here some evidence of the role of CD68/Macrosialin/LAMP4$^+$ macrophages in the tumorigenic processes and we refer to other recent reviews for a comprehensive description of the role of TAMs in cancer [144–147].

Importantly, the association of CD68/Macrosialin/LAMP4 with cancer is not only related to its expression in TAMs, but also in tumor cells [131]. For example, CD68/Macrosialin/LAMP4 was found to be highly expressed in human gliomas by both microglia and tumor cells; its expression was associated with malignancy in these tumors, and was suggested as a prognostic marker of reduced survival in human gliomas [148]. This observation is in agreement with the fact that tumor cells often express immune cells-markers to evade the immune system during the metastatic process, most frequently expression of macrophage antigens such as CD68, CD47, CD163, and DAP12 [149–151]. The mechanism explaining the expression of macrophage antigens by tumor cells is still debated, and it seems to be mediated by genetic exchange as a result of either direct macrophage-cancer cell fusion [152], or by exosome-mediated transfer [149]. CD68 was found to be expressed in mouse macrophages-derived exosomes [153], thereby supporting the hypothesis that exosomes can mediate a genetic exchange between macrophages and cancer cells and, ultimately, it could also explain the expression of CD68/Macrosialin/LAMP4 in cancer cells.

Although CD68/Macrosialin/LAMP4 is widely used as diagnostic and prognostic marker for several malignancies, the role of this protein in cancer is still to be explained and further studies investigating its mechanism of actions are needed.

3.4. BAD-LAMP/LAMP5

BAD-LAMP (Brain and Dendritic Cell associated LAMP-like molecule), also known as LAMP5 or C20orf103 is the *C. elegans* ortholog of UNC-46 and the latest characterized LAMP protein. Unlike other LAMP family members, BAD-LAMP/LAMP5 does not localize to late endosomes or lysosomes and, similarly to LAMP3 and CD68/Macrosialin/LAMP4, its expression is limited to specific tissues. BAD-LAMP/LAMP5 is a 280 amino acid protein with a transmembrane domain and a cytoplasmic tail containing a YKHM sequence, corresponding to a classic YXXΦ internalization and endosomal-targeting signal. It also contains several N-glycosylation sites, as well as four cysteine residues separated by a fixed number of amino acids, allowing for the formation of the disulfide bonds required for the "LAMP-fold" (Fig. 1) [32].

BAD-LAMP was first identified as a new LAMP family member in mice, where it is mainly expressed in specific subtypes of cortical projecting neurons. In these cells, BAD-LAMP expression

considerably increased after birth, suggesting its involvement in the late steps of neuronal differentiation. BAD-LAMP/LAMP5 can be endocytosed and directed to uncharacterized vesicles clustered in the growth cone of developing axons or in defined dendritic domains, identified as a specific class of early neuronal endosomes [32]. In *C. elegans* mutations in the BAD-LAMP ortholog, UNC-46, cause defects in most GABA-mediated behaviors, and it has been proposed as a sorting factor able to address the GABA transporter (UNC-47) to the synaptic vesicles [154]. In humans, like in mice, BAD-LAMP/LAMP5 is expressed at higher levels in the brain, but, among blood cells, it is also specifically expressed in the type I IFN-producing primary plasmacytoid dendritic cells (pDCs) and transformed pDCs (blastic pDC neoplasms or BPDCNs), for which it represents a relevant biomarker [155]. In these cells, BAD-LAMP/LAMP5 is principally localized in the ER-Golgi intermediate compartment and its expression is lost upon pDC activation by Toll-like Receptor ligands [155].

A second observation for an association between this poorly studied protein and cancer comes from the analysis of the expression of a set of genes, including BAD-LAMP/LAMP5, which has been shown to be correlated with a poor prognosis in stage II gastric cancer patients treated with chemo-radiotherapy (Table 5 and Fig. 6) [156]; however, it is not clear whether BAD-LAMP/LAMP5 expression observed in the analyzed tissues is determined by pDCs infiltration within the tumor or by a higher expression of the protein in cancer cells. Further studies are required to establish the putative role of BAD-LAMP/LAMP5 in cancer.

4. Conclusions

Correct functioning of the lysosomal compartment represents a guarantor for an efficient cell homeostasis and a critical protection against various diseases, among them cancer. Differential expression of proteins associated with the lysosomal membrane, categorized as LAMP family members, can substantially influence various processes of cancer progression. This review inspected the various LAMP proteins and their reported roles in oncogenic processes, with conflicting evidence for some of the members.

LAMP1 represents the most studied member of the family and, together with LAMP2, is involved in various oncogenic processes, such as local cancer progression, ECM adhesion and remodeling, migration, drug resistance, and metastasis. The strong potential of LAMP1 in cancer therapy encouraged the Sanofi S.A. pharmaceutical company to patent anti-LAMP1 antibodies and immunoconjugates for detection and treatment (patent number: WO2014102299). Furthermore, LAMP1 and LAMP2 expression on the plasma membrane of cancer cell renders them optimal targets for immunotherapy approaches. Nevertheless, LAMP1 has important reported roles in the immune system, thus when planning its targeting by immunotherapies, it is crucial to bear in mind the importance of specifically targeting LAMP1 and LAMP2 expressed on cancer cells. A decreased expression of LAMP1 in NK cells would reduce their perforin-mediated cytotoxicity, which represents the most efficacious NK-mediated cell death [157], thereby considerably decreasing any anti-cancer immune response. Furthermore, a better understanding of the role of LAMP1 in cancer-derived exosomes and its effects on the immune system is of paramount importance, also for future applications of exosomes in cancer immunotherapy.

The other members of the LAMP family have not yet been extensively studied, but there is growing evidence supporting their pro-tumorigenic potential. For instance, LAMP3 and CD68/Macrosialin/LAMP4, which are activated by various stimuli often present during cancer development and therapy and are closely connected with inflammation, represent additional promising targets for cancer therapy. The mechanisms by which LAMP3 expression can affect tumor progression is still to be elucidated; however, a possible explanation could be inferred from its role in the trafficking of MHC class II/peptide complexes [158], which is critical for antitumor immune response [159].

Interestingly, LAMP3, CD68/Macrosialin/LAMP4, and BAD-LAMP/LAMP5 are highly expressed in immune cells and have been shown to be associated with various types of tumors when expressed on immune cells or cancer cells. Therefore, it would be intriguing to investigate their role at the interplay between cancer and the immune system and to elucidate whether they could play a direct role in the immune response to cancer.

In conclusion, a better knowledge of the LAMP family and the role of the lysosomes in cancer progression could represent a fruitful approach in cancer research.

Conflict of Interest Statement

There are not any conflicts of interest to disclosure.

Acknowledgments

The authors thank Prof. Alberto Inga, Dr. Alessandra Bisio, Dr. Sara Zaccara, and Francesca Precazzini for helpful discussions. This work was partially supported by CIBIO Start up funds, University of Trento (to Y.C.).

References

[1] Appelqvist H, Waster P, Kagedal K, Ollinger K. The lysosome: from waste bag to potential therapeutic target. J Mol Cell Biol 2013;5:214–26.
[2] Schwake M, Schroder B, Saftig P. Lysosomal membrane proteins and their central role in physiology. Traffic 2013;14:739–48.
[3] Schroder BA, Wrocklage C, Hasilik A, Saftig P. The proteome of lysosomes. Proteomics 2010;10:4053–76.
[4] Piao S, Amaravadi RK. Targeting the lysosome in cancer. Ann NY Acad Sci 2016;1371:45–54.
[5] de Duve C. Lysosomes, a new group of cytoplasmic particles. In: Hayashi T, editor. Subcellular Particles. New York: The Ronald Press Co; 1959. p. 128–59.
[6] Turk B, Turk V. Lysosomes as "suicide bags" in cell death: myth or reality? J Biol Chem 2009;284:21783–7.
[7] Lindqvist LM, Simon AK, Baehrecke EH. Current questions and possible controversies in autophagy. Cell Death Discov 2015:1.
[8] Hoyer-Hansen M, Jaattela M. Autophagy: an emerging target for cancer therapy. Autophagy 2008;4:574–80.
[9] Li W, Yuan X, Nordgren G, et al. Induction of cell death by the lysosomotropic detergent MSDH. FEBS Lett 2000;470:35–9.
[10] Bursch W. The autophagosomal-lysosomal compartment in programmed cell death. Cell Death Differ 2001;8:569–81.
[11] Guicciardi ME, Leist M, Gores GJ. Lysosomes in cell death. Oncogene 2004; 23:2881–90.
[12] Leist M, Jaattela M. Four deaths and a funeral: from caspases to alternative mechanisms. Nat Rev Mol Cell Biol 2001;2:589–98.
[13] Leist M, Jaattela M. Triggering of apoptosis by cathepsins. Cell Death Differ 2001;8:324–6.
[14] Sancak Y, Bar-Peled L, Zoncu R, Markhard AL, Nada S, Sabatini DM. Ragulator-Rag complex targets mTORC1 to the lysosomal surface and is necessary for its activation by amino acids. Cell 2010;141:290–303.
[15] Laplante M, Sabatini DM. mTOR signaling in growth control and disease. Cell 2012;149:274–93.
[16] Guertin DA, Sabatini DM. Defining the role of mTOR in cancer. Cancer Cell 2007;12:9–22.
[17] Settembre C, Zoncu R, Medina DL, et al. A lysosome-to-nucleus signalling mechanism senses and regulates the lysosome via mTOR and TFEB. EMBO J 2012;31:1095–108.
[18] Gocheva V, Zeng W, Ke D, et al. Distinct roles for cysteine cathepsin genes in multistage tumorigenesis. Genes Dev 2006;20:543–56.
[19] Koblinski JE, Ahram M, Sloane BF. Unraveling the role of proteases in cancer. Clin Chim Acta 2000;291:113–35.
[20] Mohamed MM, Sloane BF. Cysteine cathepsins: multifunctional enzymes in cancer. Nat Rev Cancer 2006;6:764–75.
[21] Vasiljeva O, Papazoglou A, Kruger A, et al. Tumor cell-derived and macrophage-derived cathepsin B promotes progression and lung metastasis of mammary cancer. Cancer Res 2006;66:5242–50.

[22] Sevenich L, Werner F, Gajda M, et al. Transgenic expression of human cathepsin B promotes progression and metastasis of polyoma-middle-T-induced breast cancer in mice. Oncogene 2011;30:54–64.
[23] Bengsch F, Buck A, Gunther SC, et al. Cell type-dependent pathogenic functions of overexpressed human cathepsin B in murine breast cancer progression. Oncogene 2014;33:4474–84.
[24] Demchik LL, Sameni M, Nelson K, Mikkelsen T, Sloane BF. Cathepsin B and glioma invasion. Int J Dev Neurosci 1999;17:483–94.
[25] Xing W, Archer TK. Upstream stimulatory factors mediate estrogen receptor activation of the cathepsin D promoter. Mol Endocrinol 1998;12:1310–21.
[26] Tu C, Ortega-Cava CF, Chen G, et al. Lysosomal cathepsin B participates in the podosome-mediated extracellular matrix degradation and invasion via secreted lysosomes in v-Src fibroblasts. Cancer Res 2008;68:9147–56.
[27] Goetzl EJ, Boxer A, Schwartz JB, et al. Altered lysosomal proteins in neural-derived plasma exosomes in preclinical Alzheimer disease. Neurology 2015;85:40–7.
[28] Thery C, Zitvogel L, Amigorena S. Exosomes: composition, biogenesis and function. Nat Rev Immunol 2002;2:569–79.
[29] Urbanelli L, Magini A, Buratta S, et al. Signaling pathways in exosomes biogenesis, secretion and fate. Genes 2013;4:152–70.
[30] Wilke S, Krausze J, Bussow K. Crystal structure of the conserved domain of the DC lysosomal associated membrane protein: implications for the lysosomal glycocalyx. BMC Biol 2012;10:62.
[31] Fukuda M. Lysosomal membrane glycoproteins. Structure, biosynthesis, and intracellular trafficking. J Biol Chem 1991;266:21327–30.
[32] David A, Tiveron MC, Defays A, et al. BAD-LAMP defines a subset of early endocytic organelles in subpopulations of cortical projection neurons. J Cell Sci 2007;120:353–65.
[33] Eskelinen EL. Roles of LAMP-1 and LAMP-2 in lysosome biogenesis and autophagy. Mol Aspects Med 2006;27:495–502.
[34] Konecki DS, Foetisch K, Zimmer KP, Schlotter M, Lichter-Konecki U. An alternatively spliced form of the human lysosome-associated membrane protein-2 gene is expressed in a tissue-specific manner. Biochem Biophys Res Commun 1995;215:757–67.
[35] Lichter-Konecki U, Moter SE, Krawisz BR, Schlotter M, Hipke C, Konecki DS. Expression patterns of murine lysosome-associated membrane protein 2 (Lamp-2) transcripts during morphogenesis. Differentiation 1999;65:43–58.
[36] Murphy KE, Gysbers AM, Abbott SK, et al. Lysosomal-associated membrane protein 2 isoforms are differentially affected in early Parkinson's disease. Movement Disord 2015;30:1639–47.
[37] Bandyopadhyay U, Kaushik S, Varticovski L, Cuervo AM. The chaperone-mediated autophagy receptor organizes in dynamic protein complexes at the lysosomal membrane. Mol Cell Biol 2008;28:5747–63.
[38] Fujiwara Y, Hase K, Wada K, Kabuta T. An RNautophagy/DNautophagy receptor, LAMP2C, possesses an arginine-rich motif that mediates RNA/DNA-binding. Biochem Biophys Res Commun 2015;460:281–6.
[39] Perez L, McLetchie S, Gardiner GJ, Deffit SN, Zhou D, Blum JS. LAMP-2C Inhibits MHC class II presentation of cytoplasmic antigens by disrupting chaperone-mediated autophagy. J Immunol 2016;196:2457–65.
[40] Bottillo I, Giordano C, Cerbelli B, et al. A novel LAMP2 mutation associated with severe cardiac hypertrophy and microvascular remodeling in a female with Danon disease: a case report and literature review. Cardiovasc Pathol 2016;25:423–31.
[41] Csanyi B, Popoiu A, Hategan L, et al. Identification of two novel LAMP2 gene mutations in Danon disease. Can J Cardiol 2016;32:1355e23-1355.e30.
[42] Fu L, Luo S, Cai S, et al. Identification of LAMP2 mutations in early-onset Danon disease with hypertrophic cardiomyopathy by targeted next-generation sequencing. Am J Cardiol 2016;118:888–94.
[43] Rowland TJ, Sweet ME, Mestroni L, Taylor MR. Danon disease - dysregulation of autophagy in a multisystem disorder with cardiomyopathy. J Cell Sci 2016;129:2135–43.
[44] Mareninova OA, Sendler M, Malla SR, et al. Lysosome associated membrane proteins maintain pancreatic acinar cell homeostasis: LAMP-2 deficient mice develop pancreatitis. Cell Mol Gastroenterol Hepatol 2015;1:678–94.
[45] Sarafian V, Jadot M, Foidart JM, et al. Expression of Lamp-1 and Lamp-2 and their interactions with galectin-3 in human tumor cells. Int J Cancer 1998;75:105–11.
[46] Corrotte M, Castro-Gomes T, Koushik AB, Andrews NW. Approaches for plasma membrane wounding and assessment of lysosome-mediated repair responses. Methods Cell Biol 2015;126:139–58.
[47] Encarnacao M, Espada L, Escrevente C, et al. A Rab3a-dependent complex essential for lysosome positioning and plasma membrane repair. J Cell Biol 2016;213:631–40.
[48] Thomas DD, Martin CL, Weng N, Byrne JA, Groblewski GE. Tumor protein D52 expression and Ca2+-dependent phosphorylation modulates lysosomal membrane protein trafficking to the plasma membrane. Am J Physiol Cell Physiol 2010;298:C725–39.
[49] Damaghi M, Tafreshi NK, Lloyd MC, Sprung R, Estrella V, Wojtkowiak JW, et al. Chronic acidosis in the tumour microenvironment selects for over-expression of LAMP2 in the plasma membrane. Nat Commun 2015;6:8752.
[50] Agarwal AK, Srinivasan N, Godbole R, et al. Role of tumor cell surface lysosome-associated membrane protein-1 (LAMP1) and its associated carbohydrates in lung metastasis. J Cancer Res Clin 2015;141:1563–74.
[51] Garrigues J, Anderson J, Hellstrom KE, Hellstrom I. Anti-tumor antibody BR96 blocks cell migration and binds to a lysosomal membrane glycoprotein on cell surface microspikes and ruffled membranes. J Cell Biol 1994;125:129–42.
[52] Tan KP, Ho MY, Cho HC, Yu J, Hung JT, Yu AL. Fucosylation of LAMP-1 and LAMP-2 by FUT1 correlates with lysosomal positioning and autophagic flux of breast cancer cells. Cell Death Dis 2016;7:e2347.
[53] Krishnan V, Bane SM, Kawle PD, Naresh KN, Kalraiya RD. Altered melanoma cell surface glycosylation mediates organ specific adhesion and metastasis via lectin receptors on the lung vascular endothelium. Clin Exp Metastasis 2005;22:11–24.
[54] Dange MC, Agarwal AK, Kalraiya RD. Extracellular galectin-3 induces MMP9 expression by activating p38 MAPK pathway via lysosome-associated membrane protein-1 (LAMP1). Mol Cell Biol 2015;404:79–86.
[55] Jensen SS, Aaberg-Jessen C, Christensen KG, Kristensen B. Expression of the lysosomal-associated membrane protein-1 (LAMP-1) in astrocytomas. Int J Clin Exp Pathol 2013;6:1294–305.
[56] Marzinke MA, Choi CH, Chen L, Shih Ie M, Chan DW, Zhang H. Proteomic analysis of temporally stimulated ovarian cancer cells for biomarker discovery. Mol Cell Proteomics 2013;12:356–68.
[57] Tian Y, Almaraz RT, Choi CH, et al. Identification of sialylated glycoproteins from metabolically oligosaccharide engineered pancreatic cells. Clin Proteom 2015;12:11.
[58] Valor L, Teijeiro R, Aristimuno C, et al. Estradiol-dependent perforin expression by human regulatory T-cells. Eur J Clin Invest 2011;41:357–64.
[59] Alitalo K, Carmeliet P. Molecular mechanisms of lymphangiogenesis in health and disease. Cancer Cell 2002;1:219–27.
[60] Cohnen A, Chiang SC, Stojanovic A, et al. Surface CD107a/LAMP-1 protects natural killer cells from degranulation-associated damage. Blood 2013;122:1411–8.
[61] Krzewski K, Gil-Krzewska A, Nguyen V, Peruzzi G, Coligan JE. LAMP1/CD107a is required for efficient perforin delivery to lytic granules and NK-cell cytotoxicity. Blood 2013;121:4672–83.
[62] Naito T, Baba T, Takeda K, Sasaki S, Nakamoto Y, Mukaida N. High-dose cyclophosphamide induces specific tumor immunity with concomitant recruitment of LAMP1/CD107a-expressing CD4-positive T cells into tumor sites. Cancer Lett 2015;366:93–9.
[63] Hromadnikova I, Li S, Kotlabova K, Dickinson AM. Influence of in vitro IL-2 or IL-15 alone or in combination with Hsp 70 derived 14-Mer peptide (TKD) on the expression of NK cell activatory and inhibitory receptors on peripheral blood T cells, B cells and NK T cells. PLoS One 2016;11:e0151535.
[64] Kannan K, Stewart RM, Bounds W, et al. Lysosome-associated membrane proteins h-LAMP1 (CD107a) and h-LAMP2 (CD107b) are activation-dependent cell surface glycoproteins in human peripheral blood mononuclear cells which mediate cell adhesion to vascular endothelium. Cell Immunol 1996;171:10–9.
[65] Sukhai MA, Prabha S, Hurren R, et al. Lysosomal disruption preferentially targets acute myeloid leukemia cells and progenitors. J Clin Invest 2013;123:315–28.
[66] Williams M, Catchpoole D. Sequestration of AS-DACA into acidic compartments of the membrane trafficking system as a mechanism of drug resistance in rhabdomyosarcoma. Int J Mol Sci 2013;14:13042–62.
[67] Gotink KJ, Rovithi M, de Haas RR, et al. Cross-resistance to clinically used tyrosine kinase inhibitors sunitinib, sorafenib and pazopanib. Cell Oncol 2015;38:119–29.
[68] Machado E, White-Gilbertson S, van de Vlekkert D, et al. Regulated lysosomal exocytosis mediates cancer progression. Sci Adv 2015;1:e1500603.
[69] Safaei R, Larson BJ, Cheng TC, et al. Abnormal lysosomal trafficking and enhanced exosomal export of cisplatin in drug-resistant human ovarian carcinoma cells. Mol Cancer Ther 2005;4:1595–604.
[70] Kunzli BM, Berberat PO, Zhu ZW, et al. Influences of the lysosomal associated membrane proteins (Lamp-1, Lamp-2) and Mac-2 binding protein (Mac-2-BP) on the prognosis of pancreatic carcinoma. Cancer 2002;94:228–39.
[71] Meunier L, Puiffe ML, Le Page C, et al. Effect of ovarian cancer ascites on cell migration and gene expression in an epithelial ovarian cancer in vitro model. Transl Oncol 2010;3:230–8.
[72] Abba MC, Fabris VT, Hu Y, et al. Identification of novel amplification gene targets in mouse and human breast cancer at a syntenic cluster mapping to mouse ch8A1 and human ch13q34. Cancer Res 2007;67:4104–12.
[73] Sargent R, Jones D, Abruzzo LV, et al. Customized oligonucleotide array-based comparative genomic hybridization as a clinical assay for genomic profiling of chronic lymphocytic leukemia. J Mol Diagn 2009;11:25–34.
[74] Kang JU, Koo SH, Kwon KC, Park JW. AMY2A: a possible tumor-suppressor gene of 1p21.1 loss in gastric carcinoma. Int J Oncol 2010;36:1429–35.
[75] Wolfers J, Lozier A, Raposo G, et al. Tumor-derived exosomes are a source of shared tumor rejection antigens for CTL cross-priming. Nat Med 2001;7:297–303.
[76] Li Y, An J, Huang S, He J, Zhang J. Esophageal cancer-derived microvesicles induce regulatory B cells. Cell Biochem Funct 2015;33:308–13.
[77] Mogami T, Yokota N, Asai-Sato M, et al. Annexin A4 is involved in proliferation, chemo-resistance and migration and invasion in ovarian clear cell adenocarcinoma cells. PLoS One 2013;8:e80359.
[78] Wei SH, Li W, Liu Y, et al. Disturbance of autophagy-lysosome signaling molecule expression in human gastric adenocarcinoma. Oncol Lett 2014;7:635–40.
[79] Li QK, Shah P, Li Y, et al. Glycoproteomic analysis of bronchoalveolar lavage (BAL) fluid identifies tumor-associated glycoproteins from lung adenocarcinoma. J Proteome Res 2013;12:3689–96.
[80] Ni IB, Ching NC, Meng CK, Zakaria Z. Translocation t(11;14) (q13;q32) and genomic imbalances in multi-ethnic multiple myeloma patients: a Malaysian study. Hematol Rep 2012;4:e19.

[81] Saha T. LAMP2A overexpression in breast tumors promotes cancer cell survival via chaperone-mediated autophagy. Autophagy 2012;8:1643–56.
[82] Kon M, Kiffin R, Koga H, et al. Chaperone-mediated autophagy is required for tumor growth. Sci Transl Med 2011;3:109ra17.
[83] Koukourakis MI, Kalamida D, Mitrakas A, et al. Intensified autophagy compromises the efficacy of radiotherapy against prostate cancer. Biochem Biophys Res Commun 2015;461:268–74.
[84] Garg AD, Dudek AM, Agostinis P. Calreticulin surface exposure is abrogated in cells lacking, chaperone-mediated autophagy-essential gene, LAMP2A. Cell Death Dis 2013;4:e826.
[85] Stanton MJ, Dutta S, Zhang H, et al. Autophagy control by the VEGF-C/NRP-2 axis in cancer and its implication for treatment resistance. Cancer Res 2013;73:160–71.
[86] Zheng L, Terman A, Hallbeck M, et al. Macroautophagy-generated increase of lysosomal amyloid beta-protein mediates oxidant-induced apoptosis of cultured neuroblastoma cells. Autophagy 2011;7:1528–45.
[87] Bao L, Lv L, Feng J, et al. miR-487b-5p regulates temozolomide resistance of lung cancer cells through LAMP2-medicated autophagy. DNA Cell Biol 2016;35:385–92.
[88] Pols MS, Klumperman J. Trafficking and function of the tetraspanin CD63. Exp Cell Res 2009;315:1584–92.
[89] de Saint-Vis B, Vincent J, Vandenabeele S, et al. A novel lysosome-associated membrane glycoprotein, DC-LAMP, induced upon DC maturation, is transiently expressed in MHC class II compartment. Immunity 1998;9:325–36.
[90] Ozaki K, Nagata M, Suzuki M, et al. Isolation and characterization of a novel human lung-specific gene homologous to lysosomal membrane glycoproteins 1 and 2: significantly increased expression in cancers of various tissues. Cancer Res 1998;58:3499–503.
[91] Salaun B, de Saint-Vis B, Pacheco N, et al. CD208/dendritic cell-lysosomal associated membrane protein is a marker of normal and transformed type II pneumocytes. Am J Pathol 2004;164:861–71.
[92] Mason RJ, Williams MC. Type II alveolar cell. Defender of the alveolus. Am Rev Respir Dis 1977;115:81–91.
[93] Fehrenbach H. Alveolar epithelial type II cell: defender of the alveolus revisited. Respir Res 2001;2:33–46.
[94] Cunningham AC, Milne DS, Wilkes J, Dark JH, Tetley TD, Kirby JA. Constitutive expression of MHC and adhesion molecules by alveolar epithelial cells (type II pneumocytes) isolated from human lung and comparison with immunocytochemical findings. J Cell Sci 1994;107:443–9.
[95] Nagelkerke A, Bussink J, Mujcic H, et al. Hypoxia stimulates migration of breast cancer cells via the PERK/ATF4/LAMP3-arm of the unfolded protein response. Breast Cancer Res 2013;15:R2.
[96] Mujcic H, Nagelkerke A, Rouschop KM, et al. Hypoxic activation of the PERK/eIF2alpha arm of the unfolded protein response promotes metastasis through induction of LAMP3. Clin Cancer Res 2013;19:6126–37.
[97] Dominguez-Bautista JA, Klinkenberg M, Brehm N, et al. Loss of lysosome-associated membrane protein 3 (LAMP3) enhances cellular vulnerability against proteasomal inhibition. Eur J Cell Biol 2015;94:148–61.
[98] International Parkinson Disease Genomics C, Nalls MA, Plagnol V, et al. Imputation of sequence variants for identification of genetic risks for Parkinson's disease: a meta-analysis of genome-wide association studies. Lancet 2011;377:641–6649.
[99] Lill CM, Roehr JT, McQueen MB, et al. Comprehensive research synopsis and systematic meta-analyses in Parkinson's disease genetics: the PDGene database. PLoS Genet 2012;8:e1002548.
[100] Mohty M, Vialle-Castellano A, Nunes JA, Isnardon D, Olive D, Gaugler B. IFN-alpha skews monocyte differentiation into Toll-like receptor 7-expressing dendritic cells with potent functional activities. J Immunol 2003;171:3385–93.
[101] Mine KL, Shulzhenko N, Yambartsev A, et al. Gene network reconstruction reveals cell cycle and antiviral genes as major drivers of cervical cancer. Nat Commun 2013;4:1806.
[102] Zhou Z, Xue Q, Wan Y, Yang Y, Wang J, Hung T. Lysosome-associated membrane glycoprotein 3 is involved in influenza A virus replication in human lung epithelial (A549) cells. Virol J 2011;8:384.
[103] Ignatius Irudayam J, Contreras D, Spurka L, et al. Characterization of type I interferon pathway during hepatic differentiation of human pluripotent stem cells and hepatitis C virus infection. Stem Cell Res 2015;15:354–64.
[104] Nagelkerke A, Mujcic H, Bussink J, et al. Hypoxic regulation and prognostic value of LAMP3 expression in breast cancer. Cancer 2011;117:3670–81.
[105] Sun R, Wang X, Zhu H, et al. Prognostic value of LAMP3 and TP53 overexpression in benign and malignant gastrointestinal tissues. Oncotarget 2014;5:12398–3409.
[106] Kanao H, Enomoto T, Kimura T, et al. Overexpression of LAMP3/TSC403/DC-LAMP promotes metastasis in uterine cervical cancer. Cancer Res 2005;65:8640–5.
[107] Qiu X, You Y, Huang J, Wang X, Zhu H, Wang Z. LAMP3 and TP53 overexpression predicts poor outcome in laryngeal squamous cell carcinoma. Int J Clin Exp Pathol 2015;8:5519–27.
[108] Liao X, Chen Y, Liu D, Li F, Li X, Jia W. High expression of LAMP3 is a novel biomarker of poor prognosis in patients with esophageal squamous cell carcinoma. Int J Mol Sci 2015;16:17655–67.
[109] Racz A, Brass N, Heckel D, Pahl S, Remberger K, Meese E. Expression analysis of genes at 3q26-q27 involved in frequent amplification in squamous cell lung carcinoma. Eur J Cancer 1999;35:641–6.
[110] Nagelkerke A, Sweep FC, Stegeman H, et al. Hypoxic regulation of the PERK/ATF4/LAMP3-arm of the unfolded protein response in head and neck squamous cell carcinoma. Head Neck 2015;37:896–905.
[111] Mowers EE, Sharifi MN, Macleod KF. Autophagy in cancer metastasis. Oncogene 2017;36:1619-–1630.
[112] Nagelkerke A, Sieuwerts AM, Bussink J, et al. LAMP3 is involved in tamoxifen resistance in breast cancer cells through the modulation of autophagy. Endocr Relat Cancer 2014;21:101–12.
[113] Lindskog C, Fagerberg L, Hallstrom B, et al. The lung-specific proteome defined by integration of transcriptomics and antibody-based profiling. FASEB J 2014;28:5184–96.
[114] Nagelkerke A, Bussink J, van der Kogel AJ, Sweep FC, Span PN. The PERK/ATF4/LAMP3-arm of the unfolded protein response affects radioresistance by interfering with the DNA damage response. Radiother Oncol 2013;108:415–21.
[115] Pennati M, Lopergolo A, Profumo V, et al. miR-205 impairs the autophagic flux and enhances cisplatin cytotoxicity in castration-resistant prostate cancer cells. Biochem Pharmacol 2014;87:579–97.
[116] Holohan C, Van Schaeybroeck S, Longley DB, Johnston PG. Cancer drug resistance: an evolving paradigm. Nat Rev Cancer 2013;13:714–26.
[117] Bisio A, Zamborszky J, Zaccara S, et al. Cooperative interactions between p53 and NFkappaB enhance cell plasticity. Oncotarget 2014;5:12111–25.
[118] Movassagh M, Spatz A, Davoust J, et al. Selective accumulation of mature DC-Lamp+ dendritic cells in tumor sites is associated with efficient T-cell-mediated antitumor response and control of metastatic dissemination in melanoma. Cancer Res 2004;64:2192–8.
[119] Holness CL, da Silva RP, Fawcett J, Gordon S, Simmons DL. Macrosialin, a mouse macrophage-restricted glycoprotein, is a member of the lamp/lgp family. J Biol Chem 1993;268:9661–6.
[120] Kostich M, Fire A, Fambrough DM. Identification and molecular-genetic characterization of a LAMP/CD68-like protein from Caenorhabditis elegans. J Cell Sci 2000;113:2595–606.
[121] Kurushima H, Ramprasad M, Kondratenko N, Foster DM, Quehenberger O, Steinberg D. Surface expression and rapid internalization of macrosialin (mouse CD68) on elicited mouse peritoneal macrophages. J Leukocy Biol 2000;67:104–8.
[122] Graeber MB, Streit WJ, Kiefer R, Schoen SW, Kreutzberg GW. New expression of myelomonocytic antigens by microglia and perivascular cells following lethal motor neuron injury. J Neuroimmunol 1990;27:121–32.
[123] Tomita M, Yamamoto K, Kobashi H, Ohmoto M, Tsuji T. Immunohistochemical phenotyping of liver macrophages in normal and diseased human liver. Hepatology 1994;20:317–25.
[124] Athanasou NA, Puddle B, Quinn J, Woods CG. Use of monoclonal antibodies to recognise osteoclasts in routinely processed bone biopsy specimens. J Clin Pathol 1991;44:664–6.
[125] Ramprasad MP, Fischer W, Witztum JL, Sambrano GR, Quehenberger O, Steinberg D. The 94- to 97-kDa mouse macrophage membrane protein that recognizes oxidized low density lipoprotein and phosphatidylserine-rich liposomes is identical to macrosialin, the mouse homologue of human CD68. Proc Natl Acad Sci U S A 1995;92:9580–4.
[126] de Beer MC, Zhao Z, Webb NR, van der Westhuyzen DR, de Villiers WJ. Lack of a direct role for macrosialin in oxidized LDL metabolism. J Lipid Res 2003;44:674–85.
[127] Song L, Lee C, Schindler C. Deletion of the murine scavenger receptor CD68. J Lipid Res 2011;52:1542–50.
[128] Gough PJ, Gordon S, Greaves DR. The use of human CD68 transcriptional regulatory sequences to direct high-level expression of class A scavenger receptor in macrophages in vitro and in vivo. Immunology 2001;103:351–61.
[129] Gough PJ, Raines EW. Gene therapy of apolipoprotein E-deficient mice using a novel macrophage-specific retroviral vector. Blood 2003;101:485–91.
[130] Kunisch E, Fuhrmann R, Roth A, Winter R, Lungershausen W, Kinne RW. Macrophage specificity of three anti-CD68 monoclonal antibodies (KP1, EBM11, and PGM1) widely used for immunohistochemistry and flow cytometry. Ann Rehum Dis 2004;63:774–84.
[131] Gottfried E, Kunz-Schughart LA, Weber A, et al. Expression of CD68 in non-myeloid cell types. Scand J Immunol 2008;67:453–63.
[132] Boyce BF, Yao Z, Xing L. Osteoclasts have multiple roles in bone in addition to bone resorption. Crit Rev Eukaryot Gene Expr 2009;19:171–80.
[133] Ashley JW, Shi Z, Zhao H, Li X, Kesterson RA, Feng X. Genetic ablation of CD68 results in mice with increased bone and dysfunctional osteoclasts. PLoS One 2011;6:e25838.
[134] Liu C, Tao Q, Sun M, et al. Kupffer cells are associated with apoptosis, inflammation and fibrotic effects in hepatic fibrosis in rats. Lab Invest 2010;90:1805–16.
[135] Makitie T, Summanen P, Tarkkanen A, Kivela T. Tumor-infiltrating macrophages (CD68(+) cells) and prognosis in malignant uveal melanoma. Invest Ophthalmol Vis Sci 2001;42:1414–21.
[136] Foss AJ, Alexander RA, Jefferies LW, Hungerford JL, Harris AL, Lightman S. Microvessel count predicts survival in uveal melanoma. Cancer Res 1996;56:2900–3.
[137] Sanchez-Espiridion B, Martin-Moreno AM, Montalban C, et al. Immunohistochemical markers for tumor associated macrophages and survival in advanced classical Hodgkin's lymphoma. Haematologica 2012;97:1080–4.
[138] Ryder M, Ghossein RA, Ricarte-Filho JC, Knauf JA, Fagin JA. Increased density of tumor-associated macrophages is associated with decreased survival in advanced thyroid cancer. Endocr Relat Cancer 2008;15:1069–74.

[139] Wang J, Chen H, Chen X, Lin H. Expression of tumor-related macrophages and cytokines after surgery of triple-negative breast cancer patients and its implications. Med Sci Monit 2016;22:115–20.
[140] Steidl C, Lee T, Shah SP, et al. Tumor-associated macrophages and survival in classic Hodgkin's lymphoma. N Engl J Med 2010;362:875–85.
[141] Kim DW, Min HS, Lee KH, et al. High tumour islet macrophage infiltration correlates with improved patient survival but not with EGFR mutations, gene copy number or protein expression in resected non-small cell lung cancer. Br J Cancer 2008;98:1118–24.
[142] Li J, Zhang BZ, Qin YR, et al. CD68 and interleukin 13, prospective immune markers for esophageal squamous cell carcinoma prognosis prediction. Oncotarget 2016;7:15525-–15538.
[143] Chistiakov DA, Killingsworth MC, Myasoedova VA, Orekhov AN, Bobryshev YV. CD68/macrosialin: not just a histochemical marker. Lab Invest 2017;97:4–13.
[144] Pollard JW. Tumour-educated macrophages promote tumour progression and metastasis. Nat Rev Cancer 2004;4:71–8.
[145] Allavena P, Mantovani A. Immunology in the clinic review series; focus on cancer: tumour-associated macrophages: undisputed stars of the inflammatory tumour microenvironment. Clin Exp Immunol 2012;167:195–205.
[146] Noy R, Pollard JW. Tumor-associated macrophages: from mechanisms to therapy. Immunity 2014;41:49–61.
[147] Takeya M, Komohara Y. Role of tumor-associated macrophages in human malignancies: friend or foe? Pathol Int 2016;66:491–505.
[148] Strojnik T, Kavalar R, Zajc I, Diamandis EP, Oikonomopoulou K, Lah TT. Prognostic impact of CD68 and kallikrein 6 in human glioma. Anticancer Res 2009;29:3269–79.
[149] Shabo I, Svanvik J. Expression of macrophage antigens by tumor cells. Adv Exp Med Biol 2011;714:141–50.
[150] Maniecki MB, Etzerodt A, Ulhoi BP, et al. Tumor-promoting macrophages induce the expression of the macrophage-specific receptor CD163 in malignant cells. Int J Cancer 2012;131:2320–31.
[151] Steinert G, Scholch S, Niemietz T, et al. Immune escape and survival mechanisms in circulating tumor cells of colorectal cancer. Cancer Res 2014;74:1694–704.
[152] Shabo I, Midtbo K, Andersson H, et al. Macrophage traits in cancer cells are induced by macrophage-cancer cell fusion and cannot be explained by cellular interaction. BMC Cancer 2015;15:922.
[153] Hassani K, Olivier M. Immunomodulatory impact of leishmania-induced macrophage exosomes: a comparative proteomic and functional analysis. PLoS Negl Trop Dis 2013;7:e2185.
[154] Schuske K, Palfreyman MT, Watanabe S, Jorgensen EM. UNC-46 is required for trafficking of the vesicular GABA transporter. Nature Neurosci 2007;10:846–53.
[155] Defays A, David A, de Gassart A, et al. BAD-LAMP is a novel biomarker of nonactivated human plasmacytoid dendritic cells. Blood 2011;118:609–17.
[156] Lee J, Sohn I, Do IG, et al. Nanostring-based multigene assay to predict recurrence for gastric cancer patients after surgery. PLoS One 2014;9:e90133.
[157] Brodbeck T, Nehmann N, Bethge A, Wedemann G, Schumacher U. Perforin-dependent direct cytotoxicity in natural killer cells induces considerable knockdown of spontaneous lung metastases and computer modelling-proven tumor cell dormancy in a HT29 human colon cancer xenograft mouse model. Molec Cancer 2014;13:244.
[158] Barois N, de Saint-Vis B, Lebecque S, Geuze HJ, Kleijmeer MJ. MHC class II compartments in human dendritic cells undergo profound structural changes upon activation. Traffic 2002;3:894–905.
[159] Thibodeau J, Bourgeois-Daigneault MC, Lapointe R. Targeting the MHC Class II antigen presentation pathway in cancer immunotherapy. Oncoimmunology 2012;1:908–16.

Oncogene
https://doi.org/10.1038/s41388-018-0234-z

ARTICLE

Histone deacetylase 6 controls Notch3 trafficking and degradation in T-cell acute lymphoblastic leukemia cells

Marica Pinazza[1] · Margherita Ghisi[2,5] · Sonia Minuzzo[2] · Valentina Agnusdei[1] · Gianluca Fossati[3] · Vincenzo Ciminale[1,2] · Laura Pezzè[4] · Yari Ciribilli[4] · Giorgia Pilotto[2] · Carolina Venturoli[1] · Alberto Amadori[1,2] · Stefano Indraccolo[1]

Received: 7 August 2017 / Revised: 30 December 2017 / Accepted: 18 February 2018

Abstract

Several studies have revealed that endosomal sorting controls the steady-state levels of Notch at the cell surface in normal cells and prevents its inappropriate activation in the absence of ligands. However, whether this highly dynamic physiologic process can be exploited to counteract dysregulated Notch signaling in cancer cells remains unknown. T-ALL is a malignancy characterized by aberrant Notch signaling, sustained by activating mutations in Notch1 as well as overexpression of Notch3, a Notch paralog physiologically subjected to lysosome-dependent degradation in human cancer cells. Here we show that treatment with the pan-HDAC inhibitor Trichostatin A (TSA) strongly decreases Notch3 full-length protein levels in T-ALL cell lines and primary human T-ALL cells xenografted in mice without substantially reducing *NOTCH3* mRNA levels. Moreover, TSA markedly reduced the levels of Notch target genes, including *pTα*, *CR2*, and *DTX-1*, and induced apoptosis of T-ALL cells. We further observed that Notch3 was post-translationally regulated following TSA treatment, with reduced Notch3 surface levels and increased accumulation of Notch3 protein in the lysosomal compartment. Surface Notch3 levels were rescued by inhibition of dynein with ciliobrevin D. Pharmacologic studies with HDAC1, 6, and 8-specific inhibitors disclosed that these effects were largely due to inhibition of HDAC6 in T-ALL cells. HDAC6 silencing by specific shRNA was followed by reduced Notch3 expression and increased apoptosis of T-ALL cells. Finally, HDAC6 silencing impaired leukemia outgrowth in mice, associated with reduction of Notch3 full-length protein in vivo. These results connect HDAC6 activity to regulation of total and surface Notch3 levels and suggest HDAC6 as a potential novel therapeutic target to lower Notch signaling in T-ALL and other Notch3-addicted tumors.

Introduction

T-cell acute lymphoblastic leukemia (T-ALL) is a malignancy of T lymphocytes precursors characterized by a relatively unfavorable prognosis compared to B-cell ALL [1]. Molecular studies uncovered that T-ALL is a disease frequently driven by activating mutations of Notch1, which are found in more than 50% of cases [2]. Although Notch3 mutations are uncommon in patients, Notch3 overexpression is often observed in human T-ALL. Moreover, enforced expression of the active intracellular domain of Notch3 (Notch3-ICD) has been reported to cause T-cell leukemia in mouse models [3, 4]. Given some limitations of existing drugs blocking Notch signaling [5], it is important to get new insights into the biology of Notch3 to further stimulate the development of Notch-targeted therapies in cancer.

Electronic supplementary material The online version of this article (https://doi.org/10.1038/s41388-018-0234-z) contains supplementary material, which is available to authorized users.

✉ Stefano Indraccolo
stefano.indraccolo@unipd.it

[1] Istituto Oncologico Veneto IOV—IRCCS, Padova, Italy

[2] Department of Surgery, Oncology and Gastroenterological Sciences, University of Padova, Padova, Italy

[3] Italfarmaco S.P.A, Milan, Italy

[4] Laboratory of Molecular Cancer Genetics, CIBIO, University of Trento, Trento, Italy

[5] Present address: CRCT, Toulouse, France

Published online: 12 April 2018

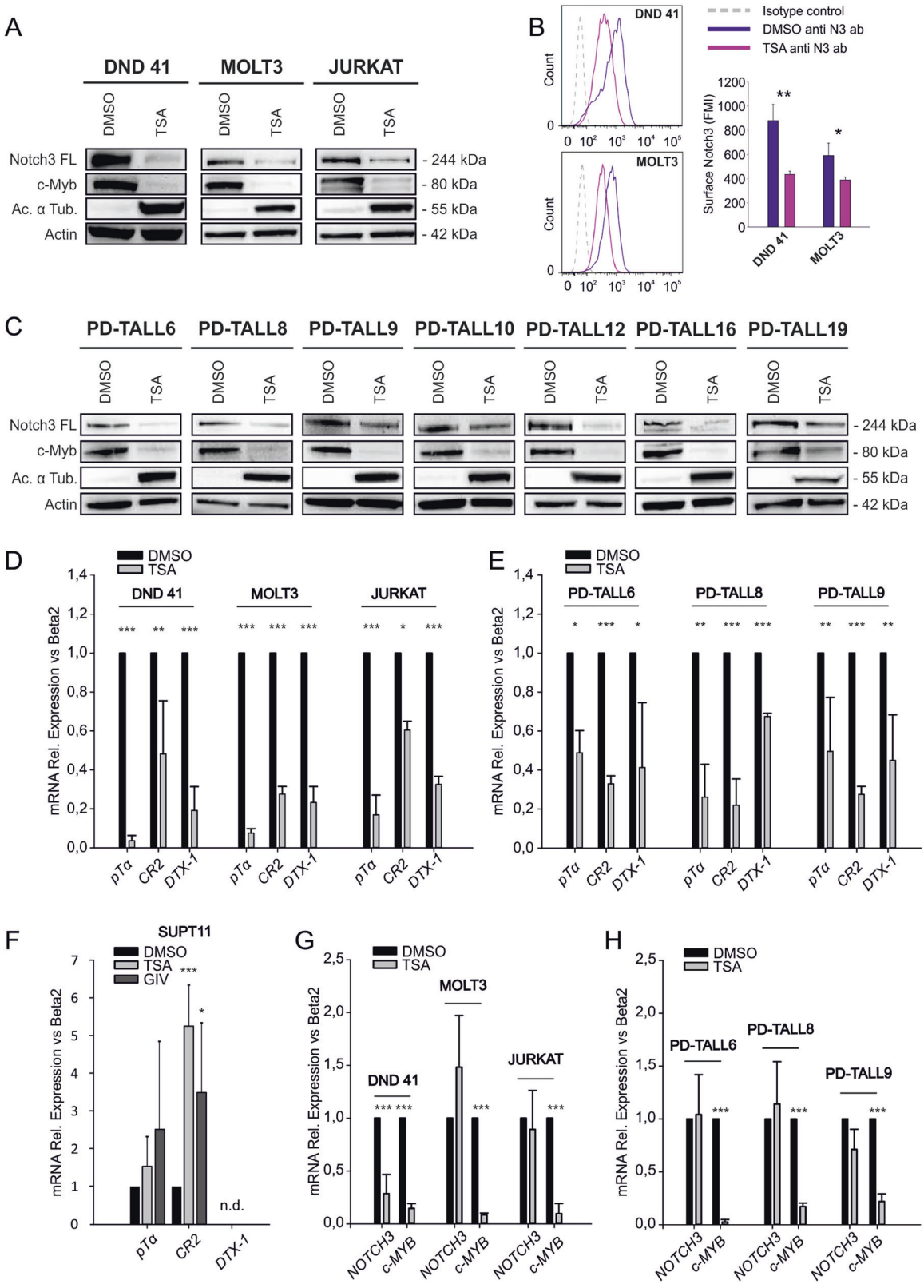

Several studies disclosed that ubiquitination and endocytosis regulate activity of both Notch and its ligands [6]. In Drosophila, Notch proteolytic processing is facilitated by dynamin-dependent endocytosis of Notch in the signal-receiving cell [7], with the contribution of the syntaxin Avalanche and the Rab5 GTPase [8]. Activated Notch,

together with Notch ligands and non-activated Notch, is subsequently internalized and channeled into early sorting endosomes. In flies, E3 ubiquitin ligases including Nedd4 and Su(dx) sort unstimulated Notch into an endosomal compartment destined for recycling and/or degradation [9]. Steady-state levels of Notch at the surface and pathway activity are modulated by this internalization process, which also limits inappropriate activation of the receptor in the absence of ligands [9]. In fact, trafficking of activated Notch into late endosomal compartments, including multivesicular bodies and degradative lysosomes, is associated with attenuation of Notch signaling [10]. In this regard, Jia et al. [11] reported that Notch3 full-length (FL) and Notch3-ICD are subjected to lysosome-dependent degradation in human cancer cells, suggesting a role of endocytosis in Notch3 degradation and signaling.

Histone deacetylases (HDACs) catalyze epigenetic regulation of chromatin promoting repression of gene expression, and also deacetylate a number of non-histone proteins, thus modulating their function [12]. Unlike other HDACs with predominant chromatin remodeling activity, HDAC6 main targets are cytoplasmic proteins, such as α-tubulin, Hsp90, and cortactin. In particular, HDAC6 inhibition determines increased acetylation of α-tubulin, thus accelerating the association of microtubules with dynein and kinesin and leading to increased routing into early endosomes [13]. Along this line, it was described that epidermal growth factor receptor (EGFR) surface levels are regulated by endocytic trafficking through a mechanism involving HDAC6 and tubulin acetylation [14, 15]. Altogether, these findings support a regulatory role for HDAC6 in endocytic cargo transport of certain transmembrane receptors but whether this might modulate expression of Notch is unknown.

Here, we investigated effects of HDAC inhibitors (HDACi) in T-ALL and found that pharmacologic or genetic inactivation of HDAC6 is followed by increased lysosomal localization of Notch3, which correlates with a reduction in signaling strength. These findings suggest that, in addition to well established approaches such as blocking antibodies and γ-secretase inhibitors [5], targeting HDAC6 is a potential novel strategy to lower Notch3 signaling in T-ALL cells.

Results

Trichostatin A downregulates Notch3 protein levels in T-ALL cells

Previous studies demonstrated that acetylation regulates Notch3-ICD stability in Notch3 transgenic mice and in one human T-ALL cell line [16]. To validate and broaden these findings, we initially investigated the effects of HDACi on Notch3 in T-ALL cells treated in vitro with the pan-HDAC inhibitor Trichostatin A (TSA) at 0.5 μM, a concentration selected on the basis of published data [16, 17]. After 16 h of treatment, whole-cell lysates were extracted and analyzed by western blot. Accumulation of acetylated α-tubulin and reduction of c-Myb, two known targets of HDACi [17], were used as read-out of TSA activity in these experiments. Interestingly, TSA decreased Notch3 FL levels in all the three cell lines tested (Fig. 1a); Notch3-ICD levels were also reduced (not shown). Following staining with an anti-human Notch3 antibody which binds an extracellular epitope of Notch3, flow cytometry analysis indicated that TSA treatment was followed by reduction of Notch3 surface levels in DND 41 and MOLT3 cells (Fig. 1b). To confirm the results obtained in cell lines, we treated T-ALL cells from several patient-derived xenografts (PDX) with distinct molecular and clinical phenotypes [18]. After 16 h of treatment, Notch3 FL and c-Myb protein levels were strongly reduced in all samples analyzed (Fig. 1c). Importantly, TSA decreased expression of the Notch target genes p*Tα, CR2*, and *DTX-1*, thus suggesting reduction of Notch signaling (Fig. 1d, e), induced apoptosis, and inhibited proliferation of T-ALL cells (Suppl. Figure 1). Effects of TSA on Notch3 levels and signaling were confirmed using the pan-HDAC inhibitor Givinostat, which is currently used in clinical trials (Suppl. Figure 2). Notably, we found no reduction of *pTα* and *CR2* levels in the SUPT11 cell line treated with panHDACi TSA or with Givinostat (Fig. 1f), indicating that HDAC inhibition fails to reduce Notch signaling in cells which do not express detectable Notch3 [19].

To investigate whether these effects were associated with inhibition of transcription, we analyzed mRNA levels of

Fig. 1 HDAC inhibition reduces Notch3 levels and signaling in T-ALL cells. **a** T-ALL cells (DND 41, MOLT3, and Jurkat) were treated with TSA (0.5 μM) or solvent (DMSO) for 16 h and protein levels analyzed by western blot. Actin was used as a loading control and tubulin acetylation and c-Myb levels as markers of HDAC inhibition. **b** TSA reduces Notch3 surface expression in T-ALL cells. DND 41 and MOLT3 cells treated with TSA or DMSO for 16 h were stained with PE anti-human Notch3 (anti-N3 Ab) or with isotype control antibody and analyzed by flow cytometry. One representative experiment of three performed is shown. Histogram reports fluorescence mean intensity (FMI) ± SD of three independent experiments (**$P < 0.01$; *$P < 0.05$). **c** TSA reduces Notch3 expression in PDX-derived T-ALL cells. T-ALL cells obtained from the spleen of xenografted mice were treated in vitro with TSA for 16 h and protein levels were analyzed by western blot. **d-h** Effects of TSA on Notch3 target genes and on Notch transcript levels. T-ALL samples, including both cell lines (**d, f, g**) and PDX T-ALL cells (**e**, **h**), were treated with TSA or Givinostat (GIV) (2 μM) for 16 h and mRNA levels of *NOTCH3, c-MYB*, or Notch target transcripts (*pTα, CR2, DTX-1*) were analyzed by qRT-PCR. n.d.: not detectable. Statistically significant differences are indicated (*$P < 0.05$, **$P < 0.01$, ***$P < 0.001$, mean ± SD of three independent experiments). Expression data are normalized to DMSO samples

NOTCH3 and *c-MYB* upon TSA treatment. Interestingly, *c-MYB* mRNA displayed >80% reduction in all samples tested. In contrast, *NOTCH3* transcripts were reduced in DND 41 but not in MOLT3 nor in Jurkat cells (Fig. 1g). Similar results were obtained in three PDX samples (PD-TALL6, PD-TALL8, and PD-TALL9) (Fig. 1h). Altogether, these results indicate that TSA regulates Notch3 expression mainly at post-transcriptional level in the majority of the T-ALL samples analyzed.

Lysosomal degradation accounts for reduced Notch3 levels in T-ALL cells treated with TSA

Several reports indicate that HDACi induce degradation of oncogenes and other cellular proteins by affecting protein stability [20]. To test whether protein degradation has a role in the effects of TSA on Notch3 protein levels, we inhibited protein translation in MOLT3 cells with cycloheximide. As expected, based on the fact that HDACi control c-Myb levels mainly at the transcriptional level (Fig. 1g and [17]), the half-life of c-Myb, roughly 8 h in MOLT3 cells, was not substantially changed by TSA. In contrast, Notch3 protein levels decreased faster in the presence of TSA (Fig. 2a, b). This result shows that TSA affects Notch3 protein stability, implying a post-translational mechanism of regulation. To investigate the molecular mechanism underlying increased Notch degradation, we treated MOLT3 and TALL1 cells with TSA in the presence of proteasome or lysosome inhibitors. Notch3 levels were rescued using the lysosome inhibitor chloroquine (CHL), suggesting involvement of the endocytic pathway. In contrast, the proteasome inhibitor MG132 further reduced Notch3 FL levels (Fig. 2c, d), whereas it increased c-Myc protein levels (Suppl. Figure 3), a transcription factor known to be degraded by the proteasome [21, 22]. Similar results were obtained in MOLT3 cells by using bafilomycin as alternative lysosome inhibitor (Suppl. Figure 4). Moreover, treatment with ciliobrevin D, a dynein inhibitor, rescued Notch3 surface levels upon TSA treatment in MOLT3 cells (Fig. 2e), confirming the importance of tubulin acetylation and vesicle transport through cytoplasmic dynein of Notch3 from the cell membrane to the lysosome. In addition, immunofluorescence and confocal microscopy analysis confirmed that MOLT3 cells treated with TSA displayed increased co-localization of Notch3 and the lysosomal marker LAMP2 (Fig. 3a–c). Fractionation assays corroborated these findings by showing that Notch3 was mainly enriched in the lysosomal fraction in T-ALL cells and upon TSA treatment there was a significant increase in the lysosome/plasma membrane ratio (Fig. 3d, e and Suppl. Figure 5). Taken together, these findings indicate that HDAC inhibition results in the accumulation of Notch3 in the lysosomal compartment.

HDAC6 modulates Notch3 expression and signaling in vitro

To identify HDAC family member(s) responsible for the effects previously characterized, we tested class-specific HDACi. In particular, we used the HDAC6 inhibitor tubacin, and two HDAC1 and HDAC8 inhibitors. Interestingly, HDAC1i and HDAC8i did not reduce Notch3 FL protein levels or Notch target genes expression and did not exert apoptotic effects in T-ALL cell lines and PDX cells (Fig. 4). On the contrary, the HDAC6-specific inhibitor tubacin reproduced effects of TSA, including reduction of Notch3 surface levels (Fig. 4), suggesting a role of this specific HDAC in the phenomenon observed. To verify activity of these compounds, we also analyzed histone 3 acetylation levels in MOLT3 and Jurkat cells. As expected, tubacin did not change histone acetylation, whereas treatment with HDAC1 and HDAC8 inhibitors increased histone 3 acetylation (Suppl. Figure 6).

Finally, HDAC6 silencing by two different shRNA in MOLT3 and TALL1 cells was followed by reduced Notch3 FL protein levels (Fig. 5a–c) and induced apoptosis in T-ALL cells (Fig. 5d), thus mimicking effects obtained with tubacin and TSA. Apoptosis induction was not observed in SUPT11 cells, which lack detectable Notch3 (Fig. 5d). Interestingly, HDAC6-mediated regulation of Notch3 FL protein seems specific for this NOTCH paralog, since HDAC6 silencing did not reduce Notch1 FL levels in MOLT3 cells (Suppl. Fig. 7).

Givinostat and HDAC6 silencing impair Notch3 expression and leukemia growth in vivo

To investigate whether modulation of Notch3 following treatment with an HDACi occurred in vivo, we treated PD-TALL12 xenografted NOD/SCID mice ($n = 5/6$ per group) with Givinostat (25 mg/kg), a panHDACi used in clinical trials, or PEG400/H_20 (vehicle). The drug was administered as a single dose upon establishment of the leukemia in the mice and animals were killed 16 h after treatment (Fig. 6a). At the time of administration of the drug, spleen and bone marrow (BM) infiltration by T-ALL cells was very high and comparable between treated and untreated mice (Suppl. Fig. 8A, B). Western blot analysis of T-ALL cells from the spleen of Givinostat-treated mice or controls showed significantly decreased Notch3 FL protein levels (Fig. 6b, c). Although survival was not an endpoint of this experiment, in our previous study we found that repeated Givinostat administration can extend survival of mice engrafted with PD-TALL12 cells [23].

Pharmacologic issues, in particular the low solubility of tubacin, prevented us from performing this experiment in mice. Therefore, we investigated whether genetic HDAC6

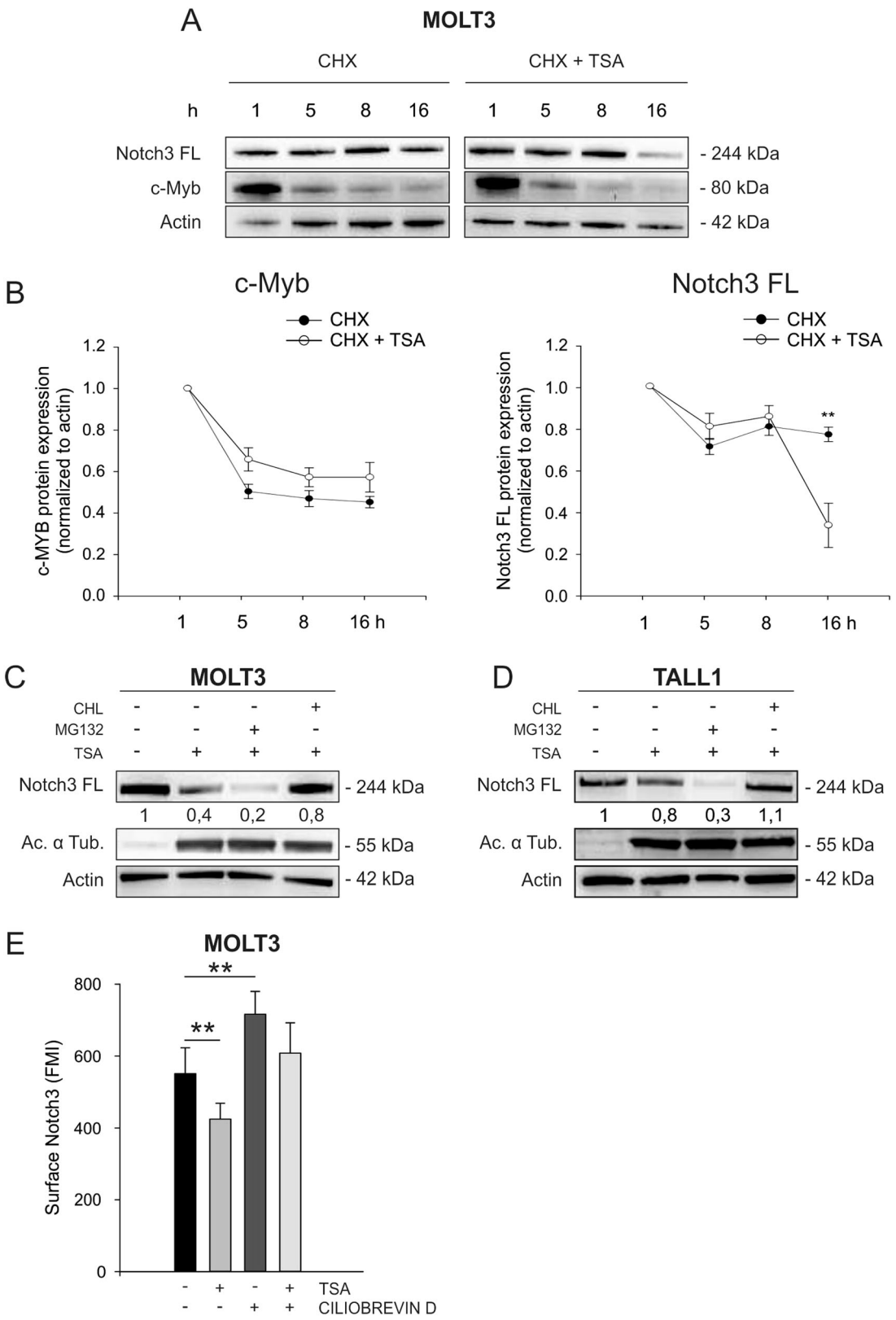
A
MOLT3
CHX
CHX + TSA
h
1
5
8
16
1
5
8
16
Notch3 FL
c-Myb
Actin
- 244 kDa
- 80 kDa
- 42 kDa
B
c-Myb
CHX
CHX + TSA
c-MYB protein expression (normalized to actin)
1.2
1.0
0.8
0.6
0.4
0.2
0.0
1
5
8
16 h
Notch3 FL
CHX
CHX + TSA
Notch3 FL protein expression (normalized to actin)
**
C
MOLT3
CHL
MG132
TSA
Notch3 FL
- 244 kDa
1
0,4
0,2
0,8
Ac. α Tub.
- 55 kDa
Actin
- 42 kDa
D
TALL1
CHL
MG132
TSA
Notch3 FL
- 244 kDa
1
0,8
0,3
1,1
Ac. α Tub.
- 55 kDa
Actin
- 42 kDa
E
MOLT3
**
**
Surface Notch3 (FMI)
800
600
400
200
0
TSA
CILIOBREVIN D

◀ **Fig. 2** HDAC inhibition promotes Notch3 degradation through the lysosomal pathway. **a** MOLT3 cells were treated with cyclohexymide (CHX, 500 μM) or with CHX plus TSA (0.5 μM). At 1, 5, 8, and 16 h, protein levels of c-Myb and Notch3 FL were analyzed. One representative western blot is reported. **b** c-Myb (left) and Notch3 FL (right) protein expression in three independent experiments was measured by densitometric analysis and normalized to Actin (**$P < 0.01$). MOLT3 (**c**) or TALL1 cell lines (**d**) were treated with TSA plus MG132 (20 μM) or chloroquine (CHL) (20 μM) for 16 h followed by western blot analysis. Numbers indicate results of densitometric analysis of Notch3 FL bands normalized to Actin. (**e**) MOLT3 were pre-treated with ciliobrevin D (20 μM) for 24 h and then with vehicle or TSA (0.5 μM) for 16 h. Cells were stained with PE anti-N3 antibody and analyzed by FACS analysis. Statistically significant differences are indicated (**$P < 0.01$, mean ± SD of three independent experiments)

inactivation would impair tumor growth by HDAC6 silencing in the Notch3-dependent cell line TALL1. To this end, we transduced TALL1 cells with a lentiviral vector encoding the firefly luciferase gene (fLUC), in order to track leukemia progression in vivo by optical imaging. TALL1 fLUC cells were then infected with shRNA or with shHDAC6 #1 and injected in NOD/SCID mice (Fig. 6d). Results show significant reduction in leukemia burden in shHDAC6#1 compared to shRNA mice, measured by optical imaging (Fig. 6e, f). At sacrifice, we measured reduction of human CD7-positive cells in the BM and in the spleen (Fig. 6g), induction of apoptosis (Fig. 6h) and reduction of Notch3 FL protein in the spleen of mice injected with HDAC6-silenced T-ALL cells (Fig. 6i). Overall, these results show that inhibition of HDAC6 activity exerts anti-leukemia effects in mice.

Discussion

Notch is constitutively internalized and it has been proposed that endocytosis modulates Notch signaling both by controlling the amount of surface levels of the receptor and by regulating its activation [24–26]. However, it has been debated whether endocytosis is required for full proteolytic processing of Notch, whereas it seems fundamental to downregulate signaling activity by lowering the potential for Notch interactions with its ligands at the cell surface (reviewed in [27]). Consistent with this model, Notch-signaling defects observed upon disruption of the activity of certain endocytosis-associated molecules, such as clathrin or dynamin [28, 29], may derive from insufficient surface Notch levels rather than selective disruption in receptor internalization. Defects in recycling or in the biosynthetic pathway might be associated with abnormal accumulation of Notch in certain intracellular compartments, such as Golgi [30].

These concepts stemmed from studies carried out in invertebrates, while there is limited information about mechanisms involved in Notch trafficking in human cancer cells, whose dysregulation might perturb Notch homeostasis leading to alterations in signaling. Conversely, interventions on Notch trafficking might represent a new therapeutic strategy to counteract aberrant Notch signaling in cancer.

Here, we describe a novel HDAC-mediated mechanism of regulation of Notch3 involving the lysosomal pathway in T-ALL cells. We report for the first time that HDAC inhibition leads to increased accumulation of Notch3 in lysosomes, reducing total and surface Notch3 levels. Our conclusions are supported by (I) reversion of HDACi effects on Notch3 levels by two different lysosome inhibitors and by blocking dynein function and (II) increased co-localization of Notch3 and the lysosomal marker LAMP2 in T-ALL cells treated with TSA by immunofluorescence studies and fractionation assays. Furthermore, involvement of HDAC6 in the control of Notch3 degradation was shown by both pharmacological inhibition and gene silencing experiments. Our findings are fitting those of previous works that demonstrated increased degradation of EGFR by the endocytic compartment following pharmacologic or genetic inactivation of HDAC6 [14, 15]. In these studies, increased microtubule acetylation accelerated lysosomal accumulation of EGFR-bearing vesicles by an HDAC6-mediated mechanism [14, 15]. We speculate that HDAC6 could also affect Notch3-FL trafficking by indirect mechanisms, namely by modulation of α-tubulin acetylation. This hypothesis stems from the above quoted studies concerning EGFR and the apparent lack of direct interactions between HDAC6 and Notch3 by immunoprecipitation studies (not shown).

Although several studies previously reported pro-apoptotic effects of HDACi in leukemia cells [reviewed in [5]], to our knowledge only one study investigated effects of HDACi on Notch3 levels. Palermo et al. [16] demonstrated that acetylation controls Notch3 stability and function in murine T-ALL cells. In this paper, Notch3-ICD acetylation increased following HDAC1 inhibition, leading to Notch3 increased ubiquitination and proteasome-dependent degradation. However, in our experiments the proteasome inhibitor MG132 did not rescue Notch3 FL degradation, indicating that increased proteosomal degradation does not account for TSA effects on Notch3 FL levels in human T-ALL cells. In fact, MG132 appeared to further reduce Notch3 FL levels when combined with TSA (Fig. 2c, d). Although further studies are needed to understand the molecular basis of this interaction, it has been reported that some proteasome inhibitors interact with dynein and up-regulate endocytosis [31], thus modulating the same biological process as HDAC6 inhibitors. Finally, Notch signaling was not impaired in T-ALL cells following treatment with an HDAC1-specific inhibitor, suggesting

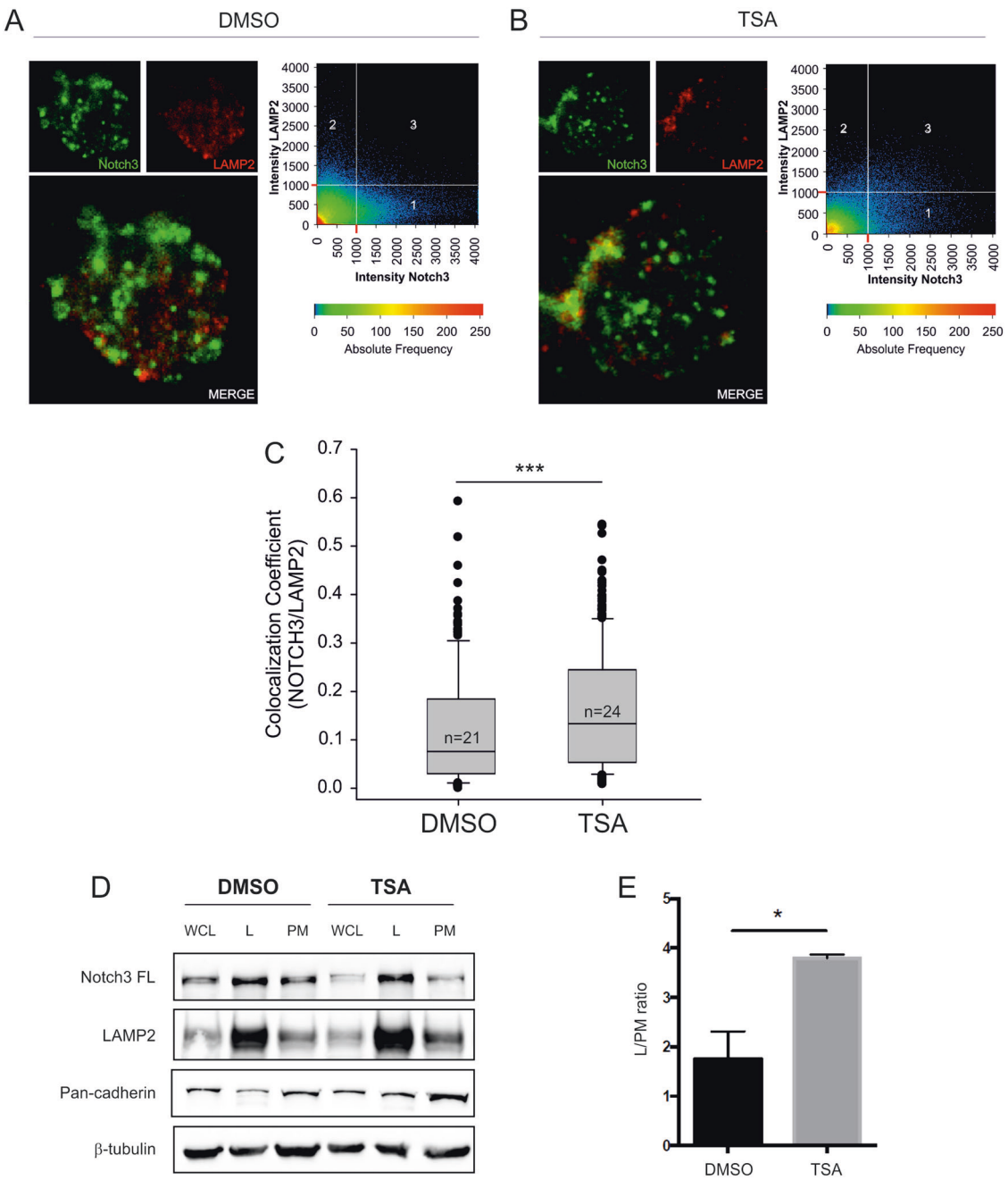

Fig. 3 TSA increases co-localization of Notch3 protein with LAMP2-positive vesicles and increases the abundance of Notch3 FL in the lysosomal compartment. MOLT3 cells were treated with DMSO or TSA (0.5 μM) for 8 h and were subsequently immuno-stained for Notch3 and LAMP2. $n = 21$ DMSO-treated cells and $n = 24$ TSA-treated cells were analyzed by z-stack laser scanning microscopy using a ×63 oil objective. Images were acquired with a resolution of 1024 × 1024 pixels. **a, b** Representative optical slices taken in the apical portion of the cells above the nucleus are shown. Scatterplots on the right-hand portion of the panels indicate the fluorescence intensity of Notch3 (*X*-axis) and LAMP2 (*Y*-axis) detected in each pixel. Detection thresholds were set at 1000 for both channels. Region 1: Notch3 single positive pixels. Region 2: LAMP2 single positive pixels. Region 3 double-positive (Notch3/LAMP2) pixels. **c** Co-localization coefficients were calculated in 21 mock-treated cells and 24 TSA-treated cells using the Zeiss Histogram software tool. At least 15 optical slices were analyzed for each cell. The values of the co-localization coefficients range between 0 and 1. Box plots reported medians, lower/upper quartiles, and outliers of all co-localization coefficients obtained for DMSO and TSA cells respectively. *** indicates $P < 0.001$ (Mann–Whitney test). **d** DND 41 cells were treated with DMSO or TSA (0.5 μM) for 8 h and 1×10^8 pelleted cells underwent subcellular fractionation. Protein extracts for each fraction were analyzed by western blot. A representative blot is reported. WCL whole-cell lysate; L lysosome; PM plasma membrane. **e** Histogram reports the quantified ratio of lysosomal enriched Notch3 FL normalized to Notch3 FL present on the plasma membrane. Expression of Notch3 FL in the different fractions was normalized to each fraction-specific proteins. Mean ± SD of two independent replicates (*$P < 0.05$, Student's *t*-test)

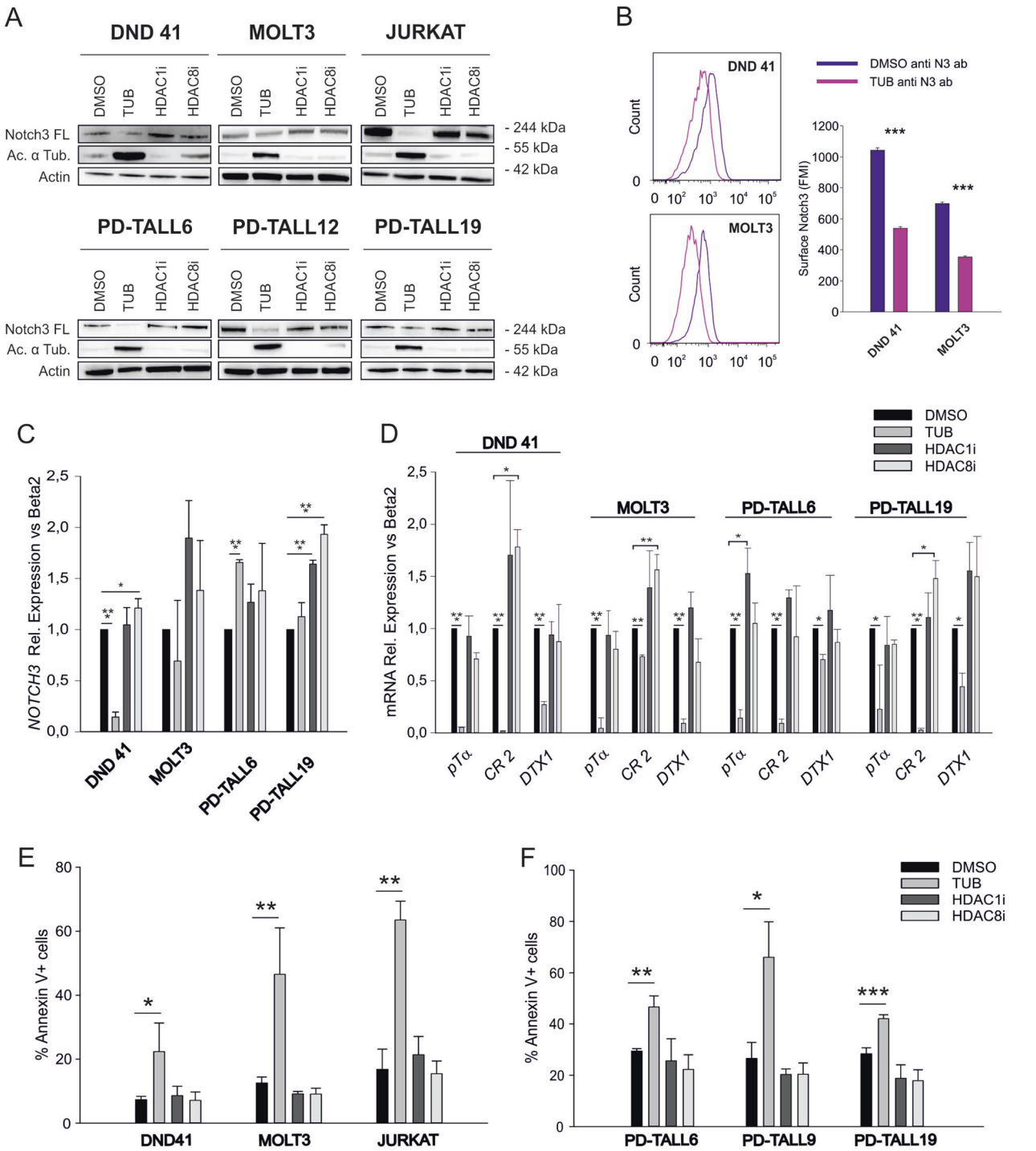

Fig. 4 Pharmacologic inhibition of HDAC6 lowers Notch3 FL protein levels and signaling, triggering apoptosis of T-ALL cells. **a** T-ALL cell lines (up) and PDX T-ALL cells (bottom) were treated in vitro for 16 h with the HDAC6 inhibitor tubacin (TUB, 2 μM), HDAC1 inhibitor (HDAC1i, 2 μM), or HDAC8 inhibitor (HDAC8i, 2 μM). Protein levels were analyzed by western blot. **b** Tubacin reduces Notch3 surface expression in T-ALL cells. DND 41 and MOLT3 cells treated with tubacin (2 μM) or DMSO for 16 h were stained with PE anti-human Notch3 (anti-N3 ab) and analyzed by flow cytometry. One representative experiment of three performed is shown. Histogram reports fluorescence mean intensity (FMI) ± SD of three independent experiments (***$P < 0.001$). Expression levels of *NOTCH3* (**c**) and Notch target genes (**d**) in T-ALL cells treated as above were analyzed by qRT-PCR (*$P < 0.05$, **$P < 0.01$, ***$P < 0.001$, mean ± SD of three independent experiments). Expression data are normalized to DMSO samples. Induction of apoptosis by HDACi in T-ALL cells (**e**) and in PDX cells (**f**) was measured by flow cytometric analysis of Annexin V staining (*$P < 0.05$, **$P < 0.01$, ***$P < 0.001$, mean ± SD of three independent experiments)

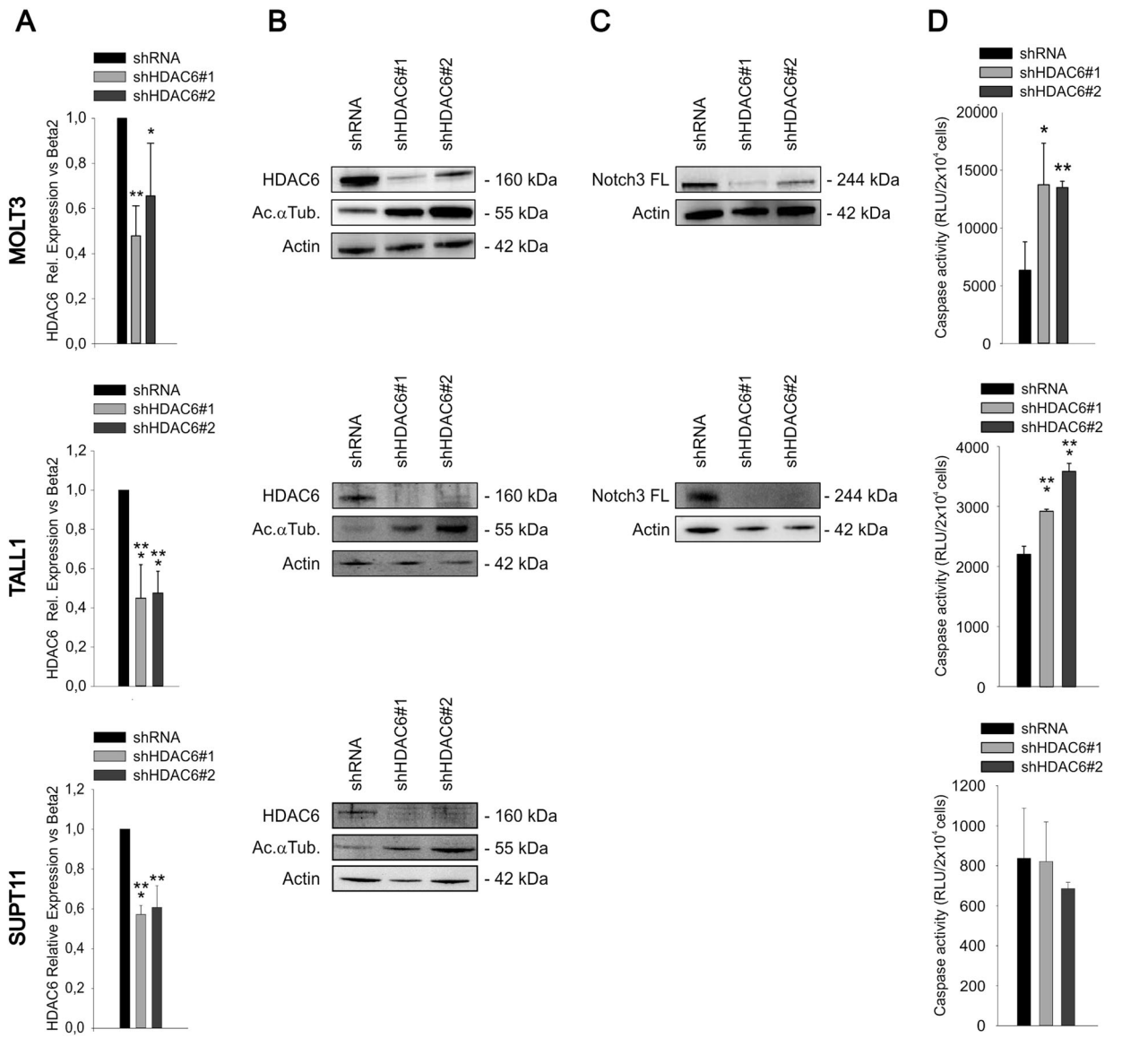

Fig. 5 Effects of HDAC6 silencing on Notch3 FL protein levels and apoptosis of T-ALL cells. MOLT3 (top), TALL1 (middle), or SUPT11 (bottom) cells were transduced with lentiviral vectors encoding a scramble shRNA or two different shHDAC6 vectors. qRT-PCR (**a**) and western blot analysis (**b**) performed 96 h after transduction, confirmed the efficacy of HDAC6 silencing by both constructs. *HDAC6* mRNA levels were normalized setting at one the shRNA sample. **c** MOLT3 or TALL1 cells expressing shHDAC6 #1 or shHDAC6 #2 showed reduced Notch3 FL protein levels. Western blot analysis was not performed in SUPT11 cells as it is known that these cells do not express detectable Notch3 [19]. **d** HDAC6 silencing was associated with increased apoptosis of T-ALL cells which express Notch3, but not in SUPT11 cells. Apoptosis was analyzed by caspase 3–7 assay 5 days after transduction of cells with the indicated LV. Relative Luminescence Units (RLU) are reported (*$P < 0.05$; **$P < 0.01$, ***$P < 0.001$, mean ± SD, three independent experiments)

that the mechanism proposed by Palermo et al. did not explain results obtained in our experiments.

Notably, shRNA against HDAC6 did not reduce Notch1 levels in MOLT3 cells (Suppl. Fig. 7). Although the reason behind this remains unknown, given the similar molecular structure of Notch1 and Notch3, this finding might underscore differential modalities of degradation of Notch1 compared with Notch3 receptors. In this regard, it is established that Notch1 undergoes ubiquitination and subsequent degradation through the proteasome by FBW7/Itch [32]. In contrast, Jia et al. [11] reported that Notch3 FL and intracellular domain are mainly subjected to lysosome-dependent degradation in various tumor cell lines. Thus, alternative routes of intracellular degradation might be involved in turnover of Notch1 and Notch3 receptors. In any case, persisting Notch1 signaling in T-ALL cells undergoing marked attenuation of Notch3 levels could partially rescue expression of Notch target genes following

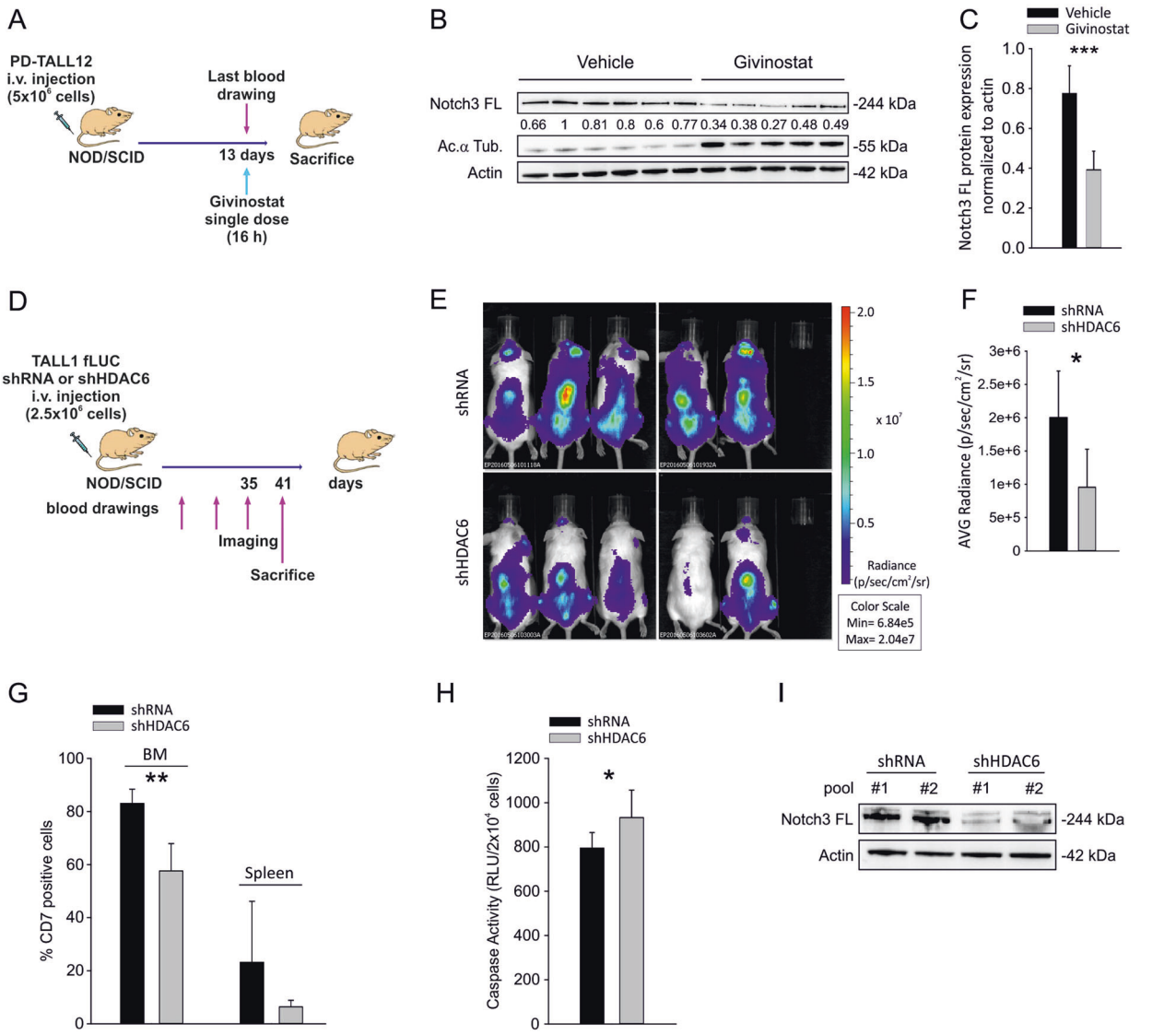

Fig. 6 Pharmacologic or genetic HDAC6 inhibition is associated with reduced Notch3 protein levels in vivo and impaired tumor growth. **a** Outline of treatment. PD-TALL12 xenografted NOD/SCID mice were randomized to receive either Givinostat (25 mg/kg) or vehicle i.p. and sacrificed 16 h after treatment. **b** Leukemic cells were recovered from the spleen of PD-TALL12 mice and Notch3 FL and acetylated α-tubulin protein levels analyzed by WB. Numbers indicate results of densitometric analysis of Notch3 FL bands normalized to Actin. **c** Columns report the mean values ± SD of Notch3 to actin ratios (densitometric analysis) in control and treated mice (***$P < 0.001$). **d** TALL1 cells were serially transduced with a lentiviral vector encoding the Firefly luciferase gene (fLUC) and with lentiviral vectors expressing either a scramble shRNA or an HDAC6-specific shRNA (shHDAC6 #1). Cells were i.v. injected in NOD/SCID mice (2.5×10^6 cells/mouse, $n = 5$ mice/group) and tumor growth was monitored by optical imaging (**e**, **f**). Representative images (**e**) and quantitative analysis (**f**) of luciferase activity at day 35 from TALL1 cells injection. Statistically significant differences in average radiance in the two groups of samples are indicated (*$P < 0.05$, mean ± SD, $n = 5$ mice/group). **g** Flow cytometric analysis of $CD7^+$ cells in the BM and spleen of shRNA and shHDAC6#1 mice at sacrifice (41 days) (**$P < 0.01$, mean ± SD, $n = 5$ mice/group). **h** Apoptosis was analyzed by caspase 3–7 assay in $CD7^+$ cells sorted from the spleen of mice at sacrifice (*$P < 0.05$, mean ± SD, $n = 5$ mice/group). **i** After sorting, T-ALL cells obtained from different mice were pooled and Notch3 FL protein levels analyzed by western blotting

HDAC6 silencing in T-ALL cells, and shield these cells from the negative consequences of Notch signaling blockade, such as apoptosis or cell cycle arrest. Speculatively, treatment with HDAC6i might exert stronger therapeutic effects in tumor cells bearing Notch3 mutations in the absence of Notch1 mutations, such as the TALL1 cell line.

In conclusion, our study disclosed that HDAC6 controls trafficking and lysosomal degradation of Notch3, by a mechanism likely involving acetylation of α-tubulin. Inhibition of HDAC6 with selective drugs may thus represent a new therapeutic approach for Notch3-addicted malignancies.

Materials and methods

In vivo experiments

PDX were established in NOD/SCID mice as previously described [18]. PDX growth was monitored using flow cytometry by testing the % of human CD5 and CD7 in blood as reported elsewhere [18]. In a set of experiments, PDX mice (at least 5 per group) were treated with Givinostat (25 mg/kg) or vehicle (PEG400/H_20) as a single dose upon establishment of the leukemia and mice were euthanized 16 h later.

In another set of experiments, TALL1 cells were serially transduced with luciferase (fLUC) encoding lentiviral vectors expressing either a HDAC6-specific shRNA or a scramble shRNA as a control and their growth in mice was monitored as previously described [33].

Cell lines

MOLT3 and Jurkat cell lines were purchased from ATCC (Manassas, VA, USA); DND 41 and TALL1 cell lines were kindly provided by academic colleagues; SUPT11 cell lines were purchased from DSMZ (Deutsche Sammlung von Mikroorganismen und Zellkulturen GmbH, Braunschweig, Germany); all these cell lines were cultured in complete RPMI medium, as reported elsewhere [33]. Cells were periodically tested for mycoplasma contamination. PDX cells were cultured in MEMα medium (Thermo Fisher Scientific) supplemented with 10% human heat inactivated AB^+ serum, 10% fetal calf serum (FCS), 1% Glutamax, 1% penicillin/streptomycin and with 20 ng/ml FLT3 ligand, 10 ng/ml IL7, 50 ng/ml SCF (Peprotech, Rocky Hill, NJ, USA), and 20 nM human insulin (Sigma Aldrich, Saint Luis, MO, USA).

The following drugs were used: 0.5 μM TSA (Sigma Aldrich), 500 μM cyclohexamide (Sigma Aldrich), 20 μM MG132 (Sigma Aldrich), 20 μM CHL (Sigma Aldrich), 2 μM tubacin (Enzo Life Science, Farmingdale, NY), 100 nM bafilomycin (Sigma Aldrich), 2 μM HDAC1i and HDAC8i (Italfarmaco, Milan, Italy), 20 μM Ciliobrevin D. At planned time points, cells were harvested and processed for assessment of cell viability, caspase assay, and RNA and protein extraction.

Flow cytometry

Detection of PDX cells in mouse samples was carried out with anti-human FITC-conjugated CD5 and PE-Cy5-conjugated CD7 antibodies (Coulter, Fullerton, CA, USA). Apoptosis was measured using Annexin V marker, as reported [23]. Surface Notch3 levels were analyzed using a PE anti-human Notch3 antibody (Biolegend, San Diego, CA, USA). Samples were analyzed on a Beckman Coulter EPICS-XL Flow Cytometer (Coulter) or a BD LSRII Flow Cytometer (BD Biosciences, San Jose, CA, USA).

Transduction with lentiviral vectors

Lentiviral vectors encoding shRNA targeting human HDAC6 (Sigma Aldrich; shHDAC6 #1: TRCN0000314909; shHDAC6 #2: TRCN0000314976) or the control shRNA vector were produced and titrated as previously reported [34].

Reverse transcription-PCR and quantitative PCR (qPCR)

Total RNA was purified by standard procedures as reported elsewhere [23]. Quantitative PCRs of cDNAs were performed with an ABI Prism 7900HT Sequencer (Thermo Fisher Scientific), as described [23]. Primer sequences are shown in Suppl. Table 1.

Immunoblot analysis

Western blot protocols have been previously published [23]. Immunoprobing was performed using the following antibodies: mouse anti-acetylated α-tubulin (Santa Cruz Biotechnologies, Dallas, TX, USA), rabbit anti-actin (Sigma Aldrich), rabbit anti-Notch3 (Abcam, Cambridge, UK), rabbit anti-Notch1 (Cell Signaling), mouse anti-c-Myb (Thermo Fisher Scientific), rabbit anti-HDAC6 (Santa Cruz Biotechnologies), rabbit anti-Histone H3 (Cell Signaling or Abcam), rabbit anti-acetyl-Histone H3 (Lys 9) (Cell Signaling), mouse anti-LAMP2 (Novus Biologicals, Littleton, CO, USA), mouse anti-Pan-cadherin (Santa Cruz Biotechnologies), mouse anti-GAPDH (Santa Cruz Biotechnologies), rabbit anti-VDAC (Cell Signaling) followed by incubation with a horseradish peroxidase-conjugated anti-rabbit or anti-mouse secondary Ab (Perkin Elmer, Waltham, MA, USA). Antigens were identified using Western Lightning plus ECL (Perkin Elmer) or ECL Select Western Blotting detection (GE Health Care) reagents and detected by UVITec Alliance LD2 (UVITec Cambridge, UK) imaging system.

Immunofluorescence analysis

The protocol for immunofluorescence analysis has been reported elsewhere [35]. Primary antibodies used included anti-Notch3 mAb (1:100; Abcam) and anti-LAMP2 mAb (1:150; Novus Biologicals, Littleton, CO, USA), both incubated overnight at 4 °C. Confocal microscopy was carried out on a Zeiss LSM 510 microscope (Zeiss, Jena, Germany) using a ×63 oil immersion objective (NA = 1.4).

$n = 21$ DMSO-treated cells and $n = 24$ TSA-treated cells were analyzed by z-stack scanning, with an optical slice of 1 µm and average of 15 optical slices/cell. Images were acquired with a resolution of 1024×1024 pixels. The co-localization coefficient (which indicates the extent of localization of Notch3 protein in LAMP2-positive vesicles) was calculated, using the Zeiss Histogram software tool, as the ratio between the Notch3/LAMP2 double-positive pixels and total number of Notch3-positive pixels.

Subcellular fractionation

Subcellular fractionation was performed by differential centrifugation in isotonic sucrose buffer with minor modification to previously described protocols [36]. Briefly, 1×10^8 pelleted cells were resuspended in 1 ml of ice-cold sucrose buffer (0.25 M sucrose in 10 mM Tris-HCl pH 7.4 and Protease Inhibitor Cocktail—Roche Diagnostic) and homogenized for 4 min (10 s ON–10 s OFF) using Kimble Kontes Pellet Pestle (Thermo Fisher Scientific). Homogenized cells were centrifuged at 4 °C at increasing speed to isolate specific cellular compartments, as schematized in Suppl. Figure 5. Pellets were resuspended in sucrose buffer and proteins were quantified using Pierce BCA Protein Assay Kit (Thermo Fisher Scientific). Twenty-five micrograms of protein extracts for each fraction were then solubilized with 3× Laemmli Sample Buffer with 0.1 M DTT, denaturated and analyzed by western blot using 7.5% or 4–15% polyacrylamide gels (BioRad, Munich, Germany). LAMP2, Pan-cadherin, GAPDH, VDAC, Histone H3, and β-tubulin were used as specific markers for lysosomes, plasma membranes, cytosol, mitochondria, nuclei, and total fractions, respectively.

Proliferation assay

Proliferation of T-ALL cells after HDAC inhibition was measured by the CellTiter 96® AQueous One Solution Cell Proliferation Assay (Promega, Madison, WI, USA).

Caspase activity assay

Caspase 3–7 activity was evaluated with the CaspaseGlo 3/7 assay kit according to the manufacturer's recommendations (Promega).

Statistical analysis

Results were expressed as mean ± standard deviation (SD). Statistical analysis was performed using Student's *t*-test or the non-parametric Mann–Whitney test, depending on the distribution of values. Differences were considered statistically significant when $P < 0.05$.

Acknowledgements We thank Adolfo Ferrando (Columbia University, New York, NY) for providing us with DND 41 and TALL1 cell lines.

Funding : AIRC (IG18803 to SI).

Compliance with ethical standards

Conflict of interest GF is an employee of Italfarmaco S.p.A., a pharmaceutical company involved in research on HDAC inhibitors. The remaining authors declare that they have no conflict of interest.

References

1. Graux C, Cools J, Michaux L, Vandenberghe P, Hagemeijer A. Cytogenetics and molecular genetics of T-cell acute lymphoblastic leukemia: from thymocyte to lymphoblast. Leukemia. 2006;20:1496–510.
2. Weng AP, Ferrando AA, Lee W, Morris JPt, Silverman LB, Sanchez-Irizarry C, et al. Activating mutations of NOTCH1 in human T cell acute lymphoblastic leukemia. Science. 2004;306:269–71.
3. Bellavia D, Campese AF, Alesse E, Vacca A, Felli MP, Balestri A, et al. Constitutive activation of NF-kappaB and T-cell leukemia/lymphoma in Notch3 transgenic mice. EMBO J. 2000;19:3337–48.
4. Bellavia D, Campese AF, Vacca A, Gulino A, Screpanti I. Notch3, another Notch in T cell development. Semin Immunol. 2003;15:107–12.
5. Gu Y, Masiero M, Banham AH. Notch signaling: its roles and therapeutic potential in hematological malignancies. Oncotarget. 2016;7:29804–23.
6. Fortini ME. Notch signaling: the core pathway and its post-translational regulation. Dev Cell. 2009;16:633–47.
7. Seugnet L, Simpson P, Haenlin M. Requirement for dynamin during Notch signaling in Drosophila neurogenesis. Dev Biol. 1997;192:585–98.
8. Lu H, Bilder D. Endocytic control of epithelial polarity and proliferation in Drosophila. Nat Cell Biol. 2005;7:1232–9.
9. Kanwar R, Fortini ME. Notch signaling: a different sort makes the cut. Curr Biol. 2004;14:R1043–5.
10. Weber U, Eroglu C, Mlodzik M. Phospholipid membrane composition affects EGF receptor and Notch signaling through effects on endocytosis during Drosophila development. Dev Cell. 2003;5:559–70.
11. Jia L, Yu G, Zhang Y, Wang MM. Lysosome-dependent degradation of Notch3. Int J Biochem Cell Biol. 2009;41:2594–8.
12. Bolden JE, Peart MJ, Johnstone RW. Anticancer activities of histone deacetylase inhibitors. Nat Rev Drug Discov. 2006;5:769–84.

13. Aldana-Masangkay GI, Sakamoto KM. The role of HDAC6 in cancer. J Biomed Biotechnol. 2011;2011:875824.
14. Deribe YL, Wild P, Chandrashaker A, Curak J, Schmidt MH, Kalaidzidis Y, et al. Regulation of epidermal growth factor receptor trafficking by lysine deacetylase HDAC6. Sci Signal. 2009;2:ra84.
15. Gao YS, Hubbert CC, Yao TP. The microtubule-associated histone deacetylase 6 (HDAC6) regulates epidermal growth factor receptor (EGFR) endocytic trafficking and degradation. J Biol Chem. 2010;285:11219–26.
16. Palermo R, Checquolo S, Giovenco A, Grazioli P, Kumar V, Campese AF, et al. Acetylation controls Notch3 stability and function in T-cell leukemia. Oncogene. 2012;31:3807–17.
17. Chambers AE, Banerjee S, Chaplin T, Dunne J, Debernardi S, Joel SP, et al. Histone acetylation-mediated regulation of genes in leukaemic cells. Eur J Cancer. 2003;39:1165–75.
18. Agnusdei V, Minuzzo S, Frasson C, Grassi A, Axelrod F, Satyal S, et al. Therapeutic antibody targeting of Notch1 in T-acute lymphoblastic leukemia xenografts. Leukemia. 2014;28:278–88.
19. Bernasconi-Elias P, Hu T, Jenkins D, Firestone B, Gans S, Kurth E, et al. Characterization of activating mutations of NOTCH3 in T-cell acute lymphoblastic leukemia and anti-leukemic activity of NOTCH3 inhibitory antibodies. Oncogene. 2016;35:6077–86.
20. Singh BN, Zhang G, Hwa YL, Li J, Dowdy SC, Jiang SW. Nonhistone protein acetylation as cancer therapy targets. Expert Rev Anticancer Ther. 2010;10:935–54.
21. Wang Z, Inuzuka H, Zhong J, Wan L, Fukushima H, Sarkar FH, et al. Tumor suppressor functions of FBW7 in cancer development and progression. FEBS Lett. 2012;586:1409–18.
22. Amati B, Sanchez-Arevalo Lobo VJ. MYC degradation: deubiquitinating enzymes enter the dance. Nat Cell Biol. 2007;9:729–31.
23. Pinazza M, Borga C, Agnusdei V, Minuzzo S, Fossati G, Paganin M, et al. An immediate transcriptional signature associated with response to the histone deacetylase inhibitor Givinostat in T acute lymphoblastic leukemia xenografts. Cell Death Dis. 2016;6:e2047.
24. McGill MA, Dho SE, Weinmaster G, McGlade CJ. Numb regulates post-endocytic trafficking and degradation of Notch1. J Biol Chem. 2009;284:26427–38.
25. Sakata T, Sakaguchi H, Tsuda L, Higashitani A, Aigaki T, Matsuno K, et al. Drosophila Nedd4 regulates endocytosis of notch and suppresses its ligand-independent activation. Curr Biol. 2004;14:2228–36.
26. Wilkin MB, Carbery AM, Fostier M, Aslam H, Mazaleyrat SL, Higgs J, et al. Regulation of notch endosomal sorting and signaling by Drosophila Nedd4 family proteins. Curr Biol. 2004;14:2237–44.
27. Conner SD. Regulation of Notch signaling through intracellular transport. Int Rev Cell Mol Biol. 2016;323:107–27.
28. Vaccari T, Lu H, Kanwar R, Fortini ME, Bilder D. Endosomal entry regulates Notch receptor activation in Drosophila melanogaster. J Cell Biol. 2008;180:755–62.
29. Windler SL, Bilder D. Endocytic internalization routes required for delta/notch signaling. Curr Biol. 2010;20:538–43.
30. Sorensen EB, Conner SD. Gamma-secretase-dependent cleavage initiates notch signaling from the plasma membrane. Traffic. 2010;11:1234–45.
31. Pacheco MT, Morais KL, Berra CM, Demasi M, Sciani JM, Branco VG, et al. Specific role of cytoplasmic dynein in the mechanism of action of an antitumor molecule, Amblyomin-X. Exp Cell Res. 2016;340:248–58.
32. Liu J, Shen JX, Wen XF, Guo YX, Zhang GJ. Targeting Notch degradation system provides promise for breast cancer therapeutics. Crit Rev Oncol Hematol. 2016;104:21–9.
33. Masiero M, Minuzzo S, Pusceddu I, Moserle L, Persano L, Agnusdei V, et al. Notch3-mediated regulation of MKP-1 levels promotes survival of T acute lymphoblastic leukemia cells. Leukemia. 2011;25:588–98.
34. Serafin V, Persano L, Moserle L, Esposito G, Ghisi M, Curtarello M, et al. Notch3 signalling promotes tumour growth in colorectal cancer. J Pathol. 2011;224:448–60.
35. Pasto A, Serafin V, Pilotto G, Lago C, Bellio C, Trusolino L, et al. NOTCH3 signaling regulates MUSASHI-1 expression in metastatic colorectal cancer cells. Cancer Res. 2014;74:2106–18.
36. Schroter CJ, Braun M, Englert J, Beck H, Schmid H, Kalbacher H. A rapid method to separate endosomes from lysosomal contents using differential centrifugation and hypotonic lysis of lysosomes. J Immunol Methods. 1999;227:161–8.

ELSEVIER

Urologic Oncology: Seminars and Original Investigations 000 (2019) 1−10

UROLOGIC ONCOLOGY

Laboratory-Kidney cancer

The role of p53 isoforms' expression and p53 mutation status in renal cell cancer prognosis

Marijana Knezović Florijan, M.D.[a], Petar Ozretić, Ph.D.[b], Maro Bujak, Ph.D.[c], Laura Pezzè, M.S.[d], Yari Ciribilli, Ph.D.[d], Željko Kaštelan, M.D., Ph.D.[e], Neda Slade, Ph.D.[b,*], Tvrtko Hudolin, M.D., Ph.D.[e]

[a] *Sestre Milosrdnice University Hospital Centre, Zagreb, Croatia*
[b] *Division of Molecular Medicine, Ruđer Bošković Institute, Zagreb, Croatia*
[c] *Division of Materials Chemistry, Ruđer Bošković Institute, Zagreb, Croatia*
[d] *Laboratory of Molecular Cancer Genetics, Centre for Integrative Biology (CIBIO), University of Trento, Povo (TN), Italy*
[e] *Department of Urology, University Hospital Centre Zagreb, Zagreb, Croatia*

Received 27 November 2018; received in revised form 13 February 2019; accepted 10 March 2019

Abstract

Objectives: To analyze p53 mutations and gene expression of p53, Δ40p53, and Δ133p53 isoforms in renal cell cancer (RCC) tissues and normal adjacent tissue (NAT) and to associate them to clinical features and outcome.

Patients and methods: Forty-one randomly selected patients, with primary, previously untreated RCC, with complete clinicopathohistological data were analyzed. NAT samples were available for 37 cases. Expression of p53, Δ40p53 and Δ133p53 was determined using RT-qPCR. A functional yeast-based assay was performed to analyze p53 mutations.

Results: More than half (56.1%) of patients harbored functional p53 mutations, and they were significantly younger than those with wild type (WT) p53 ($P = 0.032$). Expression of p53, Δ40p53, and Δ133p53 was upregulated in mutant (MT) p53 RCC compared to WT p53 RCC tissues. However, there was no difference in expression of these isoforms between MT p53 RCC tissues and NAT. Expression of Δ133p53 was significantly downregulated in WT p53 tissues compared to NAT ($P = 0.006$). Patients that harbored functional p53 mutation had better overall survival (hazard ratio 4.32, 95% confidence interval 1.46−18.82, $P = 0.006$). Multivariate analysis demonstrated that tumor stage and p53 mutation might be used as independent prognostic marker for overall survival in RCC patients.

Conclusions: Our findings support the specific events in the carcinogenesis of RCC. p53 isoforms can be differentially expressed depending on p53 mutational status.

Keywords: p53; p53 isoforms; Renal cell cancer; p53 mutation

Abbreviation: RCC, renal cell cancer; NAT, normal adjacent tissue; WT p53, wild-type p53; MT p53, mutant p53; OS, overall survival, RT-qPCR, reverse transcription quantitative polymerase chain reaction; RCF, red colony frequency; TBP, TATA binding protein; FASAY, functional analysis of separate allele in yeast.

1. Introduction

Renal cell cancer (RCC) represents 2% to 3% of all cancers, with the highest incidence in Western countries [1,2]. Over the last 2 decades the incidence of RCC is increased, mostly due to increased detection of tumors by ultrasound and computed tomography [3]. The Tumor, Nodes, Metastasis (TNM) staging system is used to assess the anatomic extent of disease [4]. The most common histologic subtype is clear cell RCC which is believed to account for 80% to 90% of all RCCs [4]. Despite of all available prognostic markers, it seems that RCC follows an unpredictable disease course [5]. To improve the prognosis of the disease course, a better understanding of critical genes associated with disease progression is required.

The p53 tumor suppressor protein is critical in the control of cell growth and the maintenance of genomic

Funding: This work was supported by Croatian Science Foundation grant IP-11-2013-1615 to NS.

*Corresponding author. Tel.: +385918961677.
E-mail address: slade@irb.hr (N. Slade).

https://doi.org/10.1016/j.urolonc.2019.03.007
1078-1439/

stability [6]. In contrast to other tumors, p53 is rarely mutated in RCCs suggesting that p53 function might be suppressed by other mechanisms [7−9]. p53 encodes 12 different isoforms that differ in their N- and C-terminus due to alternative splicing, promotor or translation initiation site [10]. The sum of their activities determines the p53-mediated cell response in a given tissue [6,11−13]. They have structural differences, different subcellular localization, they exert different effects on p53-mediated gene expression while some isoforms exhibit some functions independent of p53 [12,14−16]. The Δ40p53 isoform lacks the first 39 amino acids and has lost the first transactivating domain but still retains the second one and the entire DNA binding domain. It has reduced ability to activate transcription of p53 mediated genes by itself, but it can form complexes with p53 and modulate p53-dependent gene expression in a positive and negative manner depending on its relative levels and cellular context [10,17]. Δ133p53 and Δ160p53 isoforms, produced from internal promoter P2, lack the first 132 and 159 amino acids, respectively, and have lost both transactivating domains and a part of the first conserved cysteine box of the DNA binding domain. Δ133p53 forms heterocomplex with p53 and hence modulates gene expression in p53-independent way [13].

The expression of p53 isoforms has been shown to be dysregulated in several human cancer types, so we assume that in RCC p53 isoforms might participate in p53 inactivation, in tumor initiation and progression. The aim of this study was to analyze p53 mutation status in RCC tissues and mRNA expression of p53, Δ40p53, and Δ133p53 isoforms in RCC tissues and normal adjacent tissues (NAT), and to associate this information with clinical features and outcome.

2. Patients and methods

2.1. Patients' data

We prospectively analyzed 41 randomly selected patients with primary, previously untreated RCC, with complete clinicopathohistological data. Inclusion criteria were as followed: (1) histologically proven RCC (all cell types of RCC are eligible), (2) patients with all stages of disease according to TNM classification system, (3) patients were older than 18 years, (4) obtained written informed consent for the storage and use of their tissue and clinical information in this study. Thirty-seven patients underwent radical (90.2%), and 4 patients partial nephrectomy (9.8%) at the University Hospital Centre Zagreb, Croatia, from November 2010 until October 2013. Four patients (9.7%) had metastatic disease at the beginning of the study and 13 patients (31.7%) had locally advanced RCC defined by TNM classification (T3/T4, N0, M0). This study complied with the Helsinki Declaration and was approved by the ethical committee from the University Hospital Centre Zagreb, Zagreb. Tissue samples were collected immediately after nephrectomy and evaluated by a pathologist; areas of histologically normal adjacent renal cell tissue were available for 37 cases. All clinical information was collected prospectively from hospital information system and anonymized.

2.2. RNA extraction and RT-qPCR

Total RNA was extracted from 50 to 100 mg of tissue using TRIzol reagent (Thermo Fisher Scientific, USA) and subsequent RNA clean-up through RNeasy Mini Kit (Qiagen, USA) including DNase I treatment according to the manufacturer's instructions. Total RNA was quantified and purity assessed using the BioSpec-nano Micro-volume UV-Vis Spectrophotometer (Shimadzu, Japan). RNA was reversely transcribed using High Capacity cDNA Reverse Transcription Kit (Thermo Fisher Scientific, USA) according to the manufacturer's instructions.

Absolute copy numbers were determined using the standard curve method by qPCR using the ABI Prism 7300 Detection System (Thermo Fisher Scientific). Reactions were performed in a final volume of 25 μl using the TaqMan® Universal PCR Master Mix (Thermo Fisher Scientific) under standard thermal cycling conditions (50˚C for 2 min and 95˚C for 10 min followed by 50 cycles at 95˚C for 15 s and 60˚C for 1 min). Primers and probes sequences (Metabion, Germany) are given in Supplementary Table S1. The absolute copy numbers were calculated from standard curves generated from serial dilutions of linearized plasmid construct carrying the amplicon with known concentration to allow copy numbers determination, and normalized to the average levels of housekeeping gene TATA box-binding protein (*TBP*). Reactions were conducted in duplicates.

2.3. Functional analysis of separate allele in yeast (FASAY)

We have adapted, and *ad hoc* modified the well-established FASAY assay [18], also known as Gap Repair Assay [19], in order to screen 41 patients for *TP53* status. Briefly, cDNA obtained from RCC patients was used as template for a two-step PCR approach to amplify the *TP53* gene. The first-step PCR was performed using 25 μg of cDNA, the Go-Taq G2 Green Master Mix (Promega, USA), p53-Ex2.1-Fw (GTCACTGCCATGGAGGAGCCGCA) and p53-P4 (ACCCTTTTTGGACTTCAGGTGGCTGGAGTG) primers (Eurofins Genomics, Germany). PCR products were diluted 1:400, and used for the second-step nested PCR using again Go-Taq G2 Green Master Mix but p53-P3 (ATTTGATGCTGTCCCCGGACGATATTGAAC) and p53-Ex10-Rv (CTTCCCAGCCTGGGCATCCTTG) more internal primers. cDNAs from MCF7 (WT p53) and MDA-MB-231 (only expressing the R280K p53 mutant allele) cells were used as negative and positive controls, respectively.

Five or 10 μl of the second-step nested PCR product was added to 1.5 μl of double digested pRDI22 yeast expression plasmid (CEN/ARS, LEU2) and cotransformed in yeast using the Lithium acetate method [20] in the yeast reporter strain yIG397 that contains the ADE2 reporter gene under the control of a p53 Responsive Element. LEU2+ yeast colonies were selected on synthetic plates lacking leucine and containing limiting amount of adenine (5 mg/l). Transformant colonies were white in case of expression of WT p53, whereas MT p53 colonies appeared red. Colonies were counted, and red colony frequency (RCF) was calculated. Given the overall higher amount of background red colonies due to the two-step PCR approach (about 15−20%), samples with an RCF higher than 60% were considered heterozygous for *TP53*. Samples with an RCF below 40% were scored as homozygous wild-type, while samples with almost all red colonies (RCF = 90−100%) were considered homozygous/hemizygous *TP53* mutants. Lastly, samples with an RCF score between 40% and 60% were uncertain and were re-analyzed for a more accurate screening. However, heterozygous samples were considered mutant due to the fact that heterozygous state is often transient and the inactivation of the wild-type allele is likely to happen. Moreover, many MT p53 proteins gain oncogenic activity which overcomes the tumor suppressor activity of the remaining WT p53 allele [21].

2.4. Statistical analysis

Normality of data was tested using D'Agostino and Pearson Omnibus test. Continuous variables were log transformed prior to analyses to distribute the data normally. ANOVA and Student's t-test were used to determine the difference of p53 isoforms mRNA expression between various subgroups. Spearman's correlation coefficient was used to calculate the correlation among p53 isoforms' expression. Isoforms' expression was dichotomized into "low" and "high" by a median value. The relationship between p53 isoforms' expression and p53 mutation status to clinical parameters was interrogated using chi-square test. Overall survival (OS) was determined with Kaplan-Meier method and log-rank test, while Cox proportional-hazards regression model was used for multivariate analysis. Statistical analyses were performed using MedCalc for Windows, version 17.6 (MedCalc Software, Belgium). Two-tailed $P < 0.05$ was considered to be significant.

3. Results

3.1. p53 mutation status in RCC patients

For the analysis of p53 mutation status we used the FASAY that can distinguish inactivating mutations from functionally silent mutations. Table 1 summarizes the clinicopathological features of the cohort, as well as the results of p53 mutation analysis. More than half of the patients (56.1 %) harbored nonfunctional p53 mutations (including both homozygous [36.6%] and heterozygous [19.5%] mutants). Of note, p53 mutant cancers were associated with younger age at diagnosis (median 60 for MT p53 vs. 69 years for WT p53, $P = 0.032$).

Table 1
Summary of the patient cohort and p53 status data.

Variable	Number of patients in each category by p53 status (%)			
	Total	Wild-type p53	Mutant p53	*P* value*
Tumors, n (%)	41 (100)	18 (43.9)	23(56.1)	
Gender				0.951
Male	23 (56.1)	10	13	
Female	18 (43.9)	8	10	
Age (years)				**0.032**
Median = 64				
Range = 31−82				
<60	15 (36.6)	4	11	
60−70	14 (34.1)	5	9	
>70	12 (29.3)	9	3	
Presence of symptoms, n (%)				0.391
Asymptomatic	18 (43.9)	9	9	
Abdominal pain	14 (34.1)	7	7	
Hematuria	7 (17.1)	1	6	
Symptoms of metastatic disease	2 (4.9)	1	1	
Histological subtype, n (%)				0.577
Clear cell	35 (85.4)	16	19	
Non-clear cell	6 (14.6)	2	4	
Fuhrman grade, n (%)				0.431
1	0	0	0	
2	9 (22.0)	5	4	
3	17 (41.5)	5	12	
4	12 (29.3)	6	6	
Not available	3 (7.3)	2	1	
Tumor size (cm)				0.301
Median = 7				
Range = 2−15				
≤7 cm	19 (46.3)	10	9	
>7 cm	22 (53.7)	8	14	
Renal capsular invasion				0.453
Negative	27 (65.9)	13	14	
Positive	14 (34.1)	5	9	
Venous invasion				0.051
Negative	31 (79.5)	16	15	
Positive	8 (20.5)	1	7	
Perirenal fat invasion				0.793
Negative	29 (74.4)	13	16	
Positive	10 (25.6)	4	6	
Lymph node metastasis				0.134
Negative	31 (88.6)	11	20	
Positive	4 (11.4)	3	1	
Distant metastases				0.798
Negative	37 (90.2)	16	21	
Positive	4 (9.8)	2	2	
Tumor stage, n (%)				0.505
1	21 (51.2)	10	11	
2	3 (7.3)	1	2	
3	12 (29.3)	4	8	
4	4 (9.8)	3	1	

* χ^2 test. Significant *P* values are shown in bold.

3.2. Low expression of p53 isoforms in RCC

To determine gene expression of p53 isoforms in RCC, the mRNA expression of p53, Δ40p53 and Δ133p53 was analyzed by RT-qPCR in 41 tumors and 37 matched NATs. As shown in Supplement Table 2, Δ40p53 and Δ133p53 had remarkably weak expression compared to p53 − the p53 median expression was 8.85 times higher than the median expression of Δ40p53 and 16.32 times higher than the median expression of Δ133p53 isoform. Also, we observed significantly lower Δ133p53 expression in RCC tissues compared to NATs ($P = 0.002$) (Fig. 1). In addition, the expression of each isoform within NATs and cancer tissues regardless of p53 mutation status was highly associated with one another (Spearman's rank correlation coefficients ranged from 0.700 to 0.886, all P values < 0.05).

Table 2
The relationship of p53 isoforms expression and clinical features.

Variable	p53		*P* value*	Δ40p53		*P* value*	Δ133p53		*P* value*
	Low expression	High expression		Low expression	High expression		Low expression	High expression	
Gender			0.445			0.891			0.448
Male	13	10		11	12		13	10	
Female	8	10		9	9		8	10	
Age (years)			0.145			0.061			**0.032**
<60	6	9		7	8		5	10	
60–70	6	8		4	10		7	7	
>70	9	3		9	3		9	3	
Symptoms			0.269			0.445			0.268
Absent	11	7		10	8		11	7	
Present	10	13		10	13		10	13	
Histologic subtype			0.945			0.349			0.349
Clear cell	18	17		16	19		19	16	
Non-clear cell	3	3		4	2		2	4	
Fuhrman grade			0.302			0.159			0.510
1	0	0		0	0		0	0	
2	6	3		6	3		5	4	
3	9	8		8	9		9	8	
4	4	8		3	9		5	7	
Tumor size			**0.044**			**0.021**			0.160
≤7 cm	13	6		13	6		12	7	
>7 cm	8	14		7	15		9	13	
Renal capsular invasion			**0.040**			**0.013**			0.158
Negative	17	10		17	10		16	11	
Positive	4	10		3	11		5	9	
Venous invasion			0.937			0.587			0.936
Negative	15	16		15	16		15	16	
Positive	4	4		3	5		4	4	
Perirenal fat invasion			0.176			0.057			0.528
Negative	16	13		16	13		15	14	
Positive	3	7		2	8		4	6	
Lymph node metastasis			0.269			0.857			0.268
Negative	14	17		14	17		14	17	
Positive	3	1		2	2		3	1	
Distant metastases			0.276			0.322			0.275
Negative	20	17		19	18		20	17	
Positive	1	3		1	3		1	3	
Stage			0.573			0.572			0.893
1	12	9		12	9		11	10	
2	1	2		1	2		1	2	
3	7	5		5	7		7	5	
4	1	3		1	3		2	2	
p53 status			**0.003**			**0.009**			**0.0003**
WT	14	4		13	5		15	3	
MT	7	16		7	16		6	17	

* $\chi 2$ test. Significant P values are shown in bold.

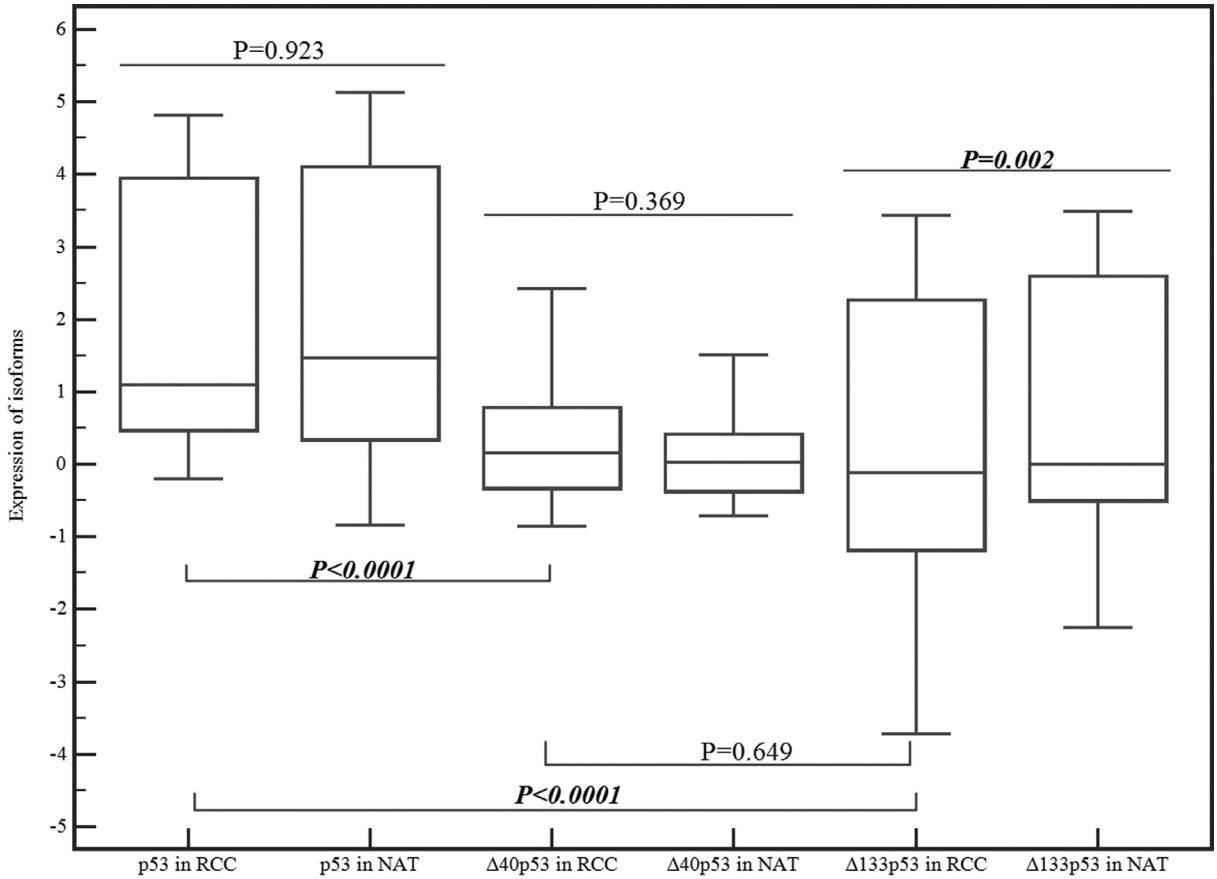

Fig. 1. Expression of p53, Δ40p53, and Δ133p53 isoforms in RCC tissues and NAT samples. Absolute quantification of p53, Δ40p53, and Δ133p53 by RT−qPCR in 41 tumors and 37 NATs. Results are shown as absolute copy numbers, expressed per standard input total RNA normalized to the average levels of housekeeping gene TATA box-binding protein (*TBP*). Values represent the median and interquartile range. Significant *P* values are shown in bold.

3.3. The expression of p53 isoforms in RCC is associated with p53 mutational status

We have further analyzed whether the expression of p53 isoforms is associated with p53 mutation status in RCC tissues (Supplementary Table S2). Cancer tissues that harbored p53 mutations had a significantly higher expression of p53, Δ40p53, and particularly Δ133p53 isoforms ($P = 0.0009$, $P = 0.004$ and $P = 0.0008$, respectively) compared to WT p53 tumors (Fig. 2A.). When compared with NATs separately in WT p53 and MT p53 RCCs, only in WT p53 cancer tissues Δ133p53 expression was significantly lower ($P = 0.006$) (Fig. 2B). We detected no significant alteration of isoform expression in MT p53 tumors compared to NATs (Fig. 2C).

3.4. The association between p53 isoforms expression and clinical features

Table 2 summarizes the association between p53 isoforms' expression and clinical features. There was no significant difference in the expression of either p53, Δ40p53 or Δ133p53 in relation to gender, presence of symptoms, Fuhrman grade, histologic type, lymph node metastases, distant metastases, and tumor stage according to TNM classification system. However, higher mRNA expression of p53 and Δ40p53 was associated with larger tumor size ($P = 0.044$ and $P = 0.021$, respectively) and more often renal capsular invasion ($P = 0.040$ and $P = 0.013$, respectively). Younger patients had higher expression of Δ133p53 isoform ($P = 0.032$).

3.5. The association of p53 isoforms expression and p53 mutational status with OS

Next, we have investigated the connection between p53 isoform expression and OS. Median follow-up was 45 months (range 2−72 months). The median values for p53, Δ40p53, and Δ133p53 were used to fractionate samples into 2 groups, a high-expressing group, and a low-expressing group. There was no difference in OS regarding the level of p53, Δ40p53, and Δ133p53 expression (Fig. 3). However, we observed difference in OS of patients harboring WT p53 compared to those with p53 mutations (hazard ratio 4.32, 95% confidence interval [CI] 1.46−18.82, $P = 0.006$) (Fig. 3D). A median OS of 27 months (95% CI:

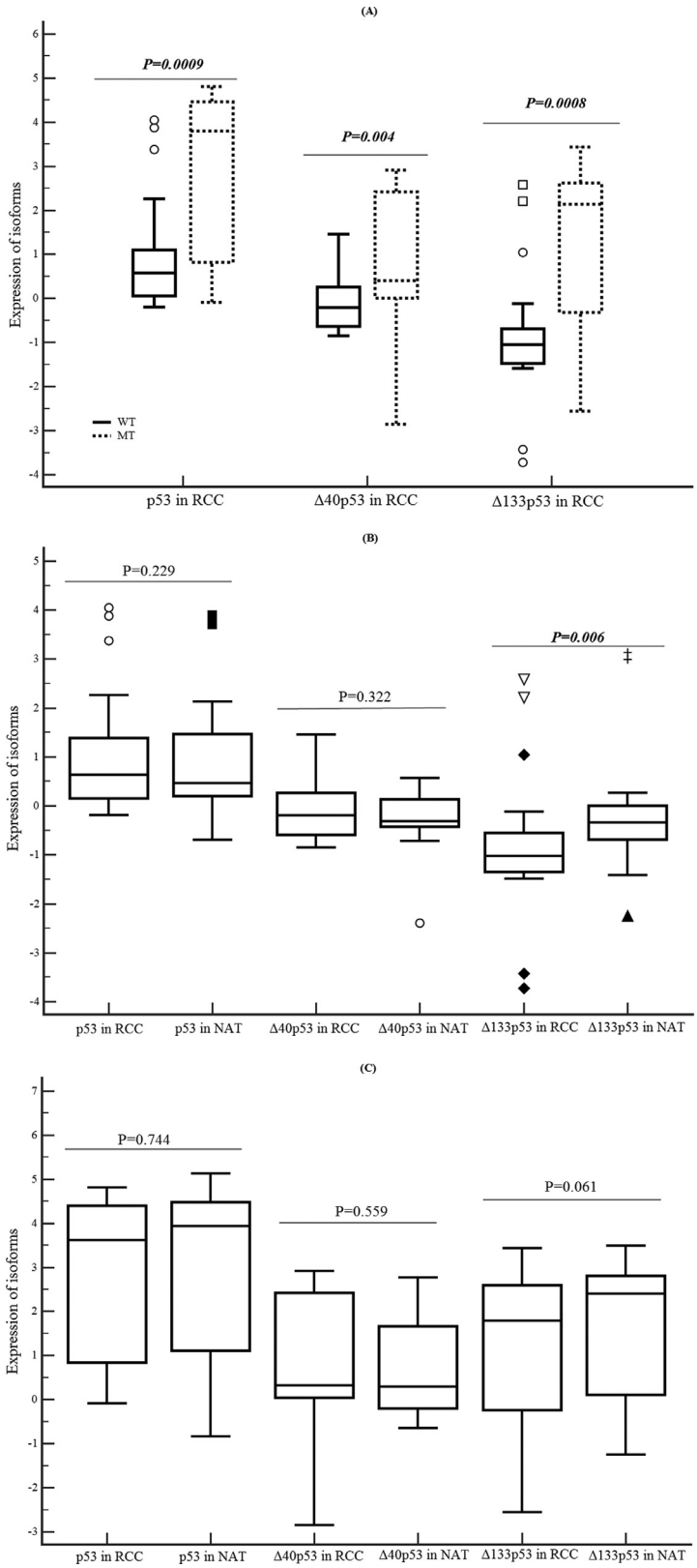

Fig. 2. Expression of p53, Δ40p53, and Δ133p53 isoforms in renal cell cancer tissues in association with p53 mutational status. Absolute quantification of p53, Δ40p53, and Δ133p53 isoforms by RT-qPCR in (A) 41 RCC tissues and (B,C) 37 matched RCC tissues and NAT in (B) wild type p53 tumors and (C) mutant p53 tumors. Results are shown as absolute copy numbers, expressed per standard input total RNA normalized to the average levels of housekeeping gene *TBP*. t-test was used for testing difference between 2 groups. Values represent median and interquartile range. Significant *P* values are shown in bold.

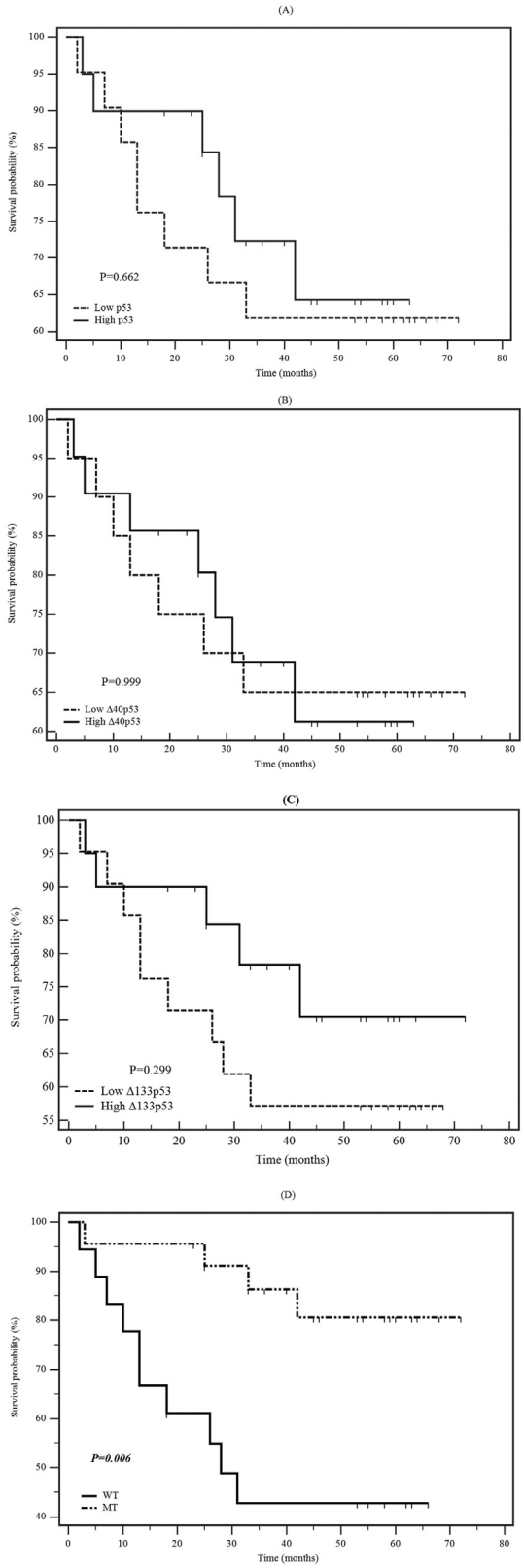

Fig. 3. Kaplan-Meier plots depicting the impact of p53 isoforms' expression and p53 mutational status on OS of patients with renal cell cancer. High (full line) or low (dotted line) expression of p53 (A), Δ40p53 (B) and Δ133p53 (C) in 41 cases. Analysis of cases with MT (dotted line) or WT (full line) in 41 cases (D). The log rank (Mantel-Cox) test *P* values are shown. Tick marks indicate censored cases.

13.0−56.8 months) was observed in patients with WT p53 while it was 53 months (95% CI: 37.4−60 months) in patients with MT p53. In the univariate analysis, Fuhrman grade, tumor stage, tumor size, and p53 mutation status were statistically significant prognostic markers for OS (Table 3). In the multivariate model, only tumor stage and p53 mutation status can be considered as independent prognostic marker (Table 3).

4. Discussion

The p53 regulates different cellular responses to stress including DNA repair, cell cycle arrest, proliferation, senescence, differentiation, cell migration, and cell death, hence maintaining cell integrity. Therefore, p53 mutations, the most common genetic changes in human cancers, often are associated with worse disease outcome. Of note, p53 isoforms have distinct and independent roles in cancer. Several clinical studies have reported that p53 isoforms are abnormally expressed in human cancers suggesting that they could contribute to cancer formation and progression [22,23]. Two independent studies have determined the expression of p53 isoforms in RCC tissues so far, using semiquantitative analysis of p53 isoforms levels. However, in both studies, p53 isoforms' expression has not been associated with clinical features and outcome [24,25]. Also, many studies have analyzed p53 mutation status using immunostaining and sequencing methods, but none of them examined the functional mutation status of p53 in RCC tissues [26,27]. The aim of this study was to determine the expression of p53, Δ40p53, and Δ133p53 isoforms in RCC and NATs, to determine the frequency of functional p53 mutations, and to associate the differential expression of isoforms and p53 mutational status with clinical features and outcome.

To this aim, we have determined the p53 status in our tumor collection using FASAY and 56.1% of tumors were identified as bearing a mutant p53 protein (either one or both alleles were mutated). The possible explanation for such a high frequency is the fact that most of the other studies have used immunochemical methods to detect p53 mutations [26,27]. In these studies, high-level expression of p53 is used as a surrogate mutation indicator due to abnormally extended half-live of mutant p53. However, in 10% to 20% of mutant p53 cases, tumors may harbor nonsense (truncating) mutations, which can lead to unstable mutant proteins, that will be expressed at low levels and falsely considered as WT p53 [9]. Furthermore, the majority of studies analyzed the central core domain of the gene (exons 4-8 or 5-8), the most common site of p53 mutations. However, approximately 15% of p53 mutations occur outside exons 5 through 8, that is in exons 4, 9, and 10, and therefore, it is likely that there will be some underestimation of p53 mutations in these studies [9].

The results of our study provide information about mRNA expression of p53 and N-truncated isoforms in RCC

Table 3
Cox regression analysis of p53 isoform expression, *TP53* status, and clinopathological parameters.

Variable (n)	Univariate		Multivariate[b]	
	HR (95% CI)	*P* value[a]	HR (95% CI)	*P* value[c]
Gender				
Male	Reference			
Female	0.458 (0.14−1.46)	0.188	/	/
Age (years)				
<60	Reference			
60−70	1.20 (0.30−4.80)	0.799	/	/
>70	2.34 (0.66−8.33)	0.188		
Presence of symptoms				
Asymptomatic	Reference			
Symptomatic	1.66 (0.56−4.98)	0.360	/	/
Histological subtype				
Clear cell	Reference			
Non-clear cell	1.09 (0.24−4.90)	0.907	/	/
Fuhrman grade				
2 and 3	Reference			
4	5.54 (1.87−16.41)	**0.002**	NS	NS
Tumor size (cm)				
≤7 cm	Reference			
>7 cm	4.38 (1.21−15.81)	**0.024**	NS	NS
Renal capsular invasion				
Negative	Reference			
Positive	2.85 (0.99−8.21)	0.052	/	/
Venous invasion				
Negative	Reference			
Positive	1.16 (0.32−4.16)	0.822	/	/
Perirenal fat invasion				
Negative	Reference			
Positive	2.01 (0.67−6.03)	0.213	/	/
Tumor stage				
Stage 1 and 2	Reference			
Stage 3 and 4	6.55 (2.02−21.20)	**0.001**	7.14 (1.65−30.83)	**0.008**
p53 status				
WT	Reference			
MT	0.23 (0.07−0.73)	**0.012**	0.12 (0.03−0.455)	**0.002**
p53				
Low expression	Reference			
High expression	0.79 (0.27−2.28)	0.663	/	/
Δ40p53				
Low expression	Reference			
High expression	1 (0.35−2.86)	0.999	/	/
Δ133p53				
Low expression	Reference			
High expression	0.56 (0.19−1.69)	0.306	/	/

[a] Variables with *P* value < 0.05 obtained from univariate analyses were used for multivariate analysis.
[b] Multivariate analysis using Cox proportional hazards regression, stepwise method.
[c] Significant *P* value < 0.05 for multivariate analysis. Reference is the parameter used as baseline for comparison. /, not included in multivariate analysis; CI, confidence interval; HR, hazard ratio; MT, mutated; NS, not significant; WT; wild type.

and NATs by RT-qPCR. Full-length p53 was the most expressed isoform in RCC tissues, while Δ40p53 and Δ133p53 were notably less expressed. This finding is consistent with study of Marabese and co-workers who had found low levels of Δ40p53 and Δ133p53 isoforms in ovarian carcinoma compared to p53 expression [28]. Also, in squamous cell carcinoma of the head and neck, Δ133p53 expression is lower compared to transactivating full-length isoforms of p53 (including p53β) [29].

We did not observe any significant difference in p53 and Δ40p53 expression in cancer tissues compared to NATs, while Δ133p53 isoform was down-regulated in cancer tissues. The lack of overexpression of p53 in RCC could be explained on the basis of the study conducted with transgenic mice exposed to ionizing radiation, which have revealed that p53 is not necessarily up-regulated in kidney tissues in response to stress and is less effective in kidney than in other tissues [30]. Moreover, it is well

accepted that full-length p53 expression is generally not modulated at the mRNA level, but rather at protein levels, often due to an array of several post-translational modifications. In contrast to this observation, another RCC study detected up-regulation of TAp53 isoforms (p53, p53β, and p53γ), but no significant alteration of Δ133p53 expression was detected in different tumor stages as compared to normal renal tissue [24]. However, down-regulation of Δ133p53β and γ was found only in early tumor phases [24]. In another RCC study, Song and collaborators observed the significant up-regulation of p53β isoform in tumor samples which correlated with tumor stage. Again, the other isoforms were expressed at different levels in both tumor and normal tissue but without statistical significance [25]. Both studies used semiquantitative analysis of p53 isoforms expression and did not analyses p53 mutation status.

We have associated the expression of p53 isoforms with p53 mutation status and found that the expression of all examined isoforms was higher in tumor tissues harboring mutant p53. In RCC tissues with WT p53 we have observed down-regulation of Δ133p53 isoform when compared to NATs. In tumors harboring MT p53 down-regulation of Δ133p53 was not observed.

As mentioned before, p53 and Δ40p53 are transcribed from P1 promoter, while Δ133p53 expression is driven by alternative promoter P2 [22], which can be activated by p53 and suppressed by Δ40p53 through suppression of p53 functions [31]. It seems that in the cases that retained WT p53, the feedback regulatory loop might be altered, resulting in lower p53 activity on P2 promoter, and down-regulation of Δ133p53 isoforms. Based on these results, we speculate that dysregulation of p53 isoforms could contribute to cancer formation in WT p53 tissues. In addition, there was a trend of higher OS in patients with higher expression levels of p53 and Δ133p53 isoforms (Fig. 3). Analysis of larger sample size might validate p53 isoform expression level as a prognostic biomarker in RCC patients.

One of the clinically most interesting findings in this study is the association of p53 mutant status with OS. Patients that harbored p53 mutation tumors had longer OS compared with patients with WT p53 tumors. This finding could be explained by the fact that patients with MT p53 tumors were significantly younger and might have less aggressive tumors (lower tumor stage) than those with WT p53 tumors since higher Fuhrman grade and tumor stage also have negative impact on OS (Fig. 3D, Table 3). Also, they had higher levels of p53, Δ40p53, and Δ133p53 isoform expression in RCC tissues and no difference in expression of isoforms in RCCs compared to NATs, suggesting that patients that have lower and dysregulated expression of p53 isoforms could have unfavorable clinical outcome even though they retained WT p53.

These observations confirm the result of a previous study showing that silent p53 mutations or mutations in noncoding regions are associated with cancer formation probably because they lead to unbalanced p53 isoforms expression despite expressing WT p53 [12]. Altogether, our results suggest that the prognostic value of isoforms depend on p53 mutation status and the cancer type.

The results of our research reveal specific combinations of isoforms expression and p53 mutation status providing additional support for specific events in kidney carcinogenesis. These findings suggest that p53 function can be lost either by specific p53 isoforms' expression or by mutations.

Our study has limitations; we analyzed RNA expression rather than protein levels on a modest number of samples. At present, RT-qPCR represents the best method to specifically detect p53 isoforms expression due to the lack of available isoform-specific antibodies. Using RT-qPCR we have focused to distinguish the expression level of N-terminal variants. However, we were not able to differentiate specifically all p53 isoforms due to excessively long amplicons for RT-qPCR and complex gene organization.

5. Conclusions

This study provides critical information on the mRNA expression level of N-terminal isoforms in RCC in relation to p53 functional mutation status. Tumors with WT p53 had lower expression of p53, Δ40p53, and Δ133p53 isoforms comparing to MT p53 harboring tumors, and down-regulation of Δ133p53 isoforms comparing to NAT. Our results underline the importance of considering both p53 mutational status and p53 isoforms' expression in RCC clinical studies. Further studies are needed to determine the role of p53 isoform network in RCC carcinogenesis.

Conflict of interest

None.

Supplementary materials

Supplementary material associated with this article can be found in the online version at https://doi.org/10.1016/j.urolonc.2019.03.007.

References

[1] ECIS - European Cancer Information System, European Union, 2018. https://ecis.jrc.ec.europa.eu. Accessed June 19, 2018.
[2] Levi F, Ferlay J, Galeone C, Lucchini F, Negri E, Boyle P, et al. The changing pattern of kidney cancer incidence and mortality in Europe. BJU Int 2008;101:949–58. https://doi.org/10.1111/j.1464-410X.2008.07451.x.
[3] Patard JJ, Rodriguez A, Rioux-Leclercq N, Guillé F, Lobel B. Prognostic significance of the mode of detection in renal tumours. BJU Int 2002;90:358–63. https://doi.org/10.1046/j.1464-410X.2002.02910.x.
[4] Ljungberg B, Bensalah K, Bex A, Canfield S, Dabestani S, Giles RH, et al. Guidelines on renal cell carcinoma. 2015. http://uroweb.org/wp-content/uploads/10-Renal-Cell-Carcinoma_LR1.pdf. Accessed November 22, 2018.

[5] Sun M, Shariat SF, Cheng C, Ficarra V, Murai M, Oudard S, et al. Prognostic factors and predictive models in renal cell carcinoma: a contemporary review. Eur Urol 2011;60:644–61. https://doi.org/10.1016/j.eururo.2011.06.041.

[6] Bourdon JC. p53 and its isoforms in cancer. Br J Cancer 2007; 97:277–82. https://doi.org/10.1038/sj.bjc.6603886.

[7] Bui MH, Zisman A, Pantuck AJ, Han KR, Wieder J, Belldegrun AS. Prognostic factors and molecular markers for renal cell carcinoma. Expert Rev. Anticancer Ther 2001;1:565–75. https://doi.org/10.1586/14737140.1.4.565.

[8] Gad S, Lefevre SH, Khoo SK, Giraud S, Vieillefond A, Vasiliu V, et al. Mutations in BHD and TP53 genes, but not in HNF1β gene, in a large series of sporadic chromophobe renal cell carcinoma. Br J Cancer 2007;96:336–40. https://doi.org/10.1038/sj.bjc.6603492.

[9] Noon AP, Vlatković N, Polański R, Maguire M, Shawki H, Parsons K, et al. p53 and MDM2 in renal cell carcinoma: biomarkers for disease progression and future therapeutic targets? Cancer 2010;116:780–902. https://doi.org/10.1002/cncr.24841.

[10] Hafsi H, Santos-Silva D, Courtois-Cox S, Hainaut P. Effects of Δ40p53, an isoform of p53 lacking the N-terminus, on transactivation capacity of the tumor suppressor protein p53. BMC Cancer 2013; 13:134. https://doi.org/10.1186/1471-2407-13-134.

[11] Bourdon JC. p53 isoforms change p53 paradigm. Mol Cell Oncol 2014;1:e969136. https://doi.org/10.4161/23723548.2014.969136.

[12] Joruiz SM, Bourdon JC. p53 isoforms: key regulators of the cell fate decision. Cold Spring Harb Perspect Med 2016;6:a026039. https://doi.org/10.1101/cshperspect.a026039.

[13] Khoury MP, Bourdon JC. p53 isoforms: an intracellular microprocessor? Genes Cancer 2011;2:453–65. https://doi.org/10.1177/1947601911408893.

[14] Bourdon J. p53 Family isoforms. Curr Pharm Biotechnol 2007;8:332–6. https://doi.org/10.2174/138920107783018444.

[15] Machado-Silva A, Perrier S, Bourdon J-C. p53 family members in cancer diagnosis and treatment. Semin Cancer Biol 2010;20:57–62. https://doi.org/10.1016/j.ejca.2007.10.011.

[16] Khoury MP, Bourdon J. The isoforms of the p53 protein. Cold Spring Harb Perspect Biol 2010;2:a000927. https://doi.org/10.1101/cshperspect.a000927.

[17] Ghosh A, Stewart D, Matlashewski G. Regulation of human p53 activity and cell localization by alternative splicing. Mol Cell Biol 2004;24: 7987–97. https://doi.org/10.1128/MCB.24.18.7987-7997.2004.

[18] Flaman JM, Frebourg T, Moreau V, Charbonnier F, Martin C, Chappuis P, et al. A simple p53 functional assay for screening cell lines, blood, and tumors. Proc Natl Acad Sci 1995;92:3963–7.

[19] Monti P, Perfumo C, Bisio A, Ciribilli Y, Menichini P, Russo D, et al. Dominant-negative features of mutant TP53 in germline carriers have limited impact on cancer outcomes. Mol Cancer Res 2011;9:271–9. https://doi.org/10.1158/1541-7786.MCR-10-0496.

[20] Andreotti V, Ciribilli Y, Monti P, Bisio A, Lion M, Jordan J, et al. p53 transactivation and the impact of mutations, cofactors and small molecules using a simplified yeast-based screening system. PLoS One 2011;6:e20643. https://doi.org/10.1371/journal.pone.0020643.

[21] Rivlin N, Brosh R, Oren M, Rotter V. Mutations in the p53 tumor suppressor gene: Important milestones at the various steps of tumorigenesis. Genes Cancer 2011;2:466–74. https://doi.org/10.1177/1947601911408889.

[22] Bourdon JC, Fernandes K, Murray-Zmijewski F, Liu G, Diot A, Xirodimas DP, et al. p53 isoforms can regulate p53 transcriptional activity. Genes Dev 2005;9:1–16. https://doi.org/10.1101/gad.1339905.

[23] Takahashi R, Giannini C, Sarkaria J, Schroeder M, Rogers J, Mastroeni D, et al. p53 isoform profiling in glioblastoma and injured brain. Oncogene 2013;32:3165–74. https://doi.org/10.1038/onc.2012.322.

[24] van den Berg L, Segun AD, Mersch S, Blasberg N, Grinstein E, Wai D, et al. Regulation of p53 isoform expression in renal cell carcinoma. Front Biosci 2010;2:1042–53. http://dx.doi.org/10.2741/162.

[25] Song W, Huo S, Lü J, Liu Z, Fang XL, Jin XB, et al. Expression of p53 isoforms in renal cell carcinoma. Chin Med J (Engl) 2009; 122:921–6.

[26] Sejima T, Miyagawa I. Expression of bcl-2, p53 oncoprotein, and proliferating cell nuclear antigen in renal cell carcinoma. Eur Urol 1999;35:242–8. https://doi.org/10.1159/000019855.

[27] Zigeuner R, Ratschek M, Rehak P, Schips L, Langner C. Value of p53 as a prognostic marker in histologic subtypes of renal cell carcinoma: a systematic analysis of primary and metastatic tumor tissue. Urology 2004;63:651–5. https://doi.org/10.1016/j.urology.2003.11.011.

[28] Marabese M, Marchini S, Marrazzo E, Mariani P, Cattaneo D, Fossati R, et al. Expression levels of p53 and p73 isoforms in stage I and stage III ovarian cancer. Eur J Cancer 2008;44:131–41. https://doi.org/10.1016/j.ejca.2007.10.011.

[29] Boldrup L, Bourdon J, Coates PJ, Sjöström B, Nylander K, et al. Expression of p53 isoforms in squamous cell carcinoma of the head and neck. Eur J Cancer 2007;43:617–23. https://doi.org/10.1016/j.ejca.2006.10.019.

[30] Slee EA, O'Connor DJ, Lu X. To die or not to die: how does p53 decide? Oncogene 2004;23:2809–18. https://doi.org/10.1038/sj.onc.1207516.

[31] Marcel V, Vijayakumar V, Fernández-Cuesta L, Hafsi H, Sagne C, Hautefeuille A, et al. p53 regulates the transcription of its Δ133p53 isoform through specific response elements contained within the TP53 P2 internal promoter. Oncogene 2010;29:2691–700. https://doi.org/10.1038/onc.2010.26.

ACKNOWLEDGEMENTS

I would like to thank my advisor Dr. Yari Ciribilli for giving me the opportunity to work in his laboratory during my PhD, allowing me to learn much, grow as a scientist, and finally become an independent researcher.

Thanks also to all the students that have joined the lab during my PhD for making this experience better: Stefano, Kalina, Irene, Francesca, Giulia and Nicolò. We were a great team, or better, “crew”. A special thank goes to Stefano, who helped me a lot with many experiments and cheered up the atmosphere , and to Kalina, for the tons of western blots she performed and for her dedication and patience.

My sincere gratitude goes to Prof. Ira Skvortsova, for hosting me in her lab, for supporting me and my ideas and for the fruitful discussions. I also want to thank all the members of her lab, Giulia, Bertram and Dragana, for helping and making me feel part of the lab, even in the short time spent together.

I also want to acknowledge Prof. Alberto Inga and all the members of his lab, for sharing ideas, reagents and precious suggestions. In particular, I want to thank Dario, a great colleague and friend who helped and supported me lots of times during these last 3 years. Thanks also to Sara for supporting me during the first year, and to Annalisa and Bosco for being always helpful.

I want to acknowledge also Prof. Marina Mione and the members of her lab, for teaching me how to perform the xenografts into zebrafish embryos and sharing materials. A special thank goes to Francesca, for her support with the transplants, but mainly for being a good friend.

Many other people contributed to making the lab and CIBIO an enjoyable workplace. In particular, I want to thank: Marco for his morning high fives and optimism, Veronica for understanding and supporting me even from abroad, Alice, Valeria, Valentina, Michele, Nicolò and Francesco for talking, laughs and lunch breaks, Blerta, Francesca, Paola, Giulia and Orsetta for sharing the lab, food, and bad music, and all the many other people that contributed to daily CIBIO life.

I acknowledge also the people working in CIBIO HTS, NGS and Cell Analysis and Separation facilities for their help and technical support.

Thanks to Dr. Mattia Forcato and Prof. Silvio Bicciato for the RNA-seq data analysis.

Last, but not least, thanks to my family. Thanks to my parents for encouraging and believing in me, and for their immeasurable support. And thanks to Elia, for giving me support, strength, love, and being always at my side, day after day.